Gene & Protein in Disease

ACCSCIENCE PUBLISHING

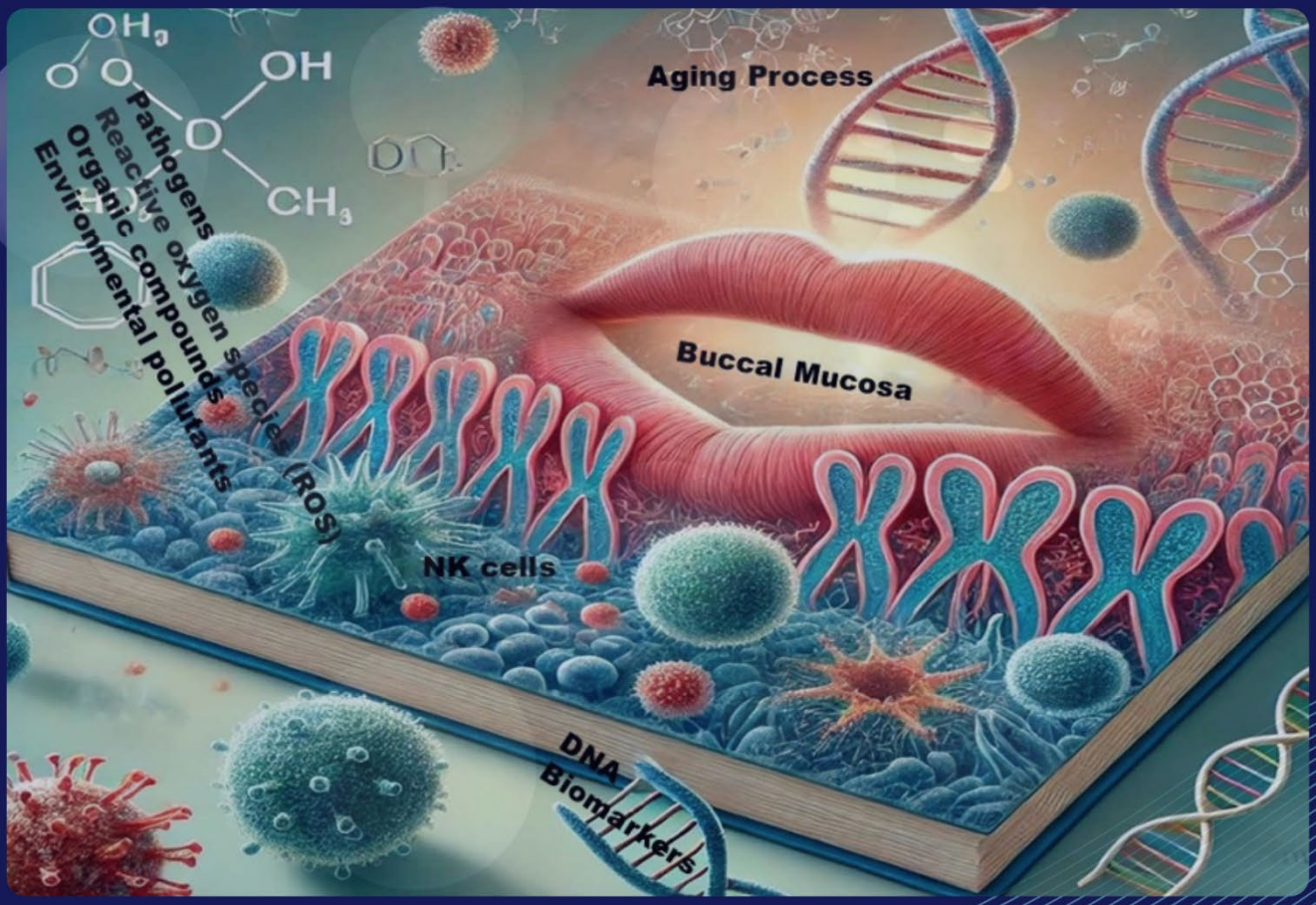

The environmental impact on aging: Insights from buccal mucosa and molecular biomarkers

ISSN: 2811-003X (Online)
Volume 3 · Issue 4
December 2024

Online ISSN: 2811-003X

Gene & Protein in Disease

Gene & Protein in Disease is an international journal for molecular and translational medicine. The journal primarily focuses on publishing investigations on the molecular bases and experimental therapeutics of human diseases.

Scan to access website:

Scan to submit papers:

About the Publisher

AccScience Publishing is a publishing company based in Singapore. We publish a range of high-quality, open-access, peer-reviewed journals and books from a broad spectrum of disciplines.

Contact Us

Managing Editor
gpd.office@accscience.sg

AccScience Publishing
8 Burn Road, #15-03 Trivex, Singapore 369977.

Volume 3 • Issue 4 • December 2024
ISSN 2811-003X (online)

GENE & PROTEIN IN DISEASE

ACCSCIENCE PUBLISHING

Access Science Without Barriers

GENE & PROTEIN IN DISEASE

ISSN: 2811-003X (online)

Editorial and Production Credits

Publisher: AccScience Publishing
Managing Editor: Juliana Meng
Production Editor: Sharmila Velapasamy
Article Layout and Typeset: Sinjore Technologies (India)

For all advertising queries, contact gpd.office@accscience.sg.

Supplementary file

Supplementary files of articles can be obtained at https://accscience.com/journal/GPD/3/4.

About the Cover

A graphic illustration of double-stranded DNA

Disclaimer

AccScience Publishing is not liable to the statements, perspectives, and opinions contained in the publications. The appearance of advertisements in the journal shall not be construed as a warranty, endorsement, or approval of the products or services advertised and/or the safety thereof. AccScience Publishing disclaims responsibility for any injury to persons or property resulting from any ideas or products referred to in the publications or advertisements. AccScience Publishing remains neutral with regard to jurisdictional claims in published maps and institutional affiliations.

Gene & Protein in Disease

Editorial Board

Youth Editorial Board Members

*Editorial Board Members as of December 19, 2024

ACCSCIENCE PUBLISHING

Volume 3 | Issue 4 | December 2024 |

Gene & Protein in Disease

https://accscience.com/journal/GPD

CONTENTS

ACCSCIENCE PUBLISHING

Gene & Protein in Disease

REVIEW ARTICLE

Understanding the fundamental mechanisms and conditions of the tumor-suppressive and oncogenic roles of sirtuins in cancer: A review

Daniela Szabóová[1], Zuzana Guľašová[2], Zdenka Hertelyová[2], and Roman Beňačka[1]*

[1]Department of Pathophysiology, Faculty of Medicine, P.J. Šafarik University, Košice, Slovakia

[2]Center of Clinical and Preclinical Research MEDIPARK, P.J. Šafarik University, Košice, Slovakia

Abstract

Silent information regulators (SIRTs) or sirtuins represent a group of class III nicotinamide adenine dinucleotide–dependent histone deacetylases. In mammals, seven types of sirtuins are distinguished, differing in their target structures, enzymatic activities, and subcellular localization. Histone deacetylation is a form of epigenetic regulation of gene expression that can cause activation or deactivation of selected genetic targets. Activation of sirtuins is part of the response to nutritional and environmental stimuli (starvation, DNA damage, and oxidative stress). Activated sirtuins subsequently stimulate specific transcriptional programs to make mitochondrial oxidative metabolism more efficient in the fight against oxidative stress or regulate proteins responsible for DNA repair after damage. As a result of their multifunctional involvement in cellular metabolism, dysregulation and aberrant expression of sirtuins have been observed in various cancers. Sirtuins play a dual role in carcinogenesis, acting as either oncogenes or tumor suppressors and affecting the proliferation, apoptosis, and survival of cancerous cells.

Keywords: Sirtuins; Oxidative stress; Cancer

***Corresponding author:**
Roman Beňačka
(roman.benacka@upjs.sk)

Citation: Szabóová D, Guľašová Z, Hertelyová Z, Beňačka R. Understanding the fundamental mechanisms and conditions of the tumor-suppressive and oncogenic roles of sirtuins in cancer: A review. *Gene Protein Dis.* 2024;3(4):4100. doi: 10.36922/gpd.4100

Received: July 1, 2024
Accepted: September 5, 2024
Published Online: October 10, 2024

1. Introduction

Silent information regulators (SIRTs) or sirtuins are a family of proteins that have attracted significant interest in biology and medicine research due to their involvement in cellular metabolism, particularly in processes related to aging, stress resistance, starvation, and survival (Figure 1).[1] Sirtuins are nicotinamide adenine dinucleotide (NAD)-dependent histone deacetylases, and different types of sirtuins possess mono–adenosine diphosphate (ADP)-ribosyltransferase, deacylase, demyristoylase, demalonylase, desuccinylase, and depalmitoylase activities. The enzymatic activity of sirtuins is dependent on NAD, and during the deacetylation reaction, histone lysines are deacetylated, and NAD is consumed in a process called hydrolysis. Simultaneously, the acetyl group bound to lysine is transferred from the target structure to the 2'-OH position of ADP-ribose, yielding 2'-O-acetyl-ADP-ribose and nicotinamide (3-pyridinecarboxamide or niacinamide).[2]

Changes in the acetylation status of lysine residues of histones represents a form of epigenetic regulation of gene expression that can cause activation or deactivation of

selected genetic targets, which allows sirtuins to influence various cellular processes, such as stress resistance and energy conservation during low-calorie situations, cell survival, transcription, DNA repair, apoptosis, inflammation, tissue regeneration, neuronal signaling, and circadian rhythm.[3,4] During caloric restriction, the tricarboxylic acid (TCA) cycle slows down due to reduced glucose and free fatty acid intake by cells. The conversion of NAD to reduced nicotinamide adenine dinucleotide (NADH) is coupled with TCA cycle reactions. Therefore, calorie restriction can raise the mitochondrial NAD/NADH ratio, whereas a high-calorie diet can lower it. As a sirtuin cosubstrate, an increase in the NAD concentration is enough to increase sirtuin activity in cells, which can act as stress adaptors.[5]

The first sirtuin ever discovered was found in the yeast *Saccharomyces cerevisiae* and named Sir2.[6] Humans have seven sirtuin isoforms homologous to yeast Sir2. SIRT1 – 7 differ in target structures, enzymatic activity, and subcellular localization (Table 1). The diversity of target structures is possibly attributed to N- and C-terminal extensions with varying sequences and lengths, which contribute to specificity in the localization and regulation of different types of human sirtuins. Different cellular localizations of sirtuins have a predisposing effect on their function. SIRT1 and 2 can be localized in the cytoplasm or nucleus, depending on the current cell cycle phase. SIRT6 is localized in the nucleus and SIRT7 in the nucleolus. Nuclear sirtuins target and interact mainly with histones and transcription factors. SIRT3 – 5 is mitochondrial sirtuins, mainly affecting mitochondrial processes.[7] The primary

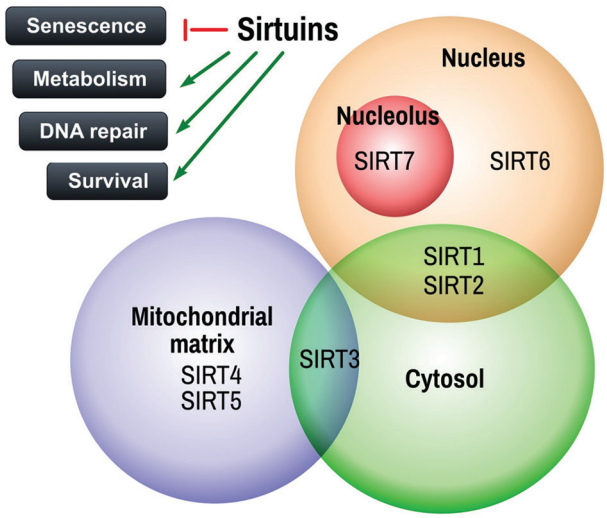

Figure 1. Subcellular localization of mammalian sirtuins. Adapted from Haigis and Sinclair.[3]
Abbreviation: SIRT: Silent information regulator.

protein structure of sirtuins consists of an evolutionarily conserved central catalytic core (containing ~275 amino acids), composed of two interconnected subdomains: a Rossmann-fold subdomain and a Zn^{2+}-binding variable module. The conserved central domain is the designated area for NAD binding and is responsible for the catalytic activity of sirtuins. The binding cleft for the nicotinamide and ribose parts of NAD and the acetyllysine substrate is formed by connected loops of subdomains of the central domain.[8] Substrate binding and catalysis are mediated by invariant amino acids situated in the binding cleft. Variations in the binding cleft's hydrophobicity and charge distribution enable distinct human sirtuins to exhibit varying levels of substrate selectivity. Despite different substrate selectivity, the homologous catalytic core allows catalysis through the same deacylation mechanism in all human sirtuins.[2]

2. Characterization of sirtuins in normal cell physiology

2.1. SIRT1

As one of the epigenetic regulators, SIRT1 is involved in the DNA damage response, acting as a histone deacetylase at the site of damage and an activator of DNA repair proteins. Histone acetylation and deacetylation are two primary epigenetic regulatory mechanisms, and modifications in histones and chromatin availability as a response to environmental factors or DNA damage can affect gene expression and regulate DNA repair. Yeast Sir proteins can repress gene transcription by modifying chromatin into its functionally inactive form, heterochromatin, by polymerizing across nucleosomes. Alterations in acetylation and methylation leading to genomic instability are currently recognized as the key features of aberrant cell proliferation and carcinogenesis.[18] SIRT1 was the first mammalian sirtuin discovered and is thus the most extensively studied sirtuin. SIRT1 shares the highest homology with Sir2, and the gene encoding SIRT1 is located on chromosome band 10q21.3 and contains nine exons and eight introns.[9] SIRT1 can be localized either in the cytoplasm or nucleus, and it is characterized by deacetylation activity, regulating fatty acid oxidation, glucose metabolism, chromatin structure, the cell cycle, and insulin secretion. Considering the impact of SIRT1 on several biological processes (e.g., cell senescence, apoptosis, oxidative stress, and inflammation), even minor changes in its expression and function can significantly affect these events.[19] The expression of *SIRT1* and the deacetylase activity of SIRT1 protein are regulated by tumor protein p53, hypermethylated in cancer 1, testis-specific protein Y-encoded-like 2, checkpoint kinase 2, and cell cycle and apoptosis regulator 2.[9]

Table 1. Characteristic activity and histone and non-histone targets of mammalian SIRT1 – SIRT7. Adapted from Carafa *et al.*[8]

Sirtuin	Intracellular localization	Histone targets	Non-histone targets	Activity	References
SIRT1	Nucleus cytosol	H1K26, H3K9, H3K14, H3K18, H3K56, H4K6, H4K12, H4K16	P53, Foxo1/3/4, HSF1, HIF-1α, NF-κB, P300, KAT5, Ku70, E2F1, PTEN, Smad3, Smad7	Deacetylase	9,10
SIRT2	Nucleuscytosol (cell cycle dependent)	H3K56ac, H4K16ac	α-tubulin, Foxo3a, EIF5A, P53, G6PD, MYC, HoxA10, Slug	Deacetylasedemyristoylase	11,12
SIRT3	Mitochondria	H3K56ac, H4K14ac	OTC, AceCS2, IDH2, HMG-CoAS2, LCAD, GDH, SOD2, SDH	Deacetylase	13
SIRT4	Mitochondria	Unknown	GDH, MCD, MTPα, PDH, MCCC, ANT2, IDE	DeacetylaseADP-ribosylase	14
SIRT5	Mitochondria	Unknown	CPS1	Deacetylasedemalonylase, desuccinylase, and deglutarylase	15
SIRT6	Nucleus	Unknown	CtIP, PARP1, NF-κB, HIF-1α, PPARγ, DNA-PK	DeacetylaseADP-ribosylase	16
SIRT7	Nucleolus	H3K18ac	HIF-1α, HIF-2α, RNA polymerase I	Deacetylase	17

Abbreviations: ADP: Adenosine diphosphate; CPS1: Carbamoyl phosphate synthetase 1; HIF-1: Hypoxia-inducible factor 1; IDH2: Isocitrate dehydrogenase 2; NF-κB: Nuclear factor kappa B; PARP1: Poly(ADP-ribose) polymerase 1; SDH: Succinate dehydrogenase; SIRT: Silent information regulator; EIF5A: Eukaryotic Translation Initiation Factor 5A; Foxo 1/3/4: Forkhead Box; G6PD: Glucose-6-phosphate dehydrogenase; HoxA10: Homeobox A10; HSF1: Heat shock transcription factor 1; KAT5: Lysine acetyltransferase 5; OTC: Ornithine transcarbamylase; PTEN: Phosphatase and tensin homolog; SOD2: Superoxide dismutase 2.

2.2. SIRT2

SIRT2 exerts various effects on different tissue types, and its main function includes the regulation of neural cell myelination in the central nervous system (brain and spinal cord) and peripheral nervous system, microtubule acetylation, and gluconeogenesis. SIRT2 has been also associated with liver diseases, such as liver fibrosis, alcoholic liver disease, or non-alcoholic fatty liver disease.[20] The gene encoding SIRT2 is located on chromosome band 19q13.2 and contains 17 exons. Alternative splicing leads to the formation of multiple isoforms of SIRT2, of which isoforms 1 and 2 are physiologically functional.[21]

SIRT2 is primarily localized in the cytoplasm and, similar to SIRT1 and 3, is characterized by deacetylation activity, which is responsible for cell cycle control, oligodendroglia proliferation, oxidative stress, and the regulation of microtubule acetylation. SIRT2 localization depends on the cell cycle phase, and it can be located in the nucleus (G2/M transition) or cytoplasm (interphase). During transition between interphase and the mitotic phase, SIRT2 is translocated into the nucleus, where its role is to regulate chromosome condensation.[22] SIRT2 is expressed in several tissues and organs, with metabolically relevant tissues (e.g., nervous system tissue, muscle, liver, pancreas, kidneys, and testes) showing the highest expression levels.[23] Due to its involvement in the regulation of neural cell myelination, SIRT2 is highly expressed in the brain and spinal cord tissue, particularly in the hippocampus, striatum, cortex, and spinal cord.[24] During glucose deprivation, SIRT2 activates phosphoenolpyruvate carboxykinase, the enzyme catalyzing gluconeogenesis.[25]

2.3. SIRT3

SIRT3 is localized exclusively in the mitochondria and, through its deacetylation activity, influences acetate metabolism, beta-oxidation, insulin secretion, oxidative stress, elimination of reactive oxygen species (ROS), inhibition of apoptosis, and prevention of tumor cell formation.[26] The gene encoding SIRT3 is located on chromosome band 11p15.5 and contains 10 exons, and the final protein has a mitochondrial-processing peptide incorporated at the N-terminal end. SIRT3 regulates several enzymes involved in key cellular metabolic pathways, such as fatty acid oxidation or the citric acid cycle. By regulating these enzymes, SIRT3 enhances mitochondrial efficiency and energy production. SIRT3 is abundantly expressed in tissues with high metabolic activity and a large number of mitochondria, including the heart, brain, kidneys, and liver. In addition, it regulates the activity of proteins essential for protection against oxidative stress, the enzymes involved in mitochondrial function, adenosine triphosphate (ATP) synthesis, and antioxidant enzymes (i.e., superoxide dismutase 2 [SOD2], catalase), thereby maintaining mitochondrial stability and decreasing the amount of ROS.[27] As a stress-responsive protein, SIRT3 regulates ROS production to prevent damage to cellular components. Due to its critical role in maintaining mitochondrial function and integrity, SIRT3 has been termed the "guardian of mitochondria."[28]

Through activation of glutamate dehydrogenase (GLUD), SIRT3 promotes glucose formation from amino acids and suppresses glucose oxidation and glycolysis by indirectly destabilizing the transcription factor hypoxia-inducible factor 1 alpha (HIF-1α).[25]

2.4. SIRT4

SIRT4 is the only mitochondrial sirtuin with ADP-ribosyltransferase activity, and its overall catalytic efficiency is up to 11-fold lower than the reported activity of other sirtuins. It inhibits mitochondrial GLUD1 activity and subsequently reduces insulin secretion. SIRT4 also possesses low deacetylase, deacylase, and lipoamidase activities, through which it affects several metabolic pathways, including ATP homeostasis, lipid oxidation, leucine catabolism, and insulin secretion. Like SIRT3, SIRT4 is also highly expressed in mitochondria-rich tissues such as the heart, liver, spleen, kidneys, testes, ovaries, and prostate. The gene encoding SIRT4 is located on chromosome bands 12q24.23 – q24.31 and contains five exons.[14]

2.5. SIRT5

In hepatic cells, SIRT5 regulates carbamoyl phosphate synthetase 1, the enzyme catalyzing the ATP-dependent reaction of carbamoyl phosphate synthesis from bicarbonate, ammonia, or glutamine, which is the first step of the urea cycle in the mitochondria of liver cells.[29] The gene encoding SIRT5 is located on chromosome band 6p23 and produces four protein isoforms: SIRT5iso1, SIRT5iso2, and SIRT5iso3 (found in the mitochondria) and SIRT5iso4 (found in the cytoplasm).[30] SIRT5 is expressed in all human tissues and organs, with the highest levels in the heart, brain, liver, kidneys, testes, and muscle tissue. Although SIRT5 is mainly localized in the mitochondrial matrix, it is also present in lower amounts in the mitochondrial intermembrane space, peroxisomes, nucleoplasm, and cytoplasm. SIRT5 has weak deacetylase activity but exhibits strong demalonylase, desuccinylase, and deglutarylase activities. In addition, SIRT5 is one of the regulators of several mitochondrial metabolism pathways, including fatty acid oxidation, amino acid degradation, glycolysis, and, most importantly, ROS and cellular respiration regulation.[31] SIRT5 also desuccinylates and activates GLUD1 and succinate dehydrogenase (SDH), key enzymes in the TCA cycle and the electron transport chain. Their activation supports the production of intermediates necessary for energy production and biosynthesis, potentially affecting the metabolic flexibility of cancer cells. Enhanced SDH activity can lead to more efficient mitochondrial respiration and ATP production, impacting the energy metabolism of tumor cells.[32]

2.6. SIRT6

Through its deacetylase and ADP-ribosyltransferase activity, SIRT6 controls longevity and several essential aging processes, including telomeric maintenance, gene expression, and DNA repair. In mammalian cells, SIRT6 is important for physiologically correct base excision DNA repair (BER) and DNA double-strand break repair (DSBR) in the case of DNA damage. SIRT6 supports DNA repair through non-homologous end joining (NHEJ) and homologous recombination.[33] It plays a crucial role in maintaining cellular homeostasis, ensuring genome stability, and regulating the inflammatory response. The gene encoding SIRT6 is located on chromosome band 19p13.3. Unlike other sirtuins, SIRT6 and SIRT7 have unique structures, as they lack a helix bundle at the NAD-binding segment of the Rossmann fold, which connects the catalytic domain to the zinc-binding domain. This distinct structure of SIRT6, even in the absence of substrates, underlies its strong affinity for binding to NAD.[34]

2.7. SIRT7

The main function of SIRT7 is to control ribosomal RNA (rRNA) transcription. It also contributes to maintaining genomic stability and DNA repair, aids in the defense against oxidative stress, and promotes cell division in certain types of cells.[35] The gene encoding SIRT7 is located on chromosome band 17q25.3. SIRT7 is localized in the nucleolus, and it mainly interacts with RNA polymerase (Pol) I and upstream binding factor. SIRT7 positively regulates rRNA gene transcription and ribosome formation. Increased SIRT7 expression results in an increased rate of RNA Pol I-mediated transcription, whereas decreased SIRT7 transcription has the opposite effect. The complete absence of SIRT7 leads to the restriction of cell proliferation and the induction of apoptosis. Reduced SIRT7 levels also lead to inefficient repair of DNA double-strand breaks through the NHEJ mechanism.[36]

SIRT7 controls rRNA gene transcription through interactions with RNA Pol I. By promoting the expression of rRNA genes, SIRT7 enhances ribosome biogenesis and protein synthesis, which can support the rapid proliferation of cancer cells.[37] SIRT7 may influence the expression and activity of HIF-1α, a transcription factor involved in cellular responses to hypoxia. HIF-1α regulates genes associated with glycolysis, angiogenesis, and cell survival, and dysregulated HIF-1α signaling is implicated in cancer progression.[38]

3. Role of sirtuins in cancer

Sirtuin dysregulation contributes to tumorigenesis by altering key cellular processes, such as energy metabolism,[39]

genome stability,[40] cell cycle regulation,[41] apoptosis,[42] and inflammation.[43] The specific effects depend on the type of sirtuin involved and the cellular context in which the dysregulation occurs. Recent research has shown that sirtuins play a dual role in cancer, exhibiting either oncogenic or tumor-suppressive characteristics depending on the tumor type, genetic makeup, and microenvironment.[44-46]

3.1. SIRT1

SIRT1 plays conflicting roles in tumorigenesis, depending on its localization and cell type. It has an oncogenic effect as an inhibitor of p53 and other tumor suppressors and can act as a tumor suppressor, negatively regulating β-catenin and survivin.[18] SIRT1 dysregulation has been proven in various cancer cell lines, such as prostate cancer[47] and melanoma; in tumor tissue samples from patients with breast cancer,[48] colorectal cancer,[49] or hepatocellular cancer;[50] and in the peripheral blood of patients with acute myeloid leukemia.[51]

p53 functions as a tumor suppressor and is linked to oxidative stress and DNA damage. Its activation induces cell cycle arrest and, if the damage is irreparable, triggers apoptosis. SIRT1 overexpression notably reduces p53-mediated apoptosis caused by DNA damage and oxidative stress by directly deacetylating lysine 382 of p53.[52] In addition, through β-catenin deacetylation, SIRT1 suppresses tumorigenesis and significantly hinders the formation and proliferation of colorectal cancer cells.[53] In breast cancer gene 1 (BRCA1) mutation–associated breast cancer cells, SIRT1 inhibits survivin, an apoptosis-suppressing protein that promotes proliferation and is often overexpressed in various cancers. Breast cancer cells with *BRCA1* mutations exhibit low *SIRT1* expression and high levels of survivin. BRCA1 binds to the SIRT1 promoter, elevating SIRT1 expression and consequently inhibiting survivin by modifying histone H3's epigenetic state. The absence of SIRT1 impedes survivin regulation by BRCA1.[54]

Studies showing SIRT1's involvement in cancer have been published for the past two decades. Early experiments on mice with overall overexpression of SIRT1 have demonstrated the dual character of SIRT1 in cancer, exhibiting both protective and promoting effects. Transgenic mice with overall SIRT1 overexpression showed lower susceptibility to aging-associated[55] and metabolic syndrome-associated cancers.[56] However, in studies with human cancer cell lines and patient tissues, SIRT1 overexpression promoted metastatic potential.[57,58]

3.2. SIRT2

SIRT2 is dysregulated in multiple tumor types,[12] gastric cancer,[59] ovarian cancer,[60] melanoma,[61] and acute myeloid leukemia.[62] SIRT2 dysregulation has been proven in both patient tissues and peripheral blood and cancer cell lines. Experiments on transgenic mice with *SIRT2* deletion have shown the development of smaller, less proliferative, and more differentiated hepatocellular tumors, suggesting the tumor-promoting characteristic of SIRT2.[63] SIRT2 can act as an oncogene and a tumor suppressor. SIRT2 promotes cell proliferation and tumor growth by further enhancing the expression of certain oncogenes (e.g., Slug – snail family transcriptional repressor 2, avian myelocytomatosis viral-related oncogene, and aldehyde dehydrogenase 1 family member A1) and inhibiting the expression of tumor suppressors (e.g., arrestin domain containing 3). It promotes the proliferation, migration, and invasiveness of tumor cells through the protein kinase B/glycogen synthase kinase 3/β-catenin signaling pathway and the inhibition of p21 through nuclear factor-kappa B (NF-κB)/Snail. However, SIRT2 may also inhibit tumor growth by deacetylating and inactivating the transcription factor NF-κB, which is involved in the inflammatory response and cancer progression. SIRT2 can prevent further tumor growth by suppressing certain oncogenes (e.g., Jumonji C domain 2A and ATP citrate lyase). SIRT2 overexpression promotes Skp2 deacetylation and degradation, resulting in increased p27 and suppression of tumor cell growth. SIRT2 also preserves genome stability by interacting with ATR Interacting Protein and the anaphase promoting complex/cyclosome, reduces the antioxidant function of Prdx-1, and prevents vascularization by inhibiting HIF-1α.[64] SIRT2 can affect tumor growth through its interaction with the surrounding tumor microenvironment and either promotes (changing the microenvironment pH, improving cell energy metabolism, and promoting immune avoidance) or inhibits (inhibiting tumor angiogenesis and fibroblast activity) cancer cell growth.[65]

3.3. SIRT3

Elevated SIRT3 expression in tumor tissue is linked to poor clinical prognosis in patients with cancer. SIRT3 dysregulation plays a role in the development and progression of various cancer cell lines, including gastric cancer,[66] colorectal cancer,[67] breast cancer,[68] and melanoma,[69] and in patient tumor tissue, including esophageal[70] and renal cancers.[71] Physiologically, SIRT3 acts as a mitochondrial tumor-suppressive protein, and impaired and aberrant mitochondrial function can lead to cancer development. Disruption in SIRT3 expression and function can result in oxidative damage, ROS accumulation, and abnormal ROS-driven signaling, leading to metabolic changes in the mitochondria.[72] SIRT3 suppresses tumor growth driven by glycolysis. In low-oxygen environments, increased SIRT3 levels reduce ROS production, inhibit glycolysis, limit cell

proliferation, and prevent HIF-1α stabilization and activity, ultimately decreasing tumor formation.[73]

SIRT3 may affect tumor growth in several ways. PDHA1 deacetylation promotes the transformation of pyruvate to acetyl coenzyme A, thereby favoring oxidative phosphorylation over glycolysis. This can inhibit the rapid proliferation of cancer cells that rely on glycolysis.[74] Deacetylation and activation of isocitrate dehydrogenase 2 and SOD2 may reduce ROS levels and generally reduce oxidative stress and DNA damage, thereby preventing genomic instability that can lead to cancer progression.[75,76]

SIRT3 deacetylates and stabilizes p53, which can suppress tumor cell growth through cell cycle arrest and apoptosis.[77] SIRT3 also deacetylates Ku70, a constituent of the NHEJ pathway involved in DNA repair. By promoting accurate DNA repair, SIRT3 helps maintain genomic integrity and prevent mutations that could lead to cancer. SIRT3 can promote apoptosis through the activity of BAX, a proapoptotic protein. By promoting apoptosis, SIRT3 helps eliminate damaged or cancerous cells.[78]

3.4. SIRT4

Low SIRT4 expression has been reported in patient tumor tissues and cell lines of thyroid,[79] lung,[80] bladder,[81] and ovarian cancers.[82] SIRT4 downregulation is associated with poor patient prognosis, as it is frequently observed in advanced-stage and metastatic tumors,[83] and SIRT4 overexpression in tumor tissue may have tumor-suppressive effects.[80] SIRT4 exerts an antiproliferative effect on damaged and cancer cells through its inhibitory effect on glutamine metabolism. Because SIRT4 exerts inhibitory effects on the proliferation of cells with damaged DNA, its expression physiologically increases during DNA damage. In many tumors, the protective effect of SIRT4 decreases due to downregulation of its expression, which can result in a tumorigenic phenotype by enhancing the proliferation of glutamine-dependent cells.[84] SIRT4 inhibits glutaminase, the enzyme responsible for converting glutamine into glutamate. Glutamine, the most abundant, free non-essential alpha-amino acid in the cell cytosol and human blood, is essential for protein synthesis. Many tumor cells rely on glutamine for rapid growth, and certain types of cancer cells cannot survive without an external glutamine supply. SIRT4 suppresses glutamine metabolism in the mitochondria of tumor cells through ADP-ribosylating GLUD, which decreases energy and glutamine availability in proliferating tumor cells. This inhibition allows time for damaged DNA to be repaired and helps maintain genome stability.[85] SIRT4 can also affect cell metabolism by inhibiting carnitine palmitoyltransferase 1A (CPT1A), which is an essential enzyme for fatty acid oxidation. CPT1A inhibition reduces the breakdown of fatty acids used for energy production, impacting cancer cells that depend on fatty acid oxidation to meet their energy demands, especially under nutrient-deprived conditions.[86] As a mitochondrial sirtuin, SIRT4 affects ROS levels and the DNA damage response. SIRT4 influences the expression and activity of SOD2 or genes involved in DNA repair mechanisms, such as BRCA1 and radiation sensitive 51 recombinase, helping to maintain low levels of ROS and thereby reducing oxidative DNA damage and genomic instability, which contribute to cancer progression.[87]

3.5. SIRT5

SIRT5 can act as an oncogene or as a tumor suppressor. It promotes cancer cell survival, proliferation, metastasis, and chemotherapy resistance. The oncogenic activity of SIRT5 has been observed in mice with SIRT5 deletion that develop colorectal[88] and breast cancer tumors.[89] SIRT5 dysregulation related to tumor proliferation has been also reported in cancer cell lines and tumor tissue samples from patients with breast cancer[89] and ovarian cancer[90] and in mononuclear and CD34+ cells of patients with acute myeloid leukemia.[91]

As a tumor suppressor, SIRT5 interacts with various proteins and post-translationally modifies them to hinder cell proliferation, disrupt the immune response, and inhibit angiogenesis and metastasis.[92] Studies have reported the association of low SIRT5 expression with poor prognosis in tissues of patients with glioblastoma[93] and thyroid cancer.[94]

3.6. SIRT6

Due to its role in maintaining genome stability and telomere integrity, SIRT6 dysregulation appears to be an important step in molecular carcinogenesis. It interacts with and deacetylates telomeric repeat–binding factor 2 (TRF2), a protein involved in the protection and maintenance of telomeres, which are sequences at the ends of chromosomes characterized by repetitive DNA. By regulating TRF2 activity, SIRT6 influences telomere integrity and stability.[95] SIRT6 also interacts with and deacetylates poly(ADP-ribose) polymerase 1 (PARP1), an enzyme involved in BER and DNA single-strand break repair,[96] and Ku70 and Ku80, which are involved in DNA DSBR.[97,98] By regulating PARP1 activity and efficient DSBR, SIRT6 promotes DNA repair and genomic stability and helps prevent chromosomal aberrations and genomic instability associated with cancer.

Depending on the biological context, SIRT6 acts as either a promoter or a tumor suppressor in tumorigenesis.[99] The tumor-suppressive function of SIRT6 has been proven

in animal experiments on mouse embryonic fibroblasts in which *SIRT6*-knockdown cells showed increased proliferation and tumorigenic characteristic.[100] *SIRT6* knockdown in human hepatocellular cancer and non-small-cell lung cancer cell lines promoted cell growth, whereas SIRT6 overexpression inhibited cell proliferation.[101,102]

In contrast, the oncogenic activity of SIRT6 has been observed in various human cancer cell lines, including ovarian cancer,[103] prostate cancer,[104] breast cancer,[105] melanoma,[106] and acute myeloid leukemia.[107]

3.7. SIRT7

Elevated SIRT7 expression has been observed in metabolically active tissues (e.g., spleen and liver), whereas low SIRT7 expression has been observed in non-proliferative tissues (e.g., brain and heart). Changes in SIRT7 expression are seen across various tumor types, including hepatocellular cancer[108] and bladder cancer,[109] indicating its significant role in cellular processes that could influence oncogenic transformation and tumor development.[110] A conflicting effect of SIRT7 on cell proliferation has also been reported. While SIRT7 downregulation in breast cancer cell lines and patient tumor tissues promotes metastatic character;,[111] in ovarian cancer cell lines, it leads to a significant reduction in cell growth and metastatic colony formation and increases apoptosis.[112] In colorectal cancer, SIRT7 has a dual character. Experiments on SIRT7-knockout mice have shown increased susceptibility of colorectal cancer cells.[113] SIRT7 knockdown in tissue samples and cell lines from patients with colorectal cancer leads to significant inhibition of cell proliferation, cell motility, and metastatic colony formation. In contrast, ectopic SIRT7 expression promotes colony formation and cell growth *in vivo* and *in vitro*.[114] Tang *et al.* revealed a possible association between SIRT7 downregulation and increased radiosensitivity triggering cell death in colorectal cell lines.[115]

4. Future prospects

Ongoing clinical trials and research will be crucial in elucidating the precise role of sirtuins in different types of cancers and in developing safe, targeted therapies that leverage the dual role of sirtuins in cellular regulation. The expression levels and activity patterns of SIRT1 – 7 may provide valuable insights into cancer diagnosis and prognosis, as previous research has shown certain dysregulation in different types of human cancers.[116,117] As shown in Figure 2, sirtuins may exert various plausible actions that interfere with multiple aspects of tumor biology. Future cancer therapies may aim to modulate sirtuin activity to restore normal cellular function, with a few modulators already in clinical trials.[118] Deus *et al.* reported

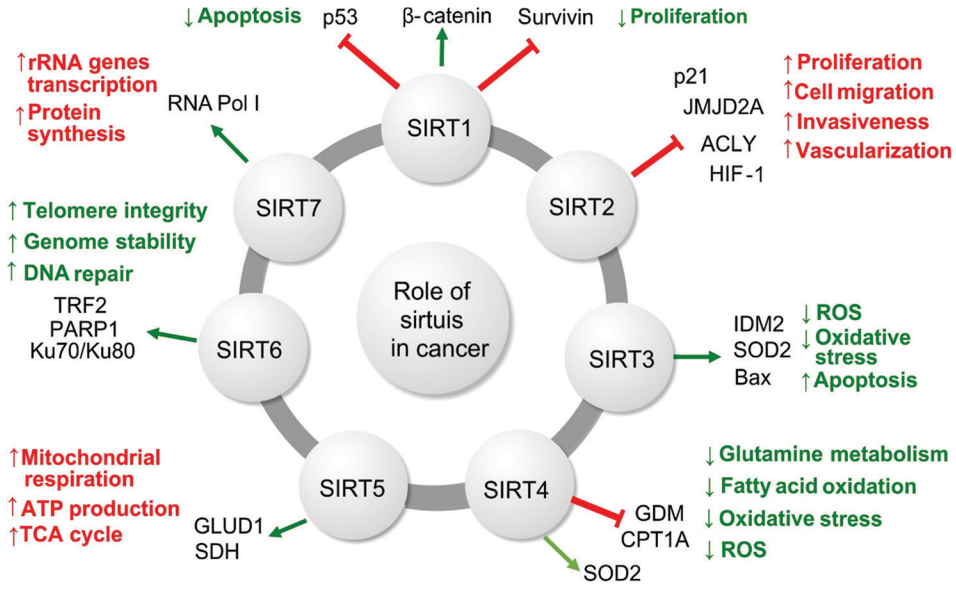

Figure 2. Role of various sirtuins as modifiers of transcriptome, proteome, and metablome in cancer.
Notes: Red: Cancerogenic effects; Green: Anticancer effects
Abbreviations: ACLY: ATP citrate lyase; ATP: Adenosine triphosphate; Bax: Bcl-2 family-associated X (core regulator of the intrinsic pathway of apoptosis); CPT1A: Carnitine palmitoyltransferase 1A; GLUD1: Glutamate dehydrogenase 1; GDM: Glutamate dehydrogenase 1 (GDH) - mitochondrial; HIF-1: Hypoxia-inducible factor 1; IDM2: Increased DNA methylation 2; JMJD2A: Jumonji C domain 2A; Ku70/Ku80: 70 kDa/80 kDa basket-shaped DNA-binding proteins; PARP1: poly(ADP-ribose) polymerase 1; RNA Pol I: RNA polymerase 1; ROS: Reactive oxygen species; rRNA: Ribosomal RNA; SDH: Succinate dehydrogenase; SOD2: Superoxide dismutase 2; TCA: Tricarboxylic acid cycle; TRF2: Telomeric repeat–binding factor 2.

that resveratrol, a sirtuin activator, has a cytotoxic effect and causes cell cycle arrest and inhibition of mitochondrial respiration in breast cancer cell lines mediated by SIRT1 and 3.[119] Synthetic SIRT1 activators SRT1720 and SRT2104 exert antiproliferative effects on cancer cells[120,121] and assist with the prevention of chemotherapy resistance.[122,123] Sirtuin inhibitors, such as cambinol and tenovins, are also being studied as potential therapeutic agents that induce apoptosis of cancer cells with defective p53 pathways and restore sensitization to chemotherapy.[124,125] The integration of sirtuin modulators in cancer treatment regimens could complement existing therapies, offering a more tailored and effective approach.[126]

5. Conclusion

Sirtuins play a pivotal role in maintaining cellular homeostasis and normal physiological functions. Altered metabolism and genomic instability are hallmark features of different types of cancer. Dysregulated expression patterns of different classes of mammalian sirtuins have been observed in tumor cells. Dysregulated sirtuins play a dual role in cancer, exhibiting both tumor-suppressive and oncogenic activities, often maintaining a delicate balance between the two. Understanding the fundamental mechanisms and conditions that dictate their divergent roles in cancer holds significant promise for sirtuins as therapeutic targets and potential biomarkers for cancer diagnosis and prognosis. Future research could delve deeper into elucidating the intricate molecular pathways underlying the dual nature of sirtuins in cancer, exploring novel therapeutic interventions that target specific sirtuin isoforms, and investigating their utility as predictive and prognostic markers in cancer management.

Acknowledgments

None.

Funding

This work was supported by VEGA grant no. 1/0622/20 of the Scientific Grant Agency of the Ministry of Education, Research and Sport of the Slovak Republic, and VVGS grant no. VVGS – 2022-2199.

Conflict of interest

The authors declare that they have no competing interests.

Author contributions

Conceptualization: Daniela Szabóová, Roman Beňačka
Writing–original draft: All authors
Writing–review & editing: Zuzana Guľašová, Zdenka Hertelyová

Ethics approval and consent to participate

Not applicable.

Consent for publication

Not applicable.

Availability of data

Not applicable.

References

1. Yamamoto H, Schoonjans K, Auwerx J. Sirtuin functions in health and disease. *Mol Endocrinol.* 2007;21:1745-1755.

   doi: 10.1210/me.2007-0079

2. Feldman JL, Dittenhafer-Reed KE, Denu JM. Sirtuin catalysis and regulation. *J Biol Chem.* 2012;287:42419-42427.

   doi: 10.1074/jbc.R112.378877

3. Haigis MC, Sinclair DA. Mammalian sirtuins: Biological insights and disease relevance. *Annu Rev Pathol.* 2010;5:253-295.

   doi: 10.1146/annurev.pathol.4.110807.092250

4. Bonkowski MS, Sinclair DA. Slowing ageing by design: The rise of NAD and sirtuin-activating compounds. *Nat Rev Mol Cell Biol.* 2016;17:679-690.

   doi: 10.1038/nrm.2016.93

5. Watroba M, Szukiewicz D. Sirtuins at the service of healthy longevity. *Front Physiol*. 2021;12:724506.

   doi: 10.3389/fphys.2021.724506

6. Blander G, Guarente L. The Sir2 family of protein deacetylases. *Annu Rev Biochem*. 2004;73:417-435.

   doi: 10.1146/annurev.biochem.73.011303.073651

7. Michishita E, Park JY, Burneskis JM, Barrett JC, Horikawa I. Evolutionarily conserved and nonconserved cellular localizations and functions of human SIRT proteins. *Mol Biol Cell.* 2005;16;4623-4635.

   doi: 10.1091/mbc.e05-01-0033

8. Carafa V, Rotili D, Forgione M, *et al*. Sirtuin functions and modulation: From chemistry to the clinic. *Clin Epigenetics*. 2016;8:61.

   doi: 10.1186/s13148-016-0224-3

9. Yang Y, Liu Y, Wang Y, *et al*. Regulation of SIRT1 and its roles in inflammation. *Front Immunol*. 2022;13:831168.

   doi: 10.3389/fimmu.2022.831168

10. Lu C, Zhao H, Liu Y, *et al*. Novel role of the SIRT1 in endocrine and metabolic diseases. *Int J Biol Sci.* 2023;19(2):484-501.

    doi: 10.7150/ijbs.78654

11. Lu W, Ji H, Wu D. SIRT2 plays complex roles in neuroinflammation neuroimmunology-associated disorders.

Front Immunol. 2023;14:1174180.

doi: 10.3389/fimmu.2023.1174180

12. Chen G, Huang P, Hu C. The role of SIRT2 in cancer: A novel therapeutic target. *Int J Cancer*. 2020;147(12):3297-3304.

doi: 10.1002/ijc.33118

13. Mishra Y, Kaundal RK. Role of SIRT3 in mitochondrial biology and its therapeutic implications in neurodegenerative disorders. *Drug Discov Today*. 2023;28(6):103583.

doi: 10.1016/j.drudis.2023.103583

14. Li Y, Zhou Y, Wang F, *et al*. SIRT4 is the last puzzle of mitochondrial sirtuins. *Bioorg Med Chem*. 2018;26(14):3861-3865.

doi: 10.1016/j.bmc.2018.07.031

15. Wang Y, Chen H, Zha X. Overview of SIRT5 as a potential therapeutic target: Structure, function and inhibitors. *Eur J Med Chem*. 2022;236:114363.

doi: 10.1016/j.ejmech.2022.114363

16. Yang Y, Zhu M, Liang J, *et al*. SIRT6 mediates multidimensional modulation to maintain organism homeostasis. *J Cell Physiol*. 2022;237(8):3205-3221.

doi: 10.1002/jcp.30791

17. Raza U, Tang X, Liu Z, Liu B. SIRT7: The seventh key to unlocking the mystery of aging. *Physiol Rev*. 2024;104(1):253-280.

doi: 10.1152/physrev.00044.2022

18. Alves-Fernandes DK, Jasiulionis MG. The role of SIRT1 on DNA damage response and epigenetic alterations in cancer. *Int J Mol Sci*. 2019;20(13):3153.

doi: 10.3390/ijms20133153

19. Singh V, Ubaid S. Role of silent information regulator 1 (SIRT1) in regulating oxidative stress and inflammation. *Inflammation*. 2020;43:1589-1598.

doi: 10.1007/s10753-020-01242-9

20. Lin L, Guo Z, He E, *et al*. SIRT2 regulates extracellular vesicle-mediated liver-bone communication. *Nat Metab*. 2023;5:821-841.

doi: 10.1038/s42255-023-00803-0

21. Rack JGM, VanLinden MR, Lutter T, Aasland R, Ziegler M. Constitutive nuclear localization of an alternatively spliced sirtuin-2 isoform. *J Mol Biol*. 2014;426:1677-1691.

doi: 10.1016/j.jmb.2013.10.027

22. Inoue T, Hiratsuka M, Osaki M, Oshimura M. The molecular biology of mammalian SIRT proteins: SIRT2 in cell cycle regulation. *Cell Cycle*. 2007;6:1011-1018.

doi: 10.4161/cc.6.9.4219

23. Wang Y, Yang J, Hong T, Chen X, Cui L. SIRT2: Controversy and multiple roles in disease and physiology. *Ageing Res Rev*. 2019;55:100961.

doi: 10.1016/j.arr.2019.100961

24. Maxwell MM, Tomkinson EM, Nobles J, *et al*. The Sirtuin 2 microtubule deacetylase is an abundant neuronal protein that accumulates in the aging CNS. *Hum Mol Genet*. 2011;20:3986-3996.

doi: 10.1093/hmg/ddr326

25. Mei Z, Zhang X, Yi J, Huang J, He J, Tao Y. Sirtuins in metabolism, DNA repair and cancer. *J Exp Clin Cancer Res*. 2016;35:182.

doi: 10.1186/s13046-016-0461-5

26. Diao Z, Ji Q, Wu Z, *et al*. SIRT3 consolidates heterochromatin and counteracts senescence. *Nucleic Acids Res*. 2021;49:4203-4219.

doi: 10.1093/nar/gkab161

27. Wang Q, Li L, Li CY, Pei Z, Zhou M, Li N. SIRT3 protects cells from hypoxia via PGC-1α- and MnSOD-dependent pathways. *Neuroscience*. 2015;286:109-121.

doi: 10.1016/j.neuroscience.2014.11.045

28. Zhang J, Xiang H, Liu J, Chen Y, He RR, Liu B. Mitochondrial sirtuin 3: New emerging biological function and therapeutic target. *Theranostics*. 2020;10:8315-8342.

doi: 10.7150/thno.45922

29. Nakagawa T, Lomb DJ, Haigis MC, Guarente L. SIRT5 Deacetylates carbamoyl phosphate synthetase 1 and regulates the urea cycle. *Cell*. 2009;137:560-570.

doi: 10.1016/j.cell.2009.02.026

30. Matsushita N, Yonashiro R, Ogata Y, *et al*. Distinct regulation of mitochondrial localization and stability of two human Sirt5 isoforms. *Genes Cells*. 2011;16:190-202.

doi: 10.1111/j.1365-2443.2010.01475.x

31. Kumar S, Lombard DB. Functions of the sirtuin deacylase SIRT5 in normal physiology and pathobiology. *Crit Rev Biochem Mol Biol*. 2018;53:311-334.

doi: 10.1080/10409238.2018.1458071

32. Wang YQ, Wang HL, Xu J, *et al*. Sirtuin5 contributes to colorectal carcinogenesis by enhancing glutaminolysis in a deglutarylation-dependent manner. *Nat Commun*. 2018;9:545.

doi: 10.1038/s41467-018-02951-4

33. Chang AR, Ferrer CM, Mostoslavsky R. SIRT6, a mammalian deacylase with multitasking abilities. *Physiol Rev*. 2020;100:145-169.

doi: 10.1152/physrev.00030.2018

34. Liu G, Chen H, Liu H, Zhang W, Zhou J. Emerging roles of SIRT6 in human diseases and its modulators. *Med Res Rev*. 2021;41:1089-1137.

doi: 10.1002/med.21753

35. Lagunas-Rangel FA. SIRT7 in the aging process. *Cell Mol*

Life Sci. 2022;79:297.

doi: 10.1007/s00018-022-04342-x

36. Tang M, Tang H, Tu B, Zhu WG. SIRT7: A sentinel of genome stability. *Open Biol*. 2021;11:210047.

doi: 10.1098/rsob.210047

37. Ford E, Voit R, Liszt G, Magin C, Grummt I, Guarente L. Mammalian Sir2 homolog SIRT7 is an activator of RNA polymerase I transcription. *Genes Dev*. 2006;20:1075-1080.

doi: 10.1101/gad.1399706

38. Hubbi ME, Hu H, Kshitiz, Gilkes DM, Semenza GL. Sirtuin-7 inhibits the activity of hypoxia-inducible factors. *J Biol Chem*. 2013;288:20768-20775.

doi: 10.1074/jbc.M113.476903

39. Varghese B, Chianese U, Capasso L, *et al*. SIRT1 activation promotes energy homeostasis and reprograms liver cancer metabolism. *J Transl Med*. 2023;21(1):627.

doi: 10.1186/s12967-023-04440-9

40. Bosch-Presegué L, Vaquero A. Sirtuin-dependent epigenetic regulation in the maintenance of genome integrity. *FEBS J*. 2015;282(9):1745-1767.

doi: 10.1111/febs.13053

41. Betsinger CN, Justice JL, Tyl MD, *et al*. Sirtuin 2 promotes human cytomegalovirus replication by regulating cell cycle progression. *mSystems*. 2023;8(6):e0051023.

doi: 10.1128/msystems.00510-23

42. Polletta L, Vernucci E, Carnevale I, *et al*. SIRT5 regulation of ammonia-induced autophagy and mitophagy. *Autophagy*. 2015;11(2):253-270.

doi: 10.1080/15548627.2015.1009778

43. Akter R, Afrose A, Rahman MR, *et al*. A comprehensive analysis into the therapeutic application of natural products as SIRT6 modulators in Alzheimer's disease, aging, cancer, inflammation, and diabetes. *Int J Mol Sci*. 2021;22(8):4180.

doi: 10.3390/ijms22084180

44. Jaiswal A, Xudong Z, Zhenyu J, Saretzki G. Mitochondrial sirtuins in stem cells and cancer. *FEBS J*. 2022;289(12):3393-3415.

doi: 10.1111/febs.15879

45. Lee H, Yoon H. Mitochondrial sirtuins: Energy dynamics and cancer metabolism. *Mol Cells*. 2024;47(2):100029.

doi: 10.1016/j.mocell.2024.100029

46. Shen H, Ma W, Hu Y, *et al*. Mitochondrial sirtuins in cancer: A revisited review from molecular mechanisms to therapeutic strategies. *Theranostics*. 2024;14(7):2993-3013.

doi: 10.7150/thno.97320

47. Wen Y, Huang H, Huang B, Liao X. HSA-miR-34a-5p regulates the SIRT1/TP53 axis in prostate cancer. *Am J Transl Res*. 2022;14(7):4493-4504.

48. Jin X, Wei Y, Xu F, *et al*. SIRT1 promotes formation of breast cancer through modulating Akt activity. *J Cancer*. 2018;9(11):2012-2023.

doi: 10.7150/jca.24275

49. Fang H, Huang Y, Luo Y, *et al*. SIRT1 induces the accumulation of TAMs at colorectal cancer tumor sites via the CXCR4/CXCL12 axis. *Cell Immunol*. 2022;371:104458.

doi: 10.1016/j.cellimm.2021.104458

50. Guo S, Li F, Liang Y, *et al*. AIFM2 promotes hepatocellular carcinoma metastasis by enhancing mitochondrial biogenesis through activation of SIRT1/PGC-1α signaling. *Oncogenesis*. 2023;12(1):46.

doi: 10.1038/s41389-023-00491-1

51. Tian WL, Guo R, Wang F, *et al*. The IRF9-SIRT1-P53 axis is involved in the growth of human acute myeloid leukemia. *Exp Cell Res*. 2018;365(2):185-193.

doi: 10.1016/j.yexcr.2018.02.036

52. Yi J, Luo J. SIRT1 and p53, effect on cancer, senescence and beyond. Biochim *Biophys Acta.* 2010;1804:1684-1689.

doi: 10.1016/j.bbapap.2010.05.002

53. Firestein R, Blander G, Michan S, *et al*. The SIRT1 deacetylase suppresses intestinal tumorigenesis and colon cancer growth. *PLoS One*. 2008;3:e2020.

doi: 10.1371/journal.pone.0002020

54. Wang RH, Zheng Y, Kim HS, *et al*. Interplay among BRCA1, SIRT1, and Survivin during BRCA1-associated tumorigenesis. *Mol Cell*. 2008;32:11-20.

doi: 10.1016/j.molcel.2008.09.011

55. Wang RH, Sengupta K, Li C, *et al*. Impaired DNA damage response, genome instability, and tumorigenesis in SIRT1 mutant mice. *Cancer Cell*. 2008;14(4):312-323.

doi: 10.1016/j.ccr.2008.09.001

56. Herranz D, Muñoz-Martin M, Cañamero M, *et al*. Sirt1 improves healthy ageing and protects from metabolic syndrome-associated cancer. *Nat Commun*. 2010;1:3.

doi: 10.1038/ncomms1001

57. Hao C, Zhu PX, Yang X, *et al*. Overexpression of SIRT1 promotes metastasis through epithelial-mesenchymal transition in hepatocellular carcinoma. *BMC Cancer.* 2014;14:978.

doi: 10.1186/1471-2407-14-978

58. Jiang K, Lyu L, Shen Z, *et al*. Overexpression of SIRT1 is a poor prognostic factor for advanced colorectal cancer. *Chin Med J* (*Engl*). 2014;127(11):2021-2024.

59. Wang J, Wu J, Wang L, Min X, Chen Z. The LINC00152/miR-138 axis facilitates gastric cancer progression by mediating SIRT2. *J Oncol*. 2021;2021:1173869.

doi: 10.1155/2021/1173869

60. Du Y, Wu J, Zhang H, Li S, Sun H. Reduced expression of SIRT2 in serous ovarian carcinoma promotes cell proliferation through disinhibition of CDK4 expression. *Mol Med Rep*. 2017;15(4);1638-1646.

doi: 10.3892/mmr.2017.6183

61. Wilking-Busch MJ, Ndiaye MA, Huang W, Ahmad N. Expression profile of SIRT2 in human melanoma and implications for sirtuin-based chemotherapy. *Cell Cycle*. 2017;16(6):574-577.

doi: 10.1080/15384101.2017.1288323

62. Deng A, Ning Q, Zhou L, Liang Y. SIRT2 is an unfavorable prognostic biomarker in patients with acute myeloid leukemia. *Sci Rep*. 2016;6:27694.

doi: 10.1038/srep27694

63. Schmidt AV, Monga SP, Prochownik EV, Goetzman ES. A novel transgenic mouse model implicates Sirt2 as a promoter of hepatocellular carcinoma. *Int J Mol Sci*. 2023;24(16):12618.

doi: 10.3390/ijms241612618

64. Zhang L, Kim S, Ren X. The clinical significance of SIRT2 in malignancies: A tumor suppressor or an oncogene? *Front Oncol*. 2020;10:1721.

doi: 10.3389/fonc.2020.01721

65. Chen J, Chan AW, To KF, *et al*. SIRT2 overexpression in hepatocellular carcinoma mediates epithelial to mesenchymal transition by protein kinase B/glycogen synthase kinase-3β/β-catenin signaling. *Hepatology*. 2013;57(6):2287-2298.

doi: 10.1002/hep.26278

66. Cui Y, Qin L, Wu J, *et al*. SIRT3 enhances glycolysis and proliferation in SIRT3-expressing gastric cancer cells. *PLoS One*. 2015;10(6):e0129834.

doi: 10.1371/journal.pone.0129834

67. Wang Y, Sun X, Ji K, *et al*. Sirt3-mediated mitochondrial fission regulates the colorectal cancer stress response by modulating the Akt/PTEN signalling pathway. *Biomed Pharmacother*. 2018;105:1172-1182.

doi: 10.1016/j.biopha.2018.06.071

68. Zu Y, Chen XF, Li Q, Zhang ST, Si LN. PGC-1α activates SIRT3 to modulate cell proliferation and glycolytic metabolism in breast cancer. *Neoplasma*. 2021;68(2):352-361.

doi: 10.4149/neo_2020_200530N584

69. George J, Nihal M, Singh CK, Zhong W, Liu X, Ahmad N. Pro-proliferative function of mitochondrial sirtuin deacetylase SIRT3 in human melanoma. *J Invest Dermatol*. 2016;136(4):809-818.

doi: 10.1016/j.jid.2015.12.026

70. Yan SM, Han X, Han PJ, Chen HM, Huang LY, Li Y. SIRT3 is a novel prognostic biomarker for esophageal squamous cell carcinoma. *Med Oncol*. 2014;31(8):103.

doi: 10.1007/s12032-014-0103-8

71. Elkady N, Aldesoky AI, Dawoud MM. Evaluation of ARK5 and SIRT3 expression in renal cell carcinoma and their clinical significance. *Diagn Pathol*. 2023;18(1):125.

doi: 10.1186/s13000-023-01409-6

72. Torrens-Mas M, Oliver J, Roca P, Sastre-Serra J. SIRT3: Oncogene and tumor suppressor in cancer. *Cancers* (*Basel*). 2017;9:90.

doi: 10.3390/cancers9070090

73. Chen Y, Fu LL, Wen X, *et al*. Sirtuin-3 (SIRT3), a therapeutic target with oncogenic and tumor-suppressive function in cancer. *Cell Death Dis*. 2014;5:e1047.

doi: 10.1038/cddis.2014.14

74. Xu L, Li Y, Zhou L, *et al*. SIRT3 elicited an anti-Warburg effect through HIF1α/PDK1/PDHA1 to inhibit cholangiocarcinoma tumorigenesis. *Cancer Med*. 2019;8:2380-2391.

doi: 10.1002/cam4.2089

75. Zou X, Zhu Y, Park SH, *et al*. SIRT3-mediated dimerization of IDH2 directs cancer cell metabolism and tumor growth. *Cancer Res*. 2017;77:3990-3999.

doi: 10.1158/0008-5472.CAN-16-2393

76. Paku M, Haraguchi N, Takeda M, *et al*. SIRT3-mediated SOD2 and PGC-1α contribute to chemoresistance in colorectal cancer cells. *Ann Surg Oncol*. 2021;28:4720-4732.

doi: 10.1245/s10434-020-09373-x

77. Chen J, Wang A, Chen Q. SirT3 and p53 deacetylation in aging and cancer. *J Cell Physiol*. 2017;232:2308-2311.

doi: 10.1002/jcp.25669

78. Luo K, Huang W, Tang S. Sirt3 enhances glioma cell viability by stabilizing Ku70-BAX interaction. *Onco Targets Ther*. 2018;11:7559-7567.

doi: 10.2147/OTT.S172672

79. Chen Z, Lin J, Feng S, *et al*. SIRT4 inhibits the proliferation, migration, and invasion abilities of thyroid cancer cells by inhibiting glutamine metabolism. *Onco Targets Ther*. 2019;12:2397-2408.

doi: 10.2147/OTT.S189536

80. Fu L, Dong Q, He J, *et al*. SIRT4 inhibits malignancy progression of NSCLCs, through mitochondrial dynamics mediated by the ERK-Drp1 pathway. *Oncogene*. 2017;36(19):2724-2736.

doi: 10.1038/onc.2016.425

81. Yin J, Cai G, Wang H, Chen W, Liu S, Huang G. SIRT4 is an independent prognostic factor in bladder cancer and

inhibits bladder cancer growth by suppressing autophagy. *Cell Div*. 2023;18(1):9.

doi: 10.1186/s13008-023-00091-w

82. Wang H, Li J, Huang R, Fang L, Yu S. SIRT4 and SIRT6 serve as novel prognostic biomarkers with competitive functions in serous ovarian cancer. *Front Genet*. 2021;12:666630.

doi: 10.3389/fgene.2021.666630

83. Wang C, Liu Y, Zhu Y, Kong C. Functions of mammalian SIRT4 in cellular metabolism and research progress in human cancer. *Oncol Lett.* 2020;20:11.

doi: 10.3892/ol.2020.11872

84. Min Z, Gao J, Yu Y. The roles of mitochondrial SIRT4 in cellular metabolism. *Front Endocrinol* (*Lausanne*). 2019;9:783.

doi: 10.3389/fendo.2018.00783

85. Cai G, Ge Z, Xu Y, Cai L, Sun P, Huang G. SIRT4 functions as a tumor suppressor during prostate cancer by inducing apoptosis and inhibiting glutamine metabolism. *Sci Rep.* 2022;12:12208.

doi: 10.1038/s41598-022-16610-8

86. Bai W, Cheng L, Xiong L, *et al*. Protein succinylation associated with the progress of hepatocellular carcinoma. *J Cell Mol Me*d. 2022;26:5702-5712.

doi: 10.1111/jcmm.17507

87. Dai Y, Liu S, Li J, *et al*. SIRT4 suppresses the inflammatory response and oxidative stress in osteoarthritis. *Am J Transl Res*. 2020;12:1965-1975.

88. Wang K, Hu Z, Zhang C, *et al*. SIRT5 contributes to colorectal cancer growth by regulating T cell activity. *J Immunol Res*. 2020;2020:3792409.

doi: 10.1155/2020/3792409

89. Abril YLN, Fernandez IR, Hong JY, *et al*. Pharmacological and genetic perturbation establish SIRT5 as a promising target in breast cancer. *Oncogene*. 2021;40(9):1644-1658.

doi: 10.1038/s41388-020-01637-w

90. Sun X, Wang S, Gai J, *et al*. SIRT5 promotes cisplatin resistance in ovarian cancer by suppressing DNA damage in a ROS-dependent manner via regulation of the Nrf2/HO-1 pathway. *Front Oncol*. 2019;9:754.

doi: 10.3389/fonc.2019.00754

91. Yan D, Franzini A, Pomicter AD, *et al*. SIRT5 is a druggable metabolic vulnerability in acute myeloid leukemia. *Blood Cancer Discov*. 2021;2(3):266-287.

doi: 10.1158/2643-3230.BCD-20-0168

92. Fabbrizi E, Fiorentino F, Carafa V, Altucci L, Mai A, Rotili D. Emerging roles of SIRT5 in metabolism, cancer, and SARS-CoV-2 infection. *Cells*. 2023;12:852.

doi: 10.3390/cells12060852

93. Chen X, Xu Z, Zeng S, *et al*. SIRT5 downregulation is associated with poor prognosis in glioblastoma. *Cancer Biomark*. 2019;24(4):449-459.

doi: 10.3233/CBM-182197

94. Yao L, Wang Y. Bioinformatic analysis of the effect of the sirtuin family on differentiated thyroid carcinoma. *Biomed Res Int*. 2022;2022:5794118.

doi: 10.1155/2022/5794118

95. Rizzo A, Iachettini S, Salvati E, *et al*. SIRT6 interacts with TRF2 and promotes its degradation in response to DNA damage. *Nucleic Acids Res*. 2017;45:1820-1834.

doi: 10.1093/nar/gkw1202

96. Mao Z, Hine C, Tian X, *et al*. SIRT6 promotes DNA repair under stress by activating PARP1. *Science*. 2011;332:1443-1446.

doi: 10.1126/science.1202723

97. Tao NN, Ren JH, Tang H, *et al*. Deacetylation of Ku70 by SIRT6 attenuates Bax-mediated apoptosis in hepatocellular carcinoma. *Biochem Biophys Res Commun*. 2017;485:713-719.

doi: 10.1016/j.bbrc.2017.02.111

98. Chen W, Liu N, Zhang H, *et al*. Sirt6 promotes DNA end joining in iPSCs derived from old mice. *Cell Rep.* 2017;18:2880-2892.

doi: 10.1016/j.celrep.2017.02.082

99. Fiorentino F, Carafa V, Favale G, Altucci L, Mai A, Rotili D. The two-faced role of SIRT6 in cancer. *Cancers* (*Basel*). 2021;13:1156.

doi: 10.3390/cancers13051156

100. Sebastián C, Zwaans BM, Silberman DM, *et al.* The histone deacetylase SIRT6 is a tumor suppressor that controls cancer metabolism. *Cell*. 2012;151(6):1185-1199.

doi: 10.1016/j.cell.2012.10.047

101. Zhang ZG, Qin CY. Sirt6 suppresses hepatocellular carcinoma cell growth via inhibiting the extracellular signalregulated kinase signaling pathway. *Mol Med Rep.* 2014;9(3):882-888.

doi: 10.3892/mmr.2013.1879

102. Han Z, Liu L, Liu Y, Li S. Sirtuin SIRT6 suppresses cell proliferation through inhibition of Twist1 expression in non-small cell lung cancer. *Int J Clin Exp Pathol.* 2014;7(8):4774-81.

103. Bae JS, Noh SJ, Kim KM, *et al*. SIRT6 is involved in the progression of ovarian carcinomas via β-catenin-mediated epithelial to mesenchymal transition. *Front Oncol*. 2018;8:538.

doi: 10.3389/fonc.2018.00538

104. Liu Y, Xie QR, Wang B, *et al*. Inhibition of SIRT6 in prostate cancer reduces cell viability and increases sensitivity to chemotherapeutics. *Protein Cell.* 2013;4(9):702-710.

doi: 10.1007/s13238-013-3054-5

105. Khongkow M, Olmos Y, Gong C, *et al*. SIRT6 modulates paclitaxel and epirubicin resistance and survival in breast cancer. *Carcinogenesis*. 2013;34(7):1476-1486.

doi: 10.1093/carcin/bgt098

106. Wang L, Guo W, Ma J, *et al*. Aberrant SIRT6 expression contributes to melanoma growth: Role of the autophagy paradox and IGF-AKT signaling. *Autophagy*. 2018;14(3):518-533.

doi: 10.1080/15548627.2017.1384886

107. Cagnetta A, Soncini D, Orecchioni S, *et al*. Depletion of SIRT6 enzymatic activity increases acute myeloid leukemia cells' vulnerability to DNA-damaging agents. *Haematologica*. 2018;103(1):80-90.

doi: 10.3324/haematol.2017.176248

108. Kim JK, Noh JH, Jung KH, *et al*. Sirtuin7 oncogenic potential in human hepatocellular carcinoma and its regulation by the tumor suppressors MiR-125a-5p and MiR-125b. *Hepatology*. 2013;57(3):1055-1067.

doi: 10.1002/hep.26101

109. Monteiro-Reis S, Lameirinhas A, Miranda-Gonçalves V, *et al*. Sirtuins' deregulation in bladder cancer: SIRT7 is implicated in tumor progression through epithelial to mesenchymal transition promotion. *Cancers* (*Basel*). 2020;12(5):1066.

doi: 10.3390/cancers12051066

110. Paredes S, Villanova L, Chua KF. Molecular pathways: Emerging roles of mammalian Sirtuin SIRT7 in cancer. *Clin Cancer Res*. 2014;20:1741-1746.

doi: 10.1158/1078-0432.CCR-13-1547

111. Huo Q, Chen S, Zhuang J, Quan C, Wang Y, Xie N. SIRT7 downregulation promotes breast cancer metastasis via LAP2α-induced chromosomal instability. *Int J Biol Sci*. 2023;19(5):1528-1542.

doi: 10.7150/ijbs.75340

112. Wang HL, Lu RQ, Xie SH, *et al*. SIRT7 exhibits oncogenic potential in human ovarian cancer cells. *Asian Pac J Cancer Prev*. 2015;16(8):3573-3537.

doi: 10.7314/apjcp.2015.16.8.3573

113. Liu X, Li C, Li Q, Chang HC, Tang YC. SIRT7 facilitates CENP-A nucleosome assembly and suppresses intestinal tumorigenesis. *iScience*. 2020;23(9):101461.

doi: 10.1016/j.isci.2020.101461

114. Yu H, Ye W, Wu J, *et al*. Overexpression of sirt7 exhibits oncogenic property and serves as a prognostic factor in colorectal cancer. *Clin Cancer Res*. 2014;20(13):3434-3445.

doi: 10.1158/1078-0432.CCR-13-2952

115. Tang M, Lu X, Zhang C, *et al*. Downregulation of SIRT7 by 5-fluorouracil induces radiosensitivity in human colorectal cancer. *Theranostics*. 2017;7(5):1346-1359.

doi: 10.7150/thno.18804

116. Zhao Q, Zhou J, Li F, *et al*. The role and therapeutic perspectives of sirtuin 3 in cancer metabolism reprogramming, metastasis, and chemoresistance. *Front Oncol*. 2022;12:910963.

doi: 10.3389/fonc.2022.910963

117. Ianni A, Kumari P, Tarighi S, Braun T, Vaquero A. SIRT7: A novel molecular target for personalized cancer treatment? *Oncogene*. 2024;43(14):993-1006.

doi: 10.1038/s41388-024-02976-8

118. Chen PT, Yeong KY. New sirtuin modulators: Their uncovering, pharmacophore, and implications in drug discovery. *Med Chem Res*. 2024;33:1064-1078.

doi: 10.1007/s00044-024-03249-5

119. Deus CM, Serafim TL, Magalhães-Novais S, *et al*. Sirtuin 1-dependent resveratrol cytotoxicity and pro-differentiation activity on breast cancer cells. *Arch Toxicol*. 2017;91(3):1261-1278.

doi: 10.1007/s00204-016-1784-x

120. Li L, Fu S, Wang J, *et al*. SRT1720 inhibits bladder cancer cell progression by impairing autophagic flux. *Biochem Pharmacol*. 2024;222:116111.

doi: 10.1016/j.bcp.2024.116111

121. Tan P, Wang M, Zhong A, *et al*. SRT1720 inhibits the growth of bladder cancer in organoids and murine models through the SIRT1-HIF axis. *Oncogene*. 2021;40(42):6081-6092.

doi: 10.1038/s41388-021-01999-9

122. Fatehi D, Soltani A, Ghatrehsamani M. SRT1720, a potential sensitizer for radiotherapy and cytotoxicity effects of NVB-BEZ235 in metastatic breast cancer cells. *Pathol Res Pract*. 2018;214(6):889-895.

doi: 10.1016/j.prp.2018.04.001

123. Han L, Long Q, Li S, *et al*. Senescent stromal cells promote cancer resistance through SIRT1 loss-potentiated overproduction of small extracellular vesicles. *Cancer Res*. 2020;80(16):3383-3398.

doi: 10.1158/0008-5472.CAN-20-0506

124. Chowdhury S, Sripathy S, Webster A, *et al*. Discovery of selective SIRT2 inhibitors as therapeutic agents in B-cell lymphoma and other malignancies. *Molecules*. 2020;25(3):455.

doi: 10.3390/molecules25030455

125. Hirai S, Endo S, Saito R, *et al*. Antitumor effects of a sirtuin inhibitor, tenovin-6, against gastric cancer cells via death receptor 5 up-regulation. *PLoS One*. 2014;9(7):e102831.

doi: 10.1371/journal.pone.0102831

126. Dai H, Sinclair DA, Ellis JL, Steegborn C. Sirtuin activators and inhibitors: Promises, achievements, and challenges. *Pharmacol Ther*. 2018;188:140-154.

doi: 10.1016/j.pharmthera.2018.03.004

ACCSCIENCE PUBLISHING

Gene & Protein in Disease

REVIEW ARTICLE

The roles of GLUT5 in cancer progression, metastasis, and drug resistance

Martin Guerrero, Gabrielle Kowkabany, and Yuping Bao*

Department of Chemical and Biological Engineering, College of Engineering, The University of Alabama, Tuscaloosa, Alabama, United States of America

Abstract

Emerging evidence has suggested that high fructose intake, particularly from added sugars and processed foods, is associated with increased cancer risk and progression. The fructose intake is believed to be mediated by the abnormal expression of glucose transporter 5 (GLUT5), the specific fructose transporter in cancer cells. The GLUT5-regulated fructose metabolism has shown to greatly affect cancer progression, metastasis, and drug resistance. This review aims to synchronize the current knowledge to highlight the underlying mechanisms of those impacts and understand the therapeutic potential of GULT5. First, we review the fructose metabolism and its alteration in cancer cells by comparing with glucose metabolism. Subsequently, the key contributors or biological pathways involved in GLUT5-asosociated tumor growth, cancer metastasis, and drug resistance are discussed. The contributions of specific pathways, metabolites, and key enzymes from the fructose metabolism process are also covered, such as enhanced glycolysis for tumor growth, epithelial-mesenchymal transition and angiogenesis for cancer metastasis, and efflux pump expression and activation of survival pathways for cancer drug resistance. The detailed analysis of these mechanisms will allow further understanding of the therapeutic potential of GLUT 5-mediated fructose metabolism in cancer therapy. In particular, targeting GLUT 5 and its-associated processes in fructose metabolism may offer promising strategies for improving cancer treatment outcomes through dietary interventions, specific GLUT5 inhibitors, or in combination.

Keywords: Fructose metabolism; GLUT5 expression; Cancer progression; Cancer metastasis; Drug resistance; Epithelial-mesenchymal transition; Matrix metalloproteinases; Pentose phosphate pathway

***Corresponding author:**
Yuping Bao
(ybao@eng.ua.edu)

Citation: Guerrero M, Kowkabany G, Bao Y. The roles of GLUT5 in cancer progression, metastasis, and drug resistance. *Gene Protein Dis.* 2024;3(4):4171. doi: 10.36922/gpd.4171

Received: July 8, 2024
Accepted: September 18, 2024
Published Online: October 15, 2024

1. Introduction

Common in human diet, fructose is a natural nutrient that can be obtained from fruits, honey, and vegetables; however, the increased intake of fructose from processed foods and drinks becomes an increasing concern.[1] The increased fructose intake directly results in abnormal expression of glucose transporter 5 (GLUT5), encoded by the solute carrier family 2 member 5 (*SLC2A5*) gene for specific fructose transport, in tissues that typically do not express GLUT5.[2] On the other hand, the upregulation of GLUT5 leads to further fructose utilization.[3] Compared to glucose that can be metabolized throughout the body, only certain tissues express GLUT5 and are able to metabolize fructose, such as small

intestine, liver, and kidney.[4] Although adipose and muscle tissues can also metabolize fructose, metabolic pathways are different. In liver, intestine, and kidney, fructose is phosphorylated at number 1 carbon by ketohexokinase (KHK), producing various intermediates for glycolysis or lipogenesis.[5] In contrast, in muscle and adipose tissue, fructose is phosphorylated at number 6 carbon by hexokinase (HK), entering glycolysis, but the process is less efficient than glucose.[5] In addition, fructose can be involved in polyol pathway, a reversible process between glucose and fructose through intermediate of sorbitol.[4] It has been shown that fructose preserves the stemness of stem cells and decreases stem cell proliferation.[6]

Recently, increasing evidence suggested the expression of GLUT5 in various cancer cells, resulting in fructose uptake and metabolism in cancer cells and affecting tumor development and progression.[7] By far, GLUT5 overexpression has been reported in various cancers, which was believed to be induced by fructose dietary uptake.[8] For example, fructose supplementation was shown to promote GLUT5 overexpression in subcutaneous tumors in nude mice.[9] The upregulation of GLUT5 in cancer cells directly increases the fructose uptake rate and metabolism. Similarly, GLUT5 upregulation was observed in colorectal cancer patient samples compared to those from healthy individuals.[10] In another study, molecular imaging clearly demonstrated the overexpression of GLUT5 protein in breast tumor in mice.[11] An analysis of 85 glioma patient samples also exhibited GLUT5 upregulation in glioma tissues that were directly associated with glioma malignancy and patient poor survival.[12] Furthermore, GLUT5 was significantly upregulated in clinical samples of prostate cancer patients when compared with their benign counterparts.[13] Overexpressed GLUT5 in human cholangiocarcinoma was also reported based on RNA sequencing data from human tissue samples and cell lines.[14] Besides GLUT5 expression, its expression levels were reported to be closely linked to malignant evolution and clinical prognosis.[9,15,16]

The upregulation of GLUT5 was believed to be resulted from the increased metabolic demands of rapidly proliferating cancer cells to enhance fructose uptake. Compared to normal cells, cancer cells not only expressed GLUT5 abnormally to use fructose as additional energy source but also exhibited altered metabolism known as the Warburg effect.[17] The Warburg effect refers to a phenomenon that cancer cells primarily use glycolysis for energy production even in the presence of oxygen. The abnormal expression of GLUT5 allows using fructose as an additional energy source and metabolic intermediates for biosynthesis.[18] In addition, fructose metabolism further altered metabolic rate. Several mechanisms associated with GLUT5-mediated fructose metabolism have been proposed, but GLUT5 expression seems the controlling step by directly increasing fructose utilization.[18] Therefore, GLUT5 emerges as a marker of cancer diagnosis and prognosis,[19,20] and inhibiting GLUT5 has been shown to be an effective approach to treating cancer through either individual or combined therapy.[21]

In this review, we focus our discussion on the impacts of GLUT5 expression and related pathways on cancer progression, metastasis, and drug resistance, highlighting the underlying mechanisms and potential therapeutic implications. Specifically, we first discuss the role of GLUT5 expression and metabolic alteration in cancer cells, such as enhanced glycolysis and the induced pentose phosphate pathway (PPP). The altered metabolism leads to high energy production and enhanced biosynthesis to support rapid cell proliferation, survival, and tumor growth. GLUT5-mediated fructose metabolism promotes epithelial-mesenchymal transition (EMT), upregulates matrix metalloproteinases (MMP), and increases angiogenesis, all of which are key players in cancer cell invasion and metastasis. Finally, we intend to understand the contribution of the elevated fructose metabolism to chemoresistance, in particular, the involved biological pathways and metabolites, such as the enhanced antioxidant defenses through NADPH production, efflux transporters modulation, and activation of pro-survival signaling pathways (*e.g.*, PI3K/AKT). These mechanisms allow cancer cells to survive oxidative stress induced by chemotherapy. Due to the direct correlation between high fructose intake and GLUT5 expression, targeting GLUT5 and related pathways offers a promising strategy for improving cancer treatment outcomes.

2. Correlation between GLUT 5 expression and cancer development

The correlation between GLUT5 expression and cancer progression is closely related to fructose uptake and altered metabolism. GLUT5, the fructose-specific transporter, facilitates fructose uptake into cancer cells, which can impact cancer development from several aspects, such as enhanced energy production, increased cell proliferation and survival, and immune evasion. In this section, we discuss the impacts of GLUT5-mediated fructose metabolism on the energy production and biosynthesis. Both the high-energy production and accelerated biosynthesis are critical elements for fast-growing cells. Here, the focus will be given on the effects of specific pathways and key players of the fructose metabolic process on cancer progression.

2.1. Metabolic alteration in cancer cells

Fructose and glucose are monosaccharide isomers with the same chemical formula (Figure 1A) but vary in their functional groups. The structural difference and their biological function led to different metabolic pathways and processing locations.[22] Both sugars can participate in glycolysis, serving as energy and carbon sources for biological systems, but the metabolic processes and key enzymes are different, as shown in Figure 2B. Glucose can be metabolized by all cell types throughout the body through several interconnected pathways to break down glucose. Glucose metabolism is the key energy source for normal cells and the metabolic processes include glycolysis, pyruvate metabolism, the tricarboxylic acid (TCA) cycle, and oxidative phosphorylation, along with glycogenesis. In addition, these processes are tightly regulated to maintain energy homeostasis in the body.

However, many types of cancer cells showed altered metabolism where glycolysis become the main energy production step even in the presence of oxygen, known as the Warburg effect.[23] This metabolic shift was believed to be driven by much higher ATP production rate of glycolysis (100 times faster) than that of TCA cycle in mitochondria.[24] The Warburg effect impacts many aspects of cancer cells, such as proliferation, metastasis, and drug resistance.[17] The resulted high ATP production rate and biosynthesis are to meet the metabolic demand of fast-growing cancer cells.

Typically, fructose is not a regular energy source for most cells. However, many studies have shown the upregulation of GLUT5 in various cancer cells, considering fructose as an additional energy source. The GLUT5 overexpression on cancer cells directly increases the fructose uptake and further induces metabolic alteration of cancer cells.[25] Fructose can enter the glycolytic pathway downstream of the rate-limiting step regulated by phosphofructokinase (Figure 1B). Due to the lack of regulation, fructose can enter glycolysis more efficiently and be metabolized more rapidly than glucose, providing a rapid source of ATP and metabolic intermediates to support cancer cell proliferation and growth. In brief, fructose is first metabolized into fructose-1-phsphate (F1P) by KHK, also known as fructokinase. This process also leads to uric acid production and stimulates the activity of glycolytic enzymes to increase the rate of glycolysis, and a subsequent high ATP production rate. The F1P-induced production of uric acid can lead to oxidative stress in mitochondria, which inhibits TCA cycle, and stimulates cell proliferation. F1P is subsequently cleaved into glyceraldehyde (GA) and dihydroxyacetone phosphate (DHAP) by aldolase B (ALDOB). These metabolites either can enter glycolysis through phosphorylated GA or be converted into fat when DHAP combines with glycerol to form glycerol-3-phosphate (G3P). This DHAP conversion leads to increased accumulation of intracellular free fatty acids.

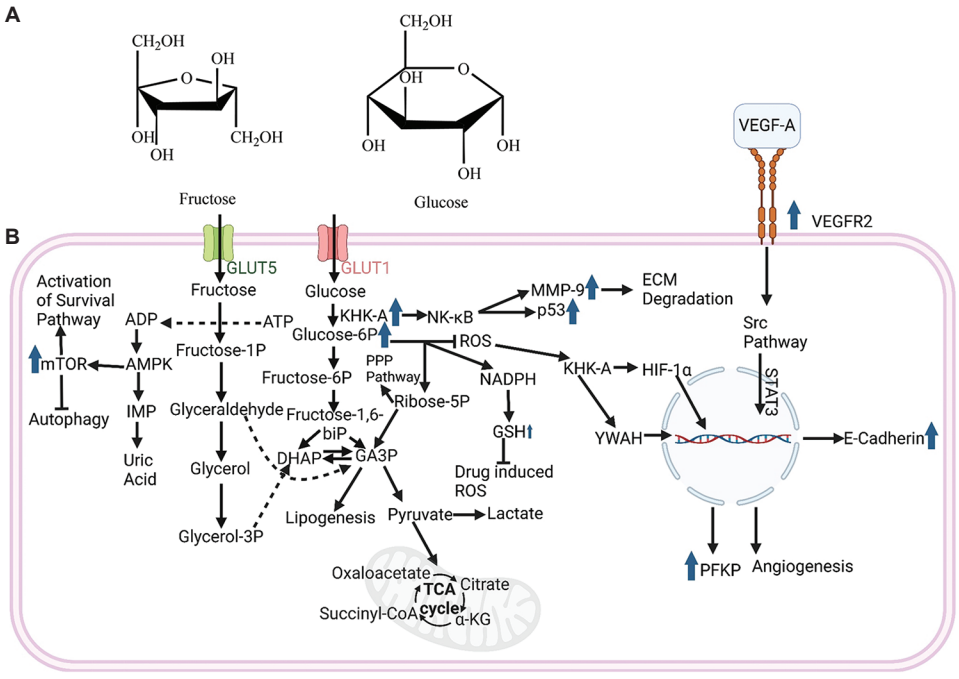

Figure 1. The illustration of (A) structures of fructose and glucose and (B) the metabolic process and key players of the fructose and glucose. Created with Biorender.com

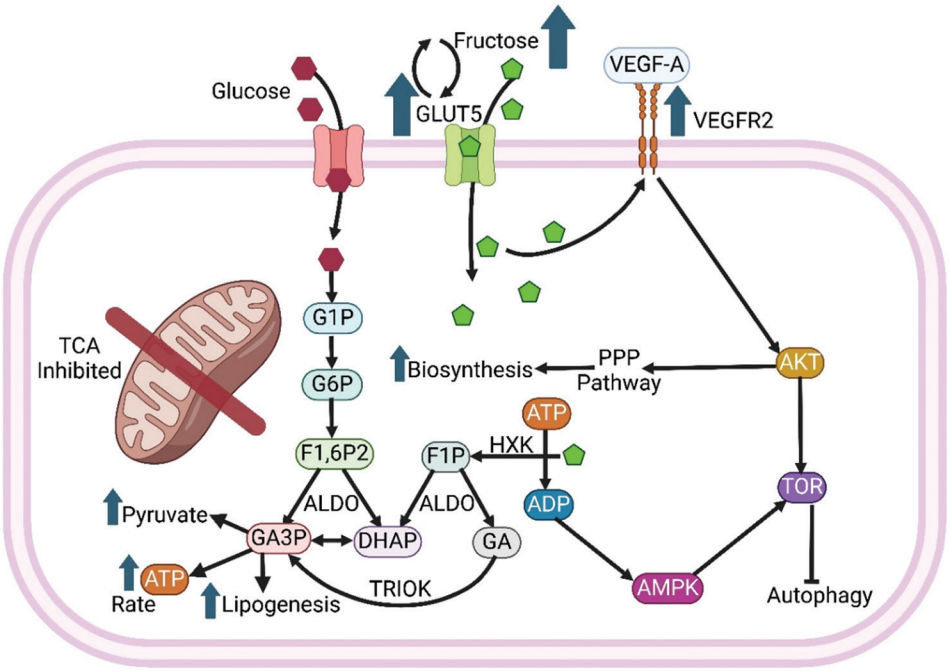

Figure 2. Illustration of pathways and key players of fructose metabolism inducing cancer cell proliferation and tumor growth. Created with Biorender.com

DHAP can also enter the glycolysis pathway and be converted to glyceraldehyde-3-phosphate. Alternatively, fructose can be phosphorylated at C6 position by HK in muscle or fat tissue, entering glycolysis directly. However, this process is not efficient because the affinity of HK to glucose is higher than fructose. In addition, excess fructose can be converted into acetyl-CoA, a substrate for fatty acid synthesis. An *in vivo* study by Goncalves *et al.*[26] reported a substantial increase in tumor size and tumor grade of intestinal tumor in mice fed with high-fructose corn syrup. The tumor growth was attributed to the activation of glycolysis and increased lipogenesis by F1P.

In addition to the impacts on glycolysis, the glycolytic intermediates of fructose metabolism in cancer cells increase PPP activity,[27] a metabolic pathway parallel to glycolysis. The PPP process generates NADPH and ribose-5-phosphate. The NADPH is essential for maintaining the redox balance and biosynthesis, such as lipid biosynthesis, while ribose-5-phosphate is critical for nucleotide synthesis, supporting DNA replication and repair in proliferating cancer cells.[28] Increased lipogenesis is necessary for the formation of cell membranes in proliferating cancer cells. Many cancer cells exhibited increased PPP activity to meet their high demand for NADPH and ribose-5-phosphate. The enhanced NADPH production helps to maintain cellular antioxidants *(e.g.*, glutathione). This reduces oxidative stress and protects cancer cells from apoptosis, supporting can cell survival and continued proliferation. Fructose-induced PPP process also causes inflationary effects in cells,[29] and dysregulation of the PPP process contributed greatly in malignant tumors.[30,31]

2.2. Increased tumor growth and survival

The key to fructose uptake and metabolism is the expression of GLUT5 in cancer cells as demonstrated by numerous studies. For example, a study by Jin *et al.*[32] suggested a direct correlation between GLUT5 expression and the proliferation of the ovarian cancer cells in fructose-rich growth medium. The animal experiments also showed that high fructose intake significantly increased tumor volume. In another study,[10] the blockade of GLUT5 with the inhibitor, N-[4-(methylsulfonyl)-2-nitrophenyl]-1,3-benzodioxol-5-amine significantly decreased the viability of colon cancer cells, but had marginal effects on the viability of normal colon epithelium cells, suggesting the critical role of GLUT5 in cancer cell proliferation. The direct correlation of GLUT5 expression and enhanced fructose uptake and tumor progression was also observed in glioma.[12] In addition, GLUT5 knockdown significantly inhibited the proliferation of glioma cells in fructose medium. Another study by Carreño *et al.*[13] not only demonstrated that GLUT5-regulated fructose uptake stimulated proliferation and invasion of prostate cancer cells *in vitro*, and increased the growth of patient-derived xenograft tumors but also confirmed the upregulation of

GLUT5 in clinical samples of prostate cancer patients when compared with their benign counterparts.[13]

Besides the direct correlation of GLUT5 expression and fructose uptake, GLUT5 overexpression also affects other key players of the fructose metabolism process. For example, it has been shown that KHK protein was upregulated by GLUT5 overexpression in colorectal cancer cells by inhibiting lysosomal degradation.[9] This GLUT5-KHK association was also observed in xenograft tumor growth *in vivo*. Suwannakul *et al.*[14] reported that fructose consumption increased xenograft tumor growth in nude mice that was directly related to GLUT5 expression and GLUT5-dependent downstream genes, such as *KHK*, aldolase B (*ALDOB*), and hypoxia-inducible factor 1 alpha (*HIF1α*). For example, it was shown that a deficiency in KHK-A suppressed the proliferation of gastric cancer cells by downregulating β-catenin, a key factor in cell growth and survival.[33] GLUT5-mediated fructose utilization has also been shown to induce lung cancer growth through enhanced lipogenesis and AMP-activated protein kinase-AMPK/mTORC1 signaling.[16] Fructose-induced mTORC1 activation was also linked to the autophagy inhibition[34] that promoted pancreatic cancer progression. In this study by Cui *et al.*[34], it was shown that GLUT5-mediated fructose metabolism activated the AMPK/TORC1 signaling pathway to inhibit glucose deficiency-induced autophagy. The typical involved pathways and key players are summarized in Figure 2.

2.3. Inflammatory and immunosuppressive effects

Fructose metabolism can activate the NF-κB (nuclear factor kappa-light-chain-enhancer of activated B-cells) pathway, a key regulator of inflammation. This activation leads to the production of pro-inflammatory cytokines such as interleukin (IL)-6, IL-1β, and tumor necrosis factor-alpha (TNF-α). For example, it has been shown that IL-6/STAT3 worked together to activate GLUT5 expression to regulate fructose metabolism and tumorigenesis.[35] In this study, a synergistic effect of inflammatory factors and fructose metabolism in facilitating tumor growth was reported in oral squamous cell carcinoma cells and prostate cancer cells. Specifically, IL-6 treatment enhanced GLUT5 expression through transcription factor STAT3 transcription that associates with GLUT5 promoter region. Similarly, Lu *et al.*[36] reported that fructose-1,6-bisphosphatase 1 (FBP1) interacted with NF-κB p65 to regulate breast tumorigenesis through PIM2 (proviral insertion in murine lymphomas 2) in nude mice. FBP1 is the rate-limiting enzyme in gluconeogenesis, a glucose formation process from non-hexose precursors (*e.g.*, glycerol, lactate, or pyruvate). FBP1 has also recently been shown to not only suppress tumor but also regulate the activities of several transcriptional factors through its non-canonical functions.[37,38] In this study, the PIM2 was confirmed as a new binding partner of FBP1 to induce FBP1 phosphorylation on Ser144. As discussed earlier, fructose metabolism also leads to increased lipogenesis, promoting the release of pro-inflammatory lipid mediators and cytokines. This lipid-driven inflammation and persistent oxidative stress can suppress effective immune responses and enhance tumor cell survival.

3. Correlation between GLUT 5 expression and cancer metastasis

The correlation between GLUT5 expression and cancer metastasis lies in several critical biochemical and physiological mechanisms. As discussed earlier, GLUT5, the fructose-specific transporter, plays a pivotal role in facilitating fructose uptake and metabolism in cancer cells. Some intermediates from the fructose metabolism process also influence cancer cell activities, such as uric acid production, activities of MMPs, and angiogenesis. In this section, we emphasize the mechanisms and key players that directly influence GLUT5-mediated cancer metastasis.

3.1. Enhanced tumor growth and metastasis

Some mechanisms promoting tumor growth discussed in section 1 also contribute to cancer metastasis, such as enhanced glycolysis and lipogenesis to meet the energy and biosynthesis needs of rapidly growing cells. In addition, fructose metabolism leads to increased uric acid production, which can induce oxidative stress and inflammation, promoting a tumor-supportive environment. Uric acid also activates aldose reductase, a key enzyme of the polyol pathway that converts glucose to fructose through sorbitol. For example, a study by Weng *et al.*[15] not only reported the role of GLUT5 upregulation in lung adenocarcinoma patient samples and its association with poor patient prognosis but also demonstrated the link between GLUT5 expression and cell migration, invasion, and metastasis.[15] In another study, Jin *et al.*[32] reported multiple effects of GLUT5 expression in ovarian cancer,[32] including cell proliferation, colony formation, and cell migration, upregulation of GLUT5 in ovarian cancer patient samples, as well as the correlation of GLUT5 expression and tumor malignancy and poor patient survival. Interestingly, the high expression of GLUT1, a glucose transporter, has been observed in primary cancer, but GLUT5 has been found to be upregulated in metastatic tumor, suggesting that GLUT5-mediated fructose metabolism greatly impacts lung cancer metastasis. Similarly, it has been reported[39] that GLUT5 overexpression promoted migration of lung cancer cells *in vitro* and reduced the overall survival of tumor-bearing mice. In this study, the metastatic effects

of GLUT5-mediated fructose metabolism were attributed to the upregulated phosphorylated AKT caused by high glycolysis rate with increased lactate production.

In addition to GLUT5 expression, other key players of the fructose metabolism also affect cancer metastasis. For example, aldolase B-mediated fructose metabolism causes preferable liver metastasis of colon cancer.[40] In addition, KHK has been shown to behave as a nuclear protein kinase to mediate fructose-induced metastasis in breast cancer.[41] In addition to dietary intake of fructose, hyperglycemia-induced fructose formation through the polyol pathway[42] also promoted metastatic behaviors of gastric cancer, such as enhanced cell migration and invasion, cytoskeletal rearrangement, and EMT. Cells experiencing EMT gain mesenchymal characteristics, which enhance metastatic potential. These behaviors are believed to be related to the activation of nuclear ketohexokinase-A (KHK-A) signaling pathways. The EMT is a common result of high reactive oxygen species (ROS) generation by cancer cells, leading to the formation of stem cell like-cancer cells, known as cancer stem cells.[43] Cancer stem cells typically have an enhanced metabolism and higher metastatic potential. A study by Park *et al.*[44] also proposed that the regulation of GLUT5 expression as a result of AKT1/3-miR-125b-5p downregulation leads to increased cell migration and drug resistance in TLR-modified colorectal cancer cells. Furthermore, it has been shown that fructose metabolism promoted glycosylation of cell surface proteins, which stimulated breast cancer migration.[45] In the same study, GLUT5-mediated fructose uptake was shown to influence the arrangement of glycan and cytoskeletal proteins in breast cancer cells, promoting sialylation by increasing the expression of sialyltransferase. Therefore, the GLUT5 expression and fructose metabolism worked synergistically to impact cancer metastasis, as illustrated in Figure 3. In addition to inhibiting GLUT5, targeting downstream enzymes may be another viable approach in cancer treatment.[46]

3.2. Activity of MMP

GLUT5-mediated fructose metabolism naturally enhances the production of uric acid and lactate, fostering an acidic tumor microenvironment. The acidic tumor microenvironment can increase the proteolytic activity of extracellular digestive enzymes, accelerating the degradation of extracellular matrix (ECM) and facilitating cancer metastasis.[47,48] Extracellular acidification directly influences the expression and activity of MMPs, which are enzymes for ECM degradation, facilitating cancer cell invasion and migration.[49] In addition, the altered tumor microenvironment is important to the function of invadopodia,[50] an actin-rich structure important for cellular crawling movements, which is essential for tumor invasion.[51] GLUT5-mediated fructose metabolism also enhanced the production of pro-inflammatory cytokines such as TNF-α and IL-6.[35] These cytokines can upregulate the expression of MMPs, particularly MMP-2 and MMP-9, through activation of transcription factors (*e.g.*, NF-κB).[52] For example, rats fed with high fructose diet exhibited elevated p65 phosphorylation, which subsequently activated NFκB, inducing enhanced MMP-9 expression.[52] FBP1 has been reported to regulate Wnt/β-catenin pathway in breast cancer,[53] where activation of Wnt/β-Catenin pathway is a signature of metastasis.[54] GLUT5-mediated fructose metabolism also increases ROS production, which can activate signaling pathways that induce MMP expression. For example, ROS-mediated expression of MMP-3 can be observed in stromal fibroblasts and cancer cells during prostate cancer progression.[55] Fructose metabolism significantly impacts the activity of MMPs primarily through mechanisms involving inflammatory responses. It has been shown that MMP9, a downstream target of HIF1α, was significantly upregulated to promote lung cancer progression.[56] Thus, therapeutic strategies targeting fructose metabolism or MMPs may serve as promising strategies to manage cancer progression and improve patient outcomes.

3.3. Angiogenesis

Angiogenesis refers to the new blood vessel formation from the existing ones, playing a crucial role in cancer progression and metastasis. GLUT5-mediated fructose uptake and metabolism is known to stimulate the production of vascular endothelial growth factor (VEGF), promoting angiogenesis. For example, an analysis of over 400 colorectal cancer specimens suggested that the levels of GLUT5 expression in vascular endothelial cells (VECs) positively correlated with microvascular density.[57] Several aspects of fructose metabolism are believed to contribute to the increased microvascular density. First, metabolites from fructose metabolism by VECs activate the ATK and Src signaling pathways that led to the enhancement of VEC proliferation, migration, and vascular formation, thus promoting angiogenesis. Second, the fructose metabolism in colorectal cancer cells increased ROS production, promoting VEGF expression. These hypotheses were further validated in clinical colorectal cancer tissues and mouse models. Many other studies also suggested that ATK signaling pathways play a key role in tumor cell migration and invasion.[58,59] It has also been shown that fructose metabolism in tumor endothelial cells (ECs) promoted angiogenesis by AMPK activation and mitochondrial respiration.[60] The effects were associated with the overexpression of GLUT5 and KHK, the key metabolizing

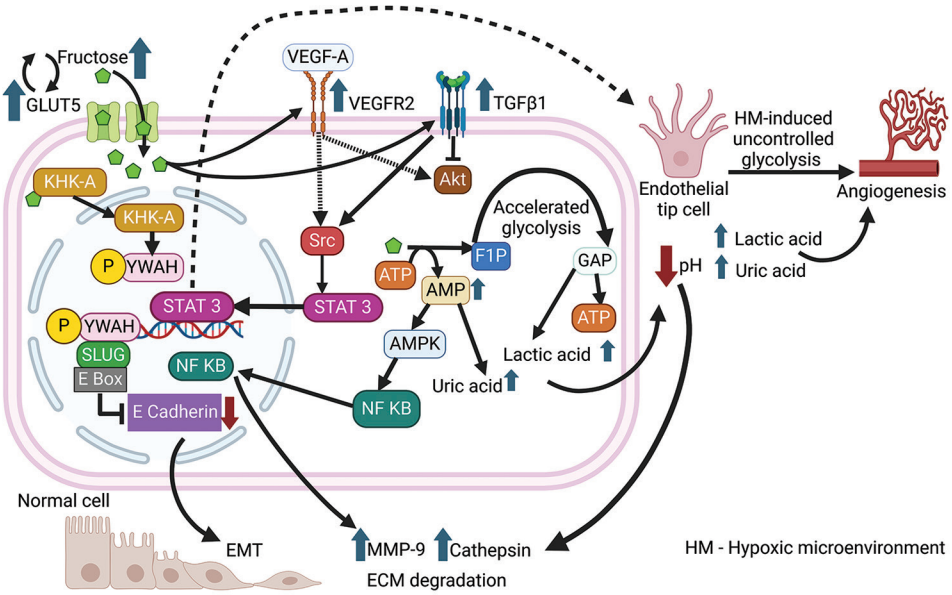

Figure 3. Illustration of pathways and key players of fructose metabolism inducing cancer metastasis. Created with Biorender.com

enzyme, in tumor ECs from hepatocellular carcinoma. An increase in tumor angiogenesis, growth, and metastasis was observed in xenografts tumors in fructose-fed mouse models or Myc/sgp53-induced liver cancer. Peng *et al.*[61] reported the KHK-A promoted liver metastasis in colorectal cancer by facilitating the phosphorylation and nuclear translocation of pyruvate kinase M2 (PKM2). This process enhances fructose metabolism and supports tumor growth. The researchers conducted *in vivo* studies in mice and *in vitro* experiments using colorectal cancer cells, demonstrating that elevated KHK-A levels increased metastasis, while silencing KHK-A reduced cancer cell invasion and proliferation.[61] Similarly, Gao *et al.*[62] showed the increased KHK levels in patient glioma tissues and glioma cell lines, which were associated with higher level of proliferation and malignancy. In addition, silencing KHK inhibited proliferation and migratory behavior of glioma cells. The KHK overexpression was also correlated with greater malignant phenotypes and overall poor patient survival. It was also suggested that the enhanced fructose metabolism by HIF1α under hypoxic conditions directly contributed to the fructose-induced EC migration. The impacts of GLUT5-mediated fructose uptake on cancer metastasis were directly verified through GLUT5 inhibition that negatively impacted cancer metastasis. For example, a comprehensive study using CRISPR/Cas9 technology to silence *SLC2A5* gene in several metastatic cancer cell lines and their xenograft mouse models exhibited effective inhibition of cancer cell proliferation and migration *in vitro* and metastases *in vivo*.[63] The direct association of increased GLUT5 expression in cancer cells with higher metastatic risk in several types of cancers indicates the potential therapeutic role of GLUT5 to reduce or prevent cancer metastasis.

4. Correlation between GLUT 5 expression and cancer drug resistance

Cancer drug resistance involves several complex mechanisms that enable cancer cells to survive and proliferate despite chemotherapeutic treatment. Many contributors are known to be related to cancer drug resistance. For example, enhanced glycolysis was directly correlated with chemoresistance in acute myeloid leukemia.[64] Here, we focus on the factors associated with GLUT5-mediated fructose metabolism

4.1. Metabolic upregulation of drug transporters

As discussed earlier, the GLUT5 abnormal expression in cancer cells increases the fructose uptake and metabolism, leading to high ATP production rate and enhanced biosynthesis. In addition, fructose is metabolized more efficiently and in an uncontrolled manner compared to glucose metabolism, providing a continuous supply of ATP and metabolic intermediates that support cell growth and survival under drug-induced stress. Therefore, the GLUT5-mediated fructose metabolism has shown much profound impacts on cancer progression and metastasis. This enhanced and continuous energy supply supports various cellular processes that contribute to drug resistance, such as repair of drug-induced damage and activation of survival pathways. The elevated energy supply

also influences the expression and activity of ATP-binding cassette (ABC) transporters, such as P-glycoprotein (P-gp). These efflux pumps drive chemotherapeutic drugs out of cancer cells, reducing drug intracellular concentrations and effectiveness. The upregulation of efflux pumps is a signature of cancer drug resistance[65] where the efflux pump expression can be influenced by several aspects of the fructose metabolism, including the activation of related signaling pathways (*e.g.*, PI3K/AKT), upregulation of ROS production, and transcriptional regulation by HIF1α. Many studies have shown that the fructose-induced metabolic alteration was closely related to multidrug resistant phenotype in various cancer.[66] For example, Shen *et al.*[9] suggested that the synergistic effects of GLUT5 and KHK during the fructose metabolism promoted the cell proliferation and chemotherapy resistance in colorectal cancer. Weng *et al.*[15] demonstrated that GLUT5 inhibition re-sensitized drug-resistant lung adenocarcinoma cells to paclitaxel treatment, a direct evidence of the role of GLUT5 expression in cancer drug resistance. The previous studies have shown that fructose metabolism caused activation of the PI3K/AKT signaling pathway,[67] which is known to regulate efflux pump expression, such as P-gp,[68] and serve as the key link modulating cancer multidrug resistance.[69] Fructose metabolism promotes PPP activity, leading to NADPH production and ribose-5-phosphate. NADPH is crucial for maintaining redox balance and reducing oxidative stress caused by chemotherapy. Fructose metabolism can activate transcription factors such as NF-κB by ROS generation and stabilize HIF1α, which both can induce efflux pump expression. Some of the key process in GLUT5-associated drug resistance is illustrated in Figure 4.

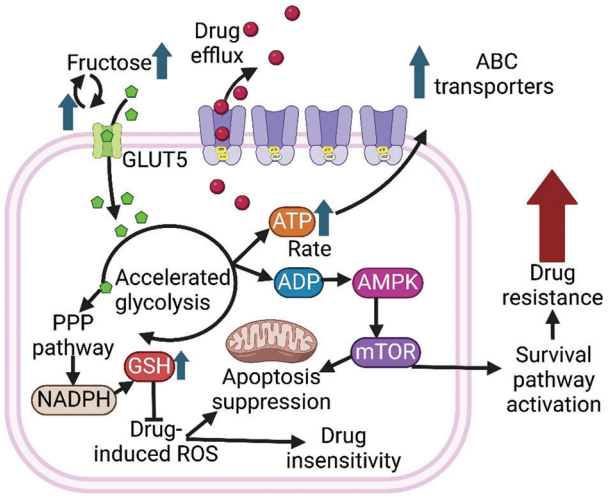

Figure 4. Illustration of pathways and key players of fructose metabolism inducing cancer drug resistance. Created with Biorender.com

4.2. Modulation of cell survival pathways

Most chemotherapeutic drugs induce cancer cell death by generating ROS. Fructose metabolism through PPP increases NADPH production, which is necessary for regenerating glutathione, a major cellular antioxidant. Glutathione can help in neutralizing ROS and protecting cancer cells from oxidative damage induced by chemotherapy.[70] NADPH also supports the activity of detoxifying enzymes such as glutathione peroxidase, which neutralizes ROS and other toxic substances, contributing to drug resistance. In addition, GLUT5-triggered high fructose utilization can cause chronic inflammation, which is known to be associated with the activation of survival pathways in cancer cells. Fructose-induced inflammation can activate the NF-κB pathway, which is known to regulate the gene expression associated with cell survival, proliferation, and drug resistance. These pathways can also upregulate anti-apoptotic proteins and downregulate pro-apoptotic proteins, making cancer cells more resistant to chemotherapy. By supporting the activation of survival pathways, GLUT5 expression helps cancer cells evade apoptosis, a key mechanism through which many chemotherapeutic agents exert their effects.

As mentioned early, fructose metabolism activates PI3K/AKT pathway that inhibits pro-apoptotic signals and caspase activation, promoting cell survival even under stressful conditions. For example, a study by Pungsrinont *et al.*[71] demonstrated the critical role of hyperactivation of PI3K-AKT-mTOR pathway in regulating pro-survival/anti-apoptotic pathways of cells as a resistance mechanism for prostate therapy. Fructose metabolism in cancer cells influences drug resistance by increasing antioxidant defenses and mitigating oxidative stress-induced damage. These adaptations allow cancer cells to survive under therapeutic pressure and maintain their proliferative capacity. Understanding the interplay between fructose metabolism, oxidative stress, and antioxidant mechanisms provides insights into potential strategies to overcome drug resistance and improve the effectiveness of cancer treatments. Shen *et al.*[9] proposed the mechanism of GLUT5-KHK axis-mediated fructose metabolism promoting proliferation and drug resistance in colorectal cancer. It has been shown that GLUT5 regulation consequent to AKT1/3-miR-125b-5p downregulation elicited drug resistance in colorectal cancer cells with elevated Toll-like receptor (TLR) expression.[44] Furthermore, fructose metabolism was shown to promote cytoprotection in melanoma tumors, making them resistant to immunotherapy.[72] Performed using immune impaired C57BL/6 mouse model bearing B16 melanoma or MC38 carcinoma tumors, the study

suggested that dietary fructose promoted tumor immune evasion. In addition, the FBP1 level is directly associated with cancer initiation and drug resistance in cervical cancer, as demonstrated in a study analyzing 140 patients with cervical cancer after radical surgery and subsequent chemoradiation therapy.[73] The results suggested that FBP1 expression was not only associated with drug resistance in cervical cancer but also the suppression of the upregulated FBP1 in carcinogenesis and restoration of cancer cell chemosensitivity to cisplatin. In addition, an analysis of 222 colorectal cancer patient samples showed that fructose-bisphosphate aldolase A played an important role in the hypoxic adaptation in colorectal cancer cells, serving as a potential target for treating drug resistance and improving poor prognosis.[74] The study showed that ALDOA had negative impacts on drug sensitivity and radiosensitivity and positive influence on cell proliferation, colony formation, and migration. Similar effects were also observed in hepatocellular carcinoma under hypoxic conditions, which have impacts on tumor malignancy[75] and renal cell carcinoma.[76] Thus, targeting glucose metabolism in cancer cells offers a viable approach to overcoming drug resistance.[77] Besides, it has been shown that inhibition of GLUT5 gene expression with trichostatin sensitized colon cancer cells to cisplatin and oxaliplatin.[78] Regardless of the impacts of GLUT5-mediated fructose mechanisms, dietary interventions could potentially contribute to cancer therapy.[79] The relationships of key metabolic pathways, such as RAF-MEK-MAPK and PI3K-Akt-mTOR pathways, with chemoresistance, as well as their potential as therapeutic targets for lung cancers, have recently been reviewed.[80]

5. Summary and future perspectives

GLUT5 represents an emerging and promising target in cancer therapy due to its role in fructose metabolism and the fact that it is overexpressed in various cancers. The upregulation of GLUT5 in various cancer cells enhanced fructose uptake and metabolism, which lead to several cascade effects. First, the increased fructose uptake promotes glycolysis, PPP activity, and lipogenesis, which collectively support tumor growth, survival, and metastasis. Second, GLUT5 expression can influence the expression and activity of MMPs, facilitating cancer cell invasion and migration. In addition, fructose metabolism enhances angiogenesis that provides pathways for cancer cells to enter the bloodstream and metastasize. Finally, the enhanced glycolysis leads to higher ATP production, upregulating the expression of ABC transporters, such as P-gp. Fructose metabolism increases NADPH levels, resulting in higher glutathione levels for ROS reduction, helping cancer cells to evade oxidative damage triggered by chemotherapy. All the above can be attributed to the overexpression of GLUT5. Therefore, targeting GLUT5 represents a promising strategy to address the multifaceted issues in cancer development and progression, so as to improve cancer treatment and prevention. By far, the majority of evidence in this regard is derived from preclinical studies in mouse models or human patient tissue samples. Therefore, the GLUT5 expression may serve as a prognostic marker, particularly in breast and colon cancer, with higher GLUT5 levels predicting poorer outcomes. To further explore the potential of using GLUT5 as a therapeutic target, the precise molecular mechanisms underlying GLUT5 overexpression-mediated cancer progression, metastasis, and drug resistance need to be elucidated. Genomic and proteomic analyses can be conducted to identify biomarkers related to fructose metabolism and GLUT5 expression for the purposes of early cancer detection and prognosis. Specific and potent GLUT5 inhibitors, for use as an individual therapy or a combined treatment with existing chemotherapy and targeted therapies, should be explored enhance therapeutic efficacy. Finally, dietary recommendations and public health policies may be developed, such as dietary guidelines or regulatory policies to recommend lower consumption of fructose, particularly obtained from added sugars and processed foods.

Acknowledgments

None.

Funding

This work was supported in part by NSF-CBET 1915873. Bao acknowledges Breast Cancer Research Foundation of the University of Alabama Center for Convergent Bioscience and Medicine Pilot Innovation Fund.

Conflict of interest

The authors declare no conflicts of interest.

Author contributions

Conceptualization: Martin Guerrero, Gabrielle Kowkabany
Visualization: Martin Guerrero, Gabrielle Kowkabany
Writing – original draft: All authors
Writing – review & editing: Yuping Bao

Ethics approval and consent to participate

Not applicable.

Consent for publication

Not applicable.

Availability of data

Not applicable.

References

1. Song A, Mao Y, Wei H. GLUT5: Structure, functions, diseases and potential applications. *Acta Biochim Biophys Sin* (*Shanghai*). 2023;55:1519-1538.

   doi: 10.3724/abbs.2023158

2. Shu R, David ES, Ferraris RP. Dietary fructose enhances intestinal fructose transport and GLUT5 expression in weaning rats. *Am J Physiol Gastrointest Liver Physiol*. 1997;272:G446-G453.

   doi: 10.1152/ajpgi.1997.272.3.G446

3. Patel C, Douard V, Yu S, Gao N, Ferraris RP. Transport, metabolism, and endosomal trafficking-dependent regulation of intestinal fructose absorption. *FASEB J*. 2015;29:4046-4058.

   doi: 10.1096/fj.15-272195

4. Hannou SA, Haslam DE, McKeown NM, Herman MA. Fructose metabolism and metabolic disease. *J Clin Invest*. 2018;128:545-555.

   doi: 10.1172/jci96702

5. Herman MA, Birnbaum MJ. Molecular aspects of fructose metabolism and metabolic disease. *Cell Metab*. 2021;33:2329-2354.

   doi: 10.1016/j.cmet.2021.09.010

6. Elsaid S, Wu X, Tee SS. Fructose vs. glucose: Modulating stem cell growth and function through sugar supplementation. *FEBS Open Bio*. 2024;14:1277-1290.

   doi: 10.1002/2211-5463.13846

7. Krause N, Wegner A. Fructose metabolism in cancer. *Cells*. 2020;9:2635.

   doi: 10.3390/cells9122635

8. Hadzi-Petrushev N, Stojchevski R, Jakimovska A, *et al*. GLUT5-overexpression-related tumorigenic implications. *Mol Med*. 2024;30:114.

   doi: 10.1186/s10020-024-00879-8

9. Shen Z, Li Z, Liu Y, *et al*. GLUT5-KHK axis-mediated fructose metabolism drives proliferation and chemotherapy resistance of colorectal cancer. *Cancer Lett*. 2022;534:215617.

   doi: 10.1016/j.canlet.2022.215617

10. Włodarczyk J, Włodarczyk M, Zielińska M, Jędrzejczak B, Dziki L, Fichna J. Blockade of fructose transporter protein GLUT5 inhibits proliferation of colon cancer cells: Proof of concept for a new class of anti-tumor therapeutics. *Pharmacol Rep*. 2021;73:939-945.

    doi: 10.1007/s43440-021-00281-9

11. Wuest M, Hamann I, Bouvet V, *et al*. Molecular imaging of GLUT1 and GLUT5 in breast cancer: A multitracer positron emission tomography imaging study in mice. *Mol Pharmacol*. 2018;93:79-89.

    doi: 10.1124/mol.117.110007

12. Su C, Li H, Gao W. GLUT5 increases fructose utilization and promotes tumor progression in glioma. *Biochem Biophy Res Commun*. 2018;500:462-469.

    doi: 10.1016/j.bbrc.2018.04.103

13. Carreño DV, Corro NB, Cerda-Infante NF, *et al*. Dietary fructose promotes prostate cancer growth. *Cancer Res*. 2021;81:2824-2832.

    doi: 10.1158/0008-5472.CAN-19-0456

14. Suwannakul N, Armartmuntree N, Thanan R, *et al*. Targeting fructose metabolism by glucose transporter 5 regulation in human cholangiocarcinoma. *Genes Dis*. 2022;9:1727-1741.

    doi: 10.1016/j.gendis.2021.09.002

15. Weng Y, Fan X, Bai Y, *et al*. SLC2A5 promotes lung adenocarcinoma cell growth and metastasis by enhancing fructose utilization. *Cell Death Dis*. 2018;4:38.

    doi: 10.1038/s41420-018-0038-5

16. Chen WL, Jin X, Wang M, *et al*. GLUT5-mediated fructose utilization drives lung cancer growth by stimulating fatty acid synthesis and AMPK/mTORC1 signaling. *JCI Insight*. 2020;5:e131596.

    doi: 10.1172/jci.insight.131596

17. Icard P, Shulman S, Farhat D, Steyaert JM, Alifano M, Lincet H. How the Warburg effect supports aggressiveness and drug resistance of cancer cells? *Drug Resist Updat*. 2018;38:1-11.

    doi: 10.1016/j.drup.2018.03.001

18. Douard V, Ferraris RP. The role of fructose transporters in diseases linked to excessive fructose intake. *J Physiol*. 2013;591:401-414.

    doi: 10.1113/jphysiol.2011.215731

19. Kannan S, Begoyan VV, Fedie JR, *et al*. Metabolism-driven high-throughput cancer identification with GLUT5-specific molecular probes. *Biosensors* (*Basel*). 2018;8:39.

    doi: 10.3390/bios8020039

20. Szablewski L. Glucose transporters as markers of diagnosis and prognosis in cancer diseases. *Oncol Rev*. 2022;16:561.

    doi: 10.4081/oncol.2022.561

21. RanaN, Aziz MA, Serya RAT, *et al*. A fluorescence-based assay to probe inhibitory effect of fructose mimics on GLUT5 transport in breast cancer cells. *ACS Bio Med Chem Au*. 2023;3:51-61.

    doi: 10.1021/acsbiomedchemau.2c00056

22. Tappy L. Metabolism of sugars: A window to the regulation of glucose and lipid homeostasis by splanchnic organs. *Clin Nutr.* 2021;40:1691-1698.

    doi: 10.1016/j.clnu.2020.12.022

23. Nakagawa T, Lanaspa MA, Millan IS, *et al*. Fructose contributes to the Warburg effect for cancer growth. *Cancer Metabol.* 2020;8:16.

    doi: 10.1186/s40170-020-00222-9

24. Vaupel P, Multhoff G. Revisiting the Warburg effect: Historical dogma versus current understanding. *J Physiol*. 2021;599:1745-1757.

    doi: 10.1113/JP278810

25. Ting KKY. Fructose-induced metabolic reprogramming of cancer cells. *Front Immunol*. 2024;15:1375461.

    doi: 10.3389/fimmu.2024.1375461

26. Goncalves MD, Lu C, Tutnauer J, *et al*. High-fructose corn syrup enhances intestinal tumor growth in mice. *Science.* 2019;363(6433):1345-1349.

    doi: 10.1126/science.aat8515

27. Patra KC, Hay N. The pentose phosphate pathway and cancer. *Trends Biochem Sci.* 2014;39(8):347-354.

    doi: 10.1016/j.tibs.2014.06.005

28. Liu H, Huang D, McArthur DL, Boros LG, Nissen N, Heaney AP. Fructose induces transketolase flux to promote pancreatic cancer growth. *Cancer Res*. 2010;70(15):6368-6376.

    doi: 10.1158/0008-5472.CAN-09-4615

29. Lodge M, Scheidemantle G, Adams VR, *et al*. Fructose regulates the pentose phosphate pathway and induces an inflammatory and resolution phenotype in Kupffer cells. *Sci Rep.* 2024;14:4020.

    doi: 10.1038/s41598-024-54272-w

30. Ghanem N, El-Baba C, Araji K, El-Khoury R, Usta J, Darwiche N. The pentose phosphate pathway in cancer: Regulation and therapeutic opportunities. *Chemotherapy.* 2021;66(5-6):179-191.

    doi: 10.1159/000519784

31. Jin L, Zhou Y. Crucial role of the pentose phosphate pathway in malignant tumors (Review). *Oncol Lett.* 2019;17:4213-4221.

    doi: 10.3892/ol.2019.10112

32. Jin C, Gong X, Shang Y. GLUT5 increases fructose utilization in ovarian cancer. *Onco Targets Ther.* 2019;12:5425-5436.

    doi: 10.2147/ott.s205522

33. Ma G, Liu S, Cai F, *et al*. Ketohexokinase-A deficiency attenuates the proliferation via reducing beta-catenin in gastric cancer cells. *Exp Cell Res.* 2024;438:114038.

    doi: 10.1016/j.yexcr.2024.114038

34. Cui Y, Tian J, Wang Z, *et al*. Fructose-induced mTORC1 activation promotes pancreatic cancer progression through inhibition of autophagy. *Cancer Res*. 2023;83(24):4063-4079.

    doi: 10.1158/0008-5472.CAN-23-0464

35. Huang X, Fang J, Lai W, *et al*. IL-6/STAT3 axis activates Glut5 to regulate fructose metabolism and tumorigenesis. *Int J Biol Sci.* 2022;18:3668-3675.

    doi: 10.7150/ijbs.68990

36. Lu C, Ren C, Yang T, *et al.* Fructose-1, 6-bisphosphatase 1 interacts with NF-κB p65 to regulate breast tumorigenesis via PIM2 induced phosphorylation. *Theranostics*. 2020;10:8606-8618.

    doi: 10.7150/thno.46861

37. Li M, Wang Z, Tao J, *et al*. Fructose-1,6-bisphosphatase 1 dephosphorylates and inhibits TERT for tumor suppression. *Nat Chem Biol*. 2024.

    doi: 10.1038/s41589-024-01623-3

38. Li Y, Fu Y, Zhang Y, *et al*. Nuclear fructose-1,6-bisphosphate inhibits tumor growth and sensitizes chemotherapy by targeting HMGB1. *Adv Sci* (*Weinh*). 2023;10:e2203528.

    doi: 10.1002/advs.202203528

39. Yang J, Dong C, Wu J, Liu D, Luo Q, Jin X. Fructose utilization enhanced by GLUT5 promotes lung cancer cell migration via activating glycolysis/AKT pathway. *Clin Transl Oncol.* 2023;25(4):1080-1090.

    doi: 10.1007/s12094-022-03015-2

40. Bu P, Chen KY, Xiang K, *et al*. Aldolase B-mediated fructose metabolism drives metabolic reprogramming of colon cancer liver metastasis. *Cell Metab*. 2018;27:1249-1262.

    doi: 10.1016/j.cmet.2018.04.003

41. Kim J, Kang J, Kang YL, *et al*. Ketohexokinase-A acts as a nuclear protein kinase that mediates fructose-induced metastasis in breast cancer. *Nat Commun*. 2020;11:5436.

    doi: 10.1038/s41467-020-19263-1

42. Kang YL, Kim J, Kwak SB, *et al*. The polyol pathway and nuclear ketohexokinase A signaling drive hyperglycemia-induced metastasis of gastric cancer. *Exp Mol Med*. 2024;56:220-234.

    doi: 10.1038/s12276-023-01153-3

43. Ghanbari Movahed Z, Rastegari-Pouyani M, Mohammadi MH, Mansouri K. Cancer cells change their glucose metabolism to overcome increased ROS: One step from cancer cell to cancer stem cell? *Biomed Pharmacother*. 2019;112:108690.

    doi: 10.1016/j.biopha.2019.108690

44. Park GB, Jeong JY, Kim D. GLUT5 regulation by AKT1/3-miR-125b-5p downregulation induces migratory activity and drug resistance in TLR-modified colorectal cancer cells, *Carcinogenesis.* 2020;41:1329-1340.

doi: 10.1093/carcin/bgaa074

45. Monzavi-Karbassi B, Hine RJ, Stanley JS, *et al*. Fructose as a carbon source induces an aggressive phenotype in MDA-MB-468 breast tumor cells. *Int J Oncol.* 2010;37:615-622.

doi: 10.3892/ijo_00000710

46. Zhang Y, Li Q, Huang Z, *et al*. Targeting glucose metabolism enzymes in cancer treatment: Current and emerging strategies. *Cancers* (*Basel*). 2022;14:4568.

doi: 10.3390/cancers14194568

47. Gillet L, Roger S, Besson P, *et al*. Voltage-gated sodium channel activity promotes cysteine cathepsin-dependent invasiveness and colony growth of human cancer cells. *J Biol Chem.* 2009;284:8680-8690.

doi: 10.1074/jbc.M806891200

48. Brisson L, Driffort V, Benoist L, *et al*. Na(V)1.5 Na+ channels allosterically regulate the NHE-1 exchanger and promote the activity of breast cancer cell invadopodia. *J Cell Sci.* 2013;12:4835-4842.

doi: 10.1074/jbc.M806891200

49. Busco G, Cardone RA, Greco MR, *et al*. NHE1 promotes invadopodial ECM proteolysis through acidification of the peri-invadopodial space. *FASEB J*. 2010;24:3903-3915.

doi: 10.1096/fj.09-149518

50. Magalhaes MAO, Larson DR, Mader CC, *et al*. Cortactin phosphorylation regulates cell invasion through a pH-dependent pathway. *J Cell Biol.* 2011;195:903-920.

doi: 10.1083/jcb.201103045

51. Debreova M, Csaderova L, Burikova M, *et al*. CAIX regulates invadopodia formation through both a pH-dependent mechanism and interplay with actin regulatory proteins. *Int J Mol Sci.* 2019;20:2745.

doi: 10.3390/ijms20112745

52. Bundalo M, Zivkovic M, Culafic T, Stojiljkovic M, Koricanac G, Stankovic A. Oestradiol treatment counteracts the effect of fructose-rich diet on matrix metalloproteinase 9 expression and NFκB activation. *Folia Biol* (*Praha*). 2015;61:233-240.

53. LiK, Ying M, Feng D, *et al*. Fructose-1,6-bisphosphatase is a novel regulator of Wnt/β-Catenin pathway in breast cancer. *Biomed Pharmacother*. 2016;84:1144-1149.

doi: 10.1016/j.biopha.2016.10.050

54. Xu X, Zhang M, Xu F, Jiang S. Wnt signaling in breast cancer: Biological mechanisms, challenges and opportunities. *Mol Cancer.* 2020;19:165.

doi: 10.1186/s12943-020-01276-5

55. Hsieh CL, Liu CM, Chen HA, *et al*. Reactive oxygen species-mediated switching expression of MMP-3 in stromal fibroblasts and cancer cells during prostate cancer progression. *Sci Rep.* 2017;7:9065.

doi: 10.1038/s41598-017-08835-9

56. Chang YC, Chan YC, Chang WM, *et al*. Feedback regulation of ALDOA activates the HIF-1α/MMP9 axis to promote lung cancer progression. *Cancer Lett.* 2017;403:28-36.

doi: 10.1016/j.canlet.2017.06.001

57. Cui Y, Liu H, Wang Z, *et al*. Fructose promotes angiogenesis by improving vascular endothelial cell function and upregulating VEGF expression in cancer cells. *J Exp Clin Cancer Res.* 2023;42:184.

doi: 10.1186/s13046-023-02765-3

58. Yoeli-Lerner M, Toker A. Akt/PKB signaling in cancer: A function in cell motility and invasion. *Cell Cycle.* 2006;5:603-605.

doi: 10.4161/cc.5.6.2561

59. Cheung M, Testa JR. Diverse mechanisms of AKT pathway activation in human malignancy. *Curr Cancer Drug Targets.* 2013;13:234-244.

doi: 10.2174/1568009611313030002

60. Fang JH, Chen JY, Zheng JL, *et al*. Fructose metabolism in tumor endothelial cells promotes angiogenesis by activating AMPK signaling and mitochondrial respiration. *Cancer Res.* 2023;83(8):1249-1263.

doi: 10.1158/0008-5472.CAN-22-1844

61. Peng CF, Yang P, Zhang DS, *et al*. KHK-A promotes fructose-dependent colorectal cancer liver metastasis by facilitating the phosphorylation and translocation of PKM2. *Acta Pharm Sin B.* 2024;14:2959-2976.

doi: 10.1016/j.apsb.2024.04.024

62. Gao W, Li N, Li Z, Xu J, Su C. Ketohexokinase is involved in fructose utilization and promotes tumor progression in glioma. *Biochem Biophys Res Commun.* 2018;503:1298-1306.

doi: 10.1016/j.bbrc.2018.07.040

63. Groenendyk J, Stoletov K, Paskevicius T, *et al*. Loss of the fructose transporter SLC2A5 inhibits cancer cell migration. *Front Cell Dev Biol.* 2022;10:896297.

doi: 10.3389/fcell.2022.896297

64. Yang Y, Pu J, Yang Y. Glycolysis and chemoresistance in acute myeloid leukemia. *Heliyon.* 2024;10:e35721.

doi: 10.1016/j.heliyon.2024.e35721

65. Ughachukwu P, Unekwe P. Efflux pump-mediated resistance in chemotherapy. *Ann Med Health Sci Res.* 2012;2:191-198.

doi: 10.4103/2141-9248.105671

66. Lopes-Rodrigues V, Di Luca A, Mleczko J, *et al*. Identification of the metabolic alterations associated with the multidrug resistant phenotype in cancer and their intercellular transfer mediated by extracellular vesicles. *Sci Rep.* 2017;7:44541.

doi: 10.1038/srep44541

67. Fontana F, Giannitti G, Marchesi S, Limonta P. The PI3K/Akt pathway and glucose metabolism: A dangerous liaison in cancer. *Int J Biol Sci.* 2024;20:3113-3125.

doi: 10.7150/ijbs.89942

68. Navaei ZN, Khalili-Tanha G, Zangouei AS, Abbaszadegan MR, Moghbeli M. PI3K/AKT signaling pathway as a critical regulator of Cisplatin response in tumor cells. *Oncol Res.* 2021;29:235-250.

doi: 10.32604/or.2022.025323

69. Liu R, Chen Y, Liu G, *et al*. PI3K/AKT pathway as a key link modulates the multidrug resistance of cancers. *Cell Death Dis*. 2020;11:797.

doi: 10.1038/s41419-020-02998-6

70. Bansal A, Simon MC. Glutathione metabolism in cancer progression and treatment resistance. *J Cell Biol.* 2018;217:2291-2298.

doi: 10.1083/jcb.201804161

71. Pungsrinont T, Kallenbach J, Baniahmad A. Role of PI3K-AKT-mTOR pathway as a pro-survival signaling and resistance-mediating mechanism to therapy of prostate cancer. *Int J Mol Sci*. 2021;22:11088.

doi: 10.3390/ijms222011088

72. Kuehm LM, Khojandi N, Piening A, *et al*. Fructose promotes cytoprotection in melanoma tumors and resistance to immunotherapy. *Cancer Immunol Res*. 2021;9:227-238.

doi: 10.1158/2326-6066.CIR-20-0396

73. Li H, Li M, Pang Y, Liu F, Sheng D, Cheng X. Fructose1,6bisphosphatase1 decrease may promote carcinogenesis and chemoresistance in cervical cancer. *Mol Med Rep.* 2017;16:8563-8571.

doi: 10.3892/mmr.2017.7665

74. Kawai K, Uemura M, Munakata K, *et al*. Fructose-bisphosphate aldolase A is a key regulator of hypoxic adaptation in colorectal cancer cells and involved in treatment resistance and poor prognosis. *Int J Oncol*. 2017;50:525-534.

doi: 10.3892/ijo.2016.3814

75. Li X, Jiang F, Ge Z, *et al*. Fructose-bisphosphate aldolase a regulates hypoxic adaptation in hepatocellular carcinoma and involved with tumor malignancy. *Dig Dis Sci*. 2019;64:3215-3227.

doi: 10.1007/s10620-019-05642-2

76. Huang Z, Hua Y, Tian Y, *et al*. High expression of fructose-bisphosphate aldolase A induces progression of renal cell carcinoma. *Oncol Rep.* 2018;39:2996-3006.

doi: 10.3892/or.2018.6378

77. Cunha A, Silva PMA, Sarmento B, Queirós O. Targeting glucose metabolism in cancer cells as an approach to overcoming drug resistance. *Pharmaceutics*. 2023;15:2610.

doi: 10.3390/pharmaceutics15112610

78. Chałaśkiewicz K, Karaś K, Zakłos-Szyda M, *et al*. Trichostatin A inhibits expression of the human SLC2A5 gene via SNAI1/SNAI2 transcription factors and sensitizes colon cancer cells to platinum compounds. *Eur J Pharmacol.* 2023;949:175728.

doi: 10.1016/j.ejphar.2023.175728

79. Taylor SR, Falcone JN, Cantley LC, Goncalves MD. Developing dietary interventions as therapy for cancer. *Nat Rev Cancer.* 2022;22:452-466.

doi: 10.1038/s41568-022-00485-y

80. Mohanty P, Pande B, Acharya R, Bhaskar L, Verma HK. Unravelling the triad of lung cancer, drug resistance, and metabolic pathways. *Diseases.* 2024;12:93.

doi: 10.3390/diseases12050093

ACCSCIENCE PUBLISHING

Gene & Protein in Disease

REVIEW ARTICLE

The environmental impact on aging: Insights from buccal mucosa and molecular biomarkers

Sima Ataollahi Eshkoor[1]* and Sara Fanijavadi[2]

[1]Department of Neurology, Medicin 3, Slagelse Hospital, Slagelse, Denmark

[2]Department of Oncology, Vejle Hospital, Vejle, Denmark

Abstract

Buccal epithelial cells serve as a primary barrier against the inhalation and ingestion of harmful substances, working alongside immune system cells such as natural killer cells to protect the body from health-damaging factors. These epithelial cells can also be used as an alternative tissue source for monitoring the genotoxic effects of external factors such as chemical exposure. This assessment can be performed using molecular biomarkers of aging, which reflect biological age and indicate cellular aging acceleration due to internal and external damage factors, such as environmental hazards. In contrast to chronological age, which merely reflects the passage of time, biological age accounts for individual variation in aging processes. Molecular biomarkers are crucial for distinguishing between normal and pathological processes in the body and for identifying the effects of external factors such as chemical exposures. The identification of specific biomarkers enhances the ability to detect and monitor adverse biological responses and accelerated aging. This review aims to highlight the routes through which environmental hazards enter the body, the application of buccal epithelial cells in assessing genetic modifications, and the introduction of potential molecular biomarkers. However, further research is necessary to elucidate the roles of these biomarkers in determining aging rates and individual variability. Understanding their implications may also help identify new therapeutic targets for preventing premature aging, treating age-related diseases, and developing potential treatments.

Keywords: Aging; Buccal cell; Biomarkers; DNA damage; Exposure; Hazards

***Corresponding author:**
Sima Ataollahi Eshkoor
(simaataolahi@yahoo.com)

Citation: Eshkoor SA, Fanijavadi S. The environmental impact on aging: Insights from buccal mucosa and molecular biomarkers. *Gene Protein Dis.* 2024;3(4):4418.
doi: 10.36922/gpd.4418

Received: August 2, 2024
Accepted: September 13, 2024
Published Online: October 23, 2024

1. Introduction

Aging is a complex and inevitable process characterized by the accumulation of damage caused by both internal and external factors. These factors may be endogenous, such as genetic predispositions, or exogenous, including environmental exposures and lifestyle influences.[1] Humans are continuously exposed to various health risks, including inherited, nutritional, and environmental hazards, which may lead to contact with toxic substances. These hazards, encountered in workplaces or industrial settings, have the potential to cause harmful effects, such as mutations, cancer, and congenital defects,[2] as well as accelerate the aging process through genetic and epigenetic changes.[3]

Hazardous substances enter the body through various routes such as the oral cavity.[4] The oral mucosal epithelium plays a crucial role in protecting the body from chemical,

microbial, and physical threats, serving as a barrier between external aggressors and underlying tissues.[5] Due to its constant exposure to environmental hazards, cells in this region, including buccal epithelial cells[6,7] and immune cells, such as natural killer (NK) cells,[8] are particularly valuable for studying genetic and epigenetic changes. Research on oral epithelial cells and oral immunity offers significant potential for identifying biomarkers of genetic damage, assessing the impacts of aging, and understanding susceptibility to age-related diseases.[5] By exploring genetic changes within these cells, researchers may gain insights into the mechanisms of aging and develop strategies for the early detection of age-related conditions.

2. Buccal mucosa

The oral mucosal epithelium acts as a barrier between the underlying tissues and the external environment,[5] protecting the body from chemical, microbial, and physical threats.[9] The oral epithelium consists of basal, prickle, intermediate, and superficial layers, which comprise structural, progenitor, and mature cells.[5,10] Due to constant exposure to environmental forces, oral mucosal epithelial cells undergo continuous shedding[11] and renewal.[12,13] Homeostasis in this tissue is maintained by a rich source of epithelial stem cells.[13] Cell division in the basal stem cells of the stratified squamous layer continuously replaces shedding cells.[11] Newly generated cells by mitosis in the basal layer of the oral epithelium migrate to the surface to replace the sloughed-off epithelial cells.[10] Potential risk factors for genetic damage in buccal cells include reactive oxygen species (ROS), viruses, seasonal changes, lifestyle factors, and chemical and physical conditions in residential and occupational settings.[14] As buccal cells form the first barrier to inhaled and ingested substances,[12,15,16] they can serve as an alternative tissue source for monitoring the genotoxic effects of chemical exposure[11,17,18] in occupational and environmental settings.[19-21]

In addition, the fact that 92% of human cancers originate in epithelial cells highlights their significance for research[20,22] and molecular studies. Furthermore, the direct exposure of buccal cells to environmental pollutants and their capability to metabolize carcinogens into reactive chemicals make them excellent sources for monitoring genotoxicity[22,23] and for examining the relationship between occupational exposure and biomarkers.[24] Accordingly, buccal cells are an accessible source for investigating DNA damage.[25-27] Interestingly, unlike blood lymphocytes, chromosomal damage in buccal cells continues to increase with age, potentially making them a valid biomarker for aging and a valuable resource for investigating genotoxicity and cytotoxicity parameters.[28]

In addition, molecular modifications in the immune system, including oral immunity and related immune cells such as NK cells, can be used to identify the aging process. Since the majority of human pathogens are transmitted across mucosal surfaces, including the oral mucosae, studying oral immunity and the role of NK cells in defending against pathogens is essential.[8] Buccal mucosal cells can be collected using cotton swabs, cytobrushes, the "swish and spit" method, or a modified version of the Guthrie card[29] for research related to identifying biomarkers and assessing risk factors such as exposure to environmental hazards.

3. Environmental exposure

Humans are exposed to inherited, nutritional, and environmental health risks.[30] Potentially harmful substances or situations, termed hazards,[31] can cause toxic effects.[32,33] These substances may be produced by agents in the workplace[23] and/or be prevalent in industrial areas, where they can induce mutations, cancer, and congenital defects.[30] Toxic materials typically enter the body by crossing barriers through dermal absorption, inhalation through the respiratory tract, or ingestion.[31,34-36] In occupational settings, inhalation is the most important route of entry for toxic materials, followed by dermal contact and ingestion. Ingestion is generally considered the least important route of entry.[4] Injection and ingestion are rare routes of chemical intake.[31] It appears that ingestion may offer some protective role against increased sensitivity to certain materials, such as metals.[37,38] However, chemical absorption more commonly occurs through other routes such as dermal adsorption of corrosive or irritants through the skin, respiratory tract, and eyes.[31]

Hazards can cause toxicological effects, including lethal or irreversible non-lethal outcomes, such as mutagenic effects after repeated or long-term exposure. The health effects of chemical exposures can be acute, chronic, local, systemic, reversible, or irreversible. The adverse biological effects of hazards are classified as very toxic, toxic, harmful, corrosive, and irritant.[31] Figure 1 illustrates the entry routes and health effects of chemical exposures. The severity of damage caused by hazards depends on the toxicity level of the chemicals, the duration of exposure, the route of entry, and the individual's susceptibility to chemical effects (Table 1).

Since toxic exposure in occupational environments can cause numerous health problems,[32,33] early identification of potential hazards is of utmost importance.[33] Workplace conditions and workers' behaviors are two major factors that increase the risk of toxic damage.[31] For example, activities such as washing hands with petrol and contaminated

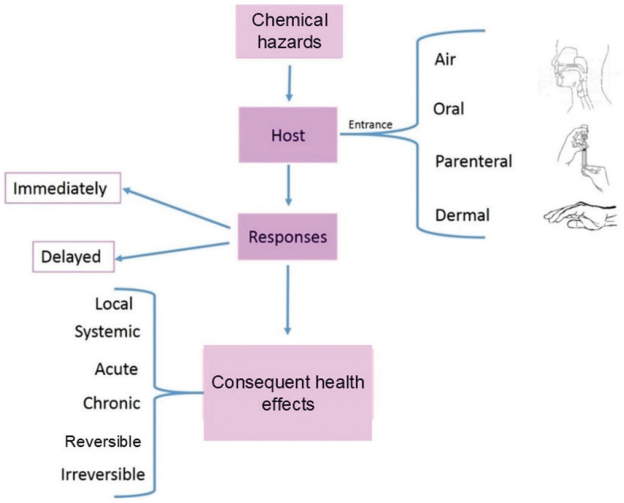

Figure 1. Entry routes of chemicals into the body and related reactions

Table 1. Factors affecting the toxicity level of chemicals in the body

Factors	Characteristics
Host	Age, heredity, gender, health status, immunology, nutrition, and hormones
Exposure dose	Concentration, rate of exposure, route of exposure, and duration
Chemicals properties	Composition (salt, free base, etc.), physical characters (particle size, liquid, solid, etc.), physical properties (instability, solubility, etc.), presence of impurities, breakdown product, and carrier
Others	Combination of chemicals, carrier

water,[30] inhaling toxic vapors,[39] and exposure to brake lining products[40] and engine ignitions can elevate the risk of genotoxicity in mechanical workshops.[30,41-45] Workers are primarily exposed to complex chemical mixtures of organic or inorganic compounds in the forms of gases, vapors, fumes, mist, and particles.[41] Once these chemicals enter or come into contact with the body, they can induce cytotoxic and genotoxic effects,[30,41-45] leading to health damage.[34-36] For instance, exposure to high concentrations of diesel exhaust is associated with an increased risk of lung and gastric cancers.[46]

One of the known health damages of environmental exposure is premature aging, which is associated with changes in metabolic rates and the body's ability to activate, detoxify, and excrete xenobiotic compounds. These changes can affect the extent of damage and toxicity, as well as the rate of aging.[47,48] In addition, environmental exposure can result in modifications in the activation of immune system cells, including NK cells,[49,50] whose maintenance is essential for healthy aging.[49]

Accordingly, occupational health is a major societal concern. Further studies are needed to identify genotoxic agents at environmental exposures, particularly in occupational settings, to protect the body from health damage.[41,51] Developing strategies to improve health and safety in workplaces, such as mechanical workshops, is essential.[46] In addition, actions should be taken to either reduce the levels of harmful chemicals or increase the protection of exposed individuals to minimize adverse health effects.[30] For instance, diluting chemicals or using less toxic substances can reduce the risk of toxicity[51] and genotoxic effects from chemical hazards.[37,52-55] These measures can help protect the body from molecular modifications caused by hazardous chemical exposure, which may accelerate biological aging.[3]

4. Aging process

Aging results from the cumulative effects of damage caused by endogenous and exogenous factors.[48,56] It can be defined in terms of both chronological and biological aging. Chronological age is measured from birth and indicates the time a person has lived. While it is linked to declining health, morbidity, and mortality, it does not accurately reflect the internal biological processes or individual variation. Therefore, the focus has shifted toward using biological markers of aging to measure biophysiological aging processes and determine biological age, which reflects the aging of cells within the body. The concept of "aging biomarkers" was first introduced by Baker and Sprott[57] in 1988 to predict functional capability based on biological parameters.

However, aging transitions an organism from full maturity to death, diminishing reproductive capability and survival.[58] It occurs in both unicellular and multicellular organisms,[59] progressing differently across tissues due to specific intrinsic cellular mechanisms. There is ongoing debate regarding whether aging originates from a specific tissue, such as the brain,[60] or affects all tissues simultaneously.[61] Despite this, aging is known to start at the cellular level due to DNA damage and reduced DNA repair capacity.[62,63] Senescent cells remain metabolically active but, morphologically, exhibit an increased volume and a flattened cytoplasm, accompanied by changes in gene expression, nuclear structure, protein processing, and metabolism.[64] Various factors, especially ROS and nitrogen species such as hydroxyl radicals, peroxyl radicals, ozone, and nitrogen oxides, induce oxidative stress, leading to DNA damage, accelerated aging, and age-related health issues.[65] The accumulation of ROS[66] and toxic metabolic byproducts in the body results in decreased physiological function, loss of homeostasis,[58] tissue atrophy, neoplasms, and reduced organ and tissue function.[67] ROS contribute to aging by causing DNA damage, mitochondrial

dysfunction, and altering protein and lipid content in the body (Figure 2). Aging has also been linked to changes in DNA methylation levels and epigenetic modifications, both of which are influenced by environmental factors such as occupational exposures. The effects of ROS on aging are thought to be mediated through histone modification and DNA methylation, processes that contribute to the regulation of gene expression.[68]

Molecular modifications in immune cells, such as NK cells, can play a critical role in the initiation and progression of senescence and age-related diseases,[69] including infection, malignancies, and inflammatory disorders. These changes are consequences of decreased immune system function and a process known as inflammaging, which refers to the chronic, low-grade inflammation associated with aging.[70] Therefore, NK cells in the buccal mucosa provide an interesting resource for assessing aging in the body.[8]

Exposure to environmental hazards can transform normal cells into abnormal ones[71] by interacting with genetic material and changing DNA and/or RNA in cells.[72] These genetic alterations can affect cellular functions, including those of immune system cells such as NK cells.[50] This transformation may occur within a latency period of 4 – 40 years following initial exposure.[71] As aging is a time-related process resulting from life-long exposure to low and natural levels of environmental agents, regular exposure to chemicals in daily occupational activities poses a higher risk of premature aging, health damage, and decreased productivity.[67] Biomarkers of aging and biological aging can assess these risks, reflecting individual-specific age-related vulnerabilities, physiological function, and overall health.[3]

5. Related molecular biological markers of aging

Aging is a heterogeneous process, with significant variability in health outcomes among individuals of the same chronological age. At the individual level, different cells, tissues, and organs age at different trajectories. Biological aging can be affected by exposure to chemical hazards, particularly through DNA damage in cells such as buccal cells, which serve as the first line of defense against foreign particles entering the body.[9]

DNA damage resulting from both internal and external factors poses a significant threat to living cells.[73] Genotoxic agents derived from exogenous or endogenous sources – including UV light, ionizing radiation, chemicals, and the intrinsic biochemical instability of DNA – can disrupt cellular homeostasis by causing DNA damage[74,75] and altering its chemical structure.[76] DNA damage, along with chromosomal changes caused by mutations, DNA adducts, DNA breaks, and alkali-labile sites,[77] can trigger[78] and accelerate the aging process.[77] The effects of chemical exposure on genotoxic materials can be monitored[30] using biomarkers, which assess molecular and cellular events in biological systems.[79,80] These biomarkers, as listed in Table 2, are categorized into three groups: exposure, susceptibility, and early effects[24,81] (Figure 3).

Exposure biomarkers measure substances, metabolites, or products resulting from the interaction of target molecules with tissue, reflecting external and/or internal

Table 2. Types of biomarkers

Biomarkers	Description
Exposure	Biomarkers of internal dose, biomarkers of biologically effective dose (e.g., DNA adducts)
Effect	DNA breaks, chromosome aberrations, micronuclei, sister chromatic exchange, biochemical effects, oxidative damage, DNA repair enzymes, metal-binding proteins
Susceptibility	Single nucleotide polymorphisms, telomere length, epigenetics, metabolism enzyme induction, varying DNA repair capacity

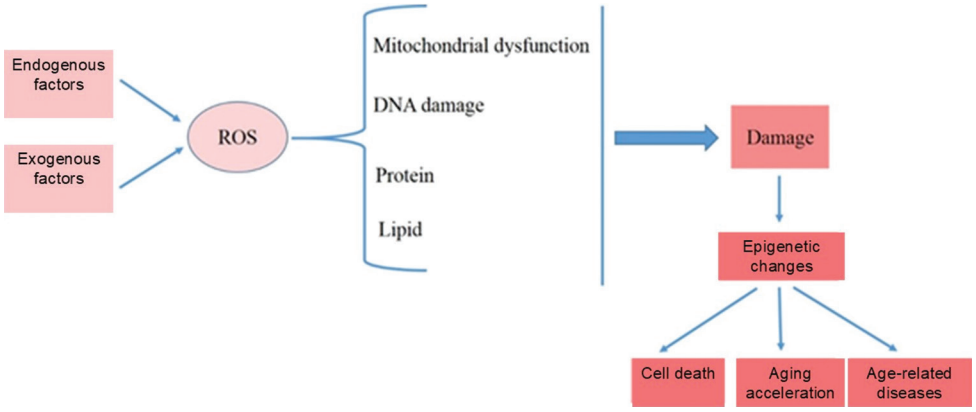

Figure 2. A schematic representation of reactive oxygen species effects on cellular senescence

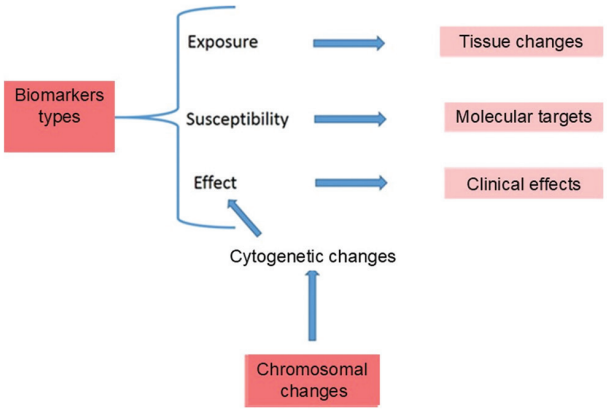

Figure 3. Biomarkers associated with environmental exposure

exposures.[24,82,83] These biomarkers indicate short-term DNA or chromosomal damage in cytogenetic analyses[30] and serve as sensitive indicators of recent human exposures to hazards.[84] Consequently, the potential risk posed by hazards and their ability to induce long-term health problems can be determined.[30] Biomarkers of effect show early health effects, such as health impairment and critical and clinical effects.[24,82,83] Biomonitoring the effects of exposure through various cytogenetic tests enables the evaluation of genotoxic effects by detecting DNA damage, such as sister chromatid exchange and micronuclei.[46] Micronuclei, an example of such biomarkers,[84] are formed due to chromosomal damage,[85] typically arising from chromosomal fragmentation or lagging.[86] This biomarker is evaluated in cells, such as buccal cells, and reflects genotoxic damage in the dividing basal cell layer of target organs 1 – 3 weeks earlier.[46] Micronucleus levels tend to increase with age.[86] The first effective biomarkers used to assess the aging process were micronuclei, sister chromatid exchange, and chromosome aberrations.[77]

Biomarkers of susceptibility indicate an individual's increased sensitivity to specific target molecules or metabolic processes, leading to a higher dose of the target compound upon exposure.[24,82,83] These biomarkers reveal the inherent or acquired capability of an organism to metabolize xenobiotic substances upon chemical exposure, resulting in variations in metabolic pathways and toxic responses among individuals. Examples of susceptibility biomarkers include cytochrome P-450 (CYPs) and glutathione transferases (GSTs).[87] Telomere shortening and epigenetic modifications are also included in this group.[88] Epigenetic biomarkers reflect stable changes to the genome that affect gene expression or silencing.[3,89] Factors such as DNA methylation levels, cell metabolism, and signal transmission control through epigenetic mechanisms play significant roles in human longevity.[68]

Moreover, changes in biomarkers related to NK cells, such as cytokines, including interferon (IFN)-γ, IFN-β, and interleukins (IL-2), as well as alterations in NK cell types, are associated with aging. NK cells may also exhibit telomere shortening, a marker of aging,[70] which can be investigated using buccal cells. This approach enhances our understanding of aging and age-related diseases and aids in designing future immune therapies targeting NK cells in the elderly population.[69] Identifying reliable biomarkers is crucial for accurate risk stratification and exploring antiaging interventions.[3] Given the challenge of pinpointing a single biomarker that reflects the intricate interaction between environmental exposures and aging, further studies are needed to identify biomarkers sensitive to mixed or low-dose exposures. In addition, a combination of biomarkers reflecting various levels of cellular organization, such as DNA, RNA, and proteins, may provide the most effective approach.

6. Interaction between molecular biomarkers and aging

Genomic damages after exposure to chemicals can occur in two forms: (i) point mutations at the nucleotide level in a gene and (ii) structural changes in chromosomes, such as chromosomal aberrations.[90] Two major perspectives on senescence include: (i) a specific genetic program for senescence and (ii) evolutionary forces, particularly reproductive success, that suggest a genetic basis for senescence.[58] Senescence results from the coordinated actions of multiple genes, and mutations in these genes can lead to premature aging.[67]

Genetic analysis of aging helps identify regulatory links between gene expressions and lifespan,[91] involving pathways such as insulin/IGF-1 signaling, PI3K, TOR, MAPK, AMPK, PKC, NF-κb, TGF-β, Notch, WNT, S6K,[92-96] and the p53/p21 and p16INK4A/pRb pathways.[64] The p16INK4A/pRb pathway can lead to premature senescence or stress-induced premature senescence. Oncogene-induced senescence is characterized by the activation of pathways involving p53 and DNA damage and is marked by tumor progression restriction without telomere shortening.[64]

DNA repair pathways play an important role in correcting damage caused by mutagens, such as DNA damage[73] and chromosomal alterations,[79] which pose significant threats to living cells. These repair processes involve cell cycle regulation[97] and mechanisms such as the SOS response,[76] utilizing ATP and NADH to remove DNA lesions.[62] It is estimated that over 130 genes in the human genome are involved in DNA repair,[98] with more than 70 genes contributing directly to the major nuclear DNA repair pathways.[99] Mutations in these repair genes

can trigger premature aging syndromes, such as Werner syndrome, Cockayne syndrome, Bloom's syndrome, and ataxia telangiectasia, suggesting possible roles of replicative senescence genes in the aging process.[62] *CDK6*, *CCND1*, and *p16* are examples of such genes that contribute to aging.[100] The *CDK6* and *CCND1* genes play crucial roles in regulating the cell cycle through the retinoblastoma pathway[101] and in growth arrest alongside the *p16* and *Rb* genes. During senescence, the *Rb* and *p53* genes are activated but gradually lose their ability to regulate cell proliferation.[91]

Many genes involved in aging are primarily located on chromosomes 1, 4, 6, 7, and 20. Telomerase suppressor genes are found on chromosomes 3 and 4, whereas the *WRN* gene, which is associated with Werner syndrome and premature aging, is localized on chromosome 8.[62] Several genes also serve as biomarkers for susceptibility to environmental damage.[102] This group includes genes from the CYP and GST families, which are crucial for the metabolism and detoxification of environmental hazards and xenobiotics.[103,104] CYP enzymes contribute to phase I xenobiotic metabolism by oxidizing compounds, leading to the formation of active substances and highly reactive mutagenic metabolites.[105] Key members of this group include CYP1A1, CYP1A2, and CYP2E1. While CYP1A1[104] and CYP1A2[105] have been documented to potentially offer protective effects against DNA damage and aging, some reports suggest paradoxical effects, particularly for CYP1A1.[106] For instance, polymorphisms in *CYP2E1* have been shown to impact aging[24,107] by inducing DNA damage.[107-109] The GST family, also involved in xenobiotic metabolism, detoxifies xenobiotics.[110] Notable members include the *GSTT1*, *GSTM1*, and *GSTP1* genes, which have been studied for their effects on aging. For instance, the absence of GSTM1[103] and GSTT1[83,102] has been associated with aging, and polymorphisms in the *GSTP1* gene have demonstrated both progressive[24,111,112] and non-progressive effects[24,113] on the aging process.

Another significant activator of cellular senescence is telomere dysfunction, which operates through the G1 DNA damage checkpoint and the upregulation of p21/p16. Telomeres are complex DNA-protein structures at the ends of eukaryotic chromosomes, and their shortening serves as a marker of DNA damage in cells.[88] By capping chromosome ends, telomeres prevent nucleolytic degradation, end-to-end fusion, irregular recombination, and other lethal cellular events.[114] Telomere length is inversely correlated with age[114] and shortens in all replicating somatic cells,[88] including NK cells, which are crucial for recognizing and eliminating senescent cells. As telomere shortening progresses with age, it gradually impairs NK cell function.[115] The functional activities of NK cells, such as cytokine production in $CD56^{bright}$ cells and cytotoxic activity in $CD56^{dim}$ cells, shift with aging – $CD56^{bright}$ cells decrease whereas $CD56^{dim}$ cells increase.[116]{Weber, 2024 #118} This shift results in impaired immunity and a heightened risk of age-related diseases.[117] These changes are associated with declines in biomarkers such as IL-2, IL-15, and $CD56^{bright}$, alongside increases in others such as IL-6,[70] IFN-γ,[118] and CD38,[119] all of which contribute to accelerated aging and age-related health issues. Consequently, these changes lead to a weakened immune response and increased inflammation associated with aging, making NK cells a significant target for interventions aimed at mitigating age-related immune decline. In addition, the function of NK

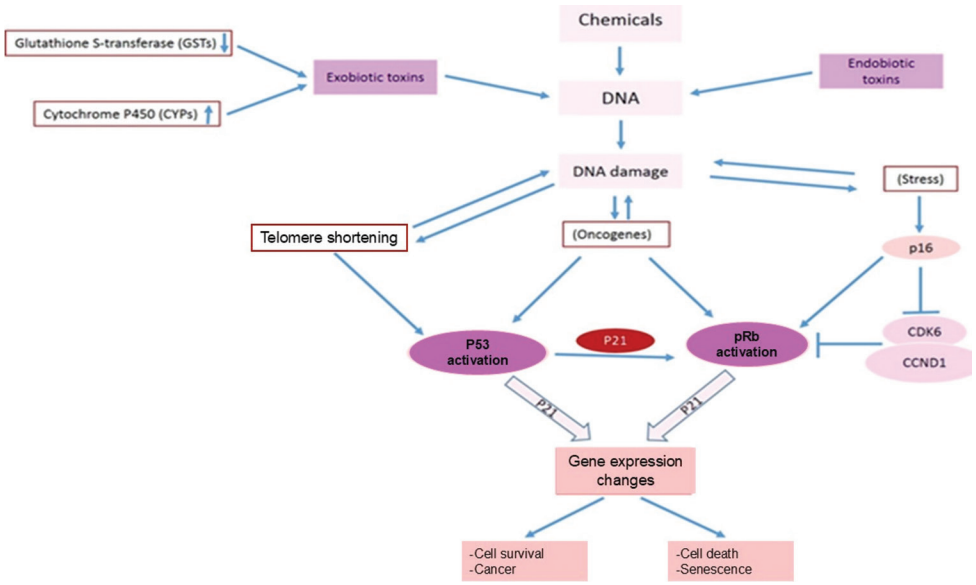

Figure 4. Consequences of DNA damage following chemical exposure

Table 3. Examples of biomolecular changes in aging

Type	Effect	Examples	References
Pathways	Mediated cell survival, growth, and DNA repair	AKT1, ATM, FOXO1, FOXO3, GHR, HIF1A, IGF1, IGF1R, PIK3CA, and PIK3CB	96
	Mediated apoptosis/senescence signaling pathway	BAX, BCL2, CDK4, CDK6, CDKN1A (P21), CDKN2A (P16), CDKN2B (P15), FAS, and TP53	96
	Autophagy/Survival	AMPK subunits (PRKAA1, PRKAA2, PRKAB2, PRKAG1, PRKAG2), SIRT1, RPS6KB1 (S6K), and TSC2	96
	Cross-talk between the aging pathways	KL, MYC, NFKB1, NFKB2, PPARGC1A, PTEN, TGFB1, and TGFBR2	96
	Sirtuins are involved in metabolic control, apoptosis, cell survival, development, inflammation, and healthy aging	Sir2, SIRT1, PGC-1α, Ku70, NF-κB, AceCS1, MEF2 and p53, FOXO transcription factors	127
	Lifespan regulation through mitochondrial DNA	PGC-1α, PGC-1β, NRF-1, and ERRα	127
	Stable housekeeping genes in aging	*18s, HPRT1, ACTB*, and *TMEM199*	128,129
Epigenetics	DNA methylation, histone modifications, non-coding RNAs		130
Natural killer cells in the buccal mucosa ($CD56^{dim}$ cells and $CD56^{bright}$ cells)	Biomarkers modifications during aging	IFN-γ, TNF-α, TNF-β, GM-CSF, CXCR3, CCR6, CCR9, CCR4, IL-10, IL-4, IL6, IL-13, IL-2, IL-15, and IL-12	69,70,117,131-137

Abbreviations: IFN-γ: Interferon-γ; TNF-α: Tumor necrosis factor-α; TNF-β: Tumor necrosis factor-β; IL: Interleukin.

cells[120] and the aging process[121] can be regulated through epigenetic changes in the body.

Epigenetics, including DNA methylation, histone modifications, and non-coding RNAs,[122] plays a crucial role in the regulation of aging. These epigenetic modifications are key regulators of gene expression[122] and influence cellular responses to environmental exposures,[99] as well as changes associated with aging.[122] Various environmental factors, such as diet, exposure to toxins, stress, smoking, and childhood trauma, can significantly impact individual epigenetic clocks and gene regulation.[123] These changes are directly linked to longevity across a wide range of organisms, from yeast to humans.[124]

Exposure to environmental chemicals can lead to changes in epigenetic biomarkers and genome function,[125,126] which accelerate aging by influencing caloric restriction, mitochondrial function, the activity of housekeeping genes, and metabolic enzyme control.[122] Figure 4 illustrates how these factors contribute to cellular senescence. Despite these findings, further efforts are needed to identify the genetic and epigenetic factors that contribute to aging and to determine their precise effects, thereby expanding the list of contributing factors (Table 3).

7. Conclusion

Given the profound impact of aging on mortality and disease susceptibility, researchers are continually developing non-invasive methods and identifying molecular biomarkers to monitor cellular damage caused by both external and internal factors. Environmental hazards are well-documented contributors to aging, leading to DNA damage and premature aging, which, in turn, increase the incidence of diseases and premature mortality. As a result, molecular biomarkers are being investigated for their potential to assess DNA damage in cells, including buccal and NK cells found in the oral mucosa, to enable the screening and diagnosis of individuals at risk of premature aging. This review aims to clarify the intricate relationship between environmental hazards, cellular senescence, and DNA damage, thereby aiding in the development of diagnostic and preventive measures. Further research is essential to fully understand the role of biomarkers in assessing DNA damage during aging and to identify new targets for strategies aimed at preventing and treating premature aging and age-related health issues.

Acknowledgments

The authors would like to acknowledge Dr. Johannes Martin Schmid from the Department of Respiratory Diseases and Allergy, Aarhus University Hospital, for his support in editing the English of this paper.

Funding

None.

Conflict of interest

The authors declare they have no competing interests.

Authors contributions

Conceptualization: All authors
Writing-original draft: All authors
Writing-review & editing: All authors

Ethics approval and consent to participate

Not applicable.

Consent for publication

Not applicable.

Availability of data

Not applicable.

References

1. Rodríguez-Rodero S, Fernández-Morera JL, Menéndez-Torre E, Calvanese V, Fernández AF, Fraga MF. Aging genetics and aging. *Aging Dis*. 2011;2(3):186-195.
2. Tulchinsky TH, Varavikova EA. Environmental and occupational health. In: *The New Public Health*. Amsterdam: Elsevier; 2014. p. 471.
3. Chen R, Wang Y, Zhang S, *et al*. Biomarkers of ageing: Current state-of-art, challenges, and opportunities. *MedComm Futur Med*. 2023;2:e50.

   doi: 10.1002/mef2.50
4. Cherrie JW, Semple S, Christopher Y, Saleem A, Hughson GW, Philips A. How important is inadvertent ingestion of hazardous substances at work? *Ann Occup Hyg*. 2006;50(7):693-704.

   doi: 10.1093/annhyg/mel035
5. Groeger S, Meyle J. Oral mucosal epithelial cells. *Front Immunol*. 2019;10:208.

   doi: 10.3389/fimmu.2019.00208
6. Farah R, Haraty H, Salame Z, Fares Y, Ojcius DM, Sadier NS. Salivary biomarkers for the diagnosis and monitoring of neurological diseases. *Biomed J*. 2018;41(2):63-87.

   doi: 10.1016/j.bj.2018.03.004
7. Langie SA, Moisse M, Declerck K, *et al*. Salivary DNA methylation profiling: Aspects to consider for biomarker identification. *Basic Clin Pharmacol Toxicol*. 2017;121:93-101.

   doi: 10.1111/bcpt.12721
8. Li H, Reeves RK. Functional perturbation of classical natural killer and innate lymphoid cells in the oral mucosa during SIV infection. *Front Immunol*. 2013;3:417.

   doi: 10.3389/fimmu.2012.00417
9. Handajani J, Tabtila U, Auliawati NR, Rohman A. Characterization of buccal cell DNA after exposure to azo compounds: A cross-sectional study. *F1000Res*. 2020;9:1053.

   doi: 10.12688/f1000research.25798.2
10. Celik A, Cavas T, Ergene-Gozukara S. Cytogenetic biomonitoring in petrol station attendants: Micronucleus test in exfoliated buccal cells. *Mutagenesis*. 2003;18(5):417-421.

    doi: 10.1093/mutage/geg022
11. Surralles J, Autio K, Nylund L, *et al*. Molecular cytogenetic analysis of buccal cells and lymphocytes from benzene-exposed workers. *Carcinogenesis*. 1997;18(4):817-823.

    doi: 10.1093/carcin/18.4.817
12. Holland N, Bolognesi C, Kirsch-Volders M, *et al*. The micronucleus assay in human buccal cells as a tool for biomonitoring DNA damage: The HUMN project perspective on current status and knowledge gaps. *Mutat Res*. 2008;659(1):93-108.

    doi: 10.1016/j.mrrev.2008.03.007
13. Papagerakis S, Pannone G, Zheng L, *et al*. Oral epithelial stem cells - Implications in normal development and cancer metastasis. *Exp Cell Res*. 2014;325(2):111-129.

    doi: 10.1016/j.yexcr.2014.04.021
14. Eshkoora SA, Ismail P, Rahman SA, Moin S, Adon MY. The association of DNA damage level with early age at the occupational exposure in the mechanical workshops workers. *Asian J Biotechnol*. 2012;4(2):83-91.

    doi: 10.3923/ajbkr.2012.83.91
15. Motgi AA, Chavan MS, Diwan NN, Chowdhery A, Channe PP, Shete MV. Assessment of cytogenic damage in the form of micronuclei in oral epithelial cells in patients using smokeless and smoked form of tobacco and non-tobacco users and its relevance for oral cancer. *J Cancer Res Ther*. 2014;10(1):165-170.

    doi: 10.4103/0973-1482.131454
16. Pradeep M, Guruprasad Y, Jose M, Saxena K, Deepa K, Prabhu V. Comparative Study of genotoxicity in different tobacco related habits using micronucleus assay in exfoliated buccal epithelial cells. *J Clin Diagn Res*. 2014;8(5):ZC21-ZC24.

    doi: 10.7860/JCDR/2014/8733.4357
17. Spivack SD, Hurteau GJ, Jain R, *et al*. Gene-environment interaction signatures by quantitative mRNA profiling in exfoliated buccal mucosal cells. *Cancer Res*. 2004;64(18):6805-6813.

    doi: 10.1158/0008-5472.CAN-04-1771
18. Chen C, Arjomandi M, Qin H, Balmes J, Tager I, Holland N. Cytogenetic damage in buccal epithelia and peripheral lymphocytes of young healthy individuals exposed to ozone. *Mutagenesis*. 2006;21(2):131-137.

doi: 10.1093/mutage/gel007

19. Manikantan P, Balachandar V, Sasikala K, Mohanadevi S. DNA damage in viscose factory workers occupationally exposed to carbon di-sulfide using buccal cell comet assay. *Braz J Oral Sci*. 2009;8(4):197-200.

doi: 10.20396/bjos.v8i4.8642078

20. Rajkokila K, Shajithanoop S, Usharani MV. Nuclear anomalies in exfoliated buccal epithelial cells of petrol station attendants in Tamilnadu, South India. *J Med Genet Genomics*. 2010;2(2):18-22.

21. Lorenzoni DC, Pinheiro LP, Nascimento HS, *et al*. Could formaldehyde induce mutagenic and cytotoxic effects in buccal epithelial cells during anatomy classes? *Med Oral Patol Oral Cir Bucal*. 2017;22(1):e58.

doi: 10.4317/medoral.21492

22. Salama SA, Serrana M, Au WW. Biomonitoring using accessible human cells for exposure and health risk assessment. *Mutat Res*. 1999;436(1):99-112.

doi: 10.1016/s1383-5742(98)00021-0

23. Eshkoor SA, Ismail P, Rahman SA, Moin S, Adon MY. Occupational exposure as a risk factor to enhance the risk of early ageing. *Asian J Biotechnol*. 2011;3(6):573-580.

doi: 10.3923/ajbkr.2011.573.580

24. Heuser VD, Erdtmann B, Kvitko K, Rohr P, da Silva J. Evaluation of genetic damage in Brazilian footwear-workers: Biomarkers of exposure, effect, and susceptibility. *Toxicology*. 2007;232(3):235-247.

doi: 10.1016/j.tox.2007.01.011

25. Borthakur G, Butryee C, Stacewicz-Sapuntzakis M, Bowen PE. Exfoliated buccal mucosa cells as a source of DNA to study oxidative stress. *Cancer Epidemiol Biomarkers Prev*. 2008;17(1):212-219.

doi: 10.1158/1055-9965.EPI-07-0706

26. Hearn R, Arblaster K. DNA extraction techniques for use in education. *Biochem Mol Biol Educ*. 2010;38(3):161-166.

doi: 10.1002/bmb.20351

27. Toy E, Yuksel S, Ozturk F, Karatas OH, Yalcin M. Evaluation of the genotoxicity and cytotoxicity in the buccal epithelial cells of patients undergoing orthodontic treatment with three light-cured bonding composites by using micronucleus testing. *Korean J Orthod*. 2014;44(3):128-135.

doi: 10.4041/kjod.2014.44.3.128

28. Franzke B, Schober-Halper B, Hofmann M, *et al*. Chromosomal stability in buccal cells was linked to age but not affected by exercise and nutrients-Vienna Active Ageing Study (VAAS), a randomized controlled trial. *Redox Biol*. 2020;28:101362.

doi: 10.1016/j.redox.2019.101362

29. Michalczyk A, Varigos G, Smith L, Ackland ML. Fresh and cultured buccal cells as a source of mRNA and protein for molecular analysis. *Biotechniques*. 2004;37(2):262-269.

doi: 10.2144/04372RR03

30. Martino-Roth MG, Viegas J, Amaral M, Oliveira L, Ferreira FLS, Erdtmann B. Evaluation of genotoxicity through micronuclei test in workers of car and battery repair garages. *Genet Mol Biol*. 2002;25(4):495-500.

doi: 10.1590/S1415-47572002000400021

31. Herber RFM, Duffus JH, Christensen JM, Olsen E, Park MV. Risk assessment for occupational exposure to chemicals. A review of current methodology (IUPAC technical report). *Pure Appl Chem*. 2001;73(6):993-1031.

doi: 10.1351/pac200173060993

32. Fairhurst S. Hazard and risk assessment of industrial chemicals in the occupational context in Europe: Some current issues. *Food Chem Toxicol*. 2003;41(11):1453-1462.

doi: 10.1016/S0278-6915(03)00193-5

33. Hassim MH, Hurme M. Occupational chemical exposure and risk estimation in process development and design. *Process Saf Environ Prot*. 2010;88(4):225-235.

doi: 10.1016/j.psep.2010.03.011

34. Dinman BD, Dinman JD. The mode of absorption, distribution, and elimination of toxic materials. In: Harris RL, editor. *Patty's Industrial Hygiene*. New York: John Wiley & Son Inc.; 2000.

doi: 10.1002/0471435139.hyg003

35. Borm PJA, Robbins D, Haubold S, *et al*. The potential risks of nanomaterials: A review carried out for ECETOC. *Part Fibre Toxicol*. 2006;3:11.

doi: 10.1186/1743-8977-3-11

36. Nielsen GD, Ovrebo S. Background, approaches and recent trends for setting health-based occupational exposure limits: A minireview. *Regul Toxicol Pharmacol*. 2008;51(3):253-269.

doi: 10.1016/j.yrtph.2008.04.002

37. Artik S, Haarhuis K, Wu X, Begerow J, Gleichmann E. Tolerance to nickel: Oral nickel administration induces a high frequency of anergic T cells with persistent suppressor activity. *J Immunol*. 2001;167(12):6794-6803.

doi: 10.4049/jimmunol.167.12.6794

38. Rustemeyer T, de Groot J, von Blomberg BME, Frosch PJ, Scheper RJ. Induction of tolerance and cross-tolerance to methacrylate contact sensitizers. *Toxicol Appl Pharmacol*. 2001;176(3):195-202.

doi: 10.1006/taap.2001.9266.

39. Moller P, Knudsen LE, Loft S, Wallin H. The Comet assay as a rapid test in biomonitoring occupational exposure to DNA-damaging agents and effect of confounding factors.

Cancer Epidemiol Biomarkers Prev. 2000;9(10):1005-1015.

40. Keshava N, Ong TM. Occupational exposure to genotoxic agents. *Mutat Res*. 1999;437(2):175-194.

doi: 10.1016/s1383-5742(99)00083-6

41. Benites CI, Amado LL, Vianna RAP, Martino-Roth MG. Micronucleus test on gas station attendants. *Genet Mol Res*. 2006;5(1):45-54.

42. Conaway CC, Schreiner CA, Cragg ST. *Mutagenicity Evaluation of Petroleum Hydrocarbons*. Vol. 7. New Jersey: Princeton Scientific Publishers Inc.; 1984. p. 1-302.

43. Loury DJ, Smith-Oliver T, Strom S, Jirtle R, Michalopoulos G, Butterworth BE. Assessment of unscheduled and replicative DNA synthesis in hepatocytes treated *in vivo* and *in vitro* with unleaded gasoline or 2,2,4-trimethylpentane. *Toxicol Appl Pharmacol*. 1986;85(1):11-23.

doi: 10.1016/0041-008x(86)90383-2

44. Nylander PO, Olofsson H, Rasmuson B, Svahlin H. Mutagenic effects of petrol in *Drosophila* melanogaster I. Effects of benzene and 1, 2-dichloroethane. *Mutat Res*. 1978;57(2):163-167.

doi: 10.1016/0027-5107(78)90263-4

45. Pitarque M, Carbonell E, Xamena N, Creus A, Marcos R. Genotoxicity of commercial petrol samples in cultured human lymphocytes. *Rev Int Contam Ambient*. 1997;13(1):15-21.

46. Garcia PV, Linhares D, Amaral AFS, Rodrigues AA. Exposure of thermoelectric power-plant workers to volatile organic compounds from fuel oil: Genotoxic and cytotoxic effects in buccal epithelial cells. *Mutat Res*. 2012;747(2):197-201.

doi: 10.1016/j.mrgentox.2012.05.008

47. Thomas RD. Age-specific carcinogenesis: Environmental exposure and susceptibility. *Environ Health Perspect*. 1995;103(Suppl 6):45-48.

doi: 10.1289/ehp.95103s645

48. Yin D, Chen K. The essential mechanisms of aging: Irreparable damage accumulation of biochemical side-reactions. *Exp Gerontol*. 2005;40(6):455-465.

doi: 10.1016/j.exger.2005.03.012

49. Tsao T, Tsai M, Hwang J, *et al*. Health effects of a forest environment on natural killer cells in humans: An observational pilot study. *Oncotarget*. 2018;9(23):16501-16511.

doi: 10.18632/oncotarget.24741

50. De Celis R, Feria-Velasco A, Bravo-Cuellar A, *et al*. Expression of NK cells activation receptors after occupational exposure to toxics: A preliminary study. *Immunol Lett*. 2008;118(2):125-131.

doi: 10.1016/j.imlet.2008.03.010

51. Unnikrishnan S, Hegde DS. An analysis of cleaner production and its impact on health hazards in the workplace. *Environ Int*. 2006;32(1):87-94.

doi: 10.1016/j.envint.2005.05.023

52. Stokinger HE. Concepts of thresholds in standards setting. An analysis of the concept and its application to industrial air limits (TLVs). *Arch Environ Health*. 1972;25(3):153-157.

doi: 10.1080/00039896.1972.10666154

53. Zielhuis RL, Notten WRF. Permissible levels for occupational exposure; Basic concepts. *Int Arch Occup Environ Health*. 1979;42(3-4):269-281.

doi: 10.1007/BF00377781

54. Henschler D. Exposure limits: History, philosophy, future developments. *Ann Occup Hyg*. 1984;28(1):79-92.

doi: 10.1093/annhyg/28.1.79

55. Hunter WJ, Aresini G, Haigh R, Papadopoulos P, von der Hude W. Occupational exposure limits for chemicals in the European Union. *Occup Environ Med*. 1997;54(4):217-222.

doi: 10.1136/oem.54.4.217

56. Semsei I. On the nature of aging. *Mech Ageing Dev*. 2000;117(1):93-108.

doi: 10.1016/s0047-6374(00)00147-0

57. Baker GT 3rd, Sprott RL. Biomarkers of aging. *Exp Gerontol*. 1988;23(4-5):223-239.

doi: 10.1016/0531-5565(88)90025-3

58. Crews DE. *Human Senescence Evolutionary and Biocultural Perspectives*. Columbus, Ohio, U.S.A: Ohio State University, Cambridge University Press; 2004. p. 302.

59. Bowen RL, Atwood CS. Living and dying for sex. A theory of aging based on the modulation of cell cycle signaling by reproductive hormones. *Gerontology*. 2004;50(5):265-290.

doi: 10.1159/000079125

60. Mattson MP, Duan W, Maswood N. How does the brain control lifespan? *Ageing Res Rev*. 2002;1(2):155-165.

doi: 10.1016/s1568-1637(01)00003-4

61. Kowald A, Kirkwood TB. Towards a network theory of ageing: A model combining the free radical theory and the protein error theory. *J Theor Biol*. 1994;168(1):75-94.

doi: 10.1006/jtbi.1994.1089

62. Wojda A, Witt M. Manifestations of ageing at the cytogenetic level. *J Appl Genet*. 2003;44(3):383-399.

63. Yadav JS, Chhillar AK. Cytogenetic damage in individuals exposed to vehicular pollution. *Int J Hum Genet*. 2002;2(2):113-117.

doi: 10.1080/09723757.2002.11885797

64. Shawi M, Autexier C. Telomerase, senescence and ageing. *Mech Ageing Dev*. 2008;129(1-2):3-10.

doi: 10.1016/j.mad.2007.11.007

65. Getof N. Anti-aging and aging factors in life. The role of free radicals. *Radiat Phys Chem*. 2007;76(10):1577-1586.

doi: 10.1016/j.radphyschem.2007.01.002

66. Beckman KB, Ames BN. The free radical theory of aging matures. *Physiol Rev*. 1998;78(2):547-581.

doi: 10.1152/physrev.1998.78.2.547

67. Vijg J. Somatic mutations and aging: A re-evaluation. *Mutat Res*. 2000;447(1):117-135.

doi: 10.1016/s0027-5107(99)00202-x

68. da Costa JP, Vitorino R, Silva GM, Vogel C, Duarte AC, Rocha-Santos T. A synopsis on aging-Theories, mechanisms and future prospects. *Ageing Res Rev*. 2016;29:90-112.

doi: 10.1016/j.arr.2016.06.005

69. Qi C, Liu Q. Natural killer cells in aging and age-related diseases. *Neurobiol Dis*. 2023;183:106156.

doi: 10.1016/j.nbd.2023.106156

70. Brauning A, Rae M, Zhu G, *et al*. Aging of the immune system: Focus on natural killer cells phenotype and functions. *Cells*. 2022;11(6):1017.

doi: 10.3390/cells11061017

71. Wojcik A, Brzeski Z, Kolodziej K, Lojko W, Letkiewicz D, Sieklucka-Dziuba M. Evaluation of toxicological threat to health caused by some carcinogenic factors in the working environment of an industrial plant. *Pol J Environ Stud*. 2000;9(6):531-536.

72. Adamus T, Mikulenkova I, Dobias L, Havrankova J, Pek T. Cytogenetic methods and biomonitoring of occupational exposure to genotoxic factors. *J Appl Biomed*. 2006;4:197-203.

doi: 10.32725/jab.2006.022

73. Verger A, Crossley M. Chromatin modifiers in transcription and DNA repair. *Cell Mol Life Sci*. 2004;61(17):2154-2162.

doi: 10.1007/s00018-004-4176-y

74. Powell CL, Swenberg JA, Rusyn I. Expression of base excision DNA repair genes as a biomarker of oxidative DNA damage. *Cancer Lett*. 2005;229(1):1-11.

doi: 10.1016/j.canlet.2004.12.002

75. Friedberg EC, McDaniel LD, Schultz RA. The role of endogenous and exogenous DNA damage and mutagenesis. *Curr Opin Genet Dev*. 2004;14(1):5-10.

doi: 10.1016/j.gde.2003.11.001

76. Hoeijmakers JHJ. Genome maintenance mechanisms for preventing cancer. *Nature*. 2001;411(6835):366-374.

doi: 10.1038/35077232

77. Bolognesi C, Lando C, Forni A, *et al*. Chromosomal damage and ageing: Effect on micronuclei frequency in peripheral blood lymphocytes. *Age Aging*. 1999;28:393-397.

doi: 10.1093/ageing/28.4.393

78. Ono T, Uehara Y, Saito Y, Ikehata H. Mutation theory of aging, assessed in transgenic mice and knockout mice. *Mech Ageing Dev*. 2002;123(12):1543-1552.

doi: 10.1016/s0047-6374(02)00090-8

79. Zhang L, Eastmond DA, Smith MT. The nature of chromosomal aberrations detected in humans exposed to benzene. *Crit Rev Toxicol*. 2002;32(1):1-42.

doi: 10.1080/20024091064165

80. Yadav AS, Jaggi S. Buccal micronucleus cytome assay-A biomarker of genotoxicity. *J Mol Biomarkers Diagn*. 2015;6:236.

doi: 10.4172/2155-9929.1000236

81. Smith MT, Zhang L. Biomarkers of leukemia risk: Benzene as a model. *Environ Health Perspect*. 1998;106:937-946.

doi: 10.1289/ehp.98106s4937

82. Nordberg GF. Biomarkers of exposure, effects and susceptibility in humans and their application in studies of interactions among metals in China. *Toxicol Lett*. 2010;192(1):45-49.

doi: 10.1016/j.toxlet.2009.06.859

83. Dusinska M, Collins AR. The comet assay in human biomonitoring: Gene-environment interactions. *Mutagenesis*. 2008;23(3):191-205.

doi: 10.1093/mutage/gen007

84. Ada AO, Yilmazer M, Suzen S, *et al*. Cytochrome P450 (CYP) and glutathione S-transferases (GST) polymorphisms (CYP1A1, CYP1B1, GSTM1, GSTP1 and GSTT1) and urinary levels of 1-hydroxypyrene in Turkish coke oven workers. *Genet Mol Biol*. 2007;30(3):511-519.

doi: 10.1590/S1415-47572007000400002

85. Bukvic N, Gentile M, Susca F, *et al*. Sex chromosome loss, micronuclei, sister chromatid exchange and aging: A study including 16 centenarians. *Mutat Res*. 2001;498(1):159-167.

doi: 10.1016/s1383-5718(01)00279-0

86. Offer T, Ho E, Traber MG, Bruno RS, Kuypers FA, Ames BN. A simple assay for frequency of chromosome breaks and loss (micronuclei) by flow cytometry of human reticulocytes. *FASEB J*. 2005;19(3):485-487.

doi: 10.1096/fj.04-2729fje

87. Mussali-Galante P, Tovar-Sánchez E, Valverde M, Rojas del Castillo E. Biomarkers of exposure for assessing environmental metal pollution: From molecules to ecosystems. *Rev Int Contam Ambient*. 2013;29:117-140.

88. Morla M, Busquets X, Pons J, Sauleda J, MacNee W, Agusti AGN. Telomere shortening in smokers with and without COPD. *Eur Respir J*. 2006;27(3):525-528.

doi: 10.1183/09031936.06.00087005

89. Pacheco KA. Epigenetics mediate environment: Gene effects on occupational sensitization. *Curr Opin Allergy Clin Immunol*. 2012;12(2):111-118.

doi: 10.1097/ACI.0b013e328351518f

90. Kasuba V, Rozgaj R, Sentija K. Cytogenetic changes in subjects occupationally exposed to benzene. *Chemosphere*. 2000;40(3):307-310.

doi: 10.1016/s0045-6535(99)00265-9

91. Cakir S. Genetics and some aging-related mechanisms. *Turk J Zool*. 2000;24(2):183-190.

92. Yu M, Zhang H, Wang B, *et al*. Key signaling pathways in aging and potential interventions for healthy aging. *Cells*. 2021;10(3):660.

doi: 10.3390/cells10030660

93. Mantovani C, Terenghi G, Magnaghi V. Senescence in adipose-derived stem cells and its implications in nerve regeneration. *Neural Regen Res*. 2014;9(1):10-15.

doi: 10.4103/1673-5374.125324

94. Lu W, Tang S, Li A, *et al*. The role of PKC/PKR in aging, Alzheimer's disease, and perioperative neurocognitive disorders. *Front Aging Neurosci*. 2022;14:973068.

doi: 10.3389/fnagi.2022.973068

95. Balistreri CR, Madonna R, Melino G, Caruso C. The emerging role of Notch pathway in ageing: Focus on the related mechanisms in age-related diseases. *Ageing Res Rev*. 2016;29:50-65.

doi: 10.1016/j.arr.2016.06.004

96. Ukraintseva S, Duan M, Arbeev K, *et al*. Interactions between genes from aging pathways may influence human lifespan and improve animal to human translation. *Front Cell Dev Biol*. 2021;9:692020.

doi: 10.3389/fcell.2021.692020

97. Ronen A, Glickman BW. Human DNA repair genes. *Environ Mol Mutagen*. 2001;37(3):241-283.

doi: 10.1002/em.1033

98. Wood RD, Mitchell M, Sgouros J, Lindahl T. Human DNA repair genes. *Science*. 2001;291(5507):1284-1289.

doi: 10.1126/science.1056154

99. Kirsch-Volders M, Fenech M. Inclusion of micronuclei in non-divided mononuclear lymphocytes and necrosis/apoptosis may provide a more comprehensive cytokinesis block micronucleus assay for biomonitoring purposes. *Mutagenesis*. 2001;16(1):51-58.

doi: 10.1093/mutage/16.1.51

100. LLeonart ME, Carnero A, Paciucci R, Wang ZQ, Shomron N. Cancer, senescence, and aging: Translation from basic research to clinics. *J Aging Res*. 2011;2011:692301.

doi: 10.4061/2011/692301

101. Eshkoora SA, Ismail P, Abdul Rahman S. Gene expression of CDK6 and CCND1 genes in basal cell carcinoma. *J Med Biol Sci*. 2008;2(2):1-9.

102. Han X, Zheng T, Foss FM, *et al*. Genetic polymorphisms in the metabolic pathway and non-Hodgkin lymphoma survival. *Am J Hematol*. 2010;85(1):51-56.

doi: 10.1002/ajh.21580

103. Eshkoorb SA, Marashi SJ, Ismail P, *et al*. Association of GSTM1 and GSTT1 with ageing in auto repair shop workers. *Genet Mol Res*. 2012;11(2):1486-1496.

doi: 10.4238/2012.May.21.5

104. Eshkoor SA, Ismail P, Rahman SA. Does CYP1A1 gene polymorphism affect cell damage biomarkers and ageing? *Turk J Biol*. 2014;38:219-225.

doi: 10.3906/biy-1308-61

105. Eshkoora SA, Ismail P, Rahman SA, Moin S. Role of the CYP1A2 gene polymorphism on early ageing from occupational exposure. *Balkan J Med Genet*. 2013;16(2):45-52.

doi: 10.2478/bjmg-2013-0031

106. Smith GB, Harper PA, Wong JM, *et al*. Human lung microsomal cytochrome P4501A1 (CYP1A1) activities: Impact of smoking status and CYP1A1, aryl hydrocarbon receptor, and glutathione S-transferase M1 genetic polymorphisms. *Cancer Epidemiol Biomarkers Prev*. 2001;10:839-853.

107. Eshkoorb SA, Ismail P, Rahman SA, Adon MY, Devan RV. Contribution of CYP2E1 polymorphism to aging in the mechanical workshop workers. *Toxicol Mech Methods*. 2013;23(4):217-222.

doi: 10.3109/15376516.2012.743637

108. Lucas D, Ferrara R, Gonzales E, Albores A, Manno M, Berthou F. Cytochrome CYP2E1 phenotyping and genotyping in the evaluation of health risks from exposure to polluted environments. *Toxicol Lett*. 2001;124(1):71-81.

doi: 10.1016/s0378-4274(00)00287-3

109. Guengerich FP, Shimada T. Activation of procarcinogens by human cytochrome P450 enzymes. *Mutat Res*. 1998;400(1):201-213.

doi: 10.1016/s0027-5107(98)00037-2

110. Pande M, Amos CI, Osterwisch DR, *et al*. Genetic variation in genes for the xenobiotic-metabolizing enzymes CYP1A1, EPHX1, GSTM1, GSTT1, and GSTP1 and susceptibility to colorectal cancer in Lynch syndrome. *Cancer Epidemiol Biomarkers Prev*. 2008;17(9):2393-2401.

doi: 10.1158/1055-9965.EPI-08-0326

111. Da Silva J, Moraes CR, Heuser VD, *et al*. Evaluation of genetic

damage in a Brazilian population occupationally exposed to pesticides and its correlation with polymorphisms in metabolizing genes. *Mutagenesis*. 2008;23(5):415-422.

doi: 10.1093/mutage/gen031

112. Pérez-Cadahía B, Laffon B, Valdiglesias V, Pásaro E, Méndez J. Cytogenetic effects induced by Prestige oil on human populations: The role of polymorphisms in genes involved in metabolism and DNA repair. *Mutat Res*. 2008;653(1):117-123.

doi: 10.1016/j.mrgentox.2008.04.002

113. Eshkoorb SA, Ismail P, Rahman SA, Moin S. Does GSTP1 polymorphism contribute to genetic damage caused by ageing and occupational exposure? *Arh Hig Rada Toksikol*. 2011;62(4):291-298.

doi: 10.2478/10004-1254-62-2011-2088

114. Wu X, Amos CI, Zhu Y, *et al*. Telomere dysfunction: A potential cancer predisposition factor. *J Natl Cancer Inst*. 2003;95(16):1211-1218.

doi: 10.1093/jnci/djg011

115. Li J, Zhang Y, You Y, *et al*. Unraveling the mechanisms of NK cell dysfunction in aging and Alzheimer's disease: Insights from GWAS and single-cell transcriptomics. *Front Immunol*. 2024;15:1360687.

doi: 10.3389/fimmu.2024.1360687

116. Weber S, Menees KB, Park J, *et al*. Distinctive $CD56^{dim}$ NK subset profiles and increased NKG2D expression in blood NK cells of Parkinson's disease patients. *NPJ Parkinsons Dis*. 2024;10(1):36.

doi: 10.1038/s41531-024-00652-y

117. Chidrawar SM, Khan N, Chan YLT, Nayak L, Moss PAH. Ageing is associated with a decline in peripheral blood $CD56^{bright}$ NK cells. *Immun Ageing*. 2006;3:10.

doi: 10.1186/1742-4933-3-10

118. Hazeldine J, Lord JM. The impact of ageing on natural killer cell function and potential consequences for health in older adults. *Ageing Res Rev*. 2013;12(4):1069-1078.

doi: 10.1016/j.arr.2013.04.003

119. Chini CC, Peclat TR, Warner GM, *et al*. CD38 ecto-enzyme in immune cells is induced during aging and regulates NAD+ and NMN levels. *Nature Metab*. 2020;2(11):1284-1304.

doi: 10.1038/s42255-020-00298-z

120. Xia M, Wang B, Wang Z, Zhang X, Wang X. Epigenetic regulation of NK cell-mediated antitumor immunity. *Front Immunol*. 2021;12:672328.

doi: 10.3389/fimmu.2021.672328

121. Lv L, Chen Q, Lu J, *et al*. Potential regulatory role of epigenetic modifications in aging-related heart failure. *Int J Cardiol*. 2024;401:131858.

doi: 10.1016/j.ijcard.2024.131858

122. Moskalev AA, Aliper AM, Smit-McBride Z, Buzdin A, Zhavoronkov A. Genetics and epigenetics of aging and longevity. *Cell Cycle*. 2014;13:1063-1077.

doi: 10.4161/cc.28433

123. Colită CI, Udristoiu I, Ancuta DL, *et al*. Epigenetics of ageing and psychiatric disorders. *J Integr Neurosci*. 2024;23(1):13.

doi: 10.31083/j.jin2301013

124. Johnson AA, Akman K, Calimport SRG, Wuttke D, Stolzing A, de Magalhaes JP. The role of DNA methylation in aging, rejuvenation, and age-related disease. *Rejuvenation Res*. 2012;15(5):483-494.

doi: 10.1089/rej.2012.1324

125. Olden K, Freudenberg N, Dowd J, Shields AE. Discovering how environmental exposures alter genes could lead to new treatments for chronic illnesses. *Health Aff* (*Millwood*). 2011;30(5):833-841.

doi: 10.1377/hlthaff.2011.0078

126. Kanherkar RR, Bhatia-Dey N, Csoka AB. Epigenetics across the human lifespan. *Front Cell Dev Biol*. 2014;2:49.

doi: 10.3389/fcell.2014.00049

127. Haigis MC, Yankner BA. The aging stress response. *Mol Cell*. 2010;40(2):333-344.

doi: 10.1016/j.molcel.2010.10.002

128. Zampieri M, Ciccarone F, Guastafierro T, *et al*. Validation of suitable internal control genes for expression studies in aging. *Mech Ageing Dev*. 2010;131(2):89-95.

doi: 10.1016/j.mad.2009.12.005

129. Hernandez-Segura A, Rubingh R, Demaria M. Identification of stable senescence-associated reference genes. *Aging Cell*. 2019;18(2):e12911.

doi: 10.1111/acel.12911

130. Pal S, Tyler JK. Epigenetics and aging. *Sci Adv*. 2016;2(7):e1600584.

doi: 10.1126/sciadv.1600584

131. Laroni A, Uccelli A. CD56bright natural killer cells: A possible biomarker of different treatments in multiple sclerosis. *J Clin Med*. 2020;9(5):1450.

doi: 10.3390/jcm9051450

132. Abel AM, Yang C, Thakar MS, Malarkannan S. Natural killer cells: Development, maturation, and clinical utilization. *Front Immunol*. 2018;9:1869.

doi: 10.3389/fimmu.2018.01869

133. Shi FD, Ljunggren HG, La Cava A, Van Kaer L. Organ-specific features of natural killer cells. *Nat Rev Immunol*. 2011;11(10):658-671.

doi: 10.1038/nri3065

134. Almeida-Oliveira A, Smith-Carvalho M, Porto LC, *et al*. Age-related changes in natural killer cell receptors from childhood through old age. *Hum Immunol*. 2011;72(4):319-329.

doi: 10.1016/j.humimm.2011.01.009

135. Campos C, Pera A, Pita-Lopez ML, *et al*. *Natural Killer Cells in Human Aging*. Cham: Springer; 2018.

doi: 10.1007/978-3-319-64597-1_27-1

136. Poli A, Michel T, Thérésine M, Andrès E, Hentges F, Zimmer J. CD56bright natural killer (NK) cells: An important NK cell subset. *Immunology*. 2009;126(4):458-465.

doi: 10.1111/j.1365-2567.2008.03027.x

137. Berahovich RD, Lai NL, Wei Z, Lanier LL, Schall TJ. Evidence for NK cell subsets based on chemokine receptor expression. *J Immunol*. 2006;177(11):7833-7840.

doi: 10.4049/jimmunol.177.11.7833

ACCSCIENCE PUBLISHING

Gene & Protein in Disease

PERSPECTIVE ARTICLE

Combination cancer therapy integrating T-cell immune checkpoint blockers and natural killer cell activation

Junyi Li and Yanzhang Wei*

Department of Biological Sciences, College of Science, Clemson University, Clemson, South Carolina, United States of America

Abstract

T-cell immune checkpoint blockers (ICBs) and natural killer (NK) cell activation have emerged as promising strategies for cancer therapy in recent years. In this approach, ICBs target inhibitory receptors on cytotoxic immune cells, such as programmed death Protein 1 (PD-1)/programmed cell death-ligand 1 (PD-L1), to enhance immune cell cytotoxicity against cancer cells in a $CD8^+$ T cell-dependent manner. Meanwhile, NK cells play a critical role in immunosurveillance through their direct cytotoxic effects, which do not require prior activation. NK cell activation is mediated by receptors such as NK Group 2 member D (NKG2D), which regulates NK cell function and cytotoxicity through the upregulation of cytokine production. Individually, these treatments target only a limited subset of cancer patients and often face great resistance rates after treatment. However, combining ICBs with NK cell activation may produce a synergistic therapeutic effect, potentially improving treatment outcomes. This perspective article discusses the mechanisms of action of T cell-related PD-1/PDL1 pathways and NK cell activation through NKG2D, examining current studies that provide a rationale for combined NK/T cell combination therapy. The potential of this dual-combination approach to enhance anti-tumor immunity is highlighted. Future perspectives suggest the potential development of chimeric antibodies targeting both T cells and NK cells as a novel therapeutic strategy for cancer treatment.

Keywords: Immune checkpoint blockers; PD-1/PD-L1; Natural killer cell activation; NKG2D

***Corresponding author:**
Yanzhang Wei
(Ywei@clemson.edu)

Citation: Li J, Wei Y. Combination cancer therapy integrating T-cell immune checkpoint blockers and natural killer cell activation. *Gene Protein Dis.* 2024;3(4):3804. doi: 10.36922/gpd.3804

Received: May 31, 2024
Accepted: August 29, 2024
Published Online: October 4, 2024

1. Introduction

Over the past several decades, immunotherapy has made remarkable strides in the treatment of human cancers.[1] For example, adoptive cell transfer, chimeric antigen receptor cell modification (CAR-T or CAR-NK), and immune checkpoint inhibitors (ICBs) have shown great clinical success.[2-4] Among these immunotherapeutic approaches, ICBs, such as monoclonal antibodies (mAb) targeting programmed death 1 (PD-1) and its ligand (PD-L1), or blocking antibodies that inhibit natural killer (NK) cell protein group 2-A (NKG2A) from interacting with tumor-expressed HLA-E, have shown promising potential in treating various cancer types by targeting distinct inhibitory checkpoints within different tumor microenvironments (TMEs).[4-8] Since the initial discovery of "classical" ICB – PD-L1/PD1 – on T cells, which act as an inhibitory receptor allowing

tumor cells to evade immunosurveillance, the majority of ICB treatments have focused on enhancing T cell-mediated tumor suppression.[9] In recent years, the United States Food and Drug Administration has approved several antibodies targeting PD-1 (nivolumab, pembrolizumab, and cemiplimab) and PD-L1 (atezolizumab and avelumab) for clinical use in various cancers, including squamous non-small cell lung cancer (NSCLC), metastatic cutaneous squamous cell carcinoma, malignant melanoma, renal cell carcinoma, bladder cancer, and hepatocellular cancer.[10-18] Simultaneously, NK cells have gained considerable attention due to their direct cytotoxicity against infected cells or tumor cells without the need for prior activation.[19-21] Notably, the activating NK cell receptor, NK cell protein group 2-D (NKG2D), provides therapeutic opportunities to target different cancer subtypes independently.[6,19,22-30] A dual-combination approach involving T-cell ICBs and NK cell activation could produce synergistic therapeutic effects, leading to improved treatment outcomes. This perspective article aims to discuss the various ICB approaches in T-cell and NK-cell activation and their associated biomarkers for predicting immunotherapeutic outcomes following ICB treatment.

2. Immune checkpoint blockers (ICBs) and NK cell activation

2.1. Effects of ICBs on T cells

ICBs are cancer immunotherapies that enhance the cytotoxicity of immune cells by targeting immunologic receptors on their surface. Compared with other therapeutic approaches, ICBs typically provide long-lasting effects with lower toxicity to healthy cells.[31,32]

Under normal conditions, the human immune system maintains a homeostatic balance between proinflammatory and anti-inflammatory responses through immune checkpoints.[31] These immune checkpoints are inhibitory or stimulatory receptors expressed by immune cells, allowing the immune system to regulate its cytotoxicity and prevent autoimmune reactions.[33-35] In many cancer cases, tumor cells within a TME can evade immunosurveillance by either expressing inhibitory signals that suppress cytotoxic immune cells or by shedding stress signals from their surface. Tumor cells can also promote the accumulation of inhibitory cells, such as regulatory T cells (Tregs) or stromal cells, within the TME.[33,35-41] By blocking these immune checkpoint functions, exhausted T cells can be restored to their normal function.[32,42] A major focus of ICB treatments is on CD 8^+ T cells,[43] with antibodies targeting the PD-1/PD-L1 pathway or CTLA-4 being widely used in clinical practice.[5,7] This perspective article will specifically focus on the PD-1/PDL1 pathway as a key target in T-cell ICB therapy.

Programmed cell death 1, also known as CD279, is a receptor that regulates $CD8^+$ T cell responses.[44] The PD-1 receptor contains a single immunoglobulin (Ig) superfamily domain and a cytoplasmic domain with a tyrosine-based inhibitory motif and an immunoreceptor tyrosine-based switch motif (ITSM).[45,46] Besides $CD8^+$ T cells, PD-1 is expressed at high levels in dendritic cells, activated T cells, and NK cells.[47-49] Its expression is upregulated by transcription factors such as forkhead box protein (FOXO1), interferon (IFN) regulatory factor 9, and NOTCH,[50-52] as well as certain common gamma-chain cytokines such as interleukin (IL)-2, IL-7, and IL-21, which recruit the NF-κB-related nuclear factor of activated T cells c1.[53,54]

Programmed cell death-ligand 1, also known as B7-H1, is the ligand for PD-1. It is expressed broadly across many immune cell types in the human body but is upregulated during inflammatory responses.[55-57] PD-L1 is a type I transmembrane glycoprotein belonging to the B7-CD28 family of the Ig superfamily.[58] In addition to immune cells, tumor cells can express PD-L1 as a means of evading immunosurveillance by inducing T cell apoptosis, upregulating IL-10 expression, and promoting $CD8^+$ T cell exhaustion.[58-60] Previous research has suggested that higher PD-L1 expression in various cancer types can significantly affect immunosuppressive activity by modulating T-cell activation through the T-cell receptor-associated protein kinase Zap70-RAS-GTPase-extracellular signal-regulated kinase and CD-28-PI3K-Akt serine-threonine kinases pathways.[61]

The primary role of the PD-1/PD-L1 pathway is to inhibit immune cell activity through the interaction of PD-1 on the cytotoxicity of immune cells with antigen-presenting cells (APCs).[62,63] Activation of PD-1 activation through PD-L1 triggers an inhibitory signal through ITSM tyrosine phosphorylation,[64] leading to the recruitment of SH2-domain-containing tyrosine phosphatase 2 and the downregulation of PI3K, serine/threonine kinase (Akt), and ZAP70 or PCK activity, directly inhibiting antigen receptor signaling.[65] PD-1 activation also affects cytokines production, such as IFN-γ, tumor necrosis factor-alpha (TNF-α), and IL-2,[66-69] and can inhibit T-cell proliferation while downregulating the anti-apoptotic protein BCL-xL.[64,69] Within the TME, the PD-1/PD-L1 pathway is associated with epithelial-mesenchymal transition, tumor malignancy, and tumor cell proliferation in various cancers, including breast, lung, and bladder cancers.[70-72]

It has been hypothesized that blocking these inhibitory pathways could prevent immune cell exhaustion, even in the TME. Therefore, various inhibitors of PD-1/PD-L1 (many of which are monoclonal antibodies) have been

developed and are now used in clinical settings. Several studies have demonstrated the efficacy of PD-1-targeting ICBs. Nivolumab, which inhibits the interaction between PD-1 and its ligand, has shown a higher survival rate in patients with non-squamous advanced NSCLC or squamous NSCLC compared to docetaxel treatment.[73] Pembrolizumab and cemiplimab, two other PD-1 inhibitors, have also shown significantly improved overall survival in patients with advanced cutaneous squamous cell carcinoma and metastatic lung cancer.[73,74] Similarly, atezolizumab and avelumab, two of the monoclonal anti-PD-L1 antibodies, have shown promising results in NSCLC and renal cell carcinoma, with response rates of 58% and disease control rates of 78%.[75-77]

2.2. NK cell activation

As previously mentioned, NK cells are critical in immunosurveillance due to their ability to exert direct cytotoxicity effects without prior activation. The cytotoxicity of NK cells is tightly regulated through activating or inhibiting receptors.

NK cells are lymphoid elements of the innate immune system, originating from $CD34^+$ hematopoietic stem cells in the bone marrow, and have the ability to infiltrate cancer tissues.[78-80] They play a critical role in mediating cytotoxicity and immune regulation in various infections, particularly in cancer. Unlike cytotoxic $CD8^+$ T cells, NK cells do not require pre-stimulation to induce cytotoxic effects. They achieve this effect through the production of perforin and granzymes, which facilitate the destruction of transformed or infected cells.[81] In addition, NK cells can activate and release various cytokines and chemokines, such as IFN-γ and CCL3/4, to enhance adaptive immunity.[82]

NK cells activate themself through receptors such as the NKG2D receptor on their surface.[83] In humans, NKG2D contains two β-sheets and two α-helices, along with four disulfide bonds.[84] Unlike the DNAM-1 signaling pathway, which utilizes the signaling element on the intracellular segment, NKG2D interacts with its adaptor proteins, DAP10 and DAP12.[85] Alternative splicing of NKG2D results in the production of two isoforms: NKG2D-S and NKG2D-L. The NKG2D-L isoform forms a homodimer, which interacts with the transmembrane domain of DAP10 in the cell membrane, leading to NK cell activation through PI3K recruitment and activation through tyrosine phosphorylation of the Tyr-X-X-Met motif.[86] This PI3K activation frequently triggers the activation of downstream pathways involving Akt and ERK, triggering Ca^{2+} mobilization and NK cell-mediated cytotoxicity.[87] In addition, research suggests that NKG2D-S can interact with both DAP10 and immunoreceptor tyrosine-based activation motif-containing DAP14, activating Zap70 and inducing IFN-γ production.[88-90]

In humans, two main ligands, major histocompatibility complex class I chain (MIC)-related Proteins A and B (MICA and MICB), bind to NKG2D.[91] MICA/B is transmembrane proteins with three extracellular domains, which are structurally similar to the α1-α3 domains of the primary histocompatibility class 1a (MHC1a) protein.[92] Some researchers suggest that cells undergoing stress or malignant transformation express higher levels of MICA/B on their cell surface than MHC1 molecules.[93]

Strategies focusing on NKG2D/NKG2D-L-mediated NK cell activation have been widely studied to enhance NK cell cytotoxicity against target cells. Soluble common γ chain-related cytokines, including IL-2 and IL-18, can positively regulate NKG2D expression in $CD16^+$ NK cells.[94,95] A low dose of IL-2 (100 U/mL) combined with IL-18 (175 ng/mL) has been shown to increase NKG2D surface expression in cancer patients without inducing IL-related toxicity.[96] In addition to targeting NKG2D on NK cells, recent studies indicate that increasing NKG2D-L expression on cancer cell surfaces enhances NK cell-mediated cytotoxicity. For example, temozolomide, an alkylating agent that induces DNA damage, has been shown to increase NKG2D-L expression, leading to tumor suppression.[97] Similarly, cisplatin-based adjuvant chemotherapy has demonstrated enhanced NK cell cytotoxicity through the upregulation of MICA through ataxia-telangiectasia-mutated and Rad3-associated protein kinase pathway in NSCLC.[98]

3. Combination cancer therapy

Tumor immunology has become a critical component in developing innovative therapeutic approaches to combat cancer. The main principle of tumor immunology is to boost the immune response by either activating positive signals or inhibiting negative signals in various immune cells. One relatively new era in this field is the use of ICBs. By targeting ICBs such as PD-1/PD-L1, ICBs restore the cytotoxic functions of T cells against cancer cells. NK cells, another population of immune cells, have also gained increasing attention for their role in treating metastatic disease. Advances in understanding NK cell cytotoxicity have led to the discovery of several promising treatments. For example, certain studies have demonstrated the effectiveness of NK cell engager (NKCE) in targeting NKG2D in the treatment of multiple myeloma. CS1xNKG2D, a linked single-chain scFv NKCE that targets the tumor surface antigen CS1, has been shown to induce dose-dependent cytotoxicity against CS1-positive multiple myeloma cells *in vitro*.[99] Similarly, 2A9-MICA, also known as BCMAxMICA, which links the scFv

region of BCMA with the extracellular domain of MICA, has shown significant potential for NK cell activation in BCMA-positive multiple myeloma cells both *in vivo* and *in vitro* through NK cell degranulation.[100]

Given that cancer cells can evade and develop resistance to single therapeutic approaches, combination therapies targeting multiple sites may provide enhanced treatment outcomes. Previous research has suggested that antibodies targeting tumor-derived soluble NKG2D ligand sMIC can reprogram NK cell homeostasis and enhance PD-L1 blockade therapy in melanoma patients by upregulating CD25 expression on NK cells.[101] In addition, ICB-resistant patients have been shown to have higher NKG2D-L expression in cancer cell surfaces, making them more susceptible to NKG2DL-mediated treatments.[102] Moreover, research suggests that alterations in PDL1-NKG2D ligand levels after radiation therapy can affect NK cell cytotoxicity in lung cancer and castration-resistant prostate cancer patients in an IL-6-dependent manner.[103,104] Specifically, through the IL-6-JAK/Stat3 or IL-6-MEK/ERK pathways, IL-6 significantly upregulates PD-L1 expression and downregulates NKG2D expression in radiation therapy-resistant cells, which further suppresses NK cell cytotoxicity.[105] Inhibitors of these pathways increase the susceptibility of target cells, enhancing NK cell cytotoxicity effects against tumor cells *in vitro* and *in vivo*.[103-105] Interestingly, the most effective cytotoxicity was observed when PD-L1 antibodies were combined with pathway inhibitors, directly upregulating NK cell activation receptor expression, underscoring the significance of combining ICBs with NK cell activation to achieve superior therapeutic outcomes. In addition, research into platinum-based chemotherapy in NSCLC patients has demonstrated upregulation of PD-L1 and downregulation of NKG2D ligand in five out of 10 NSCLC patients after chemotherapy, resulting in reduced NK cell-mediated cytotoxicity and immune evasion.[105] These findings suggest that the synergistic effect of NKG2D, PD-L1, and HLA-class 1 molecules in solid tumors after chemotherapy can suppress the immune response. A promising treatment strategy could involve targeting both NKG2D and PD-L1, either through upstream targets, such as JAK-STAT inhibitors, or by directly modulating NKG2D and PD-L1 levels. A study by Nicholas' group demonstrated that combining radiation therapy with NKG2A/PD-1 blockade effectively enhanced $CD8^+$ T cell cytotoxicity.[106] Moreover, recent research has shown that combining PD-1/PD-L1 blockade with NKCEs can enhance antitumor efficacy. For instance, EGFRxCD16axPD-L1, an NKCE that induces NK cell cytotoxicity against EGFR-positive cells through CD16a while inhibiting PD-L1 binding on NK cells, demonstrated greater cytotoxicity *in vitro* compared to bispecific NKCEs without PD-L1 blockade.[107] These findings provide a strong rationale for combining NK cell receptor targeting with ICB therapy to achieve a more robust overall immune response.

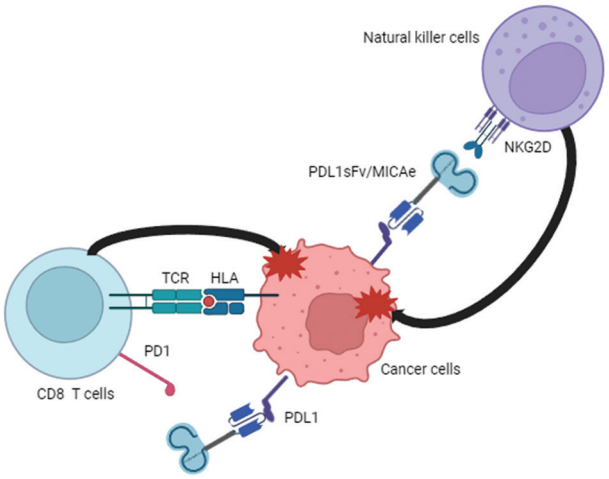

Figure 1. Schematic of the fusion protein function. The bifunctional protein PD-L1sFv/MICAe is expected to bind to the PD-L1 surface protein on tumor cells, blocking the PD-L1/PD-1 inhibitory signal and thereby activating T cells. Simultaneously, the MICAe portion of the protein is expected to bind to the NKG2D receptor on NK cells, facilitating the physical engagement of natural killer cells with tumor cells. In this way, both T cells and NK cells will be better equipped to recognize and induce apoptosis in tumor cells.
Abbreviations: HLA: Human leukocyte antigens; NKG2D: Natural killer cell protein group 2-D; PD1: Programmed cell death-1; PDL1: Programmed cell death ligand-1; TCR: T cell receptor.

In recent years, chimeric antibodies have been studied more intensively under the context of ICBs. For example, single-domain PD-L1 antibodies fused with IL-2 and IFN-γ have been shown to reduce pancreatic tumor burden by 50%.[108] A similar approach has been explored in CAR-T cell therapy, where dual CAR-T cells co-expressing NKG2D and PD-1 ligands significantly increased survival rates in murine models of peritoneal metastasis of colorectal and ovarian cancers. This combination therapy also elevated cytokine levels of IL-2, TNF-α, and IFN-γ compared to mono-treatment with single ligand CAR-T cells.[109] Beyond ICBs, the NKG2D-Fc-IL2 DNA vaccine, when combined with a therapeutic human papillomavirus type 16/E7 peptide vaccine, promoted E7-specific T-cell conjugation at the tumor site and reduced tumor growth.[110] In gastric and NSCLC models, a fusion antibody targeting αVEGFR2 and NKG2D enhanced NKG2D-positive NK cell activation and induced tumor-associated macrophage polarization *in vitro* and *in vivo*.[111] This fusion protein also demonstrated a synergic effect when combined with PD-1/PD-L1 blockade, highlighting the potential of combining NK cell activation with ICB as a promising

anti-tumor strategy.[111] In a murine tumor model, treatment with SN38, a pharmacological immuno-activator and DNA replication inhibitor, significantly reduced PD-L1 expression and enhanced FOXO3 expression.[112] This therapy also engaged tumor-infiltrating NKG2D-positive NK cells in an IFN-γ and granzyme-B-dependent manner.[112] In addition, combination therapy with anti-PD-L1 and anti-sMIC improved overall survival rates in B16DF10 melanoma mice compared to monotherapy with either anti-sMIC or PD-L1/PD-1 blockage.[101]

4. Conclusion

The data discussed above indicate that the development of a chimeric protein that simultaneously targets NKG2D and ICBs represents a novel approach to enhancing NK-cell- and T cell-mediated cytotoxicity in TME. We propose that by fusing the extracellular domain of MICA, which engages NKG2D on NK cells, with the variable regions of an anti-PD-L1 antibody, a bifunctional therapeutic agent could be created. This agent will (i) inhibit the PD-L1/PD-1 interaction between T cells and tumor cells, thereby reactivating T-cell cytotoxicity and (ii) engage with NKG2D to enhance NK cell cytotoxicity (Figure 1). Once the bifunctional fusion protein's activity is confirmed *in vitro* and in animal models, it could be rapidly advanced to clinical trials. This development would provide cancer patients, particularly those with PD-L1-positive cancers, with a promising new treatment option.

Acknowledgment

None.

Funding

None.

Conflict of interest

The authors declare no conflict of interest to any group.

Author contributions

Conceptualization: All authors
Writing – original draft: All authors
Writing – review & editing: All authors

Ethics approval and consent to participle

Not applicable.

Consent for publication

Not applicable.

Availability of data

Not applicable.

References

1. Smith SM, Wachter K, Burris HA 3rd, *et al*. Clinical cancer advances 2021: ASCO's report on progress against cancer. *J Clin Oncol*. 2021;39(10):1165-1184.
doi: 10.1200/jco.20.03420
2. Sadeghi Rad H, Monkman J, Warkiani ME, *et al*. Understanding the tumor microenvironment for effective immunotherapy. *Med Res Rev*. 2021;41(3):1474-1498.
doi: 10.1002/med.21765
3. Thorsson V, Gibbs DL, Brown SD, *et al*. The immune landscape of cancer. *Immunity*. 2018;48(4):812-830.e14.
doi: 10.1016/j.immuni.2018.03.023
4. Topalian SL, Drake CG, Pardoll DM. Immune checkpoint blockade: A common denominator approach to cancer therapy. *Cancer Cell*. 2015;27(4):450-461.
doi: 10.1016/j.ccell.2015.03.001
5. Seidel JA, Otsuka A, Kabashima K. Anti-PD-1 and anti-CTLA-4 therapies in cancer: Mechanisms of action, efficacy, and limitations. *Front Oncol*. 2018;8:86.
doi: 10.3389/fonc.2018.00086
6. André P, Denis C, Soulas C, *et al*. Anti-NKG2A mAb is a checkpoint inhibitor that promotes anti-tumor immunity by unleashing both T and NK cells. *Cell*. 2018;175(7):1731-1743.e13.
doi: 10.1016/j.cell.2018.10.014
7. Carotta S. Targeting NK cells for anticancer immunotherapy: Clinical and preclinical approaches. *Front Immunol*. 2016;7:152.
doi: 10.3389/fimmu.2016.00152
8. Sivori S, Vacca P, Del Zotto G, Munari E, Mingari MC, Moretta L. Human NK cells: Surface receptors, inhibitory checkpoints, and translational applications. *Cell Mol Immunol*. 2019;16(5):430-441.
doi: 10.1038/s41423-019-0206-4
9. Baumeister SH, Freeman GJ, Dranoff G, Sharpe AH. Coinhibitory pathways in immunotherapy for cancer. *Annu Rev Immunol*. 2016;34:539-573.
doi: 10.1146/annurev-immunol-032414-112049
10. Rolfo C, Caglevic C, Santarpia M, *et al*. Immunotherapy in NSCLC: A promising and revolutionary weapon. *Adv Exp Med Biol*. 2017;995:97-125.
doi: 10.1007/978-3-319-53156-4_5
11. Li JX, Huang JM, Jiang ZB, *et al*. Current clinical progress of PD-1/PD-L1 immunotherapy and potential combination treatment in non-small cell lung cancer. *Integr Cancer Ther*. 2019;18:1534735419890020.
doi: 10.1177/1534735419890020

12. Migden MR, Rischin D, Schmults CD, *et al*. PD-1 blockade with cemiplimab in advanced cutaneous squamous-cell carcinoma. *N Engl J Med*. 2018;379(4):341-351.

doi: 10.1056/NEJMoa1805131

13. Shirley M. Avelumab: A review in metastatic merkel cell carcinoma. *Target Oncol*. 2018;13(3):409-416.

doi: 10.1007/s11523-018-0571-4

14. Paz-Ares L, Spira A, Raben D, *et al*. Outcomes with durvalumab by tumour PD-L1 expression in unresectable, stage III non-small-cell lung cancer in the PACIFIC trial. *Ann Oncol*. 2020;31(6):798-806.

doi: 10.1016/j.annonc.2020.03.287

15. Liebl MC, Hofmann TG. Identification of responders to immune checkpoint therapy: Which biomarkers have the highest value? *J Eur Acad Dermatol Venereol*. 2019;33 Suppl 8:52-56.

doi: 10.1111/jdv.15992

16. Guo L, Zhang H, Chen B. Nivolumab as programmed death-1 (PD-1) inhibitor for targeted immunotherapy in tumor. *J Cancer*. 2017;8(3):410-416.

doi: 10.7150/jca.17144

17. Sinner F, Pinter M, Scheiner B, *et al*. Atezolizumab plus bevacizumab in patients with advanced and progressing hepatocellular carcinoma: Retrospective multicenter experience. *Cancers* (*Basel*). 2022;14(23):5966.

doi: 10.3390/cancers14235966

18. du Rusquec P, de Calbiac O, Robert M, Campone M, Frenel JS. Clinical utility of pembrolizumab in the management of advanced solid tumors: An evidence-based review on the emerging new data. *Cancer Manag Res*. 2019;11:4297-4312.

doi: 10.2147/cmar.s151023

19. Kim N, Kim HS. Targeting checkpoint receptors and molecules for therapeutic modulation of natural killer cells. *Front Immunol*. 2018;9:2041.

doi: 10.3389/fimmu.2018.02041

20. O'Sullivan TE, Sun JC, Lanier LL. Natural killer cell memory. *Immunity*. 2015;43(4):634-645.

doi: 10.1016/j.immuni.2015.09.013

21. Cao Y, Wang X, Jin T, *et al*. Immune checkpoint molecules in natural killer cells as potential targets for cancer immunotherapy. *Signal Transduct Target Ther*. 2020;5(1):250.

doi: 10.1038/s41392-020-00348-8

22. Thielens A, Vivier E, Romagné F. NK cell MHC class I specific receptors (KIR): from biology to clinical intervention. *Curr Opin Immunol*. 2012;24(2):239-245.

doi: 10.1016/j.coi.2012.01.001

23. Pende D, Falco M, Vitale M, *et al*. Killer Ig-like receptors (KIRs): Their role in NK cell modulation and developments leading to their clinical exploitation. *Front Immunol*. 2019;10:1179.

doi: 10.3389/fimmu.2019.01179

24. Sun H, Sun C. The rise of NK cell checkpoints as promising therapeutic targets in cancer immunotherapy. *Front Immunol*. 2019;10:2354.

doi: 10.3389/fimmu.2019.02354

25. McWilliams EM, Mele JM, Cheney C, *et al*. Therapeutic CD94/NKG2A blockade improves natural killer cell dysfunction in chronic lymphocytic leukemia. *Oncoimmunology*. 2016;5(10):e1226720.

doi: 10.1080/2162402x.2016.1226720

26. Seo H, Kim BS, Bae EA, *et al*. IL21 therapy combined with PD-1 and Tim-3 blockade provides enhanced NK cell antitumor activity against MHC class I-deficient tumors. *Cancer Immunol Res*. 2018;6(6):685-695.

doi: 10.1158/2326-6066.cir-17-0708

27. Seo H, Jeon I, Kim BS, *et al*. IL-21-mediated reversal of NK cell exhaustion facilitates anti-tumour immunity in MHC class I-deficient tumours. *Nat Commun*. 2017;8:15776.

doi: 10.1038/ncomms15776

28. Deng W, Gowen BG, Zhang L, *et al*. Antitumor immunity. A shed NKG2D ligand that promotes natural killer cell activation and tumor rejection. *Science*. 2015;348(6230):136-139.

doi: 10.1126/science.1258867

29. Luo Q, Luo W, Zhu Q, *et al*. Tumor-derived soluble MICA obstructs the NKG2D pathway to restrain NK cytotoxicity. *Aging Dis*. 2020;11(1):118-128.

doi: 10.14336/ad.2019.1017

30. Ames E, Canter RJ, Grossenbacher SK, *et al*. NK cells preferentially target tumor cells with a cancer stem cell phenotype. *J Immunol*. 2015;195(8):4010-4019.

doi: 10.4049/jimmunol.1500447

31. Cai X, Zhan H, Ye Y, *et al*. Current progress and future perspectives of immune checkpoint in cancer and infectious diseases. *Front Genet*. 2021;12:785153.

doi: 10.3389/fgene.2021.785153

32. Johnson DB, Nebhan CA, Moslehi JJ, Balko JM. Immune-checkpoint inhibitors: Long-term implications of toxicity. *Nat Rev Clin Oncol*. 2022;19(4):254-267.

doi: 10.1038/s41571-022-00600-w

33. Pardoll DM. The blockade of immune checkpoints in cancer immunotherapy. *Nat Rev Cancer*. 2012;12(4):252-264.

doi: 10.1038/nrc3239

34. Melero I, Rouzaut A, Motz GT, Coukos G. T-cell and

NK-cell infiltration into solid tumors: A key limiting factor for efficacious cancer immunotherapy. *Cancer Discov*. 2014;4(5):522-526.

doi: 10.1158/2159-8290.cd-13-0985

35. Melaiu O, Lucarini V, Cifaldi L, Fruci D. Influence of the tumor microenvironment on NK cell function in solid tumors. *Front Immunol*. 2019;10:3038.

doi: 10.3389/fimmu.2019.03038

36. Blank CU, Haining WN, Held W, *et al*. Defining "T cell exhaustion". *Nat Rev Immunol*. 2019;19(11):665-674.

doi: 10.1038/s41577-019-0221-9

37. Philip M, Fairchild L, Sun L, *et al*. Chromatin states define tumour-specific T cell dysfunction and reprogramming. *Nature*. 2017;545(7655):452-456.

doi: 10.1038/nature22367

38. Shim YJ, Khedraki R, Dhar J, *et al*. Early T cell infiltration is modulated by programed cell death-1 protein and its ligand (PD-1/PD-L1) interactions in murine kidney transplants. *Kidney Int*. 2020;98(4):897-905.

doi: 10.1016/j.kint.2020.03.037

39. Habif G, Crinier A, André P, Vivier E, Narni-Mancinelli E. Targeting natural killer cells in solid tumors. *Cell Mol Immunol*. 2019;16(5):415-422.

doi: 10.1038/s41423-019-0224-2

40. Huang Q, Huang M, Meng F, Sun R. Activated pancreatic stellate cells inhibit NK cell function in the human pancreatic cancer microenvironment. *Cell Mol Immunol*. 2019;1:87-89.

doi: 10.1038/s41423-018-0014-2

41. Castriconi R, Dondero A, Bellora F, *et al*. Neuroblastoma-derived TGF-β1 modulates the chemokine receptor repertoire of human resting NK cells. *J Immunol*. 2013;190(10):5321-5328.

doi: 10.4049/jimmunol.1202693

42. Yoon SR, Kim TD, Choi I. Understanding of molecular mechanisms in natural killer cell therapy. *Exp Mol Med*. 2015;47(2):e141.

doi: 10.1038/emm.2014.114

43. Robert C. A decade of immune-checkpoint inhibitors in cancer therapy. *Nat Commun*. 2020;11(1):3801.

doi: 10.1038/s41467-020-17670-y

44. Riella LV, Paterson AM, Sharpe AH, Chandraker A. Role of the PD-1 pathway in the immune response. *Am J Transplant*. 2012;12(10):2575-2587.

doi: 10.1111/j.1600-6143.2012.04224.x

45. Ishida Y, Agata Y, Shibahara K, Honjo T. Induced expression of PD-1, a novel member of the immunoglobulin gene superfamily, upon programmed cell death. *Embo J*. 1992;11(11):3887-3895.

doi: 10.1002/j.1460-2075.1992.tb05481.x

46. Neel BG, Gu H, Pao L. The "Shp'ing news: SH2 domain-containing tyrosine phosphatases in cell signaling. *Trends Biochem Sci*. 2003;28(6):284-293.

doi: 10.1016/s0968-0004(03)00091-4

47. Han Y, Liu D, Li L. PD-1/PD-L1 pathway: Current researches in cancer. *Am J Cancer Res*. 2020;10(3):727-742.

48. Ahmadzadeh M, Johnson LA, Heemskerk B, *et al*. Tumor antigen-specific CD8 T cells infiltrating the tumor express high levels of PD-1 and are functionally impaired. *Blood*. 2009;114(8):1537-1544.

doi: 10.1182/blood-2008-12-195792

49. Keir ME, Butte MJ, Freeman GJ, Sharpe AH. PD-1 and its ligands in tolerance and immunity. *Annu Rev Immunol*. 2008;26:677-704.

doi: 10.1146/annurev.immunol.26.021607.090331

50. Staron MM, Gray SM, Marshall HD, *et al*. The transcription factor FoxO1 sustains expression of the inhibitory receptor PD-1 and survival of antiviral CD8(+) T cells during chronic infection. *Immunity*. 2014;41(5):802-814.

doi: 10.1016/j.immuni.2014.10.013

51. Morimoto Y, Kishida T, Kotani SI, Takayama K, Mazda O. Interferon-β signal may up-regulate PD-L1 expression through IRF9-dependent and independent pathways in lung cancer cells. *Biochem Biophys Res Commun*. 2018;507(1-4):330-336.

doi: 10.1016/j.bbrc.2018.11.035

52. Mathieu M, Cotta-Grand N, Daudelin JF, Thébault P, Labrecque N. Notch signaling regulates PD-1 expression during CD8(+) T-cell activation. *Immunol Cell Biol*. 2013;91(1):82-88.

doi: 10.1038/icb.2012.53

53. Kinter AL, Godbout EJ, McNally JP, *et al*. The common gamma-chain cytokines IL-2, IL-7, IL-15, and IL-21 induce the expression of programmed death-1 and its ligands. *J Immunol*. 2008;181(10):6738-6746.

doi: 10.4049/jimmunol.181.10.6738

54. Oestreich KJ, Yoon H, Ahmed R, Boss JM. NFATc1 regulates PD-1 expression upon T cell activation. *J Immunol*. 2008;181(7):4832-4839.

doi: 10.4049/jimmunol.181.7.4832

55. Sharpe AH, Wherry EJ, Ahmed R, Freeman GJ. The function of programmed cell death 1 and its ligands in regulating autoimmunity and infection. *Nat Immunol*. 2007;8(3):239-245.

doi: 10.1038/ni1443

56. Yamazaki T, Akiba H, Iwai H, *et al*. Expression of

programmed death 1 ligands by murine T cells and APC. *J Immunol*. 2002;169(10):5538-5545.

doi: 10.4049/jimmunol.169.10.5538

57. Freeman GJ, Long AJ, Iwai Y, *et al*. Engagement of the PD-1 immunoinhibitory receptor by a novel B7 family member leads to negative regulation of lymphocyte activation. *J Exp Med*. 2000;192(7):1027-1034.

doi: 10.1084/jem.192.7.1027

58. Dong H, Zhu G, Tamada K, Chen L. B7-H1, a third member of the B7 family, co-stimulates T-cell proliferation and interleukin-10 secretion. *Nat Med*. 1999;5(12):1365-1369.

doi: 10.1038/70932

59. Dong H, Strome SE, Salomao DR, *et al*. Tumor-associated B7-H1 promotes T-cell apoptosis: A potential mechanism of immune evasion. *Nat Med*. 2002;8(8):793-800.

doi: 10.1038/nm730

60. Trabattoni D, Saresella M, Biasin M, *et al*. B7-H1 is up-regulated in HIV infection and is a novel surrogate marker of disease progression. *Blood*. 2003;101(7):2514-2520.

doi: 10.1182/blood-2002-10-3065

61. Zheng Y, Fang YC, Li J. PD-L1 expression levels on tumor cells affect their immunosuppressive activity. *Oncol Lett*. 2019;18(5):5399-5407.

doi: 10.3892/ol.2019.10903

62. Latchman YE, Liang SC, Wu Y, *et al*. PD-L1-deficient mice show that PD-L1 on T cells, antigen-presenting cells, and host tissues negatively regulates T cells. *Proc Natl Acad Sci U S A*. 2004;101(29):10691-10696.

doi: 10.1073/pnas.0307252101

63. Torphy RJ, Schulick RD, Zhu Y. Newly emerging immune checkpoints: Promises for future cancer therapy. *Int J Mol Sci*. 2017;18(12):2642.

doi: 10.3390/ijms18122642

64. Chemnitz JM, Parry RV, Nichols KE, June CH, Riley JL. SHP-1 and SHP-2 associate with immunoreceptor tyrosine-based switch motif of programmed death 1 upon primary human T cell stimulation, but only receptor ligation prevents T cell activation. *J Immunol*. 2004;173(2):945-954.

doi: 10.4049/jimmunol.173.2.945

65. Parry RV, Chemnitz JM, Frauwirth KA, *et al*. CTLA-4 and PD-1 receptors inhibit T-cell activation by distinct mechanisms. *Mol Cell Biol*. 2005;25(21):9543-9553.

doi: 10.1128/mcb.25.21.9543-9553.2005

66. Carter L, Fouser LA, Jussif J, *et al*. PD-1:PD-L inhibitory pathway affects both CD4(+) and CD8(+) T cells and is overcome by IL-2. *Eur J Immunol*. 2002;32(3):634-643.

doi: 10.1002/1521-4141(200203)32:3<634::aid-immu634>3.0.co;2-9

67. Ding G, Shen T, Yan C, Zhang M, Wu Z, Cao L. IFN-γ down-regulates the PD-1 expression and assist nivolumab in PD-1-blockade effect on CD8+ T-lymphocytes in pancreatic cancer. *BMC Cancer*. 2019;19(1):1053.

doi: 10.1186/s12885-019-6145-8

68. Lai X, Hao W, Friedman A. TNF-α inhibitor reduces drug-resistance to anti-PD-1: A mathematical model. *PLoS One*. 2020;15(4):e0231499.

doi: 10.1371/journal.pone.0231499

69. Keir ME, Liang SC, Guleria I, *et al*. Tissue expression of PD-L1 mediates peripheral T cell tolerance. *J Exp Med*. 2006;203(4):883-895.

doi: 10.1084/jem.20051776

70. Darvin P, Sasidharan Nair V, Elkord E. PD-L1 expression in human breast cancer stem cells is epigenetically regulated through posttranslational histone modifications. *J Oncol*. 2019;2019:3958908.

doi: 10.1155/2019/3958908

71. Takada K, Toyokawa G, Okamoto T, *et al*. A comprehensive analysis of programmed cell death ligand-1 expression with the clone SP142 antibody in non-small-cell lung cancer patients. *Clin Lung Cancer*. 2017;18(5):572-582.e1.

doi: 10.1016/j.cllc.2017.02.004

72. Nakanishi J, Wada Y, Matsumoto K, Azuma M, Kikuchi K, Ueda S. Overexpression of B7-H1 (PD-L1) significantly associates with tumor grade and postoperative prognosis in human urothelial cancers. *Cancer Immunol Immunother*. 2007;56(8):1173-1182.

doi: 10.1007/s00262-006-0266-z

73. Schiwitza A, Schildhaus HU, Zwerger B, *et al*. Monitoring efficacy of checkpoint inhibitor therapy in patients with non-small-cell lung cancer. *Immunotherapy*. 2019;11(9):769-782.

doi: 10.2217/imt-2019-0039

74. Mager L, Gardeen S, Carr DR, Shahwan KT. Cemiplimab for the treatment of advanced cutaneous squamous cell carcinoma: Appropriate patient selection and perspectives. *Clin Cosmet Investig Dermatol*. 2023;16:2135-2142.

doi: 10.2147/ccid.s381471

75. Lantuejoul S, Damotte D, Hofman V, Adam J. Programmed death ligand 1 immunohistochemistry in non-small cell lung carcinoma. *J Thorac Dis*. 2019;11(Suppl 1):S89-S101.

doi: 10.21037/jtd.2018.12.103

76. Atkins MB, Tannir NM. Current and emerging therapies for first-line treatment of metastatic clear cell renal cell carcinoma. *Cancer Treat Rev*. 2018;70:127-137.

doi: 10.1016/j.ctrv.2018.07.009

77. Herbst RS, Giaccone G, de Marinis F, *et al*. Atezolizumab for first-line treatment of PD-L1-selected patients with NSCLC.

N Engl J Med. 2020;383(14):1328-1339.

doi: 10.1056/NEJMoa1917346

78. Morvan MG, Lanier LL. NK cells and cancer: You can teach innate cells new tricks. *Nat Rev Cancer*. 2016;16(1):7-19.

doi: 10.1038/nrc.2015.5

79. Sun JC, Lanier LL. NK cell development, homeostasis and function: Parallels with CD8□ T cells. *Nat Rev Immunol*. 2011;11(10):645-657.

doi: 10.1038/nri3044

80. Yu J, Freud AG, Caligiuri MA. Location and cellular stages of natural killer cell development. *Trends Immunol*. 2013;34(12):573-582.

doi: 10.1016/j.it.2013.07.005

81. Voskoboinik I, Whisstock JC, Trapani JA. Perforin and granzymes: Function, dysfunction and human pathology. *Nat Rev Immunol*. 2015;15(6):388-400.

doi: 10.1038/nri3839

82. Vivier E, Tomasello E, Baratin M, Walzer T, Ugolini S. Functions of natural killer cells. *Nat Immunol*. 2008;9(5):503-510.

doi: 10.1038/ni1582

83. Houchins JP, Yabe T, McSherry C, Bach FH. DNA sequence analysis of NKG2, a family of related cDNA clones encoding type II integral membrane proteins on human natural killer cells. *J Exp Med*. 1991;173(4):1017-1020.

doi: 10.1084/jem.173.4.1017

84. Yabe T, McSherry C, Bach FH, *et al*. A multigene family on human chromosome 12 encodes natural killer-cell lectins. *Immunogenetics*. 1993;37(6):455-460.

doi: 10.1007/bf00222470

85. Diefenbach A, Tomasello E, Lucas M, *et al*. Selective associations with signaling proteins determine stimulatory versus costimulatory activity of NKG2D. *Nat Immunol*. 2002;3(12):1142-1149.

doi: 10.1038/ni858

86. Wu J, Song Y, Bakker AB, *et al*. An activating immunoreceptor complex formed by NKG2D and DAP10. *Science*. 1999;285(5428):730-732.

doi: 10.1126/science.285.5428.730

87. Upshaw JL, Arneson LN, Schoon RA, Dick CJ, Billadeau DD, Leibson PJ. NKG2D-mediated signaling requires a DAP10-bound Grb2-Vav1 intermediate and phosphatidylinositol-3-kinase in human natural killer cells. *Nat Immunol*. 2006;7(5):524-532.

doi: 10.1038/ni1325

88. Lanier LL, Corliss BC, Wu J, Leong C, Phillips JH. Immunoreceptor DAP12 bearing a tyrosine-based activation motif is involved in activating NK cells. *Nature*. 1998;391(6668):703-707.

doi: 10.1038/35642

89. Duan S, Guo W, Xu Z, *et al*. Natural killer group 2D receptor and its ligands in cancer immune escape. *Mol Cancer*. 2019;18(1):29.

doi: 10.1186/s12943-019-0956-8

90. Zompi S, Hamerman JA, Ogasawara K, *et al*. NKG2D triggers cytotoxicity in mouse NK cells lacking DAP12 or Syk family kinases. *Nat Immunol*. 2003;4(6):565-572.

doi: 10.1038/ni930

91. Bahram S, Bresnahan M, Geraghty DE, Spies T. A second lineage of mammalian major histocompatibility complex class I genes. *Proc Natl Acad Sci U S A*. 1994;91(14):6259-6263.

doi: 10.1073/pnas.91.14.6259

92. Zhang J, Basher F, Wu JD. NKG2D ligands in tumor immunity: Two sides of a coin. *Front Immunol*. 2015;6:97.

doi: 10.3389/fimmu.2015.00097

93. González S, López-Soto A, Suarez-Alvarez B, López-Vázquez A, López-Larrea C. NKG2D ligands: Key targets of the immune response. *Trends Immunol*. 2008;29(8):397-403.

doi: 10.1016/j.it.2008.04.007

94. Zhuang L, Fulton RJ, Rettman P, *et al*. Activity of IL-12/15/18 primed natural killer cells against hepatocellular carcinoma. *Hepatol Int*. 2019;13(1):75-83.

doi: 10.1007/s12072-018-9909-3

95. Konjević G, Mirjačić Martinović K, Vuletić A, Babović N. *In-vitro* IL-2 or IFN-α-induced NKG2D and CD161 NK cell receptor expression indicates novel aspects of NK cell activation in metastatic melanoma patients. *Melanoma Res*. 2010;20(6):459-467.

doi: 10.1097/CMR.0b013e32833e3286

96. Song H, Hur DY, Kim KE, *et al*. IL-2/IL-18 prevent the down-modulation of NKG2D by TGF-beta in NK cells via the c-Jun N-terminal kinase (JNK) pathway. *Cell Immunol*. 2006;242(1):39-45.

doi: 10.1016/j.cellimm.2006.09.002

97. Weiss T, Schneider H, Silginer M, *et al*. NKG2D-dependent antitumor effects of chemotherapy and radiotherapy against glioblastoma. *Clin Cancer Res*. 2018;24(4):882-895.

doi: 10.1158/1078-0432.ccr-17-1766

98. Okita R, Yukawa T, Nojima Y, *et al*. MHC class I chain-related molecule A and B expression is upregulated by cisplatin and associated with good prognosis in patients with non-small cell lung cancer. *Cancer Immunol Immunother*. 2016;65(5):499-509.

doi: 10.1007/s00262-016-1814-9

99. Chan WK, Kang S, Youssef Y, *et al*. A CS1-NKG2D bispecific antibody collectively activates cytolytic immune cells against multiple myeloma. *Cancer Immunol Res*. 2018;6(7):776-787.

doi: 10.1158/2326-6066.cir-17-0649

100. Wang Y, Li H, Xu W, *et al*. BCMA-targeting bispecific antibody that simultaneously stimulates NKG2D-enhanced efficacy against multiple myeloma. *J Immunother*. 2020;43(6):175-188.

doi: 10.1097/cji.0000000000000320

101. Basher F, Dhar P, Wang X, *et al*. Antibody targeting tumor-derived soluble NKG2D ligand sMIC reprograms NK cell homeostatic survival and function and enhances melanoma response to PDL1 blockade therapy. *J Hematol Oncol*. 2020;13(1):74.

doi: 10.1186/s13045-020-00896-0

102. Deng Q, Lee M, Fattah F, Koyama S, Gerber D, Akbay E. YIA23-001: Targeting NKG2D ligands is therapeutically effective in NSCLC. *J Natl Comprehensive Cancer Netw*. 2023;21(3.5):YIA23-001-YIA23-001.

doi: 10.6004/jnccn.2022.7136

103. Shen MJ, Xu LJ, Yang L, *et al*. Radiation alters PD-L1/NKG2D ligand levels in lung cancer cells and leads to immune escape from NK cell cytotoxicity via IL-6-MEK/Erk signaling pathway. *Oncotarget*. 2017;8(46):80506-80520.

doi: 10.18632/oncotarget.19193

104. Xu L, Chen X, Shen M, *et al*. Inhibition of IL-6-JAK/Stat3 signaling in castration-resistant prostate cancer cells enhances the NK cell-mediated cytotoxicity via alteration of PD-L1/NKG2D ligand levels. *Mol Oncol*. 2018;12(3):269-286.

doi: 10.1002/1878-0261.12135

105. Okita R, Maeda A, Shimizu K, Nojima Y, Saisho S, Nakata M. Effect of platinumbased chemotherapy on the expression of natural killer group 2 member D ligands, programmed cell death1 ligand 1 and HLA class I in nonsmall cell lung cancer. *Oncol Rep*. 2019;42(2):839-848.

doi: 10.3892/or.2019.7185

106. Battaglia NG, Murphy JD, Uccello TP, *et al*. Combination of NKG2A and PD-1 blockade improves radiotherapy response in radioresistant tumors. *J Immunol*. 2022;209(3):629-640.

doi: 10.4049/jimmunol.2100044

107. Bogen JP, Carrara SC, Fiebig D, Grzeschik J, Hock B, Kolmar H. Design of a trispecific checkpoint inhibitor and natural killer cell engager based on a 2 + 1 common light chain antibody architecture. *Front Immunol*. 2021;12:669496.

doi: 10.3389/fimmu.2021.669496

108. Dougan M, Ingram JR, Jeong HJ, *et al*. Targeting cytokine therapy to the pancreatic tumor microenvironment using PD-L1-specific VHHs. *Cancer Immunol Res*. 2018;6(4):389-401.

doi: 10.1158/2326-6066.cir-17-0495

109. Jiang G, Ng YY, Tay JCK, *et al*. Dual CAR-T cells to treat cancers co-expressing NKG2D and PD1 ligands in xenograft models of peritoneal metastasis. *Cancer Immunol Immunother*. 2023;72(1):223-234.

doi: 10.1007/s00262-022-03247-9

110. Kang TH, Mao CP, He L, *et al*. Tumor-targeted delivery of IL-2 by NKG2D leads to accumulation of antigen-specific CD8+ T cells in the tumor loci and enhanced anti-tumor effects. *PLoS One*. 2012;7(4):e35141.

doi: 10.1371/journal.pone.0035141

111. Pan M, Wang F, Nan L, *et al*. αVEGFR2-MICA fusion antibodies enhance immunotherapy effect and synergize with PD-1 blockade. *Cancer Immunol Immunother*. 2023;72(4):969-984.

doi: 10.1007/s00262-022-03306-1

112. Chung YM, Tsai WB, Khan PP, *et al*. FOXO3-dependent suppression of PD-L1 promotes anticancer immune responses via activation of natural killer cells. *Am J Cancer Res*. 2022;12(3):1241-1263.

ACCSCIENCE PUBLISHING

Gene & Protein in Disease

ORIGINAL RESEARCH ARTICLE

Bioinformatics analysis of therapeutic targets for idiopathic pulmonary fibrosis and exploration of immune cell infiltration patterns

Zhendong Lu[1], Umair Ali Khan Saddozai[2], Siyun Fu[1], Lingqin Zhu[3], and Jinghui Wang[1,3]*

[1]Department of Medical Oncology, Beijing Tuberculosis and Thoracic Tumor Research Institute, Beijing Chest Hospital, Capital Medical University, Beijing, China

[2]Department of Clinical Medicine, Institute of Translational Medicine, Medical College, Yangzhou University, Yangzhou, Jiangsu, China

[3]Cancer Research Center, Beijing Tuberculosis and Thoracic Tumor Research Institute, Beijing Chest Hospital, Capital Medical University, Beijing, China

Abstract

Idiopathic pulmonary fibrosis (IPF) is a severe progressive lung disease characterized by fibrotic changes in lung tissue, with limited treatment options. This study analyzed gene expression data from three gene expression omnibus datasets (GSE2052, GSE53845, and GSE110147) using R and LIMMA to identify differentially expressed genes (DEGs) in IPF samples. We identified 215 DEGs, comprising 106 upregulated and 109 downregulated genes. Weighted gene coexpression network analysis revealed five gene modules, with the module eigengene yellow showing the strongest correlation with IPF. Functional enrichment analysis of 40 consensus genes in this module indicated their significant involvement in extracellular matrix (ECM) organization. Kyoto Encyclopedia of Genes and Genomes pathway analysis revealed pathways related to protein digestion, cell adhesion molecules, and the advanced glycation end product–receptor for advanced glycation end product signaling pathway. Based on protein–protein interaction network analysis, collagen type XV alpha 1 chain (*COL15A1*) and collagen type VI alpha 3 chain (*COL6A3*) were identified as upregulated hub genes in IPF, which were regulated by microRNAs and transcription factors. Immune cell infiltration analysis showed significant changes in immune cell populations in IPF samples, with increases in memory B cells, plasma cells, and M0 macrophages and decreases in CD8 T cells, and resting natural killer cells. Potential drugs targeting COL15A1 and COL6A3 were predicted using multiple databases, revealing compounds such as (+)-JQ1, aristolochic acid I, and dexamethasone with promising binding potential. These findings suggest that *COL15A1* and *COL6A3* are central hub genes in IPF, are associated with ECM organization and immune response, and serve as therapeutic targets for IPF.

Keywords: Idiopathic pulmonary fibrosis; Weighted gene coexpression network analysis; Immune cell infiltration; MicroRNA-transcription factor-mRNA network; Molecular docking

***Corresponding author:**
Jinghui Wang
(wangjinghui@bjxkyy.cn)

Citation: Lu Z, Saddozai UAK, Fu S, Zhu L, Wang J. Bioinformatics analysis of therapeutic targets for idiopathic pulmonary fibrosis and exploration of immune cell infiltration patterns. *Gene Protein Dis*. 2024;3(4):4101. doi: 10.36922/gpd.4101

Received: July 1, 2024
Accepted: August 13, 2024
Published Online: October 10, 2024

1. Introduction

Idiopathic pulmonary fibrosis (IPF) is a chronic progressive lung disease of unknown origin, which leads to fibrotic changes in the lung interstitium. It primarily affects older individuals and is confined to the lungs. IPF is the most common type of idiopathic interstitial pneumonia, substantially impacting patients' quality of life and ultimately leading to respiratory failure and death.[1] Research indicates that the incidence of IPF ranges from 14.0 to 42.7 cases/100,000 individuals.[2] However, the influence of geographic, cultural, or racial factors on the occurrence and prevalence of IPF remains unclear.[3] IPF generally has an unfavorable prognosis, with considerable variation in its natural course and outcomes. If left untreated, patients with IPF typically have a median survival of 2 – 3 years post-diagnosis,[2] with a 5-year survival rate of only 20%.[4]

The etiological mechanisms of IPF are complex and not fully understood. Extensive research has revealed that IPF pathogenesis involves changes in genetics, epigenetics, microRNA (miRNA) regulation, cell signaling pathways, apoptosis, and autophagy.[4] miRNAs are small RNA molecules that regulate gene expression and participate in physiological processes such as tissue development, tissue repair, and cell proliferation.[5,6] The miRNA regulatory network in IPF has been extensively studied,[7] highlighting its significant role in IPF pathogenesis. In addition, various immune cells, including macrophages, monocytes, T cells, innate lymphoid cells, and neutrophils, play crucial roles in IPF development.[8,9] Therefore, examining specific changes in immune cells in patients with IPF is highly valuable for further research.

Bioinformatics analysis of microarray data is widely used to identify novel biomarkers and investigate their roles in various diseases. Weighted gene coexpression network analysis (WGCNA) is a computational biology tool that is used to construct gene coexpression networks, detect modules, and identify genes and modules of specific interest. WGCNA helps uncover potential biomarkers for different diseases.[10]

This study determined the causes and mechanisms of IPF, focusing on miRNAs, target genes, and immune cells in the tissues of patients with IPF. Three IPF tissue microarray datasets (GSE31821, GSE41177, and GSE79768) were integrated after removing batch differences. Differentially expressed genes (DEGs) were selected based on the intersection of module genes from WGCNA to identify common genes (CGs) strongly associated with IPF. Functional annotation and protein–protein interaction (PPI) analyses of CGs were conducted to identify hub genes, and a miRNA–transcription factor (TF)–mRNA network was constructed. Bioinformatics methods (CIBERSORT) were used to analyze immune infiltrations in IPF samples. In addition, potential therapeutic drugs targeting hub genes in IPF were predicted through the DrugBank database, Comparative Toxicogenomics Database (CTD), and Drug-Gene Interaction Database (DGIdb). This comprehensive analysis aimed to identify potential biomarkers or therapeutic targets for IPF.

2. Methods

2.1. Gene expression dataset

Gene expression data for IPF were obtained from the gene expression omnibus (GEO) database, a publicly accessible repository for gene expression datasets. A search was performed using the keywords "idiopathic pulmonary fibrosis" or "IPF," organism "Homo sapiens," entry type "Series," and study type "Expression profiling by array," yielding 69 microarray expression profile datasets related to IPF. After careful examination, gene expression profiles from three IPF tissue microarray datasets (GSE2052, GSE53845, and GSE110147) were collected. These datasets were based on specific platforms: GPL1739 (Amersham Biosciences CodeLink Uniset Human I Bioarray), GPL6244 ([HuGene-1_0-st] Affymetrix Human Gene 1.0 ST Array [transcript (gene) version]), and GPL6480 (Agilent-014850 Whole Human Genome Microarray 4×44K G4112F [Probe Name version]). The data can be freely accessed online through the GEO database. This study adhered to the principles of the Declaration of Helsinki (revised in 2013), with no involvement of human or animal experiments.

2.2. Analysis of RNA sequencing (RNA-seq) data and identification of DEGs associated with IPF

R software (version 4.2.2) was used to process RNA-seq data and identify DEGs associated with IPF. The preprocessing steps included gene name and probe ID matching, handling of missing data, normalization, and log2 transformation, which were performed using the LIMMA package (version 3.54.2) and impute package (version 1.72.3). The LIMMA package was used to merge three microarray expression profile datasets, and batch effects and other variations were removed using the surrogate variable analysis package (version 3.46.0). IPF DEGs were identified using LIMMA based on the criteria of a cutoff $P < 0.05$ and |log2 fold change (FC)| of >1. DEGs were visualized using the ggplot2 package (version 3.13) and pheatmap package (version 1.0.12).

2.3. Identification of IPF-associated gene modules using WGCNA

WGCNA is a systems biology approach used to identify key genes or hub genes within modules to investigate large-

scale molecular networks and reveal gene interactions and regulatory mechanisms.[10] WGCNA analysis was performed using the R language WGCNA package (version 1.72-1). The top 25% ranked genes based on variance in expression values were selected, outliers were removed, and a reliable WGCNA network was constructed. The soft-thresholding power was determined using the "pickSoftThreshold" function. An adjacency matrix was created and transformed into a topological overlap matrix (TOM). Gene dissimilarity (1-TOM) was calculated, and the dynamic tree-cutting method was used to classify genes into different modules. Modules with a dissimilarity coefficient of <0.2 (correlation coefficient of >0.8) were merged. The modules were further analyzed for correlation with clinical traits by calculating module membership (MM). This analysis revealed the module genes that were most strongly associated with clinical traits, and the correlation network between these key module genes and clinical traits was visualized. Finally, DEGs between IPF and normal control samples were integrated with the key module genes to identify CGs as the final DEGs.

2.4. Gene ontology (GO) and Kyoto encyclopedia of genes and genomes (KEGG) analyses of CGs for gene and protein annotation and pathway enrichment

GO analysis is a bioinformatics method that uses ontology-based approaches to categorize and annotate genes and proteins into three main categories: cellular component (CC), biological process (BP), and molecular function (MF). KEGG is a comprehensive bioinformatics database (https://www.genome.jp/kegg/) that provides extensive information on genes and proteins, including gene sequences, protein structures, chemical reactions, and cellular signal transduction. Analyzing data using KEGG helps in better understanding the functions of genes and proteins as well as their roles in BPs. In this study, we used the "clusterProfiler" R package (version 4.6.2) to perform GO analysis and KEGG pathway enrichment analysis of CGs. Statistically significant results were defined as an adjusted $P \leq 0.05$ and a minimum gene count of ≥2.

2.5. Analysis of PPI network and identification of hub genes

The STRING database is a specialized PPI database that stores interactions from various species, including both experimentally validated and predicted interactions. In this study, the PPI network of CGs was analyzed using the STRING database with a minimum interaction score cutoff of ≥0.4. Cytoscape_v3.10.1 was used to visualize the PPI network,[11] and the CytoHubba plugin was utilized to identify hub nodes. Each gene in the PPI network was assigned a value using 12 topological network algorithms to identify and rank the hub genes. The hub gene network was further visualized using Cytoscape_v3.10.1.

2.6. Analysis and construction of the miRNA–TF–mRNA network

The miRTarBase,[12] Starbase,[13] and TargetScan[14] databases are widely used to predict miRNA–mRNA interactions, enhancing our understanding of gene regulation. These databases contain extensive information on known miRNA–mRNA interactions, which can also be used to predict novel interactions. A Venn diagram was used to identify overlapping miRNAs from all three databases. Enrichr (http://amp.pharm.mssm.edu/Enrichr/) is a web-based platform for gene set enrichment analysis, offering a wide range of genomic libraries. The TRANSFAC and JASPAR position weight matrix sections in Enrichr were used to identify TFs regulating the expression of CGs using a *P*-value threshold of <0.05. After obtaining TF–mRNA and miRNA–mRNA interaction data, they were integrated to establish the miRNA–TF–mRNA network. Cytoscape_v3.10.1 was then used to visualize this regulatory network.

2.7. Immune cell infiltration analysis

CIBERSORT is a gene expression analysis tool that uses known gene expression data to identify and classify different cell types in a sample.[15] It estimates the proportions of each cell type, providing insights into the distribution and gene expression characteristics of various cell populations. In this study, we obtained expression profile data for 22 immune cells from the CIBERSORT website (https://cibersort.stanford.edu/). Using the CIBERSORT algorithm in R, we quantified the relative proportions of infiltrating immune cells in IPF samples. We selected significant samples with a *P*-value threshold of <0.05 and presented the results using a bar plot. To visualize the distribution of immune cell types in IPF samples, we constructed a heatmap using the "pheatmap" package (version 1.0.12) in R. In addition, we used the corrplot package (version 0.92) to generate a correlation heatmap illustrating the relationships between infiltrating immune cells. Finally, we used the vioplot package (version 0.4.0) to construct violin plots comparing the proportions of infiltrating immune cells between IPF and normal control samples.

2.8. Screening of candidate drugs targeting hub genes

The CTD (https://ctdbase.org/) is a comprehensive repository integrating information on chemical substances, genes, functional phenotypes, and disease interactions, providing gene–drug–disease interaction data to support drug screening. The DrugBank database (https://go.drugbank.com/) integrates bioinformatics and

cheminformatics, displaying drug targets, mechanisms of action, and other data, which facilitates the screening of candidate drugs targeting hub genes. DGIdb (https://www.dgidb.org/) focuses on drug–gene interactions, integrating rich data to explore the relationship between drug mechanisms and genes. The 10 key genes identified were collagen type XV alpha 1 chain (*COL15A1*), collagen type VI alpha 3 chain (*COL6A3*), asporin (*ASPN*), collagen type XIV alpha 1 chain (*COL14A1*), fibrillin 1 (*FBN1*), sulfatase 1 (*SULF1*), versican (*VCAN*), thrombospondin 2 (*THBS2*), fibroblast activation protein (*FAP*), and latent transforming growth factor beta binding protein 1 (*LTBP1*). These genes were imported into the DrugBank and DGIdb databases to search for potential drugs targeting these genes. As all 10 key genes are expressed in IPF, these hub genes were imported into the CTD to screen for compounds that can reduce the expression levels of key genes. They were considered as potential targeted drugs for IPF, with the condition that the number of genes reduced should be >5. Finally, Cytoscape was used to visualize the drugs and their interacting hub genes from the three databases.

2.9. Molecular docking

To evaluate the binding energy and interaction mode between candidate drugs/small molecules and the top two hub genes (*COL15A1* and *COL6A3*), we employed the online molecular docking platform CB-Dock2 (https://cadd.labshare.cn/cb-dock2/).[16] CB-Dock2 enables automated protein–ligand blind docking through four steps: data input, processing, cavity detection and docking, and visualization and analysis. The program automatically refines the protein structure and removes impurities. The 3D structures of COL15A1 and COL6A3 were retrieved from the PDB database (https://www.rcsb.org/) as receptors, after limiting "organisms" to "*Homo sapiens*" and "method" to "X-ray diffraction." The 3D structures of compounds were obtained from the PubChem Compound Database (https://pubchem.ncbi.nlm.nih.gov/) as ligands. Compounds whose structures were unavailable in PubChem were excluded. Docking was performed using CB-Dock2 to obtain optimal results, which were then visualized using Discovery Studio software.

2.10. Statistical analysis

In this study, all statistical analyses were conducted using R software (version 4.2.2). The R packages and versions used in each analysis are listed in each section and are available from the Bioconductor website (https://bioconductor.org/) and the R website. All statistical tests were two-sided, with a $P < 0.05$ considered to indicate statistical significance.

3. Results

3.1. DEG analysis in patients with IPF and normal controls

This study integrated gene expression microarray data from three sources: GSE2052, GSE110147, and GSE53845. The GSE2052 dataset included 13 samples from patients with IPF and 11 from normal controls. The GSE110147 dataset contained 22 samples from patients with IPF and 11 from normal controls. Similarly, the GSE53845 dataset comprised 40 samples from patients with IPF and eight from normal controls (Table 1).

Differential analysis between patients with IPF and normal controls revealed 215 DEGs, including 106 significantly upregulated and 109 significantly downregulated genes in the IPF group (Supplementary file: Table S1). The top 5 upregulated genes were transmembrane protein 100 (*TMEM100*; |logFC| = 2.810), carboxypeptidase B2 (*CPB2*; |logFC| = 2.430), vasoactive intestinal peptide receptor 1 (*VIPR1*; |logFC| = 2.424), carbonic anhydrase IV (*CA4*; |logFC| = 2.368), and advanced glycosylation end product-specific receptor (*AGER*; |logFC| = 2.033). The top 5 downregulated genes were secreted phosphoprotein 1 (*SPP1*; |logFC| = 3.894), matrix metalloproteinase 7 (*MMP7*; |logFC| = 3.218), interleukin 13 receptor alpha 2 (*IL13RA2*; |logFC| = 2.800), BPI fold containing family B member 1 (*BPIFB1*; |logFC| = 2.755), and ceruloplasmin (*CP*; |logFC| = 2.639). Figure 1A shows the heatmap of DEGs with |logFC| >1.5 and an adjusted $P < 0.05$, and Figure 1B presents the volcano plot.

3.2. Identification of gene interaction networks and modules in IPF

The upper quartile genes ($n = 2060$) were selected for clustering analysis by calculating the variation in expression values for each gene. An outlier detection threshold of 60 was established. As no samples exceeded this threshold, none of them were excluded. The optimal soft-thresholding power β value was determined to be 5, with an R-squared value of 0.8 (Appendix: Figure A1).

The dynamic tree-cutting method was used for module detection, and modules with highly correlated feature genes (dissimilarity coefficient of <0.2) were merged. Genes within the same module showed high connectivity and shared functional characteristics (Figure 2A). Each module was assigned a distinct color label, and correlation analysis was performed between module eigengenes (MEs) and clinical phenotypes (IPF and normal control samples). Five modules were identified: MEblue, MEbrown, MEturquoise, MEyellow, and MEgrey (Supplementary File: Table S2). The MEyellow module showed the strongest positive correlation

Table 1. Basic data from the three microarray databases derived from the GEO database

Dataset ID	Platform		Normal sample	IPF sample	Region
GSE2052	GPL1739	Amersham Biosciences CodeLink Uniset Human I Bioarray	11	13	USA
GSE110147	GPL6244	[HuGene-1_0-st] Affymetrix Human Gene 1.0 ST Array [transcript (gene) version]	11	22	Canada
GSE53845	GPL6480	Agilent-014850 Whole Human Genome Microarray 4×44K G4112F (Probe Name version)	8	40	USA

Abbreviations: IPF: Idiopathic pulmonary fibrosis; GEO: Gene expression omnibus.

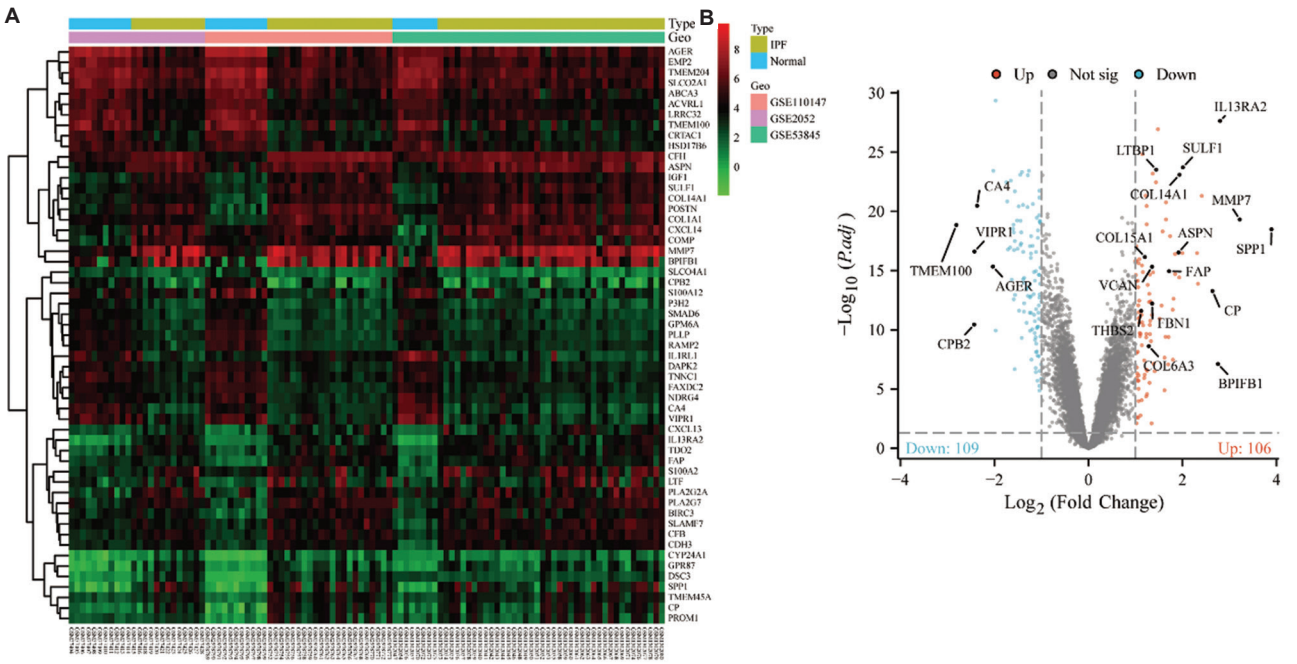

Figure 1. Heatmap and volcano plot based on the results of integrated analysis and differential gene screening of three datasets. (A) The heatmap displays tissue samples in columns and DEGs in rows, with red indicating upregulation and blue denoting downregulation. (B) In the volcano plot, red dots represent upregulated DEGs, whereas blue dots indicate downregulated DEGs.
Abbreviations: IPF: Idiopathic pulmonary fibrosis; DEGs: Differentially expressed genes.

with IPF (r = 0.84, p = 1e−28) (Figure 2B), making it the pivotal module linked to IPF phenotype.

The MM versus gene significance (GS) correlation plots were generated to illustrate the relationship between MM and GS in IPF-related modules. A strong positive correlation was observed between MM and GS in the yellow module (r = 0.93, p = 1.7e−74) (Figure 2C). By integrating and selecting DEGs and genes from the MEyellow module, a final set of 40 CGs was obtained (Figure 2D; Supplementary File: Table S3).

3.3. Functional enrichment analyses of CGs

We performed GO and KEGG pathway analyses of 40 CGs. GO analysis of CGs revealed that 73 terms were enriched (Supplementary File: Table S4). Most of the CGs were enriched in the BP category (n = 53), including extracellular matrix (ECM) organization, extracellular structure organization, ossification, external encapsulating structure organization, and heterophilic cell–cell adhesion through plasma membrane cell adhesion molecules. In the CC category (n = 11), the CGs were notably enriched in collagen trimer, collagen-containing ECM, endoplasmic reticulum lumen, basement membrane, and sarcolemma. In the MF category (n = 9), the CGs were significantly enriched in ECM structural constituent, ECM structural constituent conferring tensile strength, glycosaminoglycan binding, integrin binding, and heparin binding. In addition, KEGG pathway enrichment analysis of CGs revealed nine enriched terms. The main enriched pathways included protein digestion and absorption, malaria, cell adhesion molecules, advanced glycation end product–receptor for advanced glycation end product signaling pathway in diabetic complications, and complement and coagulation cascades (Figure 3, Supplementary File: Table S5).

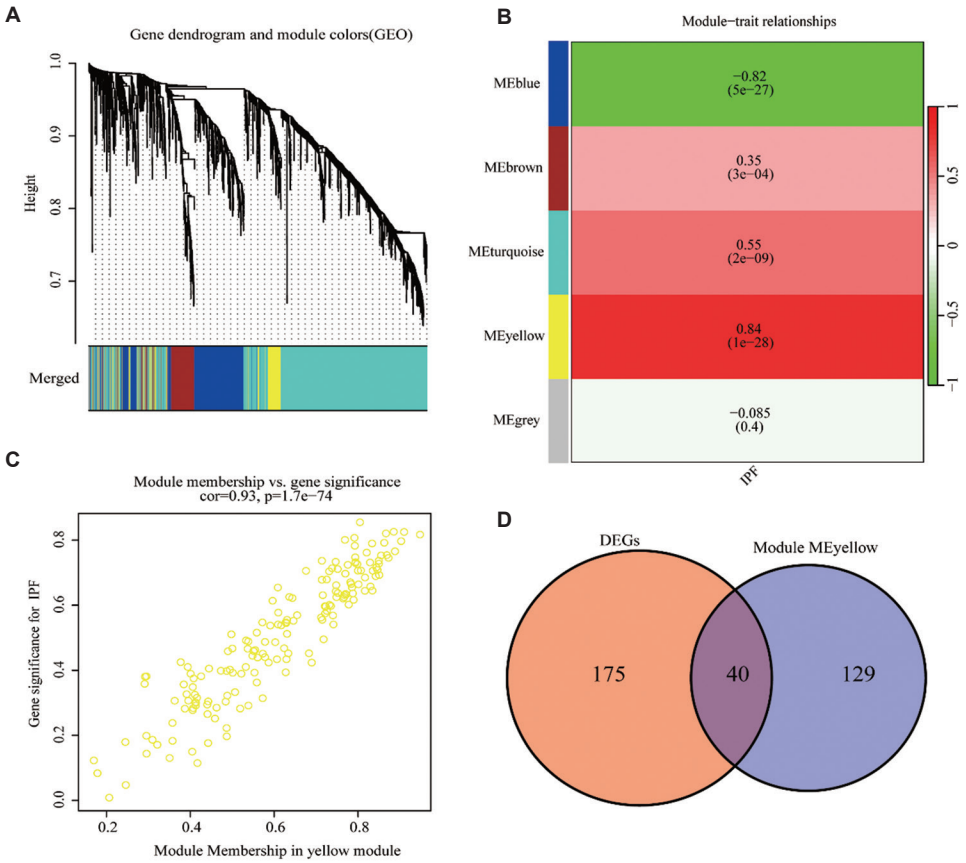

Figure 2. WGCNA and Venn diagram of DEGs and module genes. (A) WGCNA detected coexpressed gene modules associated with IPF traits, represented by different colors. (B) A heatmap showing the correlation between modules and IPF traits, with numbers indicating significance (P-value) and correlation coefficient (r). (C) A scatter plot illustrating the correlation between genes in the yellow module and IPF, using MM and GS as axes. (D) A Venn diagram indicating CGs between IPF DEGs and module genes.
Abbreviations: WGCNA: Weighted gene coexpression network analysis; IPF: Idiopathic pulmonary fibrosis; MM: Module membership; GS: Gene significance; CGs: Common genes; DEGs: Differentially expressed genes.

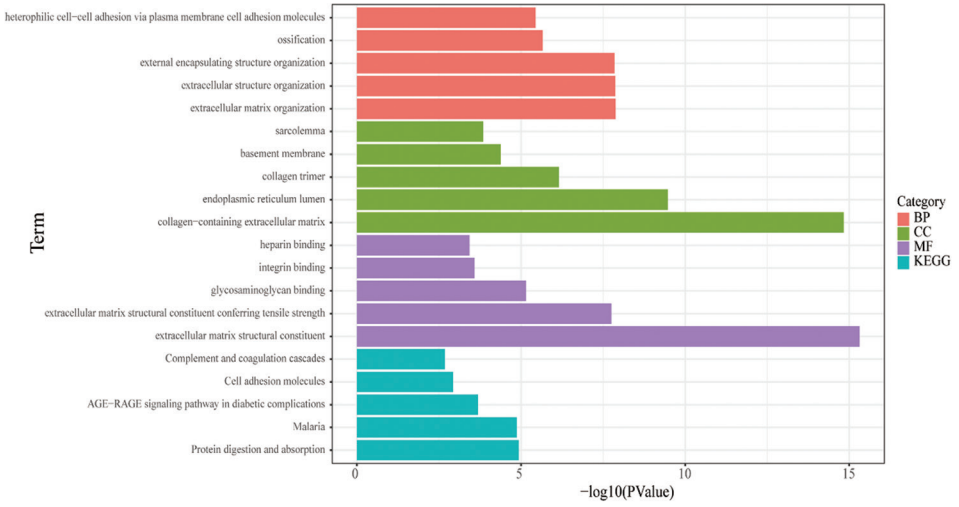

Figure 3. KEGG and GO results. The top 5 significantly enriched GO terms and KEGG pathways for CGs are shown. Red bars represent BP, green bars represent CC, purple bars represent MF, and turquoise bars represent KEGG pathways
Abbreviations: GO: Gene Ontology; KEGG: Kyoto Encyclopedia of Genes and Genomes; CGs: Common genes; BP: Biological process; CC: Cellular component; MF: Molecular function.

3.4. Identification of hub genes and construction of a PPI network in IPF

Using the STRING web tool, the CG PPI network was initially established and refined by removing disconnected nodes (Supplementary File: Table S6). The final PPI network consisted of 30 nodes and 105 edges and included 29 upregulated genes and one downregulated gene (Figure 4A). The CytoHubba (v0.1) plugin was used to identify the top 10 hub genes in this network: *COL15A1*; *COL6A3*; *ASPN*; *COL14A1*; *FBN1*; *SULF1*; *VCAN*; *THBS2*; *FAP*; *LTBP1* (Supplementary File: Table S7). Notably, *COL15A1* and *COL6A3* exhibited the highest centrality, and all hub genes were upregulated in IPF (Figure 4B).

3.5. Integration and analysis of miRNA–TF–mRNA regulatory networks in hub genes

We predicted miRNA–mRNA and TF–mRNA networks for the 10 hub genes using miRTarBase, Starbase, TargetScan, and Enrichr databases. By integrating the two data files datasets, we obtained regulatory relationship data for miRNA–TF–mRNA, resulting in a network of 28 miRNAs, 5 TFs, and 10 mRNA genes. This integrated network was visualized using Cytoscape_v3.10.1 (Figure 5, Supplementary File: Table S8). In addition, we predicted miRNA–TF–mRNA relationships for the 40 CGs; the results are presented in Appendix (Figure A2) and 3. Further analysis revealed that *COL15A1* is targeted by the TFs mindbomb E3 ubiquitin protein ligase 2 (MIB2) and runt-related transcription factor 2 (RUNX2). Similarly, *COL6A3* is targeted by the TFs high mobility group AT-hook 1 (HMGA1) and RUNX2. Furthermore, hsa-miR-29b-3p and hsa-miR-29c-3p were identified as regulators of both *COL15A1* and *COL6A3*.

3.6. Immune cell infiltration and correlation analysis in IPF

The bar chart and heatmap display the proportion of immune cells in each sample from the IPF datasets (Figure 6A and B). As shown in violin plots, the proportions of memory B cells, plasma cells, resting CD4 memory T cells, activated CD4 memory T cells, M0 macrophages, resting dendritic cells, and resting mast cells were higher, whereas the proportions of CD8 T cells, resting natural killer (NK) cells, and monocytes were lower in the IPF group than in the control group (Figure 6C). Correlation analysis revealed a positive correlation between memory B cells and regulatory T cells (Tregs) (r = 0.5) and between M1 macrophages and activated NK cells (r = 0.42). Conversely, negative correlations were observed between activated and resting mast cells (r = −0.45), between monocytes and plasma cells (r = −0.43), between neutrophils and activated NK cells (r = −0.53), and between resting CD4 memory T cells and CD8 T cells (r = −0.50) (Figure 6D).

3.7. Screening of candidate drugs targeting hub genes

To explore potential treatment methods, the DrugBank, CTD, and DGIdb databases were used to predict drugs targeting the hub genes (Figure 5). Based on DrugBank, only hyaluronic acid was identified as a compound targeting *VCAN*. Meanwhile, based on DGIdb, the following drugs or compounds targeting hub genes

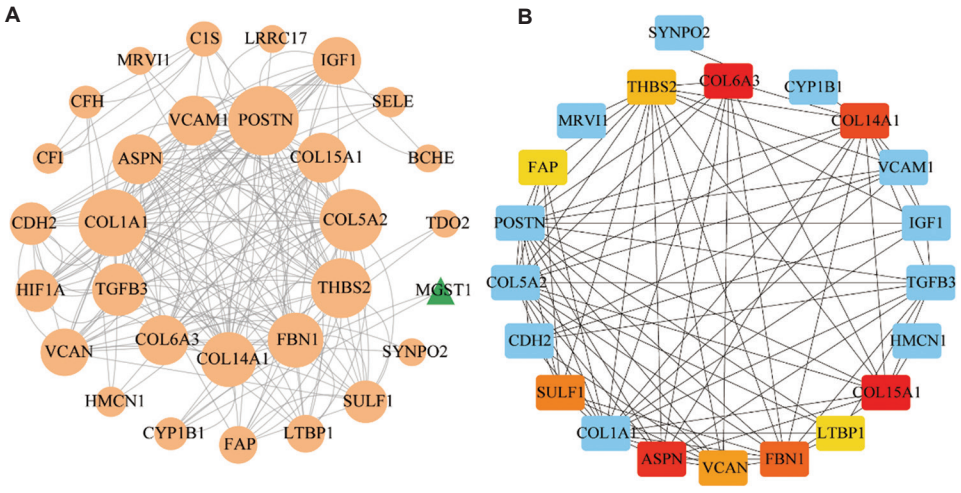

Figure 4. PPI network construction and hub gene selection. (A) Orange nodes (circles) represent upregulated genes, whereas green nodes (triangles) represent downregulated genes. The size of the node indicates the gene's importance and centrality in the network, with larger circles indicating higher importance and centrality. (B) Selection of hub genes using the DMNC algorithm, where the depth of the color represents the gene's score. Darker red colors indicate higher scores.
Abbreviations: PPI: Protein–protein interaction; CGs: Common genes.

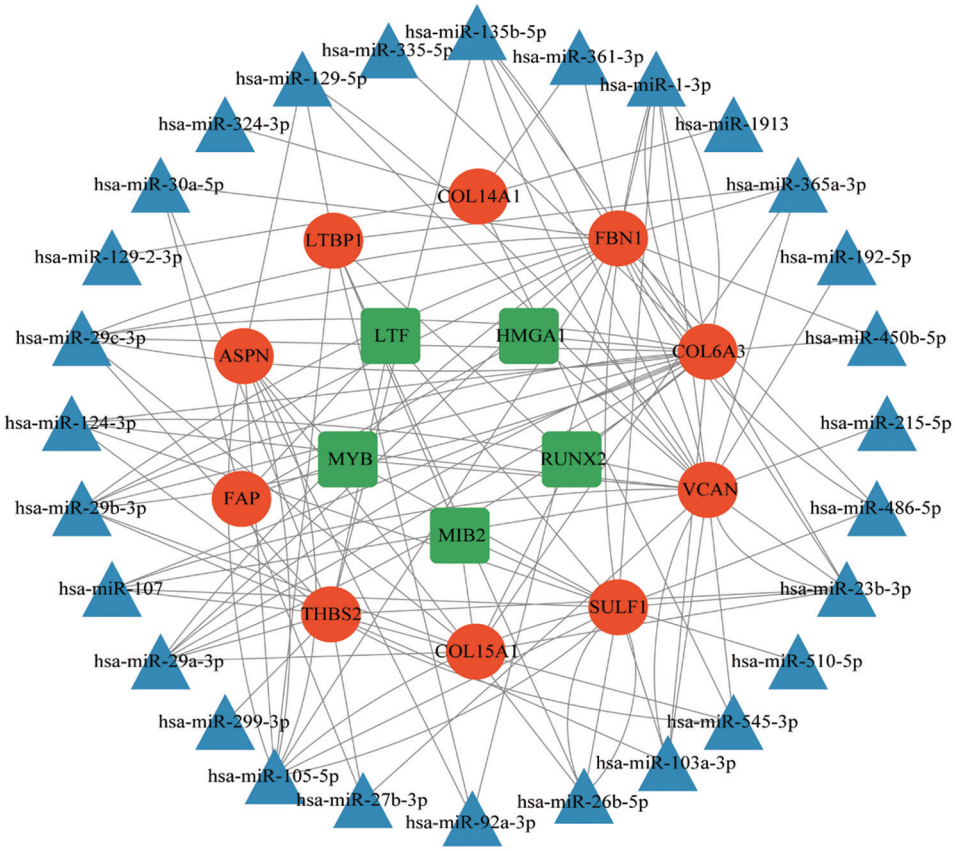

Figure 5. Construction of the miRNA–TF–mRNA regulatory network related to hub genes. Red nodes (circles) represent predicted mRNA, blue nodes (triangles) represent miRNA, and green nodes (squares) represent TFs
Abbreviations: mRNA: Messenger RNA; miRNA: MicroRNA; TFs: Transcription factors.

were identified: collagenase clostridium histolyticum (targeting *COL15A1* and *COL6A3*), ocriplasmin (targeting *COL15A1* and *COL6A3*), cyclosporine (targeting *VCAN*), bevacizumab (targeting *THBS2*), and talabostat (targeting *FAP*). In addition, CTD screening revealed more drugs or compounds, with each of them targeting ≥5 hub genes. Finally, drugs or compounds that could reduce the expression levels of hub genes were identified: aristolochic acid I, (+)-JQ1 compound, triclosan, sodium arsenite, doxorubicin, dexamethasone, valproic acid, tobacco smoke pollution, and cyclosporine (Figure 7 and Supplementary File: Table S9).

3.8. Molecular docking

The 3D structures of aristolochic acid I, (+)-JQ1 compound, triclosan, doxorubicin, dexamethasone, valproic acid, and cyclosporine were obtained from the PubChem Compound Database (2D structures were converted to 3D structures using Chem3D if needed). The 3D structures of COL15A1 (PDB ID: 3N3F; resolution: 2.005 Å) and COL6A3 (PDB ID: 6SNK; resolution: 2.2 Å) were downloaded from PDB. Molecular docking was performed using CB-Dock2, and the best ligand–receptor binding modes were selected based on "Vina score" and "cavity size." The results showed that cyclosporine was bound tightly to the COL15A1 protein receptor (Figure 8A) with a Vina score of −7.2 Furthermore, cyclosporine also exhibited high binding affinity toward the COL6A3 protein receptor (Figure 8B). Respectively, dexamethasone (Figure 8C) and (+)-JQ1 compound (Figure 8D) also displayed notable binding affinities. The detailed results are presented in Table 2. Further visualization was performed for binding results with a Vina score of <−7.0.

4. Discussion

IPF is a chronic progressive interstitial lung disease characterized by fibrosis, primarily affecting middle-aged and older individuals. Its etiology and pathogenesis remain unclear. Owing to small sample sizes in previous studies, limited research has been conducted on gene expression in IPF. This study integrated three IPF datasets to examine

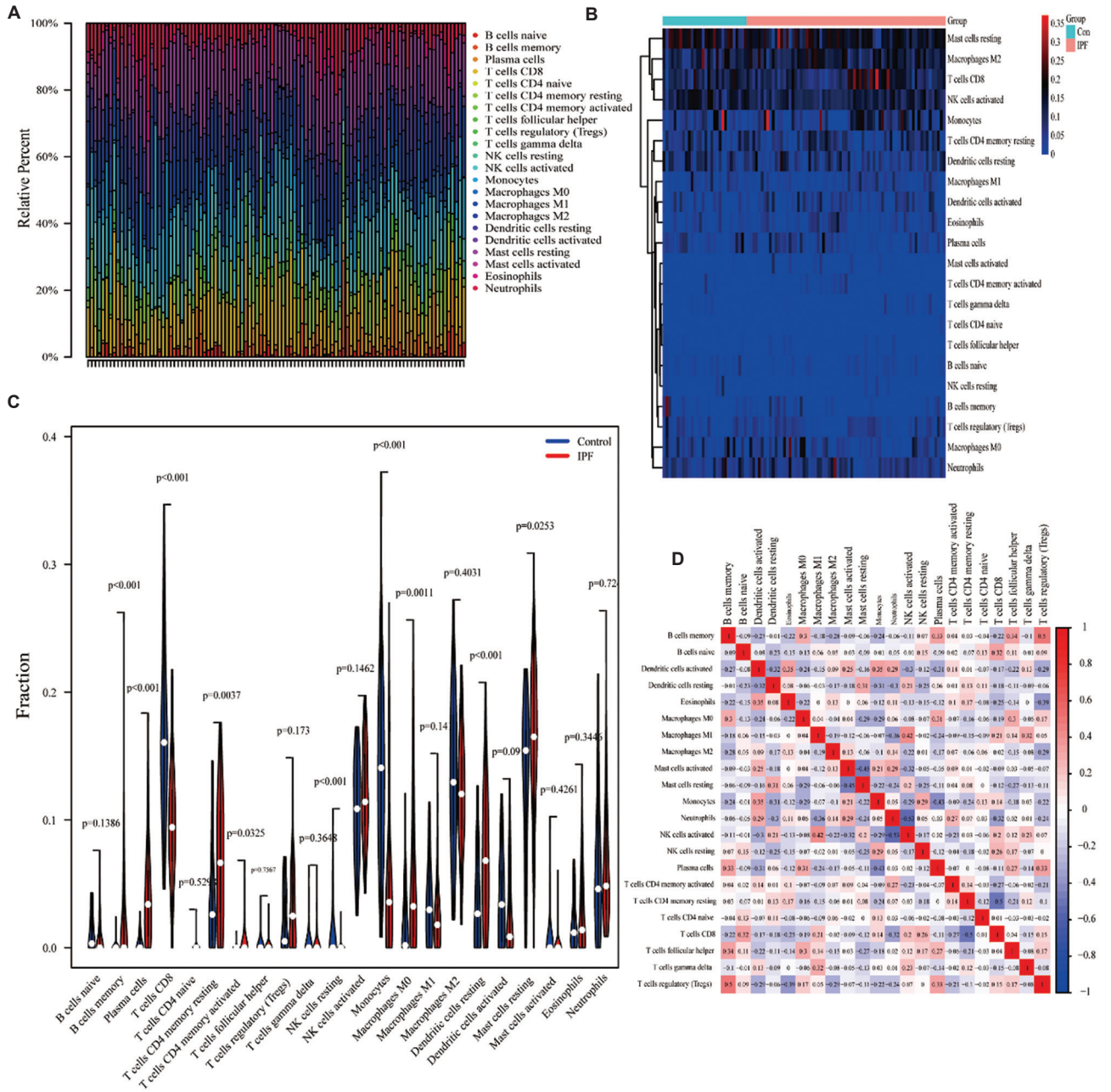

Figure 6. A bar chart and heatmap of immune cell infiltration in the IPF and normal control groups. (A) A bar chart showing the relative proportions of immune cells per sample. (B) A heatmap displaying values of immune cell infiltration per sample estimated using CIBERSORT. Violin plots illustrate the differences in immune cell infiltration and the correlation between infiltrating immune cells. (C) Based on violin plots, differences in immune cell types were evaluated between the IPF and control groups, with blue representing controls and red representing patients with IPF. (D) The correlation matrix shows relationships among 22 immune cell types, where red indicates a strong positive correlation, blue indicates a strong negative correlation, and white indicates no correlation.

Abbreviation: IPF: Idiopathic pulmonary fibrosis.

DEGs between IPF and normal control samples, identifying 215 DEGs, including 106 upregulated (e.g., *SPP1*, *MMP7*, and *IL13RA2*) and 109 downregulated (e.g., *TMEM100*, *CPB2*, and *VIPR1*) genes.

Research has shown that the upregulation of *SPP1* in lung macrophages of patients with IPF suggests the involvement of *SPP1* and *MERTK* co-expressing macrophages in tissue repair and fibrosis.[17] A previous

mouse study demonstrated increased interaction between PDIA3 and SPP1, which is linked to reduced lung function in patients with IPF.[18] Elevated blood MMP7 levels have been reported in subclinical familial pulmonary fibrosis, with the expression of *MMP7* showing a correlation with IPF severity.[19] *MMP7* knockout mice showed reduced bleomycin (BLM)-induced fibrosis, suggesting a profibrotic role of MMP7 in IPF.[20] IL13RA2 is a hallmark of IPF but cannot predict acute exacerbation.[21] Limited research has been conducted on the role of TMEM100, a transmembrane protein with diverse biological functions, in IPF, warranting further investigation.[22] CPB2, also known as plasma carboxypeptidase B, suppressed C5a-induced inflammation in autoimmune arthritis models.[23,24] However, research on CPB2 in IPF is sparse, and considering the involvement of the autoimmune system and inflammation in IPF pathogenesis, the role of CPB2 in IPF warrants further exploration. VIPR1, a G-protein-coupled receptor predominantly expressed in healthy tissues, is involved in various physiological processes, including glycogen metabolism and immune system modulation.[25] VIPR1 is associated with several cancers, with high expression levels in breast, gastric, and colorectal cancers and low expression levels in lung and liver cancers. It is associated with cancer migration, invasion, cell proliferation, and differentiation.[26,27] However, research on VIPR1 in IPF is limited, making its function worth exploring.

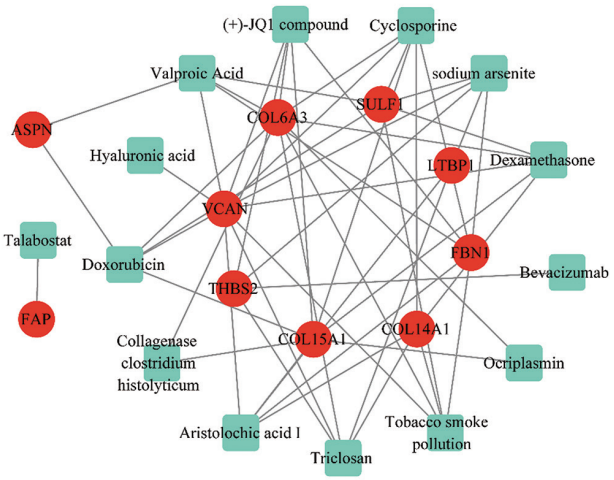

Figure 7. Prediction of potential drugs targeting hub genes using DrugBank, CTD, and DGIdb. Green squares represent drugs/compounds, and red circles represent genes
Abbreviations: CTD: Comparative Toxicogenomics Database; DGIdb: Drug-Gene Interaction Database.

Further analysis revealed *COL15A1* and *COL6A3* as hub genes. *COL15A1* encodes the alpha chain of collagen XV, primarily produced by mesenchymal cells such as myocytes and adipocytes. It possesses antiangiogenic and antitumor properties and plays a key role in maintaining tissue homeostasis in various organs, such as the liver, eye, kidney, and central nervous system.[28,29] Although research suggests a link between *COL15A1* and IPF development,[30] the mechanisms underlying this link remain poorly understood. In contrast, *COL6A3* encodes a component

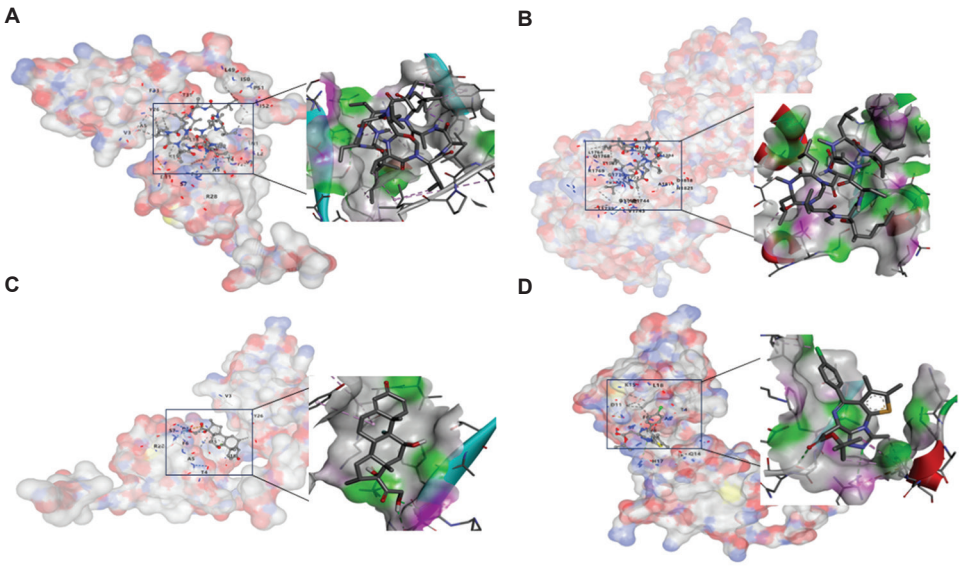

Figure 8. Macromolecular docking images of potential drugs with COL15A1 and COL6A3. (A) Molecular docking of cyclosporine and COL15A1. (B) Molecular docking of cyclosporine and COL6A3. (C) Molecular docking of dexamethasone and COL6A3. (D) Molecular docking of (+)-JQ1 compound and COL6A3.
Abbreviations: COL15A1: Collagen type XV alpha 1 chain; COL6A3: Collagen type VI alpha 3 chain.

Table 2. Molecular docking of potential therapeutic drugs/compounds with COL15A1 and COL6A3

Gene name	Compound name	Vina score (kcal/mol)	Cavity volume (Å^3)	Center (x, y, z)	Docking size (x, y, z)
COL15A1	(+)-JQ1 compound	−6.5	320	−1, 12, −9	22, 22, 22
	Aristolochic acid I	−6.0	320	−1, 12, −9	20, 20, 20
	Dexamethasone	−6.2	320	−1, 12, −9	21, 21, 21
	Doxorubicin	−6.5	320	−1, 12, −9	24, 24, 24
	Cyclosporine	−7.2	99	−12, 13, 10	26, 26, 26
COL6A3	Cyclosporine	−7.2	685	5, 28, 51	26, 26, 26
	Dexamethasone	−7.2	2075	27, 29, 40	21, 27, 21
	(+)-JQ1 compound	−9.9	2075	27, 29, 40	22, 22, 22
	Triclosan	−5.5	2075	27, 29, 40	20, 27, 20
	Valproic acid	−3.9	2075	27, 29, 40	25, 27, 18

Abbreviations: COL15A1: Collagen type XV alpha 1 chain; COL6A3: Collagen type VI alpha 3 chain.

of type VI collagen, a flexible protein found in the extracellular space.[31] It is involved in cell adhesion and has been implicated in promoting inflammation and fibrosis in diabetic kidney disease.[32] However, its role in IPF has not yet been extensively explored.

Compared with normal control samples, the proportions of B cells, plasma cells, and resting CD4 memory T cells were higher and those of CD8 T cells, resting NK cells, and monocytes were lower in IPF samples. This indicates that immune cells substantially influence IPF development. Research has revealed the presence of a large number of macrophages in the pulmonary microenvironment, specifically alveolar macrophages and interstitial macrophages.[33] Alveolar macrophages can secrete fibrogenic cytokines and chemokines, promoting the progression of pulmonary fibrosis.[34] They can also release matrix metalloproteinases to degrade the ECM, thereby reducing its deposition.[35] Evidence indicates that the M2 macrophage phenotype dominates during IPF progression,[36] highlighting the crucial role of macrophages in IPF development. According to a previous study, the number of CD8 T cells in bronchoalveolar lavage fluid of patients with IPF was correlated with the extent of lung fibrosis.[37] Another study revealed that activated CD8 T cells are associated with BLM-induced lung fibrosis.[38] B cells[39] and plasma cells[40] are closely associated with the development and progression of lung fibrosis. In addition, Treg cells, Th22 cells, Th17 cells, eosinophils, and other cell types have been implicated in IPF,[36] providing a theoretical basis for elucidating the mechanisms of IPF and the role of immune cell infiltration.

This study predicted drugs targeting hub genes using multiple databases, identifying compounds that affect the expression of hub genes, such as (+)-JQ1, aristolochic acid I, and dexamethasone. Molecular docking between COL15A1 and COL6A3 with their corresponding drugs demonstrated the binding capacity between key proteins and drugs, providing insights for future drug development.

However, our study had certain limitations. First, we focused only on genes and pathways with significant differences in expression between IPF and normal control samples. In addition, the associations between immune cell infiltration and miRNA were inferred using bioinformatics analysis, requiring further validation through *in vivo* and *in vitro* experiments. In future studies, we plan to functionally investigate key DEGs, such as *COL15A1*, *COL6A3*, *SPP1*, and *TMEM100*, with the aim to uncover crucial factors in IPF development and address clinical treatment challenges.

5. Conclusion

In this study, we conducted an integrated analysis of gene expression data to identify DEGs and key pathways in IPF. We discovered 215 DEGs, such as TMEM100, CPB2, VIPR1, SPP1, and MMP7, with significant expression changes in IPF. Functional analyses implicated these genes in ECM organization, ossification, and cell adhesion. COL15A1 and COL6A3 were identified as hub genes with upregulated expression in IPF, suggesting their potential as therapeutic targets. Immune cell infiltration patterns in IPF were also explored, revealing altered immune responses. Drug prediction and molecular docking identified (+)-JQ1, aristolochic acid I, and dexamethasone as candidates for IPF treatment. This study significantly advances our understanding of IPF pathogenesis and provides valuable insights for future therapeutic development.

Acknowledgments

The authors extend their acknowledgments to all the participants of the study for their valuable contributions to this project.

Funding

The work was supported by the Beijing Municipal Public Welfare Development and Reform Pilot Project for Medical Research Institutes (PWD&RPP-MRI; Project Number: JYY2023-14).

Conflict of interest

Umair Ali Khan Saddozai serves as the Editorial Board Member of the journal but was not in any way involved in the editorial and peer-review process conducted for this paper, directly or indirectly. Separately, the authors declare that the research was conducted in the absence of any commercial or financial relationships that could be construed as a potential conflict of interest.

Author contributions

Conceptualization: Jinghui Wang, Zhendong Lu
Formal analysis: Zhendong Lu, Siyun Fu, Lingqin Zhu, Umair Ali Khan Saddozai
Investigation: Zhendong Lu, Umair Ali Khan Saddozai
Methodology: Jinghui Wang, Zhendong Lu, Umair Ali Khan Saddozai
Writing–original draft: Zhendong Lu
Writing–review & editing: Zhendong Lu, Umair Ali Khan Saddozai

Ethics approval and consent to participate

This study is based on published data and does not involve the collection of new human or animal data. All data used in this study are sourced from previously published research articles and publicly available data sources, and no direct patient contact or intervention was involved in the study. Therefore, ethical approval is not required for this study.

Consent for publication

Not applicable.

Availability of data

The original contributions presented in this study have been included in the article. The raw data designed for this study, GSE2052, GSE53845, and GSE110147, can be obtained from the GEO database. For further inquiries, please contact the corresponding authors.

References

1. Raghu G, Collard HR, Egan JJ, *et al*. An official ATS/ERS/JRS/ALAT statement: Idiopathic pulmonary fibrosis: Evidence-based guidelines for diagnosis and management. *Am J Respir Crit Care Med*. 2011;183(6):788-824. doi: 10.1164/rccm.2009-040GL
2. Raghu G, Weycker D, Edelsberg J, Bradford WZ, Oster G. Incidence and prevalence of idiopathic pulmonary fibrosis. *Am J Respir Crit Care Med*. 2006;174(7):810-816. doi: 10.1164/rccm.200602-163OC
3. Richeldi L, Collard HR, Jones MG. Idiopathic pulmonary fibrosis. *Lancet*. 2017;389(10082):1941-1952. doi: 10.1016/S0140-6736(17)30866-8
4. Wuyts WA, Agostini C, Antoniou KM, *et al*. The pathogenesis of pulmonary fibrosis: A moving target. *Eur Respir J*. 2013;41(5):1207-1218. doi: 10.1183/09031936.00073012
5. Hwang HW, Mendell JT. MicroRNAs in cell proliferation, cell death, and tumorigenesis. *Br J Cancer* 2006;94(6):776-780. doi: 10.1038/sj.bjc.6603023
6. O'Reilly S. MicroRNAs in fibrosis: Opportunities and challenges. *Arthritis Res Ther*. 2016;18:11. doi: 10.1186/s13075-016-0929-x
7. Tzouvelekis A, Kaminski N. Epigenetics in idiopathic pulmonary fibrosis. *Biochem Cell Biol*. 2015, 93(2):159-170. doi: 10.1139/bcb-2014-0126
8. Misharin AV, Morales-Nebreda L, Reyfman PA, *et al*. Monocyte-derived alveolar macrophages drive lung fibrosis and persist in the lung over the life span. *J Exp Med*. 2017;214(8):2387-2404. doi: 10.1084/jem.20162152
9. Hams E, Armstrong ME, Barlow JL, *et al*. IL-25 and type 2 innate lymphoid cells induce pulmonary fibrosis. *Proc Natl Acad Sci U S A*. 2014;111(1):367-372. doi: 10.1073/pnas.1315854111
10. Langfelder P, Horvath S. WGCNA: An R package for weighted correlation network analysis. *BMC Bioinform*. 2008;9:559. doi: 10.1186/1471-2105-9-559.
11. Shannon P, Markiel A, Ozier O, *et al*. Cytoscape: A software environment for integrated models of biomolecular interaction networks. *Genome Res*. 2003;13(11):2498-2504. doi: 10.1101/gr.1239303
12. Huang HY, Lin YC, Li J, *et al*. miRTarBase 2020: Updates to the experimentally validated microRNA-target interaction database. *Nucleic Acids Res*. 2020;48(D1):D148-D154. doi: 10.1093/nar/gkz896
13. Yang JH, Li JH, Shao P, Zhou H, Chen YQ, Qu LH. starBase: A database for exploring microRNA-mRNA interaction maps from Argonaute CLIP-Seq and Degradome-Seq data. *Nucleic Acids Res*. 2011;39(Database issue):D202-D209.

doi: 10.1093/nar/gkq1056

14. Agarwal V, Bell GW, Nam JW, Bartel DP. Predicting effective microRNA target sites in mammalian mRNAs. *Elife.* 2015;4:e05005.

doi: 10.7554/eLife.05005

15. Chen B, Khodadoust MS, Liu CL, Newman AM, Alizadeh AA. Profiling tumor infiltrating immune cells with CIBERSORT. *Methods Mol Biol.* 2018;1711:243-259.

doi: 10.1007/978-1-4939-7493-1_12

16. Liu Y, Yang X, Gan J, Chen S, Xiao ZX, Cao Y. CB-Dock2: Improved protein-ligand blind docking by integrating cavity detection, docking and homologous template fitting. *Nucleic Acids Res.* 2022;50(W1):W159-W164.

doi: 10.1093/nar/gkac394

17. Morse C, Tabib T, Sembrat J, *et al*. Proliferating SPP1/MERTK-expressing macrophages in idiopathic pulmonary fibrosis. *Eur Respir J.* 2019;54(2):1802441.

doi: 10.1183/13993003.02441-2018

18. Kumar A, Elko E, Bruno SR, *et al*. Inhibition of PDIA3 in club cells attenuates osteopontin production and lung fibrosis. *Thorax.* 2022;77(7):669-678.

doi: 10.1136/thoraxjnl-2021-216882

19. Rosas IO, Richards TJ, Konishi K, *et al*. MMP1 and MMP7 as potential peripheral blood biomarkers in idiopathic pulmonary fibrosis. *PLoS Med.* 2008;5(4):e93.

doi: 10.1371/journal.pmed.0050093

20. Zuo F, Kaminski N, Eugui E, *et al*. Gene expression analysis reveals matrilysin as a key regulator of pulmonary fibrosis in mice and humans. *Proc Natl Acad Sci U S A.* 2002;99(9):6292-6297.

doi: 10.1073/pnas.092134099

21. Tartaglione A, Oneto A, Bandini F, Favale E. Visual evoked potentials and pattern electroretinograms in Parkinson's disease and control subjects. *J Neurol Neurosurg Psychiatry.* 1987;50(9):1243-1244.

doi: 10.1136/jnnp.50.9.1243

22. Cui H, Guo Z, Guo Z, *et al*. TMEM100 regulates neuropathic pain by reducing the expression of inflammatory factors. *Mediators Inflamm.* 2023;2023:9151967.

doi: 10.1155/2023/9151967

23. Song JJ, Hwang I, Cho KH, *et al*. Plasma carboxypeptidase B downregulates inflammatory responses in autoimmune arthritis. *J Clin Investig.* 2011;121(9):3517-3527.

doi: 10.1172/JCI46387

24. Ray K. CPB2 dampens inflammation in autoimmune arthritis. *Nat Rev Rheumatol.* 2011;7(10):558.

doi: 10.1038/nrrheum.2011.135

25. Lu S, Lu H, Jin R, Mo Z. Promoter methylation and H3K27 deacetylation regulate the transcription of VIPR1 in hepatocellular carcinoma. *Biochem Biophys Res Commun.* 2019;509(1):301-305.

doi: 10.1016/j.bbrc.2018.12.129

26. Tang B, Wu J, Zhu MX, *et al*. VPAC1 couples with TRPV4 channel to promote calcium-dependent gastric cancer progression via a novel autocrine mechanism. *Oncogene.* 2019;38(20):3946-3961.

doi: 10.1038/s41388-019-0709-6

27. Zhao L, Yu Z, Zhao B. Mechanism of VIPR1 gene regulating human lung adenocarcinoma H1299 cells. *Med Oncol.* 2019;36(11):91.

doi: 10.1007/s12032-019-1312-y

28. Heljasvaara R, Aikio M, Ruotsalainen H, Pihlajaniemi T. Collagen XVIII in tissue homeostasis and dysregulation - Lessons learned from model organisms and human patients. *Matrix Biol.* 2017;57-58:55-75.

doi: 10.1016/j.matbio.2016.10.002

29. Wang S, Zhou M, Xia Y. COL15A1 interacts with P4HB to regulate the growth and malignancy of HepG2.2.15 cells. *Biochem Biophys Res Commun.* 2023;681:20-28.

doi: 10.1016/j.bbrc.2023.09.031

30. Yu DH, Ruan XL, Huang JY, *et al*. Analysis of the interaction network of hub miRNAs-Hub genes, being involved in idiopathic pulmonary fibers and its emerging role in non-small cell lung cancer. *Front Genet.* 2020;11:302.

doi: 10.3389/fgene.2020.00302

31. Jin CY, Zheng R, Lin ZH, *et al*. Study of the collagen type VI alpha 3 (COL6A3) gene in Parkinson's disease. *BMC Neurol.* 2021;21(1):187.

doi: 10.1186/s12883-021-02215-7

32. Chen J, Luo SF, Yuan X, *et al*. Diabetic kidney disease-predisposing proinflammatory and profibrotic genes identified by weighted gene co-expression network analysis (WGCNA). *J Cell Biochem.* 2022;123(2):481-492.

doi: 10.1002/jcb.30195

33. Saradna A, Do DC, Kumar S, Fu QL, Gao P. Macrophage polarization and allergic asthma. *Transl Res.* 2018;191:1-14.

doi: 10.1016/j.trsl.2017.09.002

34. Huen SC, Moeckel GW, Cantley LG. Macrophage-specific deletion of transforming growth factor-β1 does not prevent renal fibrosis after severe ischemia-reperfusion or obstructive injury. *Am J Physiol Renal Physiol.* 2013;305(4):F477-F484.

doi: 10.1152/ajprenal.00624.2012

35. Craig VJ, Zhang L, Hagood JS, Owen CA. Matrix metalloproteinases as therapeutic targets for idiopathic pulmonary fibrosis. *Am J Respir Cell Mol Biol.* 2015;53(5):585-600.

doi: 10.1165/rcmb.2015-0020TR

36. Xu Y, Lan P, Wang T. The role of immune cells in the pathogenesis of idiopathic pulmonary fibrosis. *Medicina* (*Kaunas*). 2023;59(11):1984.

doi: 10.3390/medicina59111984

37. Papiris SA, Kollintza A, Karatza M, *et al*. CD8+ T lymphocytes in bronchoalveolar lavage in idiopathic pulmonary fibrosis. *J Inflamm*. 2007;4:14.

doi: 10.1186/1476-9255-4-14

38. Brodeur TY, Robidoux TE, Weinstein JS, Craft J, Swain SL, Marshak-Rothstein A. IL-21 promotes pulmonary fibrosis through the induction of profibrotic CD8+ T cells. *J Immunol*. 2015;195(11):5251-5260.

doi: 10.4049/jimmunol.1500777

39. Xue J, Kass DJ, Bon J, *et al*. Plasma B lymphocyte stimulator and B cell differentiation in idiopathic pulmonary fibrosis patients. *J Immunol*. 2013;191(5):2089-2095.

doi: 10.4049/jimmunol.1203476

40. Prêle CM, Miles T, Pearce DR, *et al*. Plasma cell but not CD20-mediated B-cell depletion protects from bleomycin-induced lung fibrosis. *Eur Respir J*. 2022;60(5):2101469.

doi: 10.1183/13993003.01469-2021

Appendix

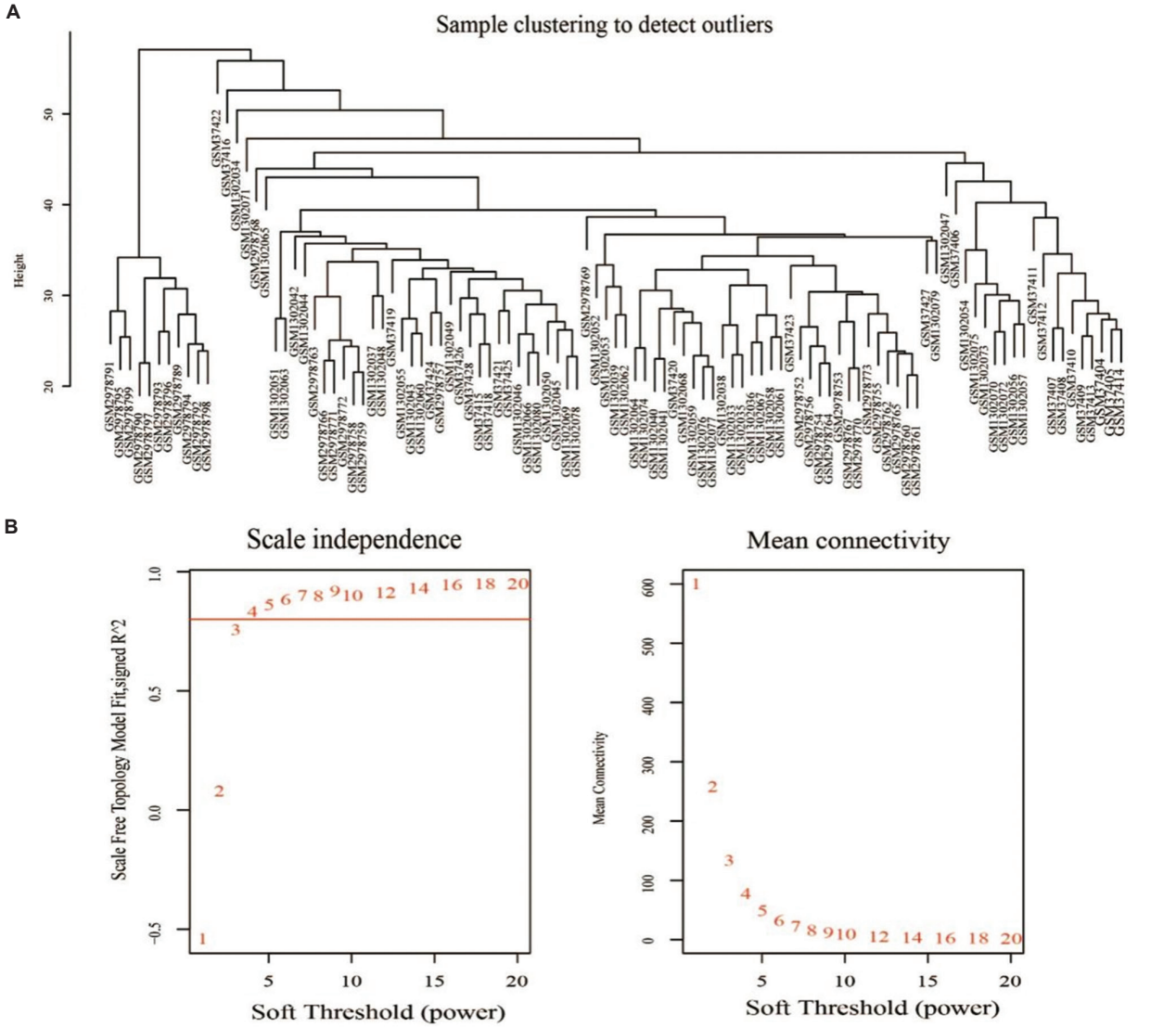

Figure A1. Hierarchical clustering of samples and screening of optimal soft-thresholding in WGCNA. (A) Sample clustering for detection of outliers. (B) Scale independence and mean connectivity plots were used to screen and filter the power β value for soft-thresholding
Abbreviation: WGCNA: Weighted gene coexpression network analysis.

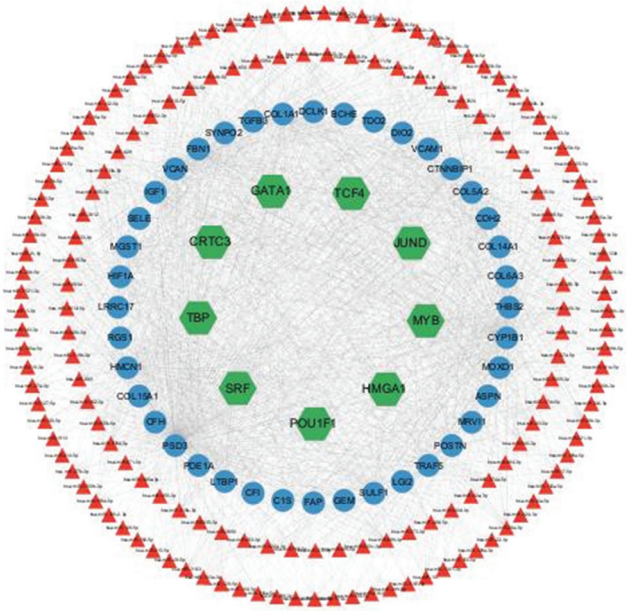

Figure A2. Construction of miRNA–TF–mRNA regulatory network related to 40 common genes. Blue nodes (circles) represent predicted mRNA, red nodes (triangles) represent miRNA, and green nodes (hexagons) represent TFs
Abbreviations: miRNA: microRNA; TF: Transcription factor.

ACCSCIENCE PUBLISHING

Gene & Protein in Disease

ORIGINAL RESEARCH ARTICLE

Interleukin-1β, interleukin-1Ra, and interleukin-8 in patients with SARS-CoV-2 infection: A correlation between vaccination and clinical outcome

Laine Andreotti Almeida[1,2], Mikaela Nagahara[3], Manuela dos Santos Bueno[1], Mônica Pezenatto Santos[1], Roger Labio[1], Spencer Luiz Marques Payão[1], and Lucas Trevizani Rasmussen[1,3]*

[1]Faculdade de Medicina de Marilia (FAMEMA) - Hemocentro, Genetics Laboratory, Marília, São Paulo, Brazil

[2]Department of Veterinary Medicine, Universidade de Marília – UNIMAR, Marília, São Paulo, Brazil

[3]Centro Universitário de Ourinhos – UNIFIO, Ourinhos, São Paulo, Brazil

Abstract

Coronavirus disease 2019 (COVID-19), an infectious disease caused by severe acute respiratory syndrome coronavirus 2 (SARS-CoV-2), was responsible for the pandemic decreed on March 11, 2020. Here, we investigated the mRNA expression of interleukin (*IL*)-*1β*, *IL-8*, and *IL-1RN* in samples collected from patients with and without SARS-CoV-2 infection, who were vaccinated or unvaccinated. This investigation was designed as a qualitative, cross-sectional, comparative, and randomized observational study. Samples were collected through nasal/oral swabs from patients symptomatic for influenza syndrome or SARS. Patients were categorized into three groups: DVAC (patients with SARS-CoV-2 infection and vaccinated), DNVAC (patients with SARS-CoV-2 infection and not vaccinated), and ND (patients without SARS-CoV-2 infection). SARS-CoV-2 was detected through reverse transcription polymerase chain reaction (RT-PCR). Gene expressions of *IL-1β*, *IL-8*, and *IL-1RN* were also evaluated using RT-PCR. Statistically significant differences in *IL-8* expression were observed among the study groups ($P = 0.033$); moreover, clinical signs and symptoms, frequency of hospitalizations, and need for intensive care units showed significant differences. These differences were noted in the DVAC group compared with those in the DNVAC and ND groups. Patients with COVID-19 showed reduced *IL-8* expression compared with those with other diseases that also cause influenza syndrome or SARS. These results suggested that the severity of clinical manifestations of patients with COVID-19 reduced after the initial two doses of the CoronaVac/Sinovac vaccine. Moreover, this vaccine reduced mortality and lethality in patients with SARS-CoV-2 infection.

Keywords: Severe acute respiratory syndrome coronavirus 2; Coronavirus disease 2019; Gene expression; Interleukins; Vaccination

***Corresponding author:**
Lucas Trevizani Rasmussen
(lucasrasmussen@unifio.edu.br)

Citation: Almeida LA, Nagahara M, Bueno MDS, *et al*. Interleukin-1β, interleukin-1Ra, and interleukin-8 in patients with SARS-CoV-2 infection: A correlation between vaccination and clinical outcome. *Gene Protein Dis.* 2024;3(4):4076. doi: 10.36922/gpd.4076

Received: June 29, 2024
Accepted: September 24, 2024
Published Online: November 4, 2024

1. Introduction

Severe acute respiratory syndrome coronavirus 2 (SARS-CoV-2) is a betacoronavirus with a positive-sense, single-stranded RNA genome.[1] SARS-CoV-2 is responsible

for the SARS that caused the coronavirus disease 2019 (COVID-19) pandemic, which was decreed on March 11, 2020, by the World Health Organization.[2,3]

The clinical manifestations of individuals infected with SARS-CoV-2 range from acute and mild respiratory conditions, such as influenza syndrome, to SARS.[4,5] In general, the severity of COVID-19 is affected by the dominance of the viral pathogenicity or inflammatory response of the host, with the latter having the probability of causing systemic hyperinflammation.[6]

Studies have shown that patients who died or required intensive care units (ICUs) with SARS due to COVID-19 had increased pro-inflammatory cytokine levels.[6-11] Some diseases, such as rheumatic, tumoral, and infectious diseases, can result in an exacerbated and uncontrolled release of pro-inflammatory cytokines,[11] such as interleukins (ILs) and tumor necrosis factor-alpha (TNF-α), leading to a cytokine storm, in which systemic inflammatory processes and multiple organ failure can occur.[6,10-12]

Pro-inflammatory cytokines correspond to extracellular glycoproteins that perform important functions in the immune response. Their intensified synthesis can result in systemic, metabolic, and hemodynamic instability, which can worsen several pathologies.[13,14] ILs consist of cytokines produced primarily by leukocytes and can be considered pro-inflammatory when they possess the ability to maximize different stages of the inflammatory process in the face of antigens that may mediate an immune response.[15]

IL-1β is a pro-inflammatory cytokine that is primarily responsible for fever. It is mainly produced by macrophages and monocytes, with higher levels of production during viral infections.[15,16] IL-1g/AR (receptor antagonist) acts as an endogenous autoregulator competing with IL-1 receptors (α and β); hence, it can be used to prevent the negative effects from the exacerbated levels of IL-1.[13,14] IL-8 is a pro-inflammatory cytokine belonging to the CXC chemokine subfamily. It is primarily produced by macrophages and can increase the levels of chemotactic factors by stimulating innate immunity and cell-mediated immunity.[15,17]

COVID-19 vaccines are currently approved for use in adults, adolescents, and children and other vaccines are still being tested.[18] Nevertheless, there is no scientific evidence for specific effective treatments that can cure COVID-19.[6,19] Hence, it is essential to understand the inflammatory response and factors, including pro-inflammatory cytokines that can influence the physiological response, for constructing therapeutic alternatives to treat individuals with COVID-19, thereby preventing systemic hyperinflammation and patient death. This study aimed to evaluate the mRNA expression of important genes associated with cytokine storm, such as *IL-1β*, *IL-8*, and *IL-1RN*, in patients with and without SARS-CoV-2 infection. At the time of this study, some patients had been vaccinated, whereas others were still unvaccinated. Moreover, the frequency of clinical manifestations was evaluated in patients with SARS-CoV-2 infection who were either vaccinated or unvaccinated.

The primary outcome measures evaluated in our study were based on the elevated levels of pro-inflammatory mediators in patients with COVID-19. These primary outcome measures could justify the systemic hyperinflammation (cytokine storm) associated with worse clinical symptoms and signs. Our secondary outcome measure compared the levels of pro-inflammatory mediators in patients who tested positive for COVID-19 and had different or similar severity. We compared patients who had been vaccinated with the CoronaVac/Sinovac vaccine, which was available at the time of this study, with those who had not been vaccinated.

2. Methods

2.1. Materials

The following materials were used in this study: QIAmp Viral RNA/QIAGEN kit (catalog number 52906, QIAGEN, Hilden, Germany); BIOGENE kit RNA/viral DNA extraction/Bioclin (reference K204, Biogene Shirley, NY, USA); Nanodrop 2000 spectrophotometer, automatic thermal cycler GeneAmp polymerase chain reaction (PCR) System 9700, and ABI Prism 7500 Fast Sequence Detection System Equipment (Thermo Scientific, Waltham, MA, USA); and High-Capacity Complementary DNA (cDNA) Reverse Transcription Kit (Applied Biosystems™, USA). Quantitative PCR (qPCR) was performed using TaqMan assays (Applied Biosystems) to evaluate IL-1β (Hs 01555410_m1), IL-8 (Hs9999034_m1), and IL-1RN (Hs00893626_m1). We also used UBC (Hs00824723_m1) and GPDH (02758991_m1).

2.2. Genetic material extraction

Viral and human RNA extraction for detecting SARS-CoV-2 was performed using the protocol described in the QIAmp Viral RNA/QIAGEN kit (catalog number 52906) to detect SARS-CoV-2 by reverse transcription PCR (RT-PCR). For gene amplification, viral/human RNA extraction was performed using the BIOGENE kit RNA/viral DNA extraction/Bioclin (reference K204). The Nanodrop 2000 spectrophotometer (Thermo Scientific, Waltham, MA, USA) was used to determine and adjust RNA concentrations.

2.3. cDNA synthesis and real-time qPCR

cDNA was synthesized using the High-Capacity cDNA Reverse Transcription Kit (Applied Biosystems™, USA), according to the manufacturer's protocol, using the automatic thermal cycler GeneAmp PCR System 9700 (Applied Biosystems) with the following conditions: 25°C for 10 min, 37°C for 60 min (2 times), 85°C for 5 min, and then 4°C at the end of the thermal cycle.

RT-PCR was used to analyze gene expression using the ABI Prism 7500 Fast Sequence Detection System Equipment. qPCR was performed using TaqMan assays to evaluate *IL-1β* (Hs 01555410_m1), *IL-8* (Hs9999034_m1), and *IL-1RN* (Hs00893626_m1). *UBC* (Hs00824723_m1) and *GPDH* (02758991_m1) were used for normalization. The reaction was performed in duplicate for each of the mentioned genes. The groups were compared with the ND group to evaluate the relative quantification (RQ) of the expression using the 2-^Ct method.[20]

2.4. Description of the study design

This was a qualitative, cross-sectional, comparative, and randomized observational study conducted at the Genetics Laboratory of the Hemocenter of the Hospital das Clínicas of the Faculty of Medicine of Marília (HC-FAMEMA) from September 2020 to December 2021 and was approved by the Research Ethics Committee (case number 4.414.477). All patients agreed to participate in the study.

2.4.1. Description of participants

We collected 127 nasal and/or oral swabs from patients of both sexes. All participants were aged ≥18 years. The swabs were stored in graduated conical tubes containing 3 mL of sterile saline solution until analysis. Sample collection was performed from September 2020 to June 2021 at the Hospital das Clínicas da Faculdade de Medicina de Marília (HC FAMEMA), São Paulo, Brazil. Patients were on the 2nd and 10th day of influenza syndrome or SARS symptoms, presenting at least three clinical manifestations that were grouped into influenza syndrome and SARS, according to the recommendations of the Brazilian Ministry of Health.

2.4.2. Description of variables/groups

Patients were divided into three groups, i.e., (1) those with SARS-CoV-2 and vaccinated (DVAC): This group was composed of patients who were symptomatic for influenza syndrome or SARS and SARS-CoV-2 who were administered two doses of the CoronaVac/Sinovac vaccine and their last dose had been administered at least 30 days before the study; (2) patients with SARS-CoV-2 and non-vaccinated (DNVAC): This group consisted of patients who were symptomatic for influenza syndrome or SARS and were not administered any dose of vaccine; and (3) patients without SARS-CoV-2 and non-vaccinated (ND): This group included patients who did not present any symptoms of influenza syndrome or SARS (Table 1). All patients who were considered SARS-CoV-2-positive were diagnosed using RT-PCR.

The CoronaVac/Sinovac vaccine was administered to the group vaccinated against COVID-19. This is an attenuated viral vaccine consisting of two doses with an interval of 14 days each, with a confirmed global efficacy of 62.3% and an efficacy of 50% and associated with serious cases.

According to the Brazilian Ministry of Health, an individual is defined as having influenza syndrome when they present with an acute respiratory condition, which should include at least two of the following clinical signs and symptoms: fever, chills, headache, myalgia, malaise, cough, runny nose, and olfactory or taste disorders. An individual is defined as having SARS when they exhibit influenza syndrome associated with dyspnea or respiratory discomfort, pressure or persistent pain in the chest, oxygen saturation of 95% in room air, or cyanosis.

2.5. Statistical analysis

Qualitative variables were described using absolute and relative frequency distributions (%). The relationship between qualitative variables was analyzed using the Chi-square association test. Quantitative variables were described using mean values and 95% confidence intervals (95% CIs). Normal distribution was confirmed using Kolmogorov–Smirnov test, and the homogeneity of variances was evaluated using Levene's test. Welch's test was used to compare the mean values of independent groups, followed by the *post hoc* Games–Howell test. A significance level of 5% was adopted, and data were analyzed using the SPSS software (version 24.0).

3. Results

3.1. SARS-CoV-2 detection

The 127 samples were categorized into three groups according to the detection of SARS-CoV-2 through

Table 1. Description of the groups analyzed in the study

	Total *n* (%)	Average age±SD	Average interval between CS and collection±SD	Gender	
				Male *n* (%)	Female *n* (%)
DVAC	40 (31.5)	40±13.48	3.92±1.48	32 (80)	8 (20)
DNVAC	43 (33.8)	46.9±15.34	4.44±1.44	22 (51.1)	21 (41.8)
ND	44 (34.6)	60.4±22.99	5.22±2.38	23 (52.2)	21 (47.3)

Abbreviations: DVAC: Vaccinated detectable (with SARS-CoV-2); DNVAC: With SARS-CoV-2 and not vaccinated; ND: Without SARS-CoV-2; SD: Standard deviation; CS: Clinical signs.

RT-PCR and the patient's vaccination status, as described in Table 1.

3.2. *IL-1β*, *IL-8*, and *IL-1RN* expression

No statistically significant difference was found in *IL-1β* expression among the study groups ($P = 0.124$) compared with that in the DVAC (mean RQ = 1.2582), DNVAC (mean RQ = 0.9789), and ND (mean RQ = 2.6107) groups (Figure 1).

The expression of *IL-8* showed a statistically significant difference among the study groups ($P = 0.033$). Patients in the DVAC group who were vaccinated but still had symptoms showed a mean RQ of 0.7847, and those in the DNVAC group who were symptomatic and had not been vaccinated showed a mean RQ of 0.9172. Finally, patients in the ND group who did not have SARS showed a mean RQ of 1.8819. Among these groups, a statistically significant difference was found between the ND group in relation to the DVAC ($P = 0.042$) and DNVAC ($P = 0.044$) groups. Comparison between the DVAC and DNVAC groups showed no statistically significant difference ($P = 0.923$) (Figure 2).

Furthermore, no statistically significant difference was found in the expression of *IL-1RN* among the DVAC (mean RQ = 1.3441), DNVAC (mean RQ = 2.3079), and ND (mean RQ = 3.9863) groups ($P = 0.118$) (Figure 3).

3.3. Frequency of clinical signs and symptoms

The study groups showed statistically significant differences in the frequency of clinical signs and symptoms, including fever ($P = 0.021$), sore throat ($P = 0.001$), fatigue and weakness ($P < 0.001$), loss of taste ($P = 0.014$), myalgia ($P < 0.001$), headache ($P < 0.001$), runny nose ($P < 0.001$), chills ($P < 0.001$), conjunctival congestion ($P < 0.001$), abdominal pain ($P = 0.002$), dyspnea ($P < 0.001$), and oxygen saturation <95% ($P < 0.001$). However, no statistically significant differences were observed in the frequency of cough ($P = 0.238$), loss of smell ($P = 0.092$), diarrhea ($P = 0.925$), and nausea and vomiting ($P = 0.084$) (Table 2).

The mean interval between the onset of clinical signs and sample collection might have influenced the analysis of the gene expression of the ILs investigated in this study. The ND group showed the highest mean expression of all ILs, as well as the highest mean and standard deviation in the interval between the onset of clinical signs and the

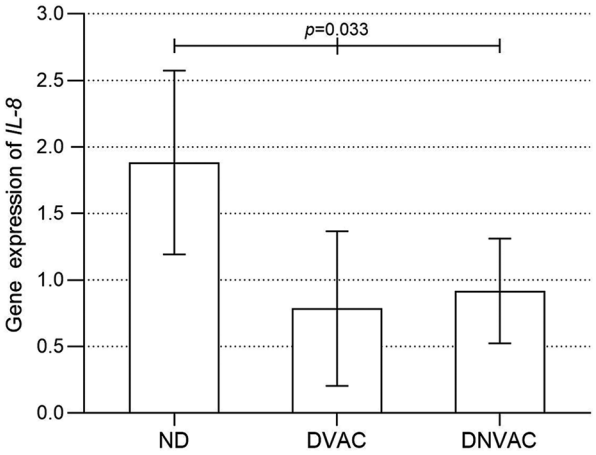

Figure 2. Analysis of *IL-8* gene expression in the ND, DVAC, and DNVAC groups
Abbreviations: DNVAC: Detectable not vaccinated; DVAC: Vaccinated detectable; ND: Not detectable; *IL*: Interleukin.

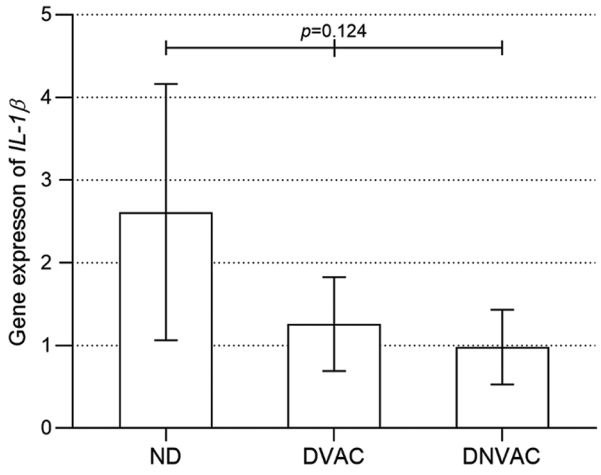

Figure 1. Analysis of *IL-1β* gene expression in the ND, DVAC, and DNVAC groups
Abbreviations: DNVAC: Detectable not vaccinated; DVAC: Vaccinated detectable; ND: Not detectable; *IL*: Interleukin.

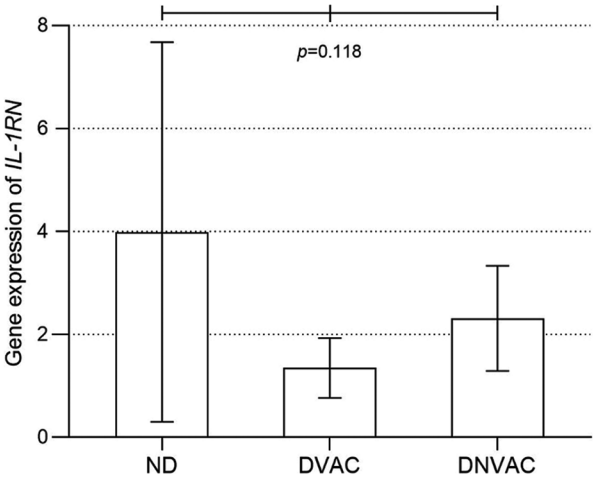

Figure 3. Analysis of *IL-1RN* gene expression in the ND, DVAC, and DNVAC groups
Abbreviations: DNVAC: Detectable not vaccinated; DVAC: Vaccinated detectable; ND: Not detectable; *IL*: Interleukin.

Table 2. Description of the frequency of patients' clinical signs and symptoms categorized into influenza syndrome and SARS

Clinical signs and symptoms	DVAC	DNVAC	ND	Total *n* (%)
Influenza syndrome				
Fever	11 (27.5)	21 (48.8)	25 (56.8)	57 (44.9)
Cough	29 (72.5)	37 (86.0)	37 (84.1)	103 (81.1)
Sore throat	26 (65.0)	24 (55.58)	11 (25.0)	61 (48.0)
Fatigue and weakness	0 (0.0)	16 (37.2)	11 (25.0)	27 (21.3)
Loss of smell	0 (0.0)	5 (11.6)	3 (6.8)	8 (6.3)
Loss of taste	10 (25.0)	4 (9.5)	2 (4.5)	16 (12.7)
Myalgia	18 (45.0)	17 (39.5)	3 (6.8)	38 (29.9)
Headache	18 (45.0)	10 (23.3)	1 (2.3)	29 (22.8)
Runny nose	27 (67.5)	17 (39.5)	2 (4.5)	46 (36.2)
Chills	9 (22.5)	0 (0.0)	0 (0.0)	9 (7.1)
Conjunctival co-management	20 (50.0)	3 (7.0)	0 (0.0)	81.1 (23)
Diarrhea	6 (15.0)	7 (16.3)	8 (18.2)	21 (16.5)
Nausea and vomiting	1 (2.5)	2 (4.7)	7 (15.9)	10 (7.9)
Abdominal pain	0 (0.0)	2 (4.7)	9 (20.5)	11 (8.7)
SARS				
Dyspnea	3 (7.5)	16 (37.2)	37 (84.1)	56 (44.1)
Oxygen saturation <95%	2 (5.0)	16 (37.2)	35 (79.5)	53 (41.7)

Abbreviations: IS: Influenza syndrome; SARS: Severe acute respiratory syndrome; DVAC: Vaccinated with SARS-CoV-2; DNVAC: With SARS-CoV-2 not vaccinated; ND: Without SARS-CoV-2. Missing values have been omitted.

collection of 5.22 (±2.38) days. Wong *et al.*[21] reported an increase in the levels of pro-inflammatory cytokines, such as IL-1β, IL-6, and IL-12, from 5 to 12 days after the onset of SARS symptoms, whereas IL-8 levels increased primarily from 9 to 14 days after the onset of symptoms.

3.4. Frequency of comorbidities and injuries and health

We observed statistically significant differences among the study groups in the frequency of the following comorbidities: diabetes ($P = 0.035$), chronic cardiovascular disease ($P < 0.001$), chronic kidney disease ($P = 0.02$), cancer ($P = 0.02$), and asthma/lung disease ($P = 0.036$). However, no statistically significant differences were observed in the frequency of smoking ($P = 0.374$), immunodeficiency ($P = 0.377$), and obesity ($P = 0.052$) (Table 3).

3.5. Frequency of ICU admissions and maintenance

The frequency of hospitalizations and ICU admissions showed a statistically significant difference among the study groups ($P < 0.0001$), as shown in Table 4.

Table 3. Description of the frequency of comorbidities and health problems in the study patients

Clinical signs and symptoms	DVAC	DNVAC	ND
Smoker	0 (0.0)	1 (2.3)	0 (0.0)
Chronic neurological disease	0.0	0.0	3 (6.8)
Diabetes	0.0	7 (16.3)	5 (11.4)
Immunodeficiency	1 (2.5)	0 (0.0)	2 (4.5)
Chronic cardiovascular disease	0 (0.0)	8 (18.6)	21 (47.7)
Chronic kidney disease	0 (0.0)	0 (0.0)	4 (9.1)
Cancer	0 (0.0)	0 (0.0)	2 (4.5)
Asthma/pulmonopathy	2 (5)	4 (9.3)	10 (22.7)
Obesity	0 (0.0)	3 (7.0)	6 (13.6)

Abbreviations: DVAC: Vaccinated detectable (with SARS-CoV-2); DNVAC: With SARS-CoV-2 and not vaccinated; ND: Without SARS-CoV-2.

Table 4. Frequency of hospitalizations and need for maintenance in the ICU in the study patients

	DVAC *n* (%)	DNVAC *n* (%)	ND *n* (%)	*P*-value
Hospitalized	1 (2.5)	10 (76.7)	39 (88.6)	<0.0001*
ICU	1 (2.5)	8 (18.6)	15 (34.1)	<0.0001*
Total	40 (100)	43 (100)	44 (100)	-

Note: * indicates a significant difference between groups according to Welch's test at $P \leq 0.05$.
Abbreviations: DVAC: Vaccinated detectable; DNVAC: Detectable not vaccinated; ND: Not detectable.

4. Discussion

Systemic hyperinflammation appears to be a relevant aspect of COVID-19. However, the expression level of various cytokines that orchestrate the inflammatory process is controversial. Huang *et al.*[12] measured the plasma concentration of several pro-inflammatory cytokines, including IL-1β, IL1-RA/RN, IL-2, IL-4, IL-5, IL-6, IL-7, IL-8, IL-9, IL-10, IL-12p70, IL-13, IL-15, and IL-17A, and confirmed increased concentrations of IL-1β, IL-1RN, IL-8, IL-9, and IL-10 in patients with COVID-19 compared with those in healthy adults. They also compared the plasma concentrations of ILs between patients with COVID-19 who required and did not require ICU admission and found that patients in the ICU showed a significant increase in the levels of IL-2, IL-7, IL-10, and TNF-α but not in the levels of IL-1β, IL-1RN, and IL-8. Another study showed that among the major cytokines whose plasma levels increase in patients with SARS, IL-2, IL-6, IL-7, GCSF, macrophage inflammatory protein 1-α, TNF-α, C-reactive protein, ferritin, and d-dimer are prominent.[6] Moreover, disease severity has been associated with elevated plasma concentrations of IFN-γ, IL-1β, IL-6,

IL-8, IP-10, and MCP-1 as well as with the period of onset of symptoms and clinical signs and analysis of these cytokines.[6,21]

According to the results shown in Table 1, the mean interval between the onset of clinical signs and sample collection may influence the analysis of the gene expression of ILs. The ND group showed the highest mean expression of all ILs as well as a higher mean and standard deviation in the interval between the onset of clinical signs and sample collection of 5.22 (±2.38) days compared with those in the DVAC (3.92 [±1.48] days) and DNVAC (4.44 [±1.44] days) groups. It is evident that this study was conducted at the beginning of the COVID-19 pandemic, respecting what was initially recommended by the Ministry of Health for the diagnosis of the disease by RT-PCR, because the literature we reviewed shows that such ILs tend to be significantly increased in longer varieties.[12,21] Wong *et al.* (2004) reported an increase in the levels of pro-inflammatory cytokines such as IL-1β, IL-6, and IL-12 after 5 – 12 days from the onset of symptoms of SARS, whereas an increase in IL-8 levels was primarily observed after 9 – 14 days from the onset of symptoms of the syndrome.[21]

As observed in this study, other studies[6,12,22,23] that examined patients with COVID-19 reported that fever, cough, fatigue, sore throat, headache, conjunctival congestion, and dyspnea were the most frequent clinical signs and symptoms in patients with influenza syndrome or SARS. However, these symptoms are non-specific, and therefore, it is difficult to differentiate them from those of other respiratory syndromes, as observed in the ND group of this study. Similarly, Chen *et al.*[23] reported that 82% of patients with COVID-19 had fever and cough, 31% had shortness of breath, 11% had muscle pain (myalgia), 8% had headache, 5% had sore throat, 2% had diarrhea, and 1% had vomiting. Moreira[24] described a symptomatology similar to that observed in the present study, showing that the most common clinical signs and symptoms at the onset of the disease are fever, cough, and fatigue, and as the disease develops and worsens, the symptoms include sputum production, headache, hemoptysis, diarrhea, and dyspnea.

In the present study, most clinical signs and symptoms showed a reduced frequency in the DVAC group compared with that in the DNVAC group, indicating a possible influence of vaccination against COVID-19 on the symptomatology of the disease. Data from the Butantan Institute[25] show that older patients suffer a higher lethality due to COVID-19 and that vaccinated individuals have a 40.4% lower lethality rate than unvaccinated patients because the vaccines can reduce the severity of the disease and consequently evolution to death. Other researchers emphasize the importance of mass vaccination against COVID-19 in containing the disease, resulting in changes in the patterns of hospitalizations and deaths and leading to an overall reduction in the rate of hospitalizations and deaths, primarily in patients aged 60 – 69 years.[26,27]

The ND group showed the occurrence of all the abovementioned comorbidities and conditions, in addition to being the group with the highest reported mean age, which might have contributed to a greater pre-disposition to comorbidities and a greater probability of aggravation of COVID-19. The increased incidence of complications and deaths is reported to be higher in individuals with risk factors and comorbidities, especially in those aged >60 years.[28]

Among the comorbidities and risk factors evaluated in our study, we observed a higher frequency of chronic cardiovascular disease, asthma/chronic lung disease, diabetes, obesity, cancer, and smoking in the analyzed groups. Mercês *et al.*[29] reported higher mortality from COVID-19 in individuals aged 70 – 79 years with comorbidities, primarily heart disease and diabetes. Tang *et al.*[30] found a higher occurrence of diabetes (20%), hypertension and cardiovascular disease (15%), chronic obstructive pulmonary disease (2%), chronic liver disease (2%), and cancer (2%) in patients with COVID-19. Similar to our study, Das Mercês *et al.* found a higher incidence of cardiopathies, diabetes, kidney disease, pneumopathy, immunosuppression, obesity, and asthma in individuals with COVID-19.[29]

The greater pre-disposition of individuals with chronic comorbidities to progress into severe cases of COVID-19 is because these individuals tend to have greater expression of *ACE-2* genes, which are responsible for the synthesis of the ACE-2 surface protein that acts as the major receptor for binding SARS-CoV-2 and establishing the infectious process. This phenomenon tends to occur primarily in individuals with chronic cardiovascular disorders and diabetes.[31]

The results of this study indicate a statistical significance for the comorbidity/risk factor cancer, which makes patients more vulnerable to injury and lethality due to COVID-19, especially those with lung and hematologic neoplasia.[32]

The need for hospitalizations and treatment in the ICU raises concerns regarding the high mortality rate of these patients. This study showed that the ND group had higher gene expression of the investigated ILs and greater severity of the clinical condition. De Sousa *et al.*[33] found that hospitalized patients with COVID-19, primarily in the interior regions of Brazil, had higher lethality among

elderly individuals. In individuals aged ≥60 years, the lethality rate was 55.4%, whereas it was 86.5% in those who required ICU care.[33] Ranzani *et al.*[34] reported high mortality in hospitalized patients with COVID-19, even in those patients aged <60 years, which reached rates of 31% in those not undergoing mechanical ventilation and 77% in those undergoing ICU treatment or mechanical ventilation.

The vaccinated group had a lower frequency of hospitalizations and maintenance in the ICU, similar to the results reported by Orellana *et al.*,[27] in which vaccinated patients showed a reduction in both the rate of hospitalizations and deaths from COVID-19. In patients aged 60 – 69 years, these authors confirmed hospitalization rates of 60.5% and 39.5% in unvaccinated and vaccinated patients, with mortality rates of 81.8% and 18.2% in unvaccinated and vaccinated patients, respectively.

The expression of *IL-8* was statistically significantly greater in the ND group than in the other groups, with the DVAC group showing the lowest expression. The other ILs and receptors showed no statistically significant difference in their expression.

It is important to emphasize that this study has a few methodological and technical limitations due to the pandemic itself. It was conducted at the time of the greatest impact of SARS-CoV-2, amidst the care of thousands of individuals, and during the rapid evolution of immunization methods. One fact is that vaccination status is inherently linked to the risk profile, which can affect groups. Numerous doubts existed and still exist concerning COVID-19; hence, the precision and generalizability of some data obtained at that time can currently be considered a bias.

5. Conclusion

A detailed analysis of the data presented in this study indicates that the presence of comorbidities is associated with an increase in the expression of ILs genes, which in turn is related to the greater severity of clinical signs and symptoms. This resulted in a significant increase in the number of hospitalizations and the need for ICU admissions, as observed in the ND and DNVAC groups.

Altogether, our findings indicated that the severity of clinical manifestations in patients with COVID-19 reduced after administering at least two initial doses of the CoronaVac/Sinovac vaccine. Moreover, among patients who received the minimum regimen of two doses of this vaccine, a reduction in the frequency of most clinical manifestations was observed, especially those associated with SARS. This reduction was accompanied by a considerable decrease in the number of hospitalizations and the need for ICU admissions. Therefore, our results reinforce that vaccination promotes a decrease in severity, mortality, and lethality in patients with SARS-CoV-2 infection, thereby contributing to a significant improvement in their clinical prognosis.

Acknowledgments

None.

Funding

This study was supported by the Sao Paulo Research Foundation (FAPESP) (case numbers: 2018/08481-1 and 2021/12017-1).

Conflict of interest

The authors declare they have no competing interests.

Author contributions

Conceptualization: Laine Andreotti Almeida, Lucas T. Rasmussen
Formal analysis: Lucas T. Rasmussen
Investigation: Laine Andreotti Almeida, Lucas T. Rasmussen, Spencer L.M. Payão, Roger Labio
Methodology: Laine Andreotti Almeida, Lucas T. Rasmussen, Spencer L.M. Payão, Roger Labio
Writing–original draft: Laine Andreotti
Writing–review & editing: Laine Andreotti Almeida, Lucas T. Rasmussen, Mônica P. Santos, Mikaela Nagahara, Manuela S. Bueno

Ethics approval and consent to participate

The study design consists of qualitative, cross-sectional, comparative, and randomized observational research and was conducted at the Genetics Laboratory of the Hemocenter of the HC-FAMEMA, from September 2020 to December 2021. All participants agreed to participate in the study. This study was approved by the Research Ethics Committee of Faculdade de Medicina de Marília (case number 4.414.477).

Consent for publication

Verbal consent was obtained from each of the subjects to publish the data.

Availability of data

Not applicable.

References

1. Lu R, Zhao X, Li J, *et al.* Genomic characterisation and epidemiology of 2019 novel coronavirus: Implications for virus origins and receptor binding. *Lancet.*

2020;395(10224):565-574.

doi: 10.1016/S0140-6736(20)30251-8

2. Sohrabi C, Alsafi Z, O'Neill N, *et al*. Corrigendum to "World Health Organization declares global emergency: A review of the 2019 novel coronavirus (COVID-19)". *Int J Surg*. 2020;77:217.

doi: 10.1016/j.ijsu.2020.02.034

3. De Souza WV, Martelli CMT, Silva AP, *et al*. The first hundred days of COVID-19 in Pernambuco State, Brazil: Epidemiology in historical context. *Cad Saude Publica*. 2020;36(11):e00228220.

doi: 10.1590/0102-311X00228220

4. Aquino EML, Silveira IH, Pescarini JM, *et al*. Social distancing measures to control the COVID-19 pandemic: Potential impacts and challenges in Brazil. *Cien Saude Colet*. 2020;25:2423-2446.

doi: 10.1590/1413-81232020256.1.10502020

5. Governo de Santa Catarina, Secretaria de Estado da Saúde, Sistema Único de Saúde, Superintendência de Vigilância em Saúde, Diretoria de Vigilância Epidemiológica de Santa Catarina. *Manual De Orientações Da Covid-19* (*Vírus SARS-CoV-2*). Florianópolis: 2020.

6. Siddiqi HK, Mehra MR. COVID-19 illness in native and immunosuppressed states: A clinical-therapeutic staging proposal. *J Heart Lung Transplant*. 2020;39(5):405-407.

doi: 10.1016/j.healun.2020.03.012

7. Bakhiet M, Taurin S. SARS-CoV-2: Targeted managements and vaccine development. *Cytokine Growth Factor Rev*. 2021;58:16-29.

doi: 10.1016/j.cytogfr.2020.11.001

8. Harrison AG, Lin T, Wang P. Mechanisms of SARS-CoV-2 transmission and pathogenesis. *Trends Immunol*. 2020;41(12):1100-1115.

doi: 10.1016/j.it.2020.10.004

9. Kirtipal N, Bharadwaj S, Kang SG. From SARS to SARS-CoV-2, insights on structure, pathogenicity and immunity aspects of pandemic human coronaviruses. *Infect Genet Evol*. 2020;85:104502.

doi: 10.1016/j.meegid.2020.104502

10. Wu C, Chen X, Cai Y, *et al*. Risk factors associated with acute respiratory distress syndrome and death in patients with coronavirus disease 2019 pneumonia in Wuhan, China. *JAMA Intern Med*. 2020;180(7):934-943.

doi: 10.1001/jamainternmed.2020.0994

11. Zhang W, Zhao Y, Zhang F, *et al*. The use of anti-inflammatory drugs in the treatment of people with severe coronavirus disease 2019 (COVID-19): The perspectives of clinical immunologists from China. *Clin Immunol*. 2020;214:108393.

doi: 10.1016/j.clim.2020.108393

12. Huang C, Wang Y, Li X, *et al*. Clinical features of patients infected with 2019 novel coronavirus in Wuhan, China. *Lancet*. 2020;395(10223):497-506.

doi: 10.1016/S0140-6736(20)30183-5

13. de Oliveira CM, Sakata RK, Issy AM, Gerola LR, Salomão R. Cytokines and pain. *Rev Bras Anestesiol*. 2011; 61: 2: 255-265.

14. Kraychete D, Calasans M, Valente C. Pro-inflammatory cytokines and pain. *Rev Bras Reumatol*. 2006;3(43):199-206.

doi: 10.1590/S0482-50042006000300007

15. Varella P, Forte W. Citokines: A review. *Rev Bras Alergia Imunopatol*. 2001;4:146-155.

16. Zhang JM, An J. Cytokines, inflammation, and pain. *Int Anesthesiol Clin*. 2007;45(2):27-37.

doi: 10.1097/AIA.0b013e318034194e

17. Raghuwanshi SK, Su Y, Singh V, Haynes K, Richmond A, Richardson RM. The chemokine receptors CXCR1 and CXCR2 couple to distinct G protein-coupled receptor kinases to mediate and regulate leukocyte functions. *J Immunol*. 2012;189(6):2824-2832.

doi: 10.4049/jimmunol.1201114

18. Tregoning JS, Flight KE, Higham SL, Wang Z, Pierce BF. Progress of the COVID-19 vaccine effort: Viruses, vaccines and variants versus efficacy, effectiveness and escape. *Nat Rev Immunol*. 2021;21(10):626-636.

doi: 10.1038/s41577-021-00592-1

19. Santos-Pinto CDB, Miranda ES, Osorio-de-Castro CGS. "Kit-covid" and the Popular Pharmacy Program in Brazil. *Cad Sáude Pública*. 2021;2:1-5.

20. Livak KJ, Schmittgen TD. Analysis of relative gene expression data using real-time quantitative PCR and the 2(-Delta Delta C(T)) Method. *Methods*. 2001;25(4):402-408.

doi: 10.1006/meth.2001.1262

21. Wong CK, Lam CW, Wu AK, *et al*. Plasma inflammatory cytokines and chemokines in severe acute respiratory syndrome. *Clin Exp Immunol*. 2004;136(1):95-103.

doi: 10.1111/j.1365-2249.2004.02415.x

22. Pascarella G, Strumia A, Piliego C, *et al*. COVID-19 diagnosis and management: A comprehensive review. *J Intern Med*. 2020;288(2):192-206.

doi: 10.1111/joim.13091

23. Chen N, Zhou M, Dong X, *et al*. Epidemiological and clinical characteristics of 99 cases of 2019 novel coronavirus pneumonia in Wuhan, China: A descriptive study. *Lancet*. 2020;395(10223):507-513.

doi: 10.1016/S0140-6736(20)30211-7

24. Moreira RS. Latent class analysis of COVID-19 symptoms in Brazil: Results of the PNAD-COVID19 survey. *Cad Saúde Pública*. 2021;37:14.

doi: 10.1590/0102-311x00238420

25. Butatã I. *Não Vacinados Representam 75% das Mortes por Covid-19, Diz Estudo Brasileiro*. São Paulo: Instituto Butantan; 2022.

26. Martins WA, de Oliveira GMM, Brandão AA, *et al*. Vaccinating patients with heart disease against COVID-19: The reasons for priority. *Arq Bras Cardiol*. 2021;116(2):213-218.

doi: 10.36660/abc.20210012

27. Orellana JDY, Cunha GMd, Leite LMdC, Domingues CMA, Horta BL. Changes in the pattern of COVID-19 hospitalizations and deaths after substantial vaccination of the elderly in Manaus, Amazonas State, Brazil. *Cad Saúde Pública*. 2022;38:PT192321.

doi: 10.1590/0102-311XPT192321

28. Barbosa AV, da Silva SM, da Silva FH, de Assunção MAS, dos Anjos FBR. Características clínicas da COVID-19. In: Latin American Publicações, editor. *Fatores de Virulência Microbianos e Terapias Emergentes*. Vol. 3. São José dos Pinhais: Latin American Publicações; 2022. p. 355.

29. Das Mercês SO, Lima FLO, de Vasconcellos Neto JRT. Association of COVID-19 with: Age and medical comorbidities. *Res Soc Dev*. 2020;9:e1299108285.

doi: 10.33448/rsd-v9i10.8285

30. Tang D, Comish P, Kang R. The hallmarks of COVID-19 disease. *PLoS Pathog*. 2020;16(5):e1008536.

doi: 10.1371/journal.ppat.1008536

31. Zheng YY, Ma YT, Zhang JY, Xie X. COVID-19 and the cardiovascular system. *Nat Rev Cardiol*. 2020;17(5):259-260.

doi: 10.1038/s41569-020-0360-5

32. Figueira K. COVID-19 em pacientes com câncer: COVID-19 in cancer patients: Managing a pandemic within a pandemic. *Braz J Implantol Health Sci*. 2020;2:6.

doi: 10.36557/2674-8169.2020v2n12p01-06

33. De Sousa EL, Gaído SB, de Sousa RA, *et al*. Profile of hospital admissions and deaths due to severe acute respiratory syndrome caused by COVID-19 in Piauí, Brazil: A descriptive study, 2020-2021. *Epidemiol Serv Saúde*. 2022;31:e2021836.

doi: 10.1590/s1679-49742022000100009

34. Ranzani OT, Bastos LSL, Gelli JBM, *et al*. Characterisation of the first 250,000 hospital admissions for COVID-19 in Brazil: A retrospective analysis of nationwide data. *Lancet Respir Med*. 2021;9(4):407-418.

doi: 10.1016/S2213-2600(20)30560-9

ACCSCIENCE PUBLISHING

Gene & Protein in Disease

ORIGINAL RESEARCH ARTICLE

Can *Epimedii herba* treat periodontitis? A prediction based on network pharmacology, molecular docking, and dynamics analysis

Junhan Wan[1,2,3], Wenwen Wang[1,2], Ningli Li[1,2], Mingzhen Yang[1,2], Yingjie Zhu[4], and Yuankun Zhai[1,2,5]*

[1]School of Stomatology, Henan University, Kaifeng, Henan, China

[2]Kaifeng Key Laboratory of Periodontal Tissue Engineering, Kaifeng, Henan, China

Abstract

Epimedii herba (EH) showed numerous activities and has the potential to treat periodontitis. However, the pharmacological mechanism has not been exhaustively elucidated. This study predicted the specific targets and mechanisms of EH to prevent and treat periodontitis. A traditional Chinese medicine system pharmacology database and analysis platform was used to screen key compounds of EH and their corresponding targets. Therapeutic Target Database and Comparative Toxicogenomics Database were used to identify targets related to periodontitis. Intersection targets were observed using a Venn diagram. The key components and corresponding protein targets of EH were searched. The intersection targets were obtained and then they were imported into the STRING database to construct a PPI network. Gene Ontology (GO) and Kyoto Encyclopedia of Genes and Genomes (KEGG) enrichment analyses were performed. Molecular docking between the screened chemical components of EH and key targets was performed using Discovery Studio 2019. The binding stability between components and target proteins was confirmed using molecular dynamics simulations. The binding stability between components and target proteins was confirmed using molecular dynamics simulations. Through network pharmacological analysis, 23 active compounds of EH were identified, including kaempferol and icariin. Based on GeneCards, GEO, and other databases, 3291 periodontitis-related genes were obtained. Venn diagram analysis revealed 137 intersection targets of EH and periodontitis, and Protein kinase B (AKT1) and Tumor necrosis factor (TNF) were identified as the key targets of EH for periodontitis treatment. GO and KEGG analyses revealed that the primary pathways mediating the therapeutic effects of EH were related to cancer, lipid, and atherosclerosis. Molecular docking showed that 8-isopentenyl-kaempferol had the best binding ability to ESR1, which was confirmed by dynamics simulations. This study demonstrated that EH can be used for periodontitis treatment, and the corresponding targets and potential mechanisms were investigated based on network pharmacology, molecular docking, and dynamics simulation analysis. Notably, 8-isopentenyl-kaempferol exhibited good binding affinity and stability to ESR1, which may partially explain the molecular mechanisms of EH for treating periodontitis. Hence, EH can be a novel choice for the clinical treatment of periodontitis in the future.

Keywords: *Epimedii herba*; Periodontitis; Network pharmacology; Molecular docking; Molecular dynamics; 8-Isopentenyl-kaempferol

***Corresponding author:**
Yuankun Zhai
(zhaiyuankun@henu.edu.cn)

Citation: Wan J, Wang W, Li N, Yang M, Zhu Y, Zhai Y. Can *Epimedii herba* treat periodontitis? A prediction based on network pharmacology, molecular docking, and dynamics analysis. *Gene Protein Dis.* 2024;3(4):4427. doi: 10.36922/gpd.4427

Received: August 2, 2024
Accepted: October 22, 2024
Published Online: November 18, 2024

[3]School and Hospital of Stomatology, China Medical University, Shenyang, Liaoning, China
[4]Medical Center of Hip, Luoyang Orthopedic-Traumatological Hospital, Luoyang, Henan, China
[5]Henan International Joint Laboratory for Nuclear Protein Regulation, Kaifeng, Henan, China

1. Introduction

Periodontitis, one of the three common oral diseases, has a high morbidity rate worldwide.[1] The progression of periodontitis not only affects the periodontal tissue but also induces or exacerbates systemic diseases such as diabetes, cardiovascular disease, and rheumatoid arthritis.[2-5] Current therapy to control the progression of periodontitis comprises basic treatments such as supragingival and subgingival scaling as well as antibiotic and surgical treatments.[6] Nevertheless, there exists a risk of increased bacterial resistance and possible toxic side effects during antibiotic treatment.[7] Therefore, it is important to develop new therapeutic strategies and explore alternative anti-inflammatory drugs that can better control and treat periodontitis.

Traditional Chinese medicine (TCM) can regulate the body's own immunity and ameliorate patient symptoms but has certain side effects.[8-10] *Epimedii herba* (EH) (common name: Yin-yang-huo in China), a herbaceous plant widely distributed in Asia and Europe, has been used alone or with other TCM to treat various diseases such as osteoporosis and sexual dysfunction for >2000 years.[11,12] Modern pharmacological studies have confirmed that EH exhibits numerous pharmacological activities, such as anti-inflammatory, immune regulatory, and antitumor effects.[13-15] Existing data have shown that the extracts of EH, icariin, and kaempferol can significantly reduce the inflammatory response.[16,17] Moreover, several studies have reported the potential of EH for treating periodontitis, which may contribute to the proliferation of human periodontal ligament cells and regeneration of alveolar bone.[18,19] However, after entering the human body, the pathways and modes of actions of EH are diverse because of multicomponent and multitarget regulation; hence, it is necessary to further explore the mechanism of core ingredients and targets for the treatment of periodontitis.[20,21]

Recently, network pharmacology has received increasing attention in TCM research as it can reveal the interaction mechanisms between the targets and active ingredients of TCM through bioinformatics technology, which systematically links drugs with diseases to identify the mode of action of TCM on diseases from the network interaction level. However, the pharmacological mechanism of EH during periodontitis treatment has not been exhaustively elucidated. Therefore, this study was conducted to reveal the action pathway of EH during periodontitis treatment from a network pharmacology perspective, explore the binding liability of EH ingredients with key targets by molecular docking and dynamics, and provide a specific basis for periodontitis treatment.

2. Methods

2.1. Collection of the active compounds and active targets of EH

The traditional Chinese medicine systems pharmacology database and analysis platform (TCMSP) was used to explore EH-active compounds. Oral bioavailability (OB) of ≥30% and drug-likeness (DL) of ≥0.18 were used to filter the active compounds, which are the key factors for evaluating absorption, distribution, metabolism, and excretion. OB of ≥30% indicated that the drugs had better OB, and DL of ≥0.18 indicated that the compounds had better solubility, chemical stability, and drug-like properties. Finally, the targets of the compounds were obtained using the UniProt (https://www.uniprot.org) database.

2.2. Collection of disease targets

"Periodontitis" was used as the keyword to input in the GeneCards database (https://www.genecards.org), OMIM database (https://omim.org), DrugBank database (https://www.drugbank.ca), TTD (https://db.idrblab.net/ttd/), and CTD (http://ctdbase.org/) to explore the targets of periodontitis. Then, using humans as the screening condition, the protein names of the disease targets were turned into gene names using the UniProt database. The GEO database was also used to screen the targets related to periodontitis. Data correction was performed in Perl, differential gene analysis was performed in the Limma package in R software (4.2.2), and the volcano map and heatmap were plotted using the ggplot2 package. p-values of <0.05 and fold-change values of >2 were considered to indicate significant differences.[22]

2.3. Screening of intersection targets

The website https://bioinfogp.cnb.csic.es/tools/venny/ was used to construct a Venn diagram and obtain the intersection targets.

2.4. Construction of the EH ingredient–target interaction network

An interaction network was constructed between the ingredients of EH and potential targets using

Cytoscape3.7.0. Nodes represented the ingredients and targets in the network, and the interactions between them were represented by edges. Then, the key ingredients were selected in the network based on the "degree" value.

2.5. Construction of a protein–protein interaction (PPI) network

The intersection targets of EH and periodontitis were input into the STRING platform (https://string-db.org), after which the tab control of "Multiple Proteins" was selected, and "Homo Sapiens" was chosen as the organism to construct the PPI network. Next, the obtained network was imported into Cytoscape 3.7.0 for further analysis. The top 10 core targets were calculated using "CytoHubba" with the highest maximal clique centrality score.

2.6. Gene functional pathway enrichment analysis

When the intersection targets were imported into the Metascape database (http://metascape.org/), the species was selected as "*H. Sapiens*" for GO and KEGG enrichment analyses. GO is an internationally standardized system for the classification of gene functions, which can be divided into cellular components (CC), molecular functions (MF), and biological processes (BP). KEGG analysis provides more insights into the biological functions of genes. We next selected the top 20 items of BP, MF, and CC and the top 20 results of KEGG enrichment analysis to construct a histogram and bubble diagram using the Weishengxin website (http://www.bioinformatics.com.cn/).

2.7. Molecular docking

The 3D structure files of the key active ingredients and targets were input into Discovery Studio 2019 for molecular docking. The PDB IDs of related proteins were 4EJN(AKT1), 7KP9(TNF), 1ALU(IL6), 6BFT(VEGFA), 1RHM(CASP3), 2OW1(MMP9), and 3OS8(ESR1). Protein preparation was performed, wherein the "Clean Protein" and "Prepare Protein" modules were used to delete redundant protein conformation and water molecules, and target proteins were hydrogenated simultaneously. Then, the protein's ligand position was selected as the active binding site. After deleting the original ligand and exposing the active binding pocket, the active site was defined as a receptor in the docking system. Next, hydrogenation and energy optimization were also performed on the key effective ingredient. Then, the CDocker module was used to connect the original ligand to the active pocket and calculate the root mean square deviation (RMSD) of the molecular conformations. RMSD values of <2.0 Å indicate that the molecular conformation obtained by docking can reduce the ligand and receptor binding affinity, thereby confirming the rationality of the selected docking methods and parameter settings. Finally, the CDocker module was used to connect the key active ingredients of EH to the processed protein to perform molecular docking. The higher the negative CDocker interaction energy (−CIE) value of the docking, the more stable the docking system between the chemical ingredients and protein receptors.

2.8. Molecular dynamics

Gromacs-2022.04GPU was used to perform molecular dynamics simulations between the active ingredient and target protein with the best bonding ability in the molecular docking results. The ATB website (http://atb.uq.edu.au/) was used to convert the active ingredient files into the molecular structure and topology files; the built-in commands in Gromacs-2022.04GPU were used to convert the protein files into the molecular structure files. Then, using the TIP3P model as water molecules, chloride, and sodium ions were added to the system to leave the system at a normal saline concentration. The topology files of the chemical components were prepared using the PDB-2gmx module, and the receptor proteins were subjected to the latest charmm36-jul2022 force field. After optimizing the energy of the system, the temperature should be maintained at 36.85°C, and the pressure should be maintained at 1 atm within a simulation period of 50 ns.

3. Results

3.1. Collection of the active compounds and targets of EH

Based on TCMSP, 23 effective active ingredients of EH were obtained, as shown in Table 1. A total of 199 targets related to the active ingredients of EH were obtained.

3.2. Acquisition of periodontitis-related targets

Two periodontitis-related datasets were obtained from the GEO database, namely, GSE10334 and GSE16134, which contained 183 and 241 samples, respectively. Both datasets covered the gingival tissues of patients with periodontitis and healthy people. Figure 1 shows the volcano map and heatmap of differential genes in periodontitis. After deleting duplicate gene targets, 3291 periodontitis-related targets were obtained from GeneCards, DrugBank, TTD, CTD, and GEO databases.

3.3. Screening of the intersection targets of EH and periodontitis

By constructing a Venn diagram, 137 intersection targets were obtained, as depicted in Figure 2.

3.4. Construction of the EH ingredient–target interaction network

The EH ingredient–target interaction network (Figure 3) consisted of 219 nodes and 439 edges. Each pathway

Table 1. Active ingredients of *Epimedii herba* and their major parameters

No.	Molecule ID	Active ingredients	OB/%	DL
1	MOL001510	24-Epicampesterol	37.58	0.71
2	MOL001645	Linoleyl acetate	42.10	0.20
3	MOL001771	Poriferast-5-en-3beta-ol	36.91	0.75
4	MOL001792	DFV	32.76	0.18
5	MOL003044	Chryseriol	35.85	0.27
6	MOL003542	8-Isopentenyl-kaempferol	38.04	0.39
7	MOL000359	Sitosterol	36.91	0.75
8	MOL000422	Kaempferol	41.88	0.24
9	MOL004367	Olivil	62.23	0.41
10	MOL004373	Anhydroicaritin	45.41	0.44
11	MOL004380	C-Homoerythrinan	39.14	0.49
12	MOL004382	Yinyanghuo A	56.96	0.77
13	MOL004384	Yinyanghuo C	45.67	0.50
14	MOL004386	Yinyanghuo E	51.63	0.55
15	MOL004388	8-Tetrahydro-1H-isochromeno[3,4-h] isoquinolin-2-ium	60.64	0.66
16	MOL004391	8-(3-Methylbut-2-enyl)-2-phenyl-chromone	48.54	0.25
17	MOL004394	Anhydroicaritin-3-O-alpha-L-rhamnoside	41.58	0.61
18	MOL004396	1,2-Bis (4-hydroxy-3-methoxyphenyl) propan-1,3-diol	52.31	0.22
19	MOL004425	Icariin	41.58	0.61
20	MOL004427	Icariside A7	31.91	0.86
21	MOL000006	Luteolin	36.16	0.25
22	MOL000622	Magnograndiolide	63.71	0.19
23	MOL000098	Quercetin	46.43	0.28

Abbreviations: OB, Oral bioavailability; DL, Drug-likeness; DFV: 4',7-Dihydroxyflavanone.

corresponded to multiple targets, and each target connected multiple pathways, reflecting the mechanism of the multicomponents, multitargets, and multipathways of EH in treating periodontitis.

3.5. Analysis of the PPI network

After analyses using the STRING platform, the common targets of EH and periodontitis were inputs into Cytoscape 3.7.0 to perform further topological analysis, as depicted in Figure 4. As illustrated in Figure 5, the top 10 key targets, namely, AKT1, TNF, IL6, TP53, VEGFA, IL1B, CASP3, PTGS2, MMP9, and ESR1, were screened according to the degree value using the network topology analysis plug-in "cytoHubba."

3.6. GO and KEGG pathway enrichment analyses

The results of GO functional enrichment analysis (Figure 6A) showed that in BP, the response to inorganic substances and cellular response to organic cyclic compounds played a vital role. The membrane raft, transcription regulator complex, and vesicle lumen played major roles in CC. Among MFs, DNA-binding transcription factor binding, cytokine receptor binding, and protein homodimerization activity played a major role.

The results of the KEGG pathway enrichment analysis (Figure 6B) demonstrated that EH primarily participated in regulating the signaling pathways related to cancer, lipid, and atherosclerosis; AGE–RAGE signaling pathway in diabetic complications; chemical carcinoma receptor activation; and MAPK activation to treat periodontitis.

3.7. Molecular docking

The RMSD values of the target proteins AKT1, TNF, IL6, VEGFA, CASP3, MMP9, and ESR1 with their ligands were <2.0 Å, as shown in Table 2, indicating that the docking methods and parameter settings were reasonable and could be used for the next step of docking with EH components. After the molecular docking of 8-(3-methylbut-2-enyl)-2-phenyl-chromone, 8-isopentenyl-kaempferol, anhydroicaritin, chryseriol, DFV, kaempferol, luteolin, quercetin, and Yinyanghuo C with the targets AKT1, TNF, IL6, VEGFA, CASP3, MMP9, and ESR1, the results

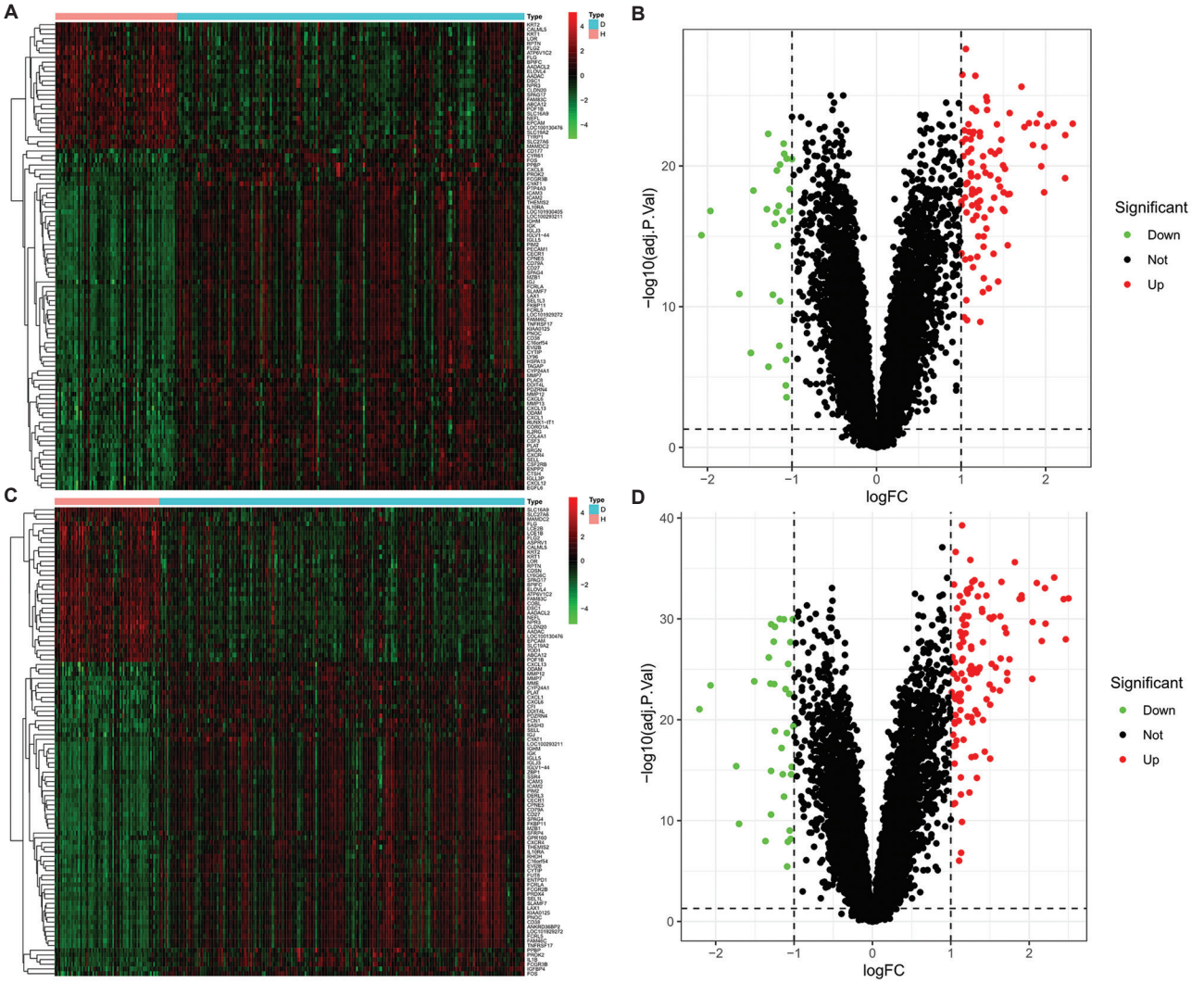

Figure 1. Volcano map and heatmap of differential genes in periodontitis from the GEO database. (A and B) Heatmap and volcano map of the GSE10334 dataset, respectively. (C and D) Heatmap and volcano map of the GSE16134 dataset, respectively. In the volcano plot, red represents upregulated genes, and green represents downregulated genes

(Table 3 and Figure 7) showed that all the compounds had good binding abilities with the proteins. Among them, 8-isopentenyl-kaempferol exhibited the highest − CIE value with ESR1.

3.8. Molecular dynamics

The results of the molecular dynamics simulations (Figure 8) further confirmed that the binding of 8-isopentenyl-kaempferol with ESR1 was stable. RMSD can reveal the position change of the protein conformation during molecular dynamics, and its trend of change is also an important representation to judge whether the simulation has reached stability. As shown in Figure 8A, the conformation of the complex reached a relatively stable state at approximately 10 ns and fluctuated slightly at approximately 0.25 nm. The root mean square fluctuation (RMSF) can characterize the flexibility and intensity of protein amino acids throughout the simulation. The overall structure was relatively stable during the simulations, and the active site region was located near the protein residues 315, 334, and 465, as there were several peaks between residues 300 and 550, as illustrated in Figure 8B. The radius of gyration (Rg) can be used to characterize the tightness of the protein structure and the looseness of the peptide chain, which also indicates the stability of the protein during the simulation. Based on Figure 8C, we can conclude that Rg fluctuated obviously at the beginning of the simulation and reached a relatively stable state at 10 ns, which corresponds to the RMSD results. The number of H-bonds can also indicate the binding stability between molecules. Results

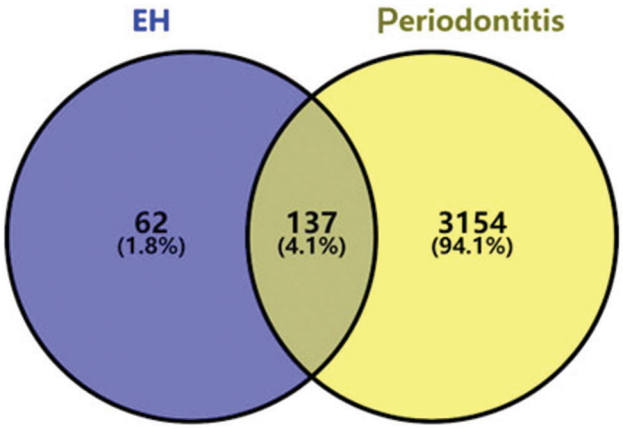

Figure 2. Intersection targets of *Epimedii herba* (EH) and periodontitis. Blue represents the target number for the active ingredients of EH, yellow represents the target number for periodontitis, and the middle part represents the intersection targets

showed that the number of H-bonds gradually increased after 10 ns, and the system tended to be stable, as depicted in Figure 8D. Solvent accessible surface area (SASA) is another key factor of protein stabilization, which similarly stabilized after 10 ns, as illustrated in Figure 8E.

Molecular mechanics Poisson–Boltzmann surface area (MMPBSA) is one of the most common methods to estimate binding free energies, which can be used to accurately estimate the affinity of ligand–protein binding and calculate the binding free energy generated by the docking of the ligand–protein complex.[23,24] The total binding free energies of MMPBSA included GGAS and GSOLV. The GGAS is composed of van der Waals force and electrostatic energy, which are −38.31 and −8.42 kcal/mol, respectively. The GSOLV consists of a polar solvation energy of 30.99 kcal/mol and a non-polar solvation energy of −5.59 kcal/mol. Therefore, the total binding free energy was 21.33 kcal/mol, indicating that the binding was relatively stable, as depicted in Figure 9A.

During the binding process, the amino acid residues participate in the formation of the binding site pocket. The total contributing energy of the amino acid residues was 7.67 kcal/mol, and LEU:346, MET:421, LEU:387, MET:388, LEU:391, PHE:404, ILE:424, LEU:349, and LEU:384 contributed significantly to the binding free energies, as illustrated in Figure 9B. LEU:346 and MET:421 contributed prominently with the binding energies of −2.69 and −2.20 kcal/mol, respectively.

4. Discussion

Periodontitis is a widespread disease worldwide that can induce an inflammatory response and cause tooth loss, destruction of periodontal supporting tissues, and other systemic diseases through subgingival plaque and its products.[25] Therefore, timely treatment of periodontitis is of considerable importance to improve the quality of life of patients with periodontitis. With the development of bioinformatics, network pharmacology provides us with a new entry point for research. Furthermore, molecular docking and molecular dynamics are neoteric means of new drug research and development, as they are cost-effective, can save more time, and provide an accurate possibility to identify new targeted drugs for periodontitis. As a disease caused by microorganisms and mediated by host inflammation, the treatment of periodontitis should not only exert anti-inflammatory effects but also increase the body's immune regulation to promote the regeneration of periodontal tissue.[6,26] TCM can not only inhibit the inflammatory response but also control the elimination of dental plaque (the initial factor of periodontitis) to kill microorganisms and promote the body's immune regulation to achieve periodontal tissue regeneration.[27-29] EH, a TCM that has been used for several years worldwide, has recently been proven to exert anti-inflammatory and immune-regulating effects.[16,30] In this study, network pharmacology, molecular docking, and molecular dynamics methods were used to screen the pharmacological components of EH for the prevention and treatment of periodontitis, explore its molecular mechanism, and provide novel ideas for the clinical treatment of periodontitis.

OB and DL screening revealed 8-(3-methylbut-2-enyl)-2-phenyl-chromone, 8-isopentenyl-kaempferol, anhydroicaritin, chryseriol, DFV, kaempferol, luteolin, quercetin, and Yinyanghuo C as the major active ingredients of EH. According to the PPI network, AKT1, TNF, IL6, TP53, VEGFA, IL1B, CASP3, PTGS2, MMP9, and ESR1 were screened as the top 10 key targets, through which EH may play a vital role in periodontitis treatment. GO enrichment analysis revealed that EH participated in the processes of cellular response to organic cyclic compounds, membrane raft, DNA-binding transcription factor binding, and other reaction processes. KEGG pathway enrichment analysis revealed that pathways related to cancer, lipid, and atherosclerosis as well as AGE–RAGE signaling pathways in diabetic complications might be primarily involved in periodontitis treatment with EH. The results of molecular docking and molecular dynamics simulation demonstrated that the active components of EH had good binding ability to the key targets, suggesting that EH plays a vital role in periodontitis treatment. These methods also confirmed the predicted results of network pharmacology to a certain extent.

Regarding the anti-inflammatory effects of EH, previous studies have reported that icariin can alleviate

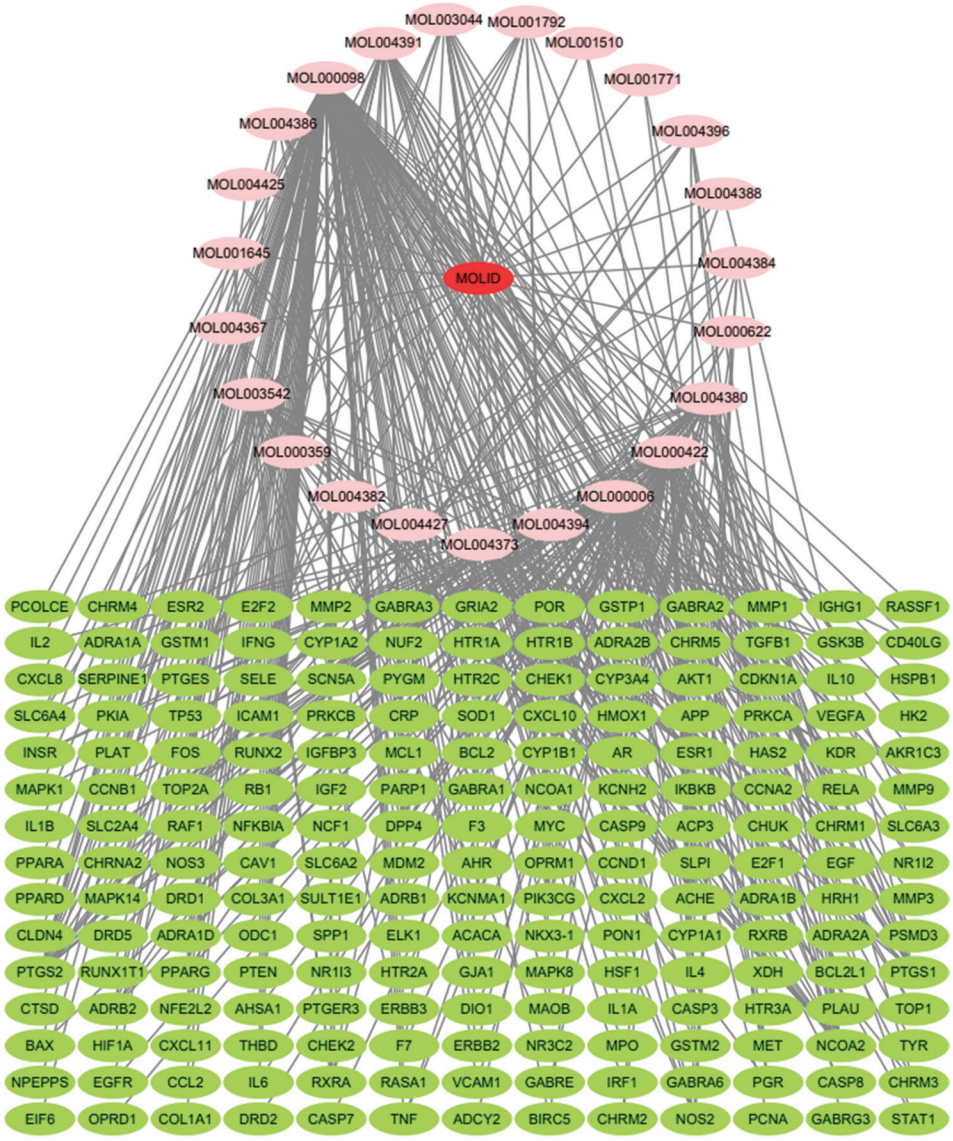

Figure 3. *Epimedii herba* (EH) ingredient–target interaction network. Pink nodes represent the active ingredients of EH, and green nodes represent the potential targets of EH

not only the LPS-induced acute inflammatory response involving the PI3K/Akt and nuclear factor-kappa B (NF-κB) signaling pathway but also the interleukin-1β-induced inflammatory response in human nucleus pulposus cells.[31,32] Moreover, kaempferol, a polyphenol from *Epimedium*, has been found to exert potential anti-inflammatory effects.[17] Kaempferol has been used to treat several diseases with its multiple biological properties, including antitumor, anti-inflammatory, and antioxidant activities;[33] it can also help improve the body's antioxidant defense against free radicals; regulate cell signaling pathways related to apoptosis, angiogenesis, and inflammation; maintain normal cell vitality; and play a role in protecting tissue cells.[34] The anti-inflammatory activities of these components have extensively demonstrated the potential of EH for treating periodontitis.

Network pharmacology analyses showed that the antiperiodontitis activity of psoralen was associated with several key targets, such as AKT1, TNF, and MMP9. AKT1, also known as protein kinase β, is closely related to cell proliferation and can protect the endothelial barrier and prevent abnormal vascular permeability, which may exhibit some correlation with the remission of periodontal disease.[35,36] TNF is an active cytokine that can induce an inflammatory response and cell death.[37]

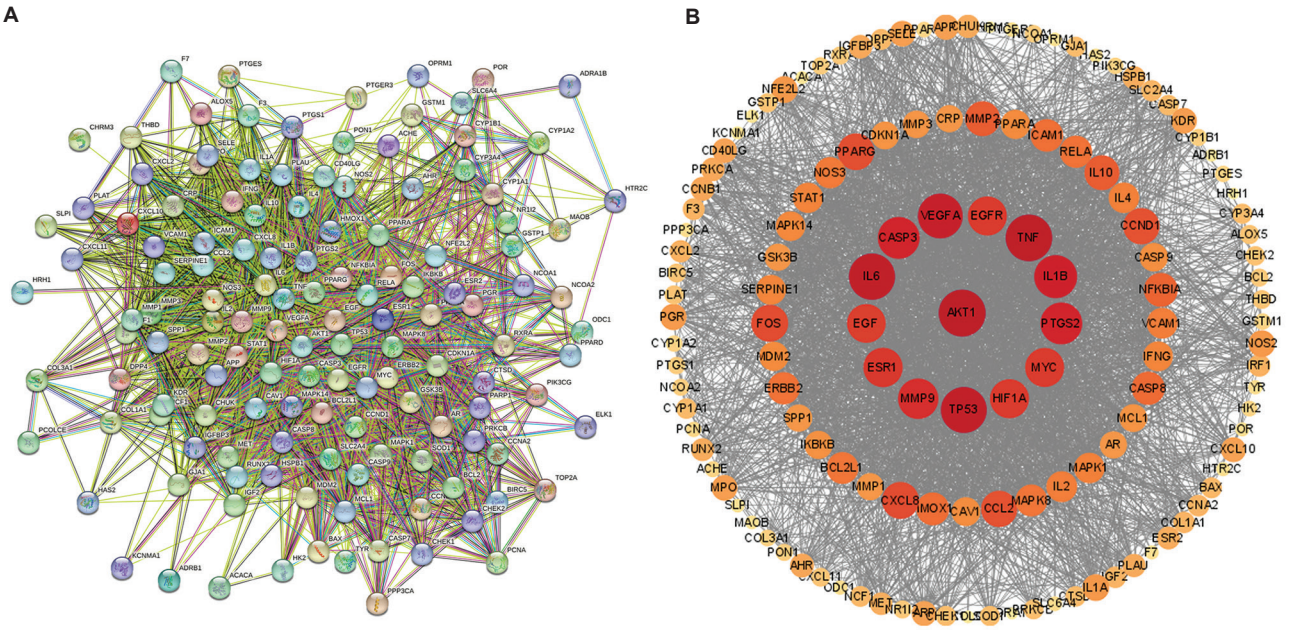

Figure 4. Protein–protein interaction (PPI) network. (A) PPI network of key targets of *Epimedii herba* (EH) for periodontitis. (B) PPI network of targets screened according to the degree value, represented by node size and color depth

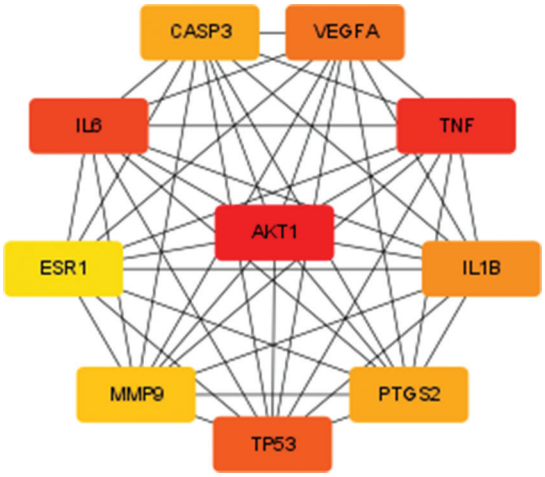

Figure 5. Key targets of *Epimedii herba* (EH) for periodontitis. The top 10 key targets based on the degree value, with darker colors representing greater degree value

Molecular docking results showed that the active components of EH had a higher −CIE value with MMP9 and ESR1, suggesting that they are the primary targets of EH in periodontitis treatment. MMP9 is closely associated with inflammation, with its expression significantly increasing in inflammatory diseases such as chronic periodontitis and rheumatoid arthritis.[38] MMP9 is also a potential biomarker of periodontitis, which can process the neutrophil chemotactic factor IL-8 and then improve its chemotactic effect on inflammatory neutrophils. In fact, it has been reported that the levels of MMP9 in serum, GCF, and saliva of patients with periodontitis were significantly higher than those in healthy people, suggesting a positive correlation between MMP9 and periodontitis development.[39] The occurrence of periodontal inflammation is also closely associated with oxidative stress. For instance, excessive reactive oxygen species produced by periodontal inflammation can aggravate the inflammatory response and activate osteoclasts, resulting in alveolar bone resorption in patients with periodontitis. Furthermore, MMP9, as a key gene regulating oxidative stress, can affect the differentiation process of osteoclasts, aggravate the inflammation of periodontal tissue, and induce the further absorption of periodontal supporting tissues.[22] Another key target, ESR1, exerted the best binding effect with 8-isopentenyl-kaempferol. Genetic polymorphisms involved in estrogen activity may contribute to women's susceptibility to periodontitis, and the estrogen receptor alpha gene (ESR1) PvuII and XbaI polymorphisms are associated with metabolic and pro-inflammatory factors in PCOS.[40] ESR1 is related to the development of bone resorption, which plays a vital role in bone metabolism, as observed in people who have bone loss after menopause or get osteopenia with ESR1 defect.[41,42] Through multiple pathways and cytokines, ESR1 can inhibit osteoclast differentiation and longevity, inducing the apoptosis of osteoclasts.[43] Another possible pathway is that ESR1 in osteoclasts induces Fas ligand expression, which in turn causes cell death through an autocrine mechanism.[44] ESR1 can also inhibit the NF-κB-mediated transcription of the IL-6 promoter by reducing the NF-κB DNA-binding activity, thereby regulating inflammation, immunity, and stress responses.[45] Therefore, it can be concluded that

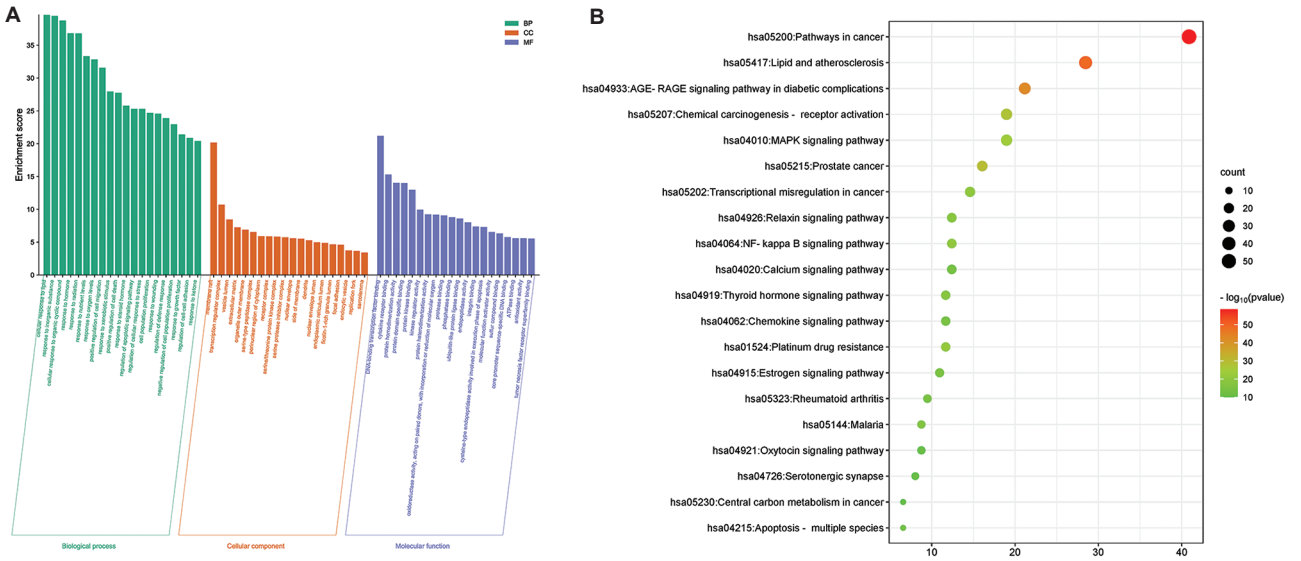

Figure 6. Gene Ontology (GO) functional analysis and Kyoto Encyclopedia of Genes and Genomes (KEGG) pathway enrichment analysis. A: GO histogram, green represents biological processes (BP), orange indicates cellular components (CC), and blue indicates molecular functions (MF). B: Bubble plot of KEGG pathway analysis; darker colors and smaller *p*-values indicate more significant enrichment

Table 2. RMSD values

RMSD(Å)	Gene name (protein molecule)						
	AKT1 (4EJN)	TNF (7KP9)	IL6 (1ALU)	VEGFA (6BFT)	CASP3 (1RHM)	MMP9 (2OW1)	ESR1 (3OS8)
	0.8867	0.8649	1.6702	0.915	1.8978	0.3482	0.3963

Abbreviation: AKT1: Protein kinase B; CASP3: Caspase-3; ESR1: Estrogen receptor; IL6: Interleukin-6; MMP9: Matrix metalloproteinase-9; RMSD: Root mean square deviation; TNF: Tumor necrosis factor VEGFA: Vascular endothelial growth factor A.

Table 3. Molecular docking results of the active components and key targets of EH

Key targets (protein) Active ingredients	−CIE						
	AKT1 (4EJN)	TNF (7KP9)	IL6 (1ALU)	VEGFA (6BFT)	CASP3 (1RHM)	MMP9 (2OW1)	ESR1 (3OS8)
8-(3-Methylbut-2-enyl)-2-phenyl-chromone	41.4055	38.5565	26.4379	26.4365	16.7762	40.487	42.9618
8-Isopentenyl-kaempferol	50.4215	42.7286	27.1504	34.7559	22.0006	38.8674	**55.0661**
Anhydroicaritin	51.9299	44.596	N/A	34.412	22.2191	54.5735	49.1107
Chryseriol	40.9433	44.7695	30.0842	27.1465	20.5928	55.5964	44.7241
DFV	38.6591	38.7429	31.6587	26.2254	17.4715	48.1983	40.9704
Kaempferol	43.3774	40.5597	31.7986	26.355	22.6086	44.9292	43.0489
Luteolin	45.1168	41.8853	29.5019	29.3159	17.8122	53.5428	44.3276
Quercetin	42.6345	42.7105	31.6144	27.2352	17.6754	46.5599	46.3985
Yinyanghuo C	50.0232	46.3035	20.9673	32.2408	24.0419	51.8019	44.1256

Abbreviations: AKT1: Protein kinase B; CASP3: Caspase-3; DFV: 4',7-Dihydroxyflavanone; ESR1: Estrogen receptor; IL6: Interleukin-6; MMP9: Matrix metalloproteinase-9; TNF: Tumor necrosis factor VEGFA: Vascular endothelial growth factor A. Numbers in bold represent the highest -CIE value, which mains the best binding stability.

ESR1 can downregulate the abundance of osteoclasts and slow down the resorption process of the alveolar bone and other periodontal supporting tissues, thereby achieving the purpose of periodontitis treatment. Using molecular docking and molecular dynamics techniques, we further confirmed the binding activity between the EH-active component and MMP9, suggesting that MMP9 should be a primary target of EH to exert its antiperiodontitis activity.

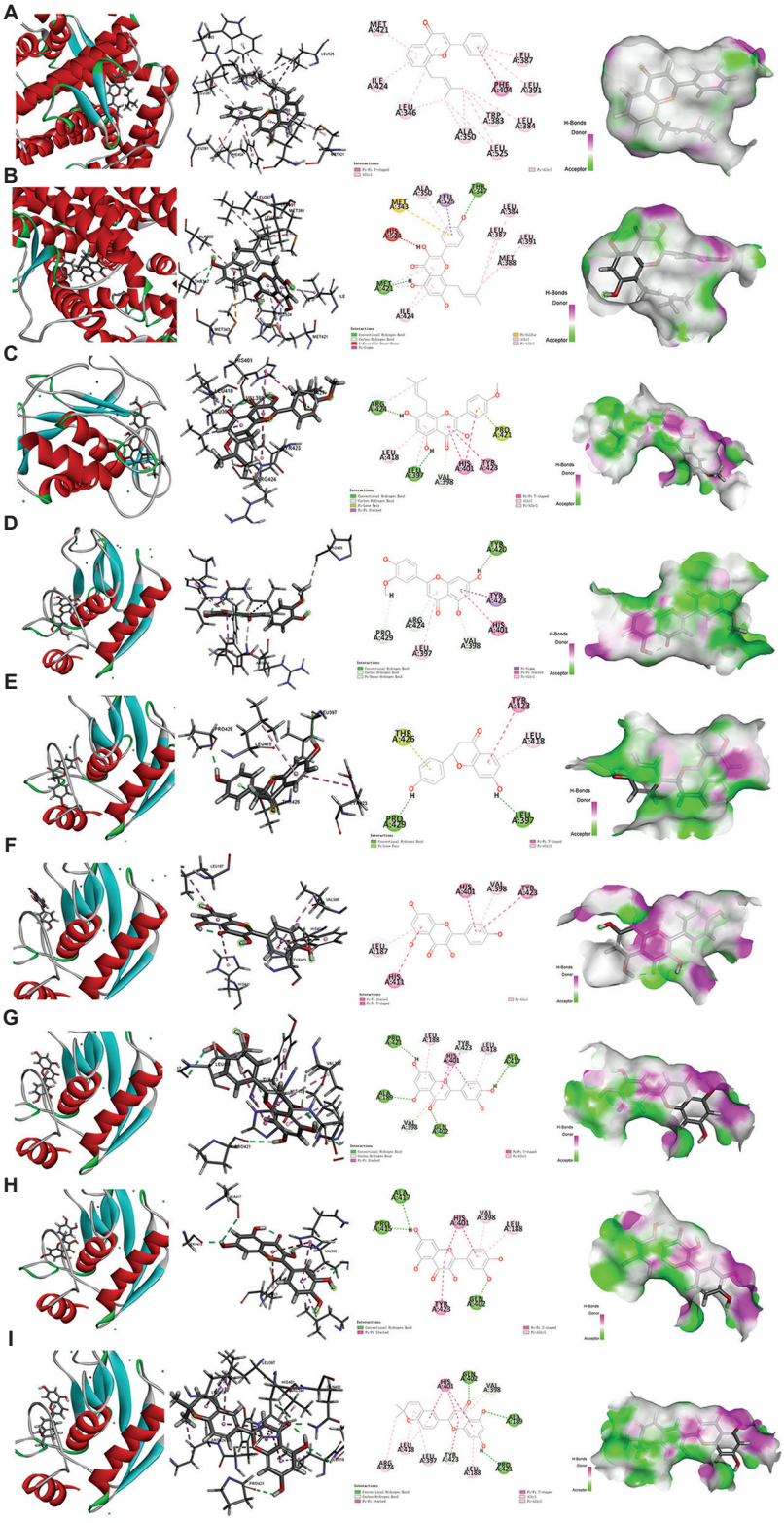

Figure 7. Schematic of the optimal molecular docking results of the key active components with key targets, showing hydrogen bonds, van der Waals forces, and π–π interactions with amino acid residues of the active targets and proteins. A and B represent the molecular docking results of 8-(3-methylbut-2-enyl)-2-phenyl-chromone and 8-isopentenyl-kaempferol with ESR1. C–I represent the molecular docking results of anhydroicaritin, chryseriol, DFV, kaempferol, luteolin, quercetin, and Yinyanghuo C with MMP9

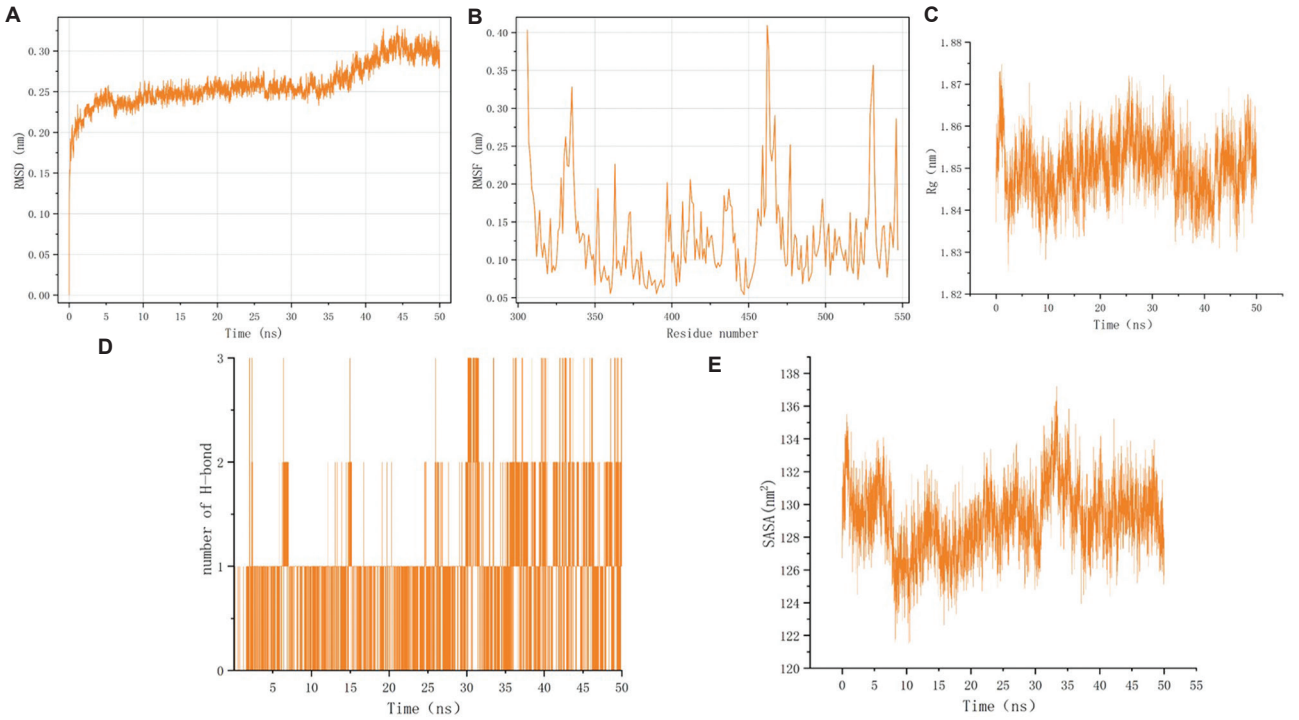

Figure 8. Results of molecular dynamics simulations. Panels (A) to (E) represent the root mean square deviation (RMSD), root mean square fluctuation (RMSF), radius of gyration (Rg), number of H-bonds, and SASA results of the molecular dynamics simulations, respectively

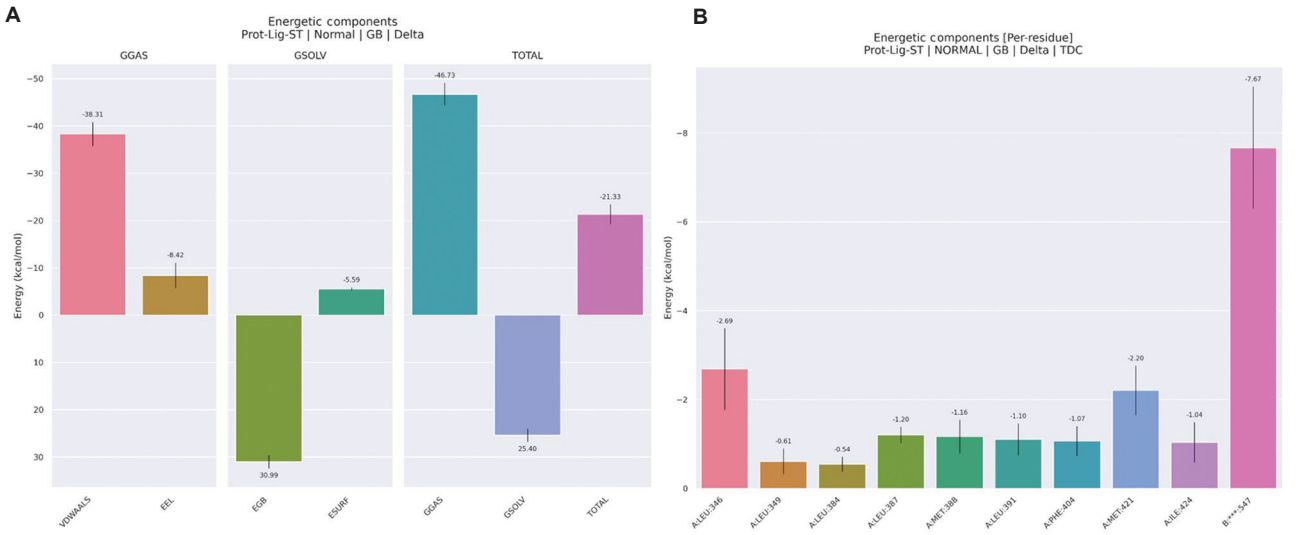

Figure 9. MMPBSA calculations. (A) From left to right, the bars represent van der Waals force, electrostatic energy, polar solvation energy, and non-polar solvation energy, respectively, and the TOTAL represents the average binding free energies. (B) Energy contribution of different amino acid residues; the last bar represents the ligand's energy, which is also the sum of energies

5. Conclusion

The prevention and treatment of periodontitis by EH is a complex process involving multiple components, targets, pathways, and links. The ingredients 8-(3-Methylbut-2-enyl)-2-phenyl-chromone, 8-isopentenyl-kaempferol, anhydroicaritin, chryseriol, DFV, kaempferol, luteolin, quercetin, and Yinyanghuo C were involved in the treatment process through pathways related to cancer, lipid, and atherosclerosis; AGE–RAGE signaling pathway in diabetic complications; and other key signaling pathways regulating the expression of the core targets of AKT1,

TNF, IL6, TP53, VEGFA, IL1B, CASP3, PTGS2, MMP9, and ESR1. These ingredients play an anti-inflammatory role, promote the regeneration of periodontal tissue, and provide a new drug alternative for the clinical treatment of periodontitis. Nevertheless, there is still a long way to go before the clinical application of these drugs, and further laboratory research and clinical trials are warranted.

Acknowledgments

None.

Funding

This work was supported by grants from the Foundation of Science and Technology Department of Henan Province, China (no. 212102310103); Natural Science Foundation of Education Department of Henan Province, China (no. 21A320004); Foundation of the National Health Commission of Henan Province, China (no. Wjlx2020017); Foundation of the Educational Administration Department of Henan University, China (no. HDXJJG2020-83); and Foundation of Science & Technology Department of Kaifeng City, Henan Province, China (no. 2203015).

Conflict of interest

Yuankun Zhai is an Editorial Board Member of this journal but was not in any way involved in the editorial and peer-review process conducted for this paper, directly or indirectly. Separately, other authors declared that they have no known competing financial interests or personal relationships that could have influenced the work reported in this paper.

Author contributions

Conceptualization: Yuankun Zhai
Investigation: Junhan Wan, Mingzhen Yang
Methodology: Junhan Wan, Yingjie Zhu
Writing – original draft: Junhan Wan
Writing – review & editing: Wenwen Wang, Ningli Li, Yuankun Zhai

Ethics approval and consent to participate

Not applicable.

Consent for publication

Not applicable.

Availability of data

The datasets used and analyzed in the current study are available from the corresponding author upon reasonable request.

References

1. Slots J. Periodontitis: Facts, fallacies and the future. *Periodontol 2000*. 2017;75(1):7-23.

   doi: 10.1111/prd.12221

2. Graves DT, Correa JD, Silva TA. the oral microbiota is modified by systemic diseases. *J Dent Res*. 2019;98(2):148-156.

   doi: 10.1177/0022034518805739

3. Qin H, Li G, Xu X, *et al*. The role of oral microbiome in periodontitis under diabetes mellitus. *J Oral Microbiol*. 2022;14(1):2078031.

   doi: 10.1080/20002297.2022.2078031

4. Sanz M, Del Castillo AM, Jepsen S, *et al*. Periodontitis and cardiovascular diseases: Consensus report. *J Clin Periodontol*. 2020;47(3):268-288.

   doi: 10.1111/jcpe.13189

5. De Molon RS, Rossa C Jr., Thurlings RM, Cirelli JA, Koenders MI. Linkage of periodontitis and rheumatoid arthritis: Current evidence and potential biological interactions. *Int J Mol Sci*. 2019;20(18):4541.

   doi: 10.3390/ijms20184541

6. Kwon T, Lamster IB, Levin L. Current concepts in the management of periodontitis. *Int Dent J*. 2021;71(6):462-476.

   doi: 10.1111/idj.12630

7. Bessa LJ, Botelho J, Machado V, Alves R, Mendes JJ. Managing oral health in the context of antimicrobial resistance. *Int J Environ Res Public Health*. 2022;9(24):16448

   doi: 10.3390/ijerph192416448

8. Xu H, Zhou S, Quet R, *et al*. Icariin prevents oestrogen deficiency-induced alveolar bone loss through promoting osteogenesis via STAT3. *Cell Prolif*. 2020;53(2):e12743.

   doi: 10.1111/cpr.12743

9. Wu J, Zhou J, Chen X, *et al*. Attenuation of LPS-induced inflammation by ICT, a derivate of icariin, via inhibition of the CD14/TLR4 signaling pathway in human monocytes. *Int Immunopharmacol*. 2012;12(1):74-79.

   doi: 10.1016/j.intimp.2011.10.015

10. Sun S, Liu L, Tian X, *et al*. Icariin attenuates high glucose-induced apoptosis, oxidative stress, and inflammation in human umbilical venous endothelial cells. *Planta Med*. 2019;85(6):473-482.

    doi: 10.1055/a-0837-0975

11. Ma H, He X, Yang Y, Li M, Hao D, Jia Z. The genus epimedium: An ethnopharmacological and phytochemical review. *J Ethnopharmacol*. 2011;134(3):519-541.

    doi: 10.1016/j.jep.2011.01.001

12. Wang S, Ma J, Zeng Y, *et al*. Icariin, an up-and-coming

bioactive compound against neurological diseases: Network pharmacology-based study and literature review. *Drug Des Devel Ther*. 2021;15:3619-3641.

doi: 10.2147/DDDT.S310686

13. Sze SC, Tong Y, Ng TB, Cheng CL, Cheung HP. Herba Epimedii: Anti-oxidative properties and its medical implications. *Molecules*. 2010;15(11):7861-7870.

doi: 10.3390/molecules15117861

14. He W, Sun H, Yang B, Zhang D, Kabelitz D. Immunoregulatory effects of the herba epimediia glycoside icariin. *Arzneimittelforschung*. 1995;45(8):910-913.

15. Verma A, Aggarwal K, Agrawal R, Pradhan K, Goyal A. Molecular mechanisms regulating the pharmacological actions of icariin with special focus on PI3K-AKT and Nrf-2 signaling pathways. *Mol Biol Rep*. 2022;49(9):9023-9032.

doi: 10.1007/s11033-022-07778-3

16. Bi Z, Zhang W, Yan X. Anti-inflammatory and immunoregulatory effects of icariin and icaritin. *Biomed Pharmacother*. 2022;151:113180.

doi: 10.1016/j.biopha.2022.113180

17. Alam W, Khan H, Shah MA, Cauli O, Saso L. Kaempferol as a dietary anti-inflammatory agent: Current therapeutic standing. *Molecules*. 2020;25(18):4073.

doi: 10.3390/molecules25184073

18. Zheng X, Dong Z, Liang Z, *et al*. Photothermally responsive icariin and carbon nanofiber modified hydrogels for the treatment of periodontitis. *Front Bioeng Biotechnol*. 2023;11:1207011.

doi: 10.3389/fbioe.2023.1207011

19. Zhang X, Han N, Li G, *et al*. Local icariin application enhanced periodontal tissue regeneration and relieved local inflammation in a minipig model of periodontitis. *Int J Oral Sci*. 2018;10(2):19.

doi: 10.1038/s41368-018-0020-3

20. Han Y, Sun H, Zhang A, Yan G, Wang XJ. Chinmedomics, a new strategy for evaluating the therapeutic efficacy of herbal medicines. *Pharmacol Ther*. 2020;216:107680.

doi: 10.1016/j.pharmthera.2020.107680

21. Lou Y, Ma M, Jiang Y, *et al*. Ferroptosis: A new strategy for traditional Chinese medicine treatment of stroke. *Biomed Pharmacother*. 2022;156:113806.

doi: 10.1016/j.biopha.2022.113806

22. Zhang Z, Zheng Y, Bian X, *et al*. Identification of key genes and pathways associated with oxidative stress in periodontitis. *Oxid Med Cell Longev*. 2022;2022:9728172.

doi: 10.1155/2022/9728172

23. Valdes-Tresanco MS, Valdés-Tresanco ME, Valiente PA, Moreno E. gmx_MMPBSA: A new tool to perform end-state free energy calculations with GROMACS. *J Chem Theory Comput*. 2021;17(10):6281-6291.

doi: 10.1021/acs.jctc.1c00645

24. Poli G, Granchi C, Rizzolio F, Tuccinardi T. Application of MM-PBSA methods in virtual screening. *Molecules*. 2020;25(8):1971.

doi: 10.3390/molecules25081971

25. Di Stefano M, Polizzi A, Santonocito S, Romano A, Lombardi T, Isola G. Impact of oral microbiome in periodontal health and periodontitis: A critical review on prevention and treatment. *Int J Mol Sci*. 2022;23(9):5142.

doi: 10.3390/ijms23095142

26. Hajishengallis G, Darveau RP, Curtis MA. The keystone-pathogen hypothesis. *Nat Rev Microbiol*. 2012;10(10):717-725.

doi: 10.1038/nrmicro2873

27. Liu X, Niu Y, Xie W, Wei D, Du Q. Tanshinone IIA promotes osteogenic differentiation of human periodontal ligament stem cells via ERK1/2-dependent Runx2 induction. *Am J Transl Res*. 2019;11(1):340-350.

28. Cao CF, Sun XP. Herbal medicine for periodontal diseases. *Int Dent J*. 1998;48(3 Suppl 1):316-322.

doi: 10.1111/j.1875-595x.1998.tb00722.x

29. Chan Y, Lai CH, Yang HW, Lin YY, Chan CH. The evaluation of Chinese herbal medicine effectiveness on periodontal pathogens. *Am J Chin Med*. 2003;31(5):751-761.

doi: 10.1142/S0192415X03001417

30. Shen R, Wang JH. The effect of icariin on immunity and its potential application. *Am J Clin Exp Immunol*. 2018;7(3):50-56.

31. Xu CQ, Liu BJ, Wu JF, *et al*. Icariin attenuates LPS-induced acute inflammatory responses: Involvement of PI3K/Akt and NF-kappaB signaling pathway. *Eur J Pharmacol*. 2010;642(1-3):146-153.

doi: 10.1016/j.ejphar.2010.05.012

32. Hua W, Zhang Y, Wu X, *et al*. Icariin attenuates interleukin-1beta-induced inflammatory response in human nucleus pulposus cells. *Curr Pharm Des*. 2018;23(39):6071-6078.

doi: 10.2174/1381612823666170615112158

33. Devi KP, Malar DJ, Nabavi SF, *et al*. Kaempferol and inflammation: From chemistry to medicine. *Pharmacol Res*. 2015;99:1-10.

doi: 10.1016/j.phrs.2015.05.002

34. Chen AY, Chen YC. A review of the dietary flavonoid, kaempferol on human health and cancer chemoprevention. *Food Chem*. 2013;138(4):2099-2107.

doi: 10.1016/j.foodchem.2012.11.139

35. Mundi PS, Sachdev J, McCourt C, Kalinsky K. AKT in

cancer: New molecular insights and advances in drug development. *Br J Clin Pharmacol*. 2016;82(4):943-956.

doi: 10.1111/bcp.13021

36. Alwhaibi A, Verma A, Adil MS, Somanath PR. The unconventional role of Akt1 in the advanced cancers and in diabetes-promoted carcinogenesis. *Pharmacol Res*. 2019;145:104270.

doi: 10.1016/j.phrs.2019.104270

37. Van Loo G, Bertrand MJM. Death by TNF: A road to inflammation. *Nat Rev Immunol*. 2022;23:289-303.

doi: 10.1038/s41577-022-00792-3

38. Zhang H, Liu L, Jiang C, Pan K, Deng J, Wan C. MMP9 protects against LPS-induced inflammation in osteoblasts. *Innate Immun*. 2020;26(4):259-269.

doi: 10.1177/1753425919887236

39. Checchi V, Maravic T, Bellini P, *et al*. The role of matrix metalloproteinases in periodontal disease. *Int J Environ Res Public Health*. 2020;17(14):4923.

doi: 10.3390/ijerph17144923

40. Silva FS, Sóter MO, Sales MF, *et al*. Estrogen receptor alpha gene (ESR1) PvuII and XbaI polymorphisms are associated to metabolic and proinflammatory factors in polycystic ovary syndrome. *Gene*. 2015;560(1):44-49.

doi: 10.1016/j.gene.2015.01.037

41. Musacchio E, Binotto P, Silva-Netto F, Perissinotto E, Sartori L. Bone-related polymorphisms and dental status in older men and women. Results of the longitudinal Pro.V.A. study. *J Dent Sci*. 2022;17(1):528-534.

doi: 10.1016/j.jds.2021.06.023

42. Langdahl BL, Løkke E, Carstens M, Stenkjaer LL, Eriksen EF. A TA repeat polymorphism in the estrogen receptor gene is associated with osteoporotic fractures but polymorphisms in the first exon and intron are not. *J Bone Miner Res*. 2000;15(11):2222-2230.

doi: 10.1359/jbmr.2000.15.11.2222

43. Deng L, Guo Y. Estrogen effects on orthodontic tooth movement and orthodontically-induced root resorption. *Arch Oral Biol*. 2020;118:104840.

doi: 10.1016/j.archoralbio.2020.104840

44. Krum SA, Brown M. Unraveling estrogen action in osteoporosis. *Cell Cycle*. 2008;7(10):1348-1352.

doi: 10.4161/cc.7.10.5892

45. Gao Y, Guo Z, Liu Y. Analysis of the potential molecular biology of triptolide in the treatment of diabetic nephropathy: A narrative review. *Medicine* (*Baltimore*). 2022;101(48):e31941.

doi: 10.1097/MD.0000000000031941

ACCSCIENCE PUBLISHING

Gene & Protein in Disease

ORIGINAL RESEARCH ARTICLE

Pre-metastatic niche in oral squamous cell carcinoma: Insights from a transcriptomic meta-analysis

Ana Kelly Fernandes Duarte[1†], Heloisa de Almeida Freitas[1†], Genilda Castro de Omena Neta[2], Rodger Marcel Lima Rocha[1], Thaysa Kelly Barbosa Vieira[2], Karol Fireman de Farias[2], Bruna Del Vechio Koike[3], Carolinne de Sales Marques[4], and Carlos Alberto de Carvalho Fraga[2*]

[1]Institute of Pharmaceutical Sciences, Federal University of the Alagoas, Maceió, Alagoas, Brazil

[2]Medical and Nursing Science Complex, Federal University of the Alagoas, Arapiraca, Alagoas, Brazil

[3]Medical College, Federal University of the San Francisco Valley, Petrolina, Pernambuco, Brazil

[4]Department of Genetics, Institute of Biological and Health Sciences, Federal University of the Alagoas, Maceió, Alagoas, Brazil

Abstract

Primary tumors can precondition a pre-metastatic niche, promoting the colonization of circulating neoplastic cells and influencing the secondary tumor microenvironment. Nevertheless, the mechanisms underlying the formation of this niche, as well as perineural invasion in oral squamous cell carcinoma (OSCC), are not well-elucidated. The study aims to identify differentially expressed genes (DEGs) and related pathways associated with pre-metastatic niche and perineural invasion in OSCC. We evaluated metastatic and non-metastatic primary tumor samples, healthy oral tissues, OSCC samples, metastatic lymph nodes from patients with OSCC, and normal lymph node samples. The GEO2R tool was applied to identify mRNAs differentially expressed between tissues exhibiting features of a pre-metastatic niche and normal tissue samples, including selected non-metastatic and metastatic OSCC samples. We also performed an analysis of perineural invasion-negative and perineural invasion-positive tumor samples. Our data revealed that *SERPINE1*, *SPP1*, *CALCA*, and *MMP13* genes were upregulated. These upregulated genes are associated with several cancer-related pathways, while downregulated genes are mainly associated with immune responses, axon guidance, and the neurotrophin signaling pathway. Given the upregulation of the circadian rhythm pathway in metastatic lymph nodes, we also performed a correlation analysis that allows users to compute function-specific parameters, with resulting figures dynamically displayed to conveniently access the tumor's immunological, clinical, and genomic features. Downregulation of the circadian rhythm gene *PER3* and upregulation of *Bhlhe40* were associated with poor survival outcomes. In conclusion, we postulate that during lymph node invasion, OSCCs activate axonal guidance genes, such as *SERPENE1*, *L1AM*, *CXCR4*, and *SPP1*. As neoplastic cells establish themselves, circadian rhythm genes are upregulated, contributing to immune evasion and promoting tumor growth.

Keywords: Metastasis; Circadian rhythm; Oral cancer; Cancer microenvironment

[†]These authors contributed equally to this work.

***Corresponding author:**
Carlos Alberto de Carvalho Fraga (carlos.fraga@arapiraca.ufal.br)

Citation: Duarte AKF, Freitas HA, Neta GCO, *et al.* Pre-metastatic niche in oral squamous cell carcinoma: Insights from a transcriptomic meta-analysis. *Gene Protein Dis.* 2024;3(4):2971. doi: 10.36922/gpd.2971

Received: February 19, 2024
Accepted: July 16, 2024
Published Online: November 20, 2024

1. Introduction

Metastasis involves the spread of cancer cells from the primary tumor site to surrounding tissues and distant organs.[1] Neoplastic cells circulating in the blood are often likened to metastatic "seeds" that have the ability to fertilize a microenvironmental "soil" of organs secondary to the tumor.[2] However, reaching another site in the body does not guarantee the formation of a metastatic tumor, where successful invasion and proliferation of neoplastic cells depends on their interaction with the local microenvironment.[3] Primary tumor cells are capable of modifying a microenvironment distant from the primary tumor locus before the arrival of metastatic cells, creating what is known as the pre-metastatic niche.[4]

A pre-requisite for metastasis spread is the ability of these cells to exit the bloodstream, peripheral nerves, and lymphatic vessels, reach the stroma, and exhibit a pre-dilection to lodge in specific organs.[5-7] The local microenvironment, characterized by early changes that dictate the pattern of metastatic spread, is referred to as the "pre-metastatic niche."[8] Mechanical forces within vascular channels govern the initial dispersion of cells originating from primary tumors to distant sites.[1] The attachment, extravasation, survival, and proliferation of neoplastic cells are important for metastatic growth. In response to cytokines such as vascular endothelial growth factor receptors and matrix metalloproteinases (MMPs), tumor-associated cells, such as hematopoietic progenitor cells and macrophages, modify the distant sites, allowing cancer cell adhesion, invasion, and growth.[4]

Neoplastic cells can reach secondary sites through nerves found in the peripheral nervous system, a process called perineural invasion.[7,9,10] The mechanism underlying perineural invasion is not well understood. Cancer cells must acquire mechanisms that enable their survival outside the primary environment, facilitating communication with the nerve microenvironment in several tumors, including oral squamous cell carcinoma (OSCC).[11,12]

OSCC is a malignant neoplasia that can affect different regions of the oral cavity.[5] The main risk factors include substances such as tobacco and alcohol, chronic lesions, human papillomavirus (HPV) infection, and ultraviolet radiation.[5,13-16] These pathological factors influence several metabolic processes, disrupt cellular homeostasis, and induce genomic changes, which can promote carcinogenesis in the long run.[17-19]

Globally, approximately 20 million new cancer cases are reported annually, with nearly 10 million cancer-related deaths.[20] The majority of cancer-related deaths are due to metastasis.[14] In patients with oral cancer, metastasis development is well characterized, and studies have shown the association between poor survival rate and lymph node metastasis in oral cancer patients.[14,18] In this study, we performed a bioinformatic analysis to identify differentially expressed genes (DEGs) and pathways associated with the pre-metastatic niche and perineural invasion in OSCC.

2. Methods

2.1. Data retrieval and processing

The Gene Expression Omnibus (GEO) database (www.ncbi.nlm.nih.gov/geo) is one of the leading platforms for the storage and distribution of gene expression data generated through microarray technology, accessible through a free, public web interface. We evaluated GEO datasets with metastatic and non-metastatic primary tumor samples (GSE2280), healthy oral tissues and OSCC samples (GSE31056), and metastatic lymph nodes from patients with OSCC and normal lymph node samples (GSE70604). GEO2R was applied to screen mRNAs differentially expressed between tissues exhibiting features of a pre-metastatic niche and normal tissue samples.

2.2. RNA-seq and clinical information data from The Cancer Genome Atlas

The Cancer Genome Atlas (TCGA) analyses were performed as previously described.[21] The selected cancer subtypes included non-metastatic and metastatic OSCC samples. We also performed an analysis of perineural invasion-negative and perineural invasion-positive tumor samples. Co-expressed upregulated and downregulated DEGs from the gene expression profiles were combined and identified using Venn Diagram 2.1.0 (http://bioinfogp.cnb.csic.es/tools/venny/index.html). A significance threshold of adjusted $P < 0.05$ and a log of fold change (logFC) ≥ 1 was set as the cut-off criterion.

2.3. Functional enrichment analysis

We performed gene list collection and functional enrichment analysis as previously described.[21] The data of associated genes and pathways for Kyoto Encyclopedia of Genes and Genomes (KEGG) analyses are available on the Database for Annotation, Visualization, and Integrated Discovery (DAVID) platform (https://david.ncifcrf.gov/), which acts as a data warehouse whose central objective is to extract meaningful biological information such as functions and pathways of genes and proteins. KEGG analyses were performed using the DAVID platform to annotate DEG functions and evaluate their pathway enrichment.

2.4. Oral cancer expression analyses

Additional web resources were used as sources of information and analytical tools for head and neck cancer

expression studies. Survival analysis of the TCGA data was performed using TCGAbiolinks.[22] Kaplan–Meier plots were constructed to explore the association between clinical outcomes and gene expression, allowing for the visualization of survival differences. We further explored protein expression using The Human Protein Atlas.

3. Results

3.1. Identification of differentially expressed genes, gene ontology enrichment, and functional classification

To evaluate key factors that contribute to the development and progression of the pre-metastatic niche in OSCC, we evaluated GEO datasets, including metastatic and non-metastatic primary tumor samples (GSE2280), healthy oral tissues and OSCC samples (GSE31056), and metastatic lymph nodes from patients with OSCC and normal lymph node samples (GSE70604).

In the GSE2280 dataset (metastatic and non-metastatic primary tumor samples), downregulated DEGs indicated the inactivation of the "intestinal immune network for IgA production" and "cytokine-cytokine receptor interaction" pathways. In contrast, upregulation of the "calcium signaling pathway," "neuroactive ligand-receptor interaction," "long-term potentiation," "dilated cardiomyopathy," "gonadotropin-releasing hormone (GnRH) signaling pathway," and "gap junction" were observed (Table 1).

In the GSE31056 dataset (healthy oral tissues and OSCC samples), the top six downregulated pathways were "drug metabolism," "fatty acid metabolism," "metabolism of xenobiotics by cytochrome P450," "peroxisome proliferator-activated receptor signaling pathway," "dilated cardiomyopathy," and "valine, leucine, and isoleucine degradation." We observed that "cell cycle," "extracellular matrix (ECM)-receptor interaction," "DNA replication," "focal adhesion," "p53 signaling pathway," and "pathways in cancer" were more active in OSCC samples compared with normal tissue (Table 2).

Finally, in the GSE70604 dataset (metastatic lymph nodes), we observed inactivated immune response pathways and activated "ECM-receptor interaction," "focal adhesion," "pathways in cancer," "circadian rhythm," "steroid hormone biosynthesis," and "adherens junction" pathways (Table 3).

3.2. Overview of The Cancer Genome Atlas cancer transcriptomic analysis

To validate the GEO2R results, we evaluated the TCGA data, obtaining gene expression data from metastatic and non-metastatic specimens. A separate analysis was conducted, and DAVID functional analysis showed that downregulated DEGs in non-metastatic tissue were mainly associated with "drug metabolism," "metabolism of xenobiotics by cytochrome P450," "retinol metabolism," "calcium signaling pathway," "dilated cardiomyopathy," "hypertrophic cardiomyopathy, "and "steroid hormone biosynthesis" pathways. In contrast, the "ECM-receptor interaction," "focal adhesion," "cytokine-cytokine receptor interaction," "neuroactive ligand-receptor interaction," "graft-versus-host disease," "natural killer cell-mediated cytotoxicity," "systemic lupus erythematosus," and "pathways in cancer" were more active in the same group of specimens (Tables S1 and S2).

Similarly, in metastatic samples, downregulated DEGs were linked to the inactivation of "drug metabolism," "metabolism of xenobiotics by cytochrome P450," and "retinol metabolism" pathways. On the other hand, upregulated DEGs in metastatic samples were associated with "ECM-receptor interaction," "focal adhesion," "cytokine-cytokine receptor interaction," "neuroactive ligand-receptor interaction," "systemic lupus erythematosus," "pathways in cancer," and "cell cycle" pathways. We found similar results in both perineural invasion-negative and perineural invasion-positive analyses (Tables S3 and S4).

3.3. Differentially expressed genes and pre-metastatic niche-related genes

Using Entrez Gene and GeneCards analyses, we identified 473 pre-metastatic niche-related genes. A Venn diagram was created to illustrate the overlap between the DEGs identified in the meta-analysis and those related to the pre-metastatic niche. The data showed that *SERPINE1*, *SPP1, CALCA*, and *MMP13* genes were consistently upregulated across all GEO and TCGA datasets. According to the list of 473 pre-metastatic niche-related genes, the GSE70604 dataset (lymph node samples) showed 68 upregulated and 61 downregulated genes. DAVID analysis showed those the upregulated genes are associated with several cancer-related pathways, while the downregulated genes are mainly associated with immune response, axon guidance, and the neurotrophin signaling pathway (Table 4). These findings were validated using immunohistochemical analysis from The Human Protein Atlas (Figure 1).

We found a positive correlation between *CALCA*, *SERPINE1*, *MMP13*, *SPP1*, and *MMP13* in TCGA cancer samples (Figure 2). Survival analysis showed that the overexpression of *SERPINE1*, *SPP1*, and *L1CAM* (axon guidance) was associated with poor survival, while the low

Table 1. Functional annotation analysis of upregulated differentially expressed genes overlapping in non-metastatic and metastatic oral squamous cell carcinoma tissue (GSE2280) using the Database for Annotation, Visualization, and Integrated Discovery tool

Term	%	P-value	Genes	Fold enrichment	Bonferroni	Benjamini	FDR
hsa04020: Calcium signaling pathway	4.9208211	1,33E-05	*PRKCA, ADCY2, ERBB4, TNNC1, ADCY8, ERBB3, HTR4, GRM1, ITPR2, PLCB4, GRIN2C, CHRM2, GRIN2D, AVPR1A, GNAS, PLCB1*	3.820435763	0.001542344	0.001542344	0.01517981
hsa04080: Neuroactive ligand-receptor interaction	4.69208211	9.06E-04	*F2RL3, GABRB3, OPRK1, ADCYAP1R1, NPY2R, GLRA2, HTR4, GRIA3, NPY1R, GRM1, GRIN2C, CHRM2, GRIN2D, MAS1, AVPR1A, MC5R*	2.626549587	0.099814658	0.051219023	1.02888658
hsa04720: Long-term potentiation	2.34604106	0.00100663	*PRKCA, PLCB4, ADCY8, GRIN2C, GRIN2D, PLCB1, GRM1, ITPR2*	4.94409334	0.110261827	0.038194164	1.14245075
hsa05414: Dilated cardiomyopathy	2.63929619	0.00135363	*LAMA2, ACTC1, ADCY2, ADCY8, TNNC1, SGCD, GNAS, CACNB4,* TTN	4.111121092	0.145404555	0.038520247	1.53349617
hsa04912: GnRH signaling pathway	2.63929619	0.00203465	*PRKCA, ADCY2, PLCB4, ADCY8, GNAS, MAPK8, MMP14, PLCB1, ITPR2*	3.859419801	0.210424573	0.046152985	2.29687361
hsa04540: Gap junction	2.34604106	0.00476122	*PRKCA, ADCY2, PLCB4, ADCY8, GNAS, PLCB1, GRM1, ITPR2*	3.777509518	0.425135434	0.088141208	5.29938542
hsa04730: Long-term depression	2.05278592	0.00543626	*PRKCA, PLCB4, GNAS, GRIA3, PLCB1, GRM1, ITPR2*	4.263384837	0.46864598	0.086372552	6.02962223
hsa04270: Vascular smooth muscle contraction	2.34604106	0.016069	*PRKCA, ADCY2, PLCB4, ADCY8, AVPR1A, GNAS, PLCB1, ITPR2*	3.001770956	0.847278993	0.209344407	16.8743914
hsa04510: Focal adhesion	3.22580645	0.01963648	*PRKCA, LAMA2, PAK4, BCL2, COL6A1, MAPK8, COL2A1, COL11A2, THBS1, RAPGEF1, SPP1*	2.299864315	0.899790642	0.225556375	20.2487751
hsa05416: Viral myocarditis	1.75953079	0.02542281	*LAMA2, MYH3, HLA-DRB4, SGCD, MYH8, MYH10*	3.551390991	0.94957056	0.258231453	25.4570748
hsa04916: Melanogenesis	2.05278592	0.02878173	*PRKCA, TYRP1, ADCY2, PLCB4, ADCY8, GNAS, PLCB1*	2.971450038	0.966212655	0,265062564	28.3361616
hsa04070: Phosphatidylinositol signaling system	1.75953079	0.02976164	*PRKCA, PIK3C2G, PLCB4, PLCB1, ITPK1, ITPR2*	3.40741568	0.969946202	0.253279147	29.1567617
hsa04512: ECM-receptor interaction	1.75953079	0.04746861	*LAMA2, COL6A1, COL2A1, COL11A2, THBS1, SPP1*	3.001770956	0.996451879	0.352054709	42.5833939
hsa05410: Hypertrophic cardiomyopathy	1.75953079	0.0495208	*LAMA2, ACTC1, TNNC1, SGCD, CACNB4,* TTN	2.966456004	0.997237237	0.343493808	43.9789683
hsa04640: Hematopoietic cell lineage	1.75953079	0.0516248	*IL9R, IL5, FCGR1A, HLA-DRB4, CD22, ITGAM*	2.931962329	0.997863506	0.336287319	45.3775838
hsa04530: Tight junction	2.05278592	0.09593184	*PRKCA,* CTTN, *MYH3, CLDN11, MYH8, CTNNA3, MYH10*	2.195325028	0.999991695	0.518652728	68.3548824

Note: $P<0.05$ was considered statistically significant.
Abbreviations: ECM: Extracellular matrix; FDR: False discovery rate; GnRH: Gonadotropin-releasing hormone.

Table 2. Functional annotation analysis of upregulated differentially expressed genes overlapping in normal and oral squamous cell carcinoma tissue (GSE31056) using the Database for Annotation, Visualization, and Integrated Discovery tool

Term	%	*P*-value	Genes	Fold enrichment	Bonferroni	Benjamini	FDR
hsa04110: Cell cycle	3.29768271	1.94E-12	*MAD1L1, DBF4, TGFB3, PRKDC, TTK, PKMYT1, CHEK1, SFN, PTTG1, TGFB1, CCNE2, CCNE1, CDC45, MCM7, CDKN2A, TFDP2, BUB1, CCNA1, CCNA2, CDC7, CDC6, CDK1, SKP2, CDK6, CDC20, MCM2, MCM4, MCM5, CDC25B, CCNB1, MAD2L1, YWHAH, CCNB2, PLK1, GSK3B, PCNA, BUB1B*	3.744179104	3.11E-10	3.11E-10	2.34E-09
hsa04512: ECM-receptor interaction	2.67379679	1.98E-12	*TNC, COL3A1, ITGB4, HMMR, LAMB3, CD44, ITGAV, ITGB6, COL6A3, COL6A1, AGRN, COL11A1, THBS2, FN1, SPP1, COL4A2, COL4A1, ITGA2, ITGA3, ITGA4, COL5A3, COL5A2, COL5A1, COL4A6, SDC1, ITGA6, ITGA5, COL1A2, LAMC2, COL1A1*	4.517590618	3.16E-10	1.58E-10	2.39E-09
hsa03030: DNA replication	1.24777184	1.62E-06	*POLA2, MCM2, RNASEH2A, MCM4, MCM5, RPA3, PRIM1, RFC5, RFC4, MCM7, POLE2, PRIM2, PCNA, FEN1*	4.919154229	2.60E-04	8.65E-05	0.00195894
hsa04510: Focal adhesion	3.20855615	4.88E-06	*PGF, TNC, COL3A1, ITGB4, LAMB3, RAC2, PAK2, ITGAV, COL6A3, ITGB6, COL6A1, SHC1, COL11A1, THBS2, FN1, SPP1, COL4A2, COL4A1, MET, ITGA2, ACTN1, ITGA3, ITGA4, COL5A3, COL5A2, COL5A1, COL4A6, FLNA, VEGFC, PPP1CA, ITGA6, ITGA5, GSK3B, COL1A2, LAMC2, COL1A1*	2.265537982	7.80E-04	1.95E-04	0.00589215
hsa04115: p53 signaling pathway	1.60427807	1.32E-05	*BID, CDK1, CDK6, CHEK1, PMAIP1, SFN, GTSE1, SESN3, CCNB1, CCNE2, CCNE1, CDKN2A, CCNB2, SERPINB5, BAX, RRM2, SERPINE1, IGFBP3*	3.34833187	0.002110583	4.22E-04	0.01594371
hsa05200: Pathways in cancer	3.74331551	0.00173278	*BID, WNT5A, PGF, MMP9, EGLN3, TGFB3, TGFB1, MMP1, WNT2, CCNE2, CCNE1, LAMB3, CDKN2A, RAC2, ITGAV, SLC2A1, TGFA, CCNA1, FN1, COL4A2, COL4A1, RELA, MET, SKP2, BRCA2, ITGA2, CDK6, BIRC5, FADD, ITGA3, FZD2, STAT1, DAPK3, COL4A6, FZD6, NRAS, VEGFC, CBLC, ITGA6, GSK3B, BAX, LAMC2*	1.619721514	0.242313769	0.045194528	2.07235604

(*Cont'd...*)

Table 2. (*Continued*)

Term	%	*P*-value	Genes	Fold enrichment	Bonferroni	Benjamini	FDR
hsa00240: Pyrimidine metabolism	1.51515152	0.0027625	*DTYMK, UPP1, POLA2, POLR2D, PNP, NME7, TK1, CMPK2, PRIM1, TYMS, TYMP, POLE2, RRM2, PRIM2, CDA, UCK2, NT5E*	2.263550668	0.357643837	0.061272775	3.28513461
hsa04114: Oocyte meiosis	1.60427807	0.00518584	*CDK1, PKMYT1, AURKA, CDC20, PTTG1, ITPR3, CCNE2, CCNB1, CCNE1, PPP1CA, CCNB2, YWHAH, MAD2L1, RPS6KA1, PLK1, BUB1, FBXO5, CALML5*	2.069877883	0.56477551	0.098762684	6.08511781
hsa05222: Small cell lung cancer	1.3368984	0.00548348	*COL4A2, COL4A1, RELA, SKP2, ITGA2, CDK6, ITGA3, COL4A6, CCNE2, CCNE1, LAMB3, ITGA6, ITGAV, LAMC2, FN1*	2.258795309	0.585121834	0.093126459	6.42383747
hsa05322: Systemic lupus erythematosus	1.42602496	0.01006257	*HIST1H2BD, HIST1H2BE, HIST1H2AG, HIST1H2BF, HIST1H2BG, HIST1H2AE, HIST1H2BH, ACTN1, C1QC, C1QB, CD86, HIST1H2BK, CD80, HIST2H2BE, HIST1H2BI, SNRPB, HIST1H3D, HIST1H2AM, FCGR3B, HIST1H4H*	2.044323835	0.8017381	0.149402844	11.4957646
hsa04060: Cytokine-cytokine receptor interaction	2.85204991	0.01345636	*CXCL1, CSF2, TNFRSF21, CXCL5, OSMR, TNFRSF12A, CXCL3, TGFB3, CXCL9, CXCL6, IL7R, CXCL11, CCL5, CCL4, TGFB1, CXCL10, IL12RB2, CCL20, IL1RAP, IL1B, IL1A, IL2RB, TNFSF4, MET, IL24, CCL18, CCL11, INHBA, VEGFC, TNFSF10, CXCL13, CXCL16*	1.544947021	0.885551997	0.178856747	15.0907417
hsa05412: Arrhythmogenic right ventricular cardiomyopathy	1.15864528	0.01488495	*ITGB4, ACTN1, ITGA2, GJA1, ITGA3, CDH2, ITGA4, CACNA2D3, DSG2, ITGA6, ITGA5, ITGAV, ITGB6*	2.163688138	0.909236245	0.181234808	16.563565
hsa05020: Prion diseases	0.71301248	0.01750244	*C1QB, BAX, IL1B, STIP1, PRNP, CCL5, C1QC, IL1A*	2.891257996	0.940702468	0.195329275	19.2014569
hsa04810: Regulation of actin cytoskeleton	2.31729055	0.03041059	*DIAPH 3, ITGB4, ITGA2, ACTN1, ITGA3, ITGB2, ITGA4, MYH9, ARPC1A, ARPC1B, NRAS, PFN1, PPP1CA, PFN2, RAC2, PAK2, ITGA6, ITGAX, ITGA5, ITGAV, RRAS2, ITGB6, CFL1, MSN, FN1, F2R*	1.529677195	0.992854084	0.297383376	31.1268342

(*Cont'd...*)

Table 2. (*Continued*)

Term	%	*P*-value	Genes	Fold enrichment	Bonferroni	Benjamini	FDR
hsa04062: Chemokine signaling pathway	2.04991087	0.03634854	*CXCL1, LYN, CXCL5, HCK, CXCL3, RELA, CXCL9, CXCL6, CCL5, STAT1, CXCL11, CCL4, CCL18, CXCL10, CCL11, NRAS, CCL20, RAC2, CXCL13, CXCL16, GSK3B, GNB5, SHC1*	1.555790566	0.997325777	0.326279374	36.0507054
hsa05219: Bladder cancer	0.71301248	0.04377802	*NRAS, VEGFC, TYMP, CDKN2A, PGF, MMP9, DAPK3, MMP1*	2.409381663	0.999224833	0.360872932	41.7563079
hsa04620: Toll-like receptor signaling pathway	1.24777184	0.05258336	*RELA, CXCL9, TLR2, FADD, CXCL11, STAT1, CCL5, CCL4, CXCL10, CD86, CD80, IRF7, IL1B, SPP1*	1.753361903	0.999823575	0.398536221	47.9122636
hsa04514: Cell adhesion molecules	1.51515152	0.05422803	*F11R, ICAM1, CD276, ITGB2, ITGA4, CDH2, CDH3, SDC1, CD86, CD80, ITGA6, ITGAV, ICOS, CLDN1, CNTN1, CNTNAP2, VCAN*	1.629070556	0.999866393	0.390788167	48.9936622
hsa05212: Pancreatic cancer	0.98039216	0.05441853	*VEGFC, CDKN2A, RAC2, PGF, RELA, TGFB3, TGFA, BRCA2, CDK6, STAT1, TGFB1*	1.932524876	0.99987063	0.375748489	49.1175775
hsa04623: Cytosolic DNA-sensing pathway	0.80213904	0.06456243	*DDX58, RELA, IRF7, PYCARD, IL1B, CCL5, CCL4, AIM2, CXCL10*	2.069877883	0.999976966	0.413701946	55.3308922
hsa05410: Hypertrophic cardiomyopathy	1.06951872	0.06876775	*ITGA6, ITGA5, ITGAV, ITGB6, ITGB4, TGFB3, ITGA2, ITGA3, ITGA4, CACNA2D3, TPM4, TGFB1*	1.785776997	0.999988798	0.418899192	57.6962219
hsa04640: Hematopoietic cell lineage	1.06951872	0.07355873	*CSF2, CD38, CD44, ITGA6, TFRC, ITGA5, IL1B, ITGA2, ITGA3, ITGA4, IL7R, IL1A*	1.765012149	0.999995092	0.426312252	60.2506497
hsa05120: Epithelial cell signaling in Helicobacter pylori infection	0.8912656	0.0842849	*CXCL1, ATP6V1C1, F11R, ADAM10, LYN, PTPRZ1, RELA, MET, ADAM17, CCL5*	1.860184372	0.999999239	0.458017547	65.4648659
hsa05211: Renal cell carcinoma	0.8912656	0.09709066	*NRAS, VEGFC, PAK2, PGF, MET, SLC2A1, EGLN3, TGFB3, TGFA, TGFB1*	1.807036247	0.99999992	0.493832462	70.8654463

Note: $P<0.05$ was considered statistically significant.
Abbreviations: ECM: Extracellular matrix; FDR: False discovery rate.

expression of *CXCR4* (axon guidance) and *CALCA* was associated with a good prognosis (Figure 3).

Given the observed upregulation of the circadian rhythm pathway in metastatic lymph nodes, we further performed a correlation analysis using TIMER, a web server that allows users to input function-specific parameters, with resulting figures dynamically displayed to conveniently access the tumor immunological, clinical, and genomic features. We observed that the downregulation of the circadian rhythm gene *PER3* and upregulation of *BHLHE40* were associated with poor survival outcomes (Figure 4).

4. Discussion

Over the past decade, substantial efforts have been made to unravel the mechanisms that underpin the formation of the pre-metastatic niche and its role in metastasis.[4] Integrating

Table 3. Functional annotation analysis of upregulated differentially expressed genes overlapping in non-metastatic and metastatic lymph nodes (GSE70604) using the Database for Annotation, Visualization, and Integrated Discovery tool

Term	%	*P*-value	Genes	Fold enrichment	Bonferroni	Benjamini	FDR
hsa04512: ECM-receptor interaction	1.94497154	9.89E-15	*TNC, COL3A1, ITGB4, ITGB5, SDC4, SDC2, GP9, LAMB4, LAMB3, GP6, CD44, COMP, COL6A3, ITGB6, COL6A2, COL6A1, AGRN, LAMB1, COL11A2, THBS1, COL11A1, THBS2, THBS3, SPP1, THBS4, COL4A2, ITGA2, ITGA3, COL5A3, COL5A2, COL5A1, COL4A6, LAMA1, LAMA4, SDC1, LAMA3, ITGA6, COL1A2, LAMC2, LAMC1, COL1A1*	3.709961563	1.80E-12	1.80E-12	1.22E-11
hsa04510: Focal adhesion	2.65654649	3.22E-08	*HRAS, PDGFA, TLN2, BCAR1, PAK6, COL11A2, COL11A1, EGFR, ACTN4, ACTN1, FLNC, CCND1, CRKL, JUN, VEGFA, COL1A2, LAMC2, LAMC1, COL1A1, CAV2, CAV1, ERBB2, TNC, COL3A1, ITGB4, ITGB5, IGF1R, LAMB4, LAMB3, RAC3, COMP, ITGB6, RAC1, COL6A3, COL6A2, COL6A1, LAMB1, EGF, THBS1, THBS2, THBS3, THBS4, SPP1, COL4A2, FLT1, ITGA2, ITGA3, CAPN2, COL5A3, COL5A2, COL5A1, COL4A6, LAMA1, LAMA4, LAMA3, ITGA6*	2.117662807	5.85E-06	2.93E-06	3.97E-05
hsa05200: Pathways in cancer	3.13092979	2.91E-04	*HRAS, PDGFA, WNT3A, MITF, TGFB3, FGF10, GLI2, MMP1, WNT2, FOS, CDKN2A, CDKN2B, SLC2A1, TGFA, RALA, CCNA1, EGFR, PLD1, CTBP2, RXRA, SKP2, CDK6, FGF21, CTNNA1, JUP, CCDC6, CCND1, CRKL, JUN, VEGFA, LAMC2, LAMC1, GSTP1, FGFR2, FGFR3, ERBB2, EGLN3, PML, TFG, CDH1, TCF7L2, TCF7L1, ARNT, LAMB4, IGF1R, LAMB3, RAC3, RAC1, LAMB1, EGF, COL4A2, BMP2, MSH3, FZD1, ITGA2, ITGA3, STAT1, COL4A6, DVL1, FZD6, NRAS, LAMA1, LAMA4, CDKN1A, LAMA3, ITGA6*	1.529448759	0.05162259	0.017512425	0.35873138
hsa00140: Steroid hormone biosynthesis	0.75901328	5.09E-04	*CYP1B1, CYP3A7, CYP11A1, HSD17B2, HSD17B1, SULT2B1, COMT, CYP7B1, AKR1C2, AKR1C4, HSD11B1, SRD5A3, UGT2A1, HSD11B2, SRD5A1, SULT1E1*	2.643790213	0.088437113	0.022882798	0.62585637
hsa04520: Adherens junction	1.04364326	6.66E-04	*EGFR, PARD3, ACTN4, PTPRF, BAIAP2, WASF1, ERBB2, LMO7, ACTN1, CTNND1, CDH1, FER, SNAI2, CTNNA1, TCF7L2, TCF7L1, IGF1R, RAC3, RAC1, WASL, YES1, INSR*	2.171684817	0.114132053	0.023946108	0.81832442
hsa05219: Bladder cancer	0.66413662	0.00203832	*EGFR, HRAS, FGFR3, ERBB2, CDH1, MMP1, NRAS, TYMP, CCND1, CDKN1A, CDKN2A, VEGFA, EGF, THBS1*	2.533632287	0.310200033	0.060015855	2.48646729
hsa05412: Arrhythmogenic right ventricular cardiomyopathy	0.9487666	0.00354163	*ACTN4, LMNA, ITGB4, ACTN1, ITGA2, ITGB5, GJA1, ITGA3, CTNNA1, CACNA2D2, TCF7L2, TCF7L1, JUP, ITGA6, SGCG, ITGB6, DSP, DSC2, CACNA1D, SGCB*	2.000236016	0.475715932	0.088119152	4.28374905
hsa04710: Circadian rhythm	0.28462998	0.02002098	*NPAS2, CSNK1E, PER2, PER1, BHLHE40, PER3*	3.508106244	0.974796926	0.368778637	22.0864146

(*Cont'd...*)

Table 3. (*Continued*)

Term	%	*P*-value	Genes	Fold enrichment	Bonferroni	Benjamini	FDR
hsa00010: Glycolysis/ Gluconeogenesis	0.71157495	0.02094904	*ALDOA, LDHA, HK2, FBP1, PFKP, PGAM2, ALDH3B2, BPGM, ADH7, PGM2, ALDH7A1, TPI1, ALDH1A3, HK3, ENO1*	1.900224215	0.978788841	0.348277506	22.9920687
hsa04144: Endocytosis	1.66034156	0.02255403	*FGFR2, PARD3, FGFR4, HRAS, CLTB, FGFR3, LDLR, CHMP4C, ERBB3, ASAP2, HSPA1A, ASAP3, HSPA1B, IGF1R, HSPA2, HSPA6, NEDD4L, EGF, AGAP2, SH3GL3, EGFR, EPN3, PLD1, DNM1L, FLT1, RAB4A, PRKCI, PSD2, RAB31, PSD, ACAP3, NEDD4, ACAP2, ARAP3, CLTCL1, SH3GL1*	1.445822772	0.984264428	0.339780642	24.5355185
hsa04530: Tight junction	1.28083491	0.02452481	*CLDN8, HRAS, PARD3, OCLN, GNAI3, ZAK, CLDN4, GNAI1, AMOTL1, LLGL1, CTTN, YES1, PPP2R2C, F11R, MAGI2, ACTN4, CNKSR3, PRKCI, ACTN1, CTNNA1, NRAS, CGN, CLDN1, CLDN2, RAB13, TJP2, MYH10*	1.531523994	0.989101832	0.336902192	26.3918352
hsa00051: Fructose and mannose metabolism	0.4743833	0.0275831	*ALDOA, TPI1, PFKFB4, AKR1B10, HK3, PFKFB2, HK2, PFKP, FBP1, PMM2*	2.2355579	0.993846036	0.345721104	29.1895597
hsa04115: p53 signaling pathway	0.75901328	0.0279472	*STEAP3, RPRM, CDK6, CHEK1, SFN, SESN3, EI24, CCND1, TP53I3, CDKN1A, CDKN2A, SERPINB5, GADD45G, SERPINE1, PERP, THBS1*	1.78844632	0.994251507	0.327553095	29.5160473
hsa05216: Thyroid cancer	0.42694497	0.02917712	*NRAS, CCDC6, HRAS, CCND1, RXRA, TFG, CDH1, TCF7L2, TCF7L1*	2.358899026	0.995434584	0.319512697	30.608716
hsa04960: Aldosterone-regulated sodium reabsorption	0.52182163	0.03566208	*ATP1B1, SGK1, ATP1B3, HSD11B1, HSD11B2, NEDD4L, SCNN1G, SFN, SCNN1B, INSR, SCNN1A*	2.039265011	0.9986519	0.356352414	36.1169647
hsa05222: Small cell lung cancer	0.85388994	0.04327485	*COL4A2, RXRA, SKP2, ITGA2, CDK6, ITGA3, COL4A6, LAMA1, LAMB4, CCND1, LAMA4, LAMB3, LAMA3, ITGA6, CDKN2B, LAMC2, LAMC1, LAMB1*	1.628763613	0.999681383	0.395419278	42.0691502
hsa00150: Androgen and estrogen metabolism	0.4743833	0.04579641	*AKR1C4, HSD17B2, HSD17B1, SRD5A3, HSD11B1, HSD11B2, SULT2B1, UGT2A1, SRD5A1, SULT1E1*	2.054296449	0.999802907	0.394604143	43.9253923
hsa04810: Regulation of actin cytoskeleton	1.80265655	0.0479246	*FGFR2, FGFR4, ENAH, HRAS, FGFR3, PDGFA, WASF1, BCAR1, DIAPH 3, ITGB4, FGF10, ITGB5, BDKRB1, BDKRB2, ITGAM, PAK6, PFN2, RAC3, ITGB6, RAC1, EGF, EGFR, LIMK2, ACTN4, BAIAP2, ITGA2, ACTN1, ITGA3, FGF21, NCKAP1, NRAS, CRKL, CHRM3, ITGA6, CYFIP1, WASL, CD14, MYH10*	1.343414329	0.999868724	0.391383657	45.4493499
hsa04012: ErbB signaling pathway	0.85388994	0.05773379	*EGFR, HRAS, NRG4, ERBB3, ERBB2, PAK6, NRAS, CDKN1A, EIF4EBP1, CRKL, JUN, HBEGF, TGFA, AREG, NRG1, EGF, ABL2, NRG2*	1.572599351	0.999980066	0.434268405	51.9938358

(*Cont'd...*)

Table 3. (*Continued*)

Term	%	*P*-value	Genes	Fold enrichment	Bonferroni	Benjamini	FDR
hsa04360: Axon guidance	1.13851992	0.07534992	*HRAS, GNAI3, PLXNA1, LIMK2, PLXNA2, EFNA1, GNAI1, EFNB1, DPYSL5, EPHB3, EPHB4, EPHA2, PAK6, NRAS, EPHA4, UNC5B, RAC3, SEMA3F, RAC1, SEMA4B, SEMA3C, NFATC4, RHOD, SRGAP1*	1.414120346	0.999999357	0.50977612	61.9675645
hsa04916: Melanogenesis	0.90132827	0.09220218	*HRAS, GNAI3, GNAI1, WNT3A, MITF, EDN1, FZD1, TCF7L2, TCF7L1, FZD6, DVL1, WNT2, NRAS, PLCB3, MC1R, CALML3, CREB3L1, CALML5, PLCB1*	1.458757983	0.999999977	0.567579927	69.6906156

Note: $P<0.05$ was considered statistically significant.
Abbreviations: ECM: Extracellular matrix; FDR: False discovery rate.

Table 4. Functional annotation analysis of upregulated differentially expressed genes overlapping in non-metastatic and metastatic lymph nodes (GSE70604) associated with pre-metastatic niche-related genes using the Database for Annotation, Visualization, and Integrated Discovery tool

Term	%	*P*-value	Genes	Fold enrichment	Bonferroni	Benjamini	FDR
hsa04660: T cell receptor signaling pathway	2.22222222	3.75E-14	*TNF, CD8A, CD8B, NFKBIE, CD247, NFKB1, MAP3K7, KRAS, RASGRP1, ICOS, MAP3K8, PPP3CB, ZAP70, PIK3CA, CD4, PIK3R5, NFATC3, AKT3, CD28, NFATC1, TEC, AKT2, PIK3CG, PTPN6, ITK, PTPRC, IL5, CD3G, CD3D, CD3E, PIK3CD, CTLA4, MALT1, VAV1, CARD11, MAPK1, LAT, PRKCQ, CBLB, PLCG1, FYN, CD40LG, LCK, IKBKG, MAP3K14, GRAP2, LCP2*	3.24474585	6.90E-12	6.90E-12	4.64E-11
hsa05340: Primary immunodeficiency	1.13475177	1.01E-12	*CIITA, PTPRC, CD3D, CD8A, CD8B, RFX5, CD3E, CD40, IL7R, RFXAP, BTK, DCLRE1C, CD19, CD40LG, ICOS, LCK, IKBKG, AIRE, ZAP70, CD4, AICDA, IL2RG, CD79A, BLNK*	5.11269376	1.86E-10	9.30E-11	1.25E-09
hsa04662: B cell receptor signaling pathway	1.65484634	1.07E-11	*NFKBIE, NFKB1, CD72, BTK, KRAS, DAPP1, RASGRP3, RAC2, PPP3CB, PIK3CA, CD22, PIK3R5, INPP5D, NFATC3, AKT3, AKT2, NFATC1, BLNK, SYK, PIK3CG, PTPN6, CR2, LYN, PIK3CD, MALT1, VAV1, PRKCB, CARD11, MAPK1, CD19, FCGR2B, PLCG2, IKBKG, CD79B, CD79A*	3.47947214	1.96E-09	6.54E-10	1.32E-08
hsa04640: Hematopoietic cell lineage	1.74940898	4.52E-11	*CSF3, TNF, HLA-DRB1, CD8A, CD8B, FCER2, HLA-DRB3, KIT, IL7R, IL11, FLT3LG, IL4R, MS4A1, CD2, CD22, CD4, GP1BA, CD5, CSF2RA, CD7, CR2, IL5, CD3G, CD3D, IL7, CD3E, FLT3, CD1C, CD1B, ITGA4, IL6R, CD1E, CD1D, CD37, CD19, IL3RA, HLA-DRA*	3.207819	8.31E-09	2.08E-09	5.58E-08

(*Cont'd*...)

Table 4. (*Continued*)

Term	%	*P*-value	Genes	Fold enrichment	Bonferroni	Benjamini	FDR
hsa05330: Allograft rejection	1.04018913	2.68E-10	*HLA-DQB1, TNF, IL5, HLA-DRB1, HLA-DRB3, FASLG, GZMB, CD40, HLA-DMB, HLA-E, HLA-DQA2, HLA-DMA, HLA-DQA1, HLA-G, HLA-F, CD40LG, IL12A, HLA-DPA1, HLA-DOA, HLA-DOB, CD28, HLA-DRA*	4.55645161	4.93E-08	9.85E-09	3.31E-07
hsa04672: Intestinal immune network for IgA production	1.1820331	1.77E-09	*HLA-DQB1, IL5, HLA-DRB1, HLA-DRB3, TNFRSF17, TNFSF12, ITGA4, CD40, IL15, HLA-DMB, HLA-DQA2, CXCL12, HLA-DMA, HLA-DQA1, CCR9, CXCR4, CD40LG, ICOS, AICDA, HLA-DPA1, MAP3K14, HLA-DOA, HLA-DOB, CD28, HLA-DRA*	3.80408762	3.25E-07	5.41E-08	2.18E-06
hsa04514: Cell adhesion molecules (CAMs)	2.12765957	2.17E-09	*HLA-DQB1, ITGAL, CADM3, HLA-DRB1, CD8A, CD8B, HLA-DRB3, CLDN5, L1CAM, HLA-DMB, HLA-DMA, VCAM1, ICOS, CD2, CD22, ESAM, CD4, HLA-DOA, CD6, SELPLG, HLA-DOB, SPN, CD28, SELP, PTPRC, SELL, ICAM2, ICAM3, CTLA4, NFASC, CD276, ITGA4, CD40, HLA-E, HLA-DQA2, HLA-G, HLA-DQA1, HLA-F, CD40LG, CNTN2, HLA-DPA1, JAM2, SELE, CD226, HLA-DRA*	2.54182218	3.99E-07	5.70E-08	2.68E-06
hsa04940: Type I diabetes mellitus	1.04018913	1.17E-08	*HLA-DQB1, ICA1, TNF, HLA-DRB1, PTPRN2, HLA-DRB3, FASLG, GZMB, HLA-DMB, HLA-E, HLA-DQA2, HLA-DMA, HLA-DQA1, HLA-G, HLA-F, IL12A, HLA-DPA1, HLA-DOA, HLA-DOB, LTA, CD28, HLA-DRA*	3.90552995	2.15E-06	2.69E-07	1.44E-05
hsa04650: Natural killer cell-mediated cytotoxicity	2.03309693	3.08E-08	*ITGAL, CD244, KLRC2, MICA, TNF, CD247, KLRK1, FASLG, CD48, SH2D1A, KRAS, RAC2, PPP3CB, ZAP70, PIK3CA, PIK3R5, NFATC3, NFATC1, SYK, PIK3CG, PRKCA, PTPN6, BRAF, ICAM2, PIK3CD, GZMB, HLA-E, VAV1, HLA-G, PRKCB, NCR3, HCST, TNFRSF10A, MAPK1, LAT, IFNAR2, TNFRSF10B, PLCG1, FYN, ULBP1, LCK, PLCG2, LCP2*	2.41059026	5.67E-06	6.30E-07	3.81E-05
hsa04062: Chemokine signaling pathway	2.55319149	3.09E-08	*ADCY4, ADCY1, ADCY7, PREX1, STAT5B, CXCR2, NFKB1, CXCL12, CXCR5, CXCR4, PIK3CA, GNG2, CSK, PLCB2, AKT3, GNG7, AKT2, PIK3CG, ROCK1, BRAF, LYN, NCF1, PIK3CD, PRKCB, CCR9, MAPK1, CCR7, CCR4, CCR3, CX3CR1, FGR, CXCL5, CXCL2, PF4, CCL22, DOCK2, KRAS, CCL20, RAC2, CCL21, RASGRP2, PIK3R5, ITK, HCK, CCL19, VAV1, CCL17, CCL14, CXCL13, IKBKG, GRK6, RAP1A, JAK2, GRK5*	2.15307291	5.68E-06	5.68E-07	3.81E-05

(*Cont'd...*)

Table 4. (*Continued*)

Term	%	*P*-value	Genes	Fold enrichment	Bonferroni	Benjamini	FDR
hsa05310: Asthma	0.75650118	8.65E-07	*HLA-DQB1, FCER1A, TNF, IL5, HLA-DRB1, HLA-DRB3, CD40, HLA-DMB, HLA-DMA, HLA-DQA2, HLA-DQA1, CD40LG, HLA-DPA1, HLA-DOA, HLA-DOB, HLA-DRA*	4.11366164	1.59E-04	1.45E-05	0.0010698
hsa04060: Cytokine-cytokine receptor interaction	3.02600473	1.16E-06	*IL21R, FASLG, CXCR2, IL15, TNFSF12, CXCL12, IL11, FLT3LG, ACVR1B, TNFRSF11B, CXCR5, CXCR4, IL4R, LTB, LTA, CSF2RA, GHR, TNFRSF17, TNFRSF14, IL6R, CD40, CCR9, TNFRSF10A, IFNAR2, TNFRSF9, CCR7, TNFRSF10B, RELT, CCR4, CD40LG, CCR3, CX3CR1, IL12A, NGFR, CSF3, TNF, CXCL5, TNFRSF25, CXCL2, TNFRSF8, PF4, KIT, IL7R, CCL22, TNFRSF1B, IL23A, IL12RB1, CCL20, CCL21, IL10RA, IL2RG, CD27, IL2RB, IL23R, IL5, IL7, FLT3, CCL19, KDR, CCL17, TSLP, CCL14, CXCL13, IL3RA*	1.82131584	2.13E-04	1.77E-05	0.00142939
hsa04664: Fc epsilon RI signaling pathway	1.32387707	1.28E-06	*TNF, BTK, KRAS, RAC2, PIK3CA, PIK3R5, INPP5D, AKT3, AKT2, SYK, PRKCA, PIK3CG, FCER1A, IL5, LYN, PIK3CD, MAP2K4, VAV1, PRKCB, MAPK1, LAT, PLA2G4A, PLCG1, FYN, PLCG2, MAPK8, PLA2G2D, LCP2*	2.67651703	2.36E-04	1.81E-05	0.00158281
hsa05332: Graft-versus-host disease	0.85106383	3.39E-06	*HLA-DQB1, TNF, HLA-DRB1, HLA-DRB3, FASLG, GZMB, HLA-DMB, HLA-E, HLA-DQA2, HLA-DMA, HLA-DQA1, HLA-G, HLA-F, HLA-DPA1, HLA-DOA, HLA-DOB, CD28, HLA-DRA*	3.44123618	6.24E-04	4.46E-05	0.00419502
hsa05320: Autoimmune thyroid disease	0.9929078	3.46E-06	*HLA-DQB1, IL5, HLA-DRB1, HLA-DRB3, CTLA4, FASLG, GZMB, CD40, HLA-DMB, HLA-E, HLA-DQA2, HLA-DMA, HLA-DQA1, HLA-G, HLA-F, CD40LG, HLA-DPA1, HLA-DOA, HLA-DOB, CD28, HLA-DRA*	3.07012248	6.36E-04	4.24E-05	0.00427531
hsa04666: Fc gamma R-mediated phagocytosis	1.37115839	2.73E-05	*MARCKSL1, PIP5K1B, ARPC4, PIP5K1A, DOCK2, RAC2, PIKFYVE, PIK3CA, PIK3R5, INPP5D, AKT3, SYK, AKT2, PRKCA, PIK3CG, PTPRC, LYN, NCF1, HCK, PIK3CD, VAV1, PRKCB, MAPK1, LAT, PLA2G4A, PLCG1, FCGR2B, CFL2, PLCG2*	2.27604569	0.0050155	3.14E-04	0.0337775
hsa05223: Non-small cell lung cancer	0.89834515	1.34E-04	*PRKCA, PIK3CG, FHIT, BRAF, RXRB, PIK3CD, TP53, STK4, PRKCB, MAPK1, RASSF5, KRAS, PLCG1, CASP9, PLCG2, PIK3CA, PIK3R5, AKT3, AKT2*	2.62341153	0.02430181	0.00144613	0.16516041

(*Cont'd*...)

Table 4. (*Continued*)

Term	%	*P*-value	Genes	Fold enrichment	Bonferroni	Benjamini	FDR
hsa04612: Antigen processing and presentation	1.1820331	1.42E-04	*HLA-DQB1, KLRC2, HLA-DRB1, CD8A, CD8B, HLA-DRB3, HLA-DMB, HLA-DMA, RFXAP, CD74, CD4, HLA-DOA, HLA-DOB, LTA, CIITA, RFX5, CREB1, CTSS, HLA-E, HLA-DQA2, HLA-G, HLA-DQA1, HLA-F, HLA-DPA1, HLA-DRA*	2.24578667	0.02573915	0.00144763	0.17504864
hsa04630: Jak-STAT signaling pathway	1.79669031	2.34E-04	*CSF3, STAT5A, STAT5B, IL21R, IL15, IL7R, IL11, STAT4, IL12RB1, IL23A, IL4R, IL10RA, PIK3CA, IL2RG, PIK3R5, AKT3, CSF2RA, GHR, AKT2, PIK3CG, PTPN6, IL2RB, IL23R, IL5, IL7, PIK3CD, CREBBP, IL6R, TSLP, IFNAR2, CBLB, EP300, CCND3, PIAS4, CCND2, IL12A, JAK2, IL3RA*	1.82792546	0.04214707	0.0022638	0.28890247
hsa05416: Viral myocarditis	1.04018913	2.59E-04	*HLA-DQB1, ITGAL, HLA-DRB1, HLA-DRB3, CD40, HLA-DMB, HLA-E, HLA-DQA2, HLA-DMA, HLA-DQA1, HLA-G, HLA-F, RAC2, CASP9, CD40LG, FYN, MYH11, HLA-DPA1, HLA-DOA, HLA-DOB, CD28, HLA-DRA*	2.31031349	0.0465486	0.0023805	0.31975393
hsa04210: Apoptosis	1.1820331	3.12E-04	*PIK3CG, TNF, DFFB, PIK3CD, TP53, FASLG, NFKB1, BIRC3, ATM, IRAK4, TNFRSF10A, PRKAR2B, TNFRSF10B, CASP9, RIPK1, IKBKG, PRKAR1A, PPP3CB, PIK3CA, EXOG, PIK3R5, MAP3K14, IL3RA, AKT3, AKT2*	2.14253211	0.05587998	0.00273444	0.3856018
hsa04070: Phosphatidylinositol signaling system	1.04018913	4.84E-04	*PRKCA, PIK3CG, PIK3C2G, PIK3C2B, PIK3CD, PIP5K1B, ITPKB, PIP5K1A, ITPR1, PRKCB, DGKA, DGKB, PLCG1, PIKFYVE, PLCG2, PIK3CA, PIK3R5, INPP4B, INPP5D, INPP4A, PIP4K2A, PLCB2*	2.21665214	0.08514472	0.0040368	0.59612239
hsa05221: Acute myeloid leukemia	0.85106383	0.00110129	*PIK3CG, TCF7, BRAF, FLT3, STAT5A, STAT5B, PIK3CD, LEF1, NFKB1, PIM2, KIT, MAPK1, KRAS, IKBKG, PIK3CA, PIK3R5, AKT3, AKT2*	2.31393467	0.18351616	0.0087764	1.35299791
hsa04270: Vascular smooth muscle contraction	1.32387707	0.0013631	*GNA13, ADCY4, ADCY1, ADCY7, ADORA2A, PPP1R12B, MRVI1, PLCB2, PRKCA, RAMP3, RAMP2, ARHGEF1, ROCK1, BRAF, PRKCH, NPR1, NPR2, ITPR1, PRKCB, SPDYA, MAPK1, PRKCQ, PLA2G4A, AVPR1A, MYH11, GUCY1B3, CACNA1F, PLA2G2D*	1.86400293	0.22196387	0.01040311	1.67217376
hsa04670: Leukocyte transendothelial migration	1.37115839	0.00144942	*ITGAL, SIPA1, CLDN5, MMP2, CXCL12, VCAM1, RAC2, CXCR4, PIK3CA, ESAM, PIK3R5, RHOH, PRKCA, PIK3CG, ITK, ROCK1, NCF1, NCF4, PIK3CD, ITGA4, VAV1, PRKCB, RASSF5, CYBB, PLCG1, PLCG2, RAP1A, TXK, JAM2*	1.83240966	0.23424074	0.01061872	1.77719479

(*Cont'd...*)

Table 4. (*Continued*)

Term	%	*P*-value	Genes	Fold enrichment	Bonferroni	Benjamini	FDR
hsa04370: VEGF signaling pathway	0.9929078	0.00153595	*PRKCA, PIK3CG, PIK3CD, SRC, KDR, PRKCB, MAPK1, PLA2G4A, KRAS, PLCG1, RAC2, CASP9, PLCG2, PPP3CB, PIK3CA, PIK3R5, PLA2G2D, NFATC3, AKT3, NFATC1, AKT2*	2.08768328	0.24635315	0.01081918	1.8823596
hsa05215: Prostate cancer	1.08747045	0.00263771	*PIK3CG, FGFR1, TCF7, BRAF, CREB1, CREBBP, PIK3CD, TP53, LEF1, FOXO1, NFKB1, CCNE2, MAPK1, KRAS, CDKN1B, EP300, CASP9, IKBKG, PIK3CA, PIK3R5, PDGFD, AKT3, AKT2*	1.92683449	0.38490568	0.01783823	3.21249119
hsa05220: Chronic myeloid leukemia	0.94562648	0.00375763	*PIK3CG, BCR, BRAF, STAT5A, STAT5B, PIK3CD, TP53, SMAD4, NFKB1, MECOM, MAPK1, ACVR1B, CBLB, KRAS, CDKN1B, IKBKG, PIK3CA, PIK3R5, AKT3, AKT2*	1.98826979	0.49977907	0.02443597	4.54753719
hsa05200: Pathways in cancer	2.88416076	0.00575604	*FGF5, STAT5A, ARNT2, STAT5B, FOXO1, FASLG, NFKB1, NFKB2, MMP2, FLT3LG, CCNE2, ACVR1B, CASP9, PIK3CA, AKT3, CSF2RA, AKT2, PRKCA, PIK3CG, BCR, BRAF, RXRB, PIK3CD, TP53, LEF1, MECOM, STK4, PRKCB, MAPK1, EP300, PIAS4, NCOA4, MAPK8, TRAF1, FGFR1, WNT16, KIT, KRAS, RAC2, PIK3R5, AXIN2, TRAF5, COL4A4, FZD8, TCF7, EPAS1, VHL, FLT3, CREBBP, SMAD4, APPL1, BIRC3, FZD4, RASSF5, CBLB, CDKN1B, PLCG1, ETS1, IKBKG, PLCG2, PTCH2*	1.38663633	0.65429531	0.03596393	6.88786138
hsa04722: Neurotrophin signaling pathway	1.32387707	0.00627781	*NFKBIE, FASLG, NFKB1, IRAK4, KRAS, MAP3K3, SH2B3, PIK3CA, PIK3R5, SH2B2, CSK, AKT3, ARHGDIB, AKT2, PIK3CG, BRAF, PIK3CD, TP53, RPS6KA5, MAPK1, RPS6KA3, CAMK4, PLCG1, RPS6KA2, PLCG2, RAP1A, MAPK8, NGFR*	1.68361555	0.68612434	0.03788883	7.49016567
hsa05210: Colorectal cancer	0.9929078	0.00636178	*PIK3CG, FZD8, TCF7, BRAF, PIK3CD, TP53, SMAD4, LEF1, APPL1, FZD4, MAPK1, ACVR1B, KRAS, RAC2, CASP9, PIK3CA, PIK3R5, MAPK8, AXIN2, AKT3, AKT2*	1.86400293	0.69096704	0.03717238	7.58676142
hsa00562: Inositol phosphate metabolism	0.70921986	0.00976227	*PIK3CG, PIK3C2G, PIK3C2B, PIK3CD, PIP5K1B, ITPKB, PIP5K1A, PLCG1, PIKFYVE, PLCG2, PIK3CA, INPP4B, INPP4A, PIP4K2A, PLCB2*	2.07111437	0.83553906	0.05484734	11.4214764

(*Cont'd...*)

Table 4. (*Continued*)

Term	%	*P*-value	Genes	Fold enrichment	Bonferroni	Benjamini	FDR
hsa05212: Pancreatic cancer	0.85106383	0.01240542	*PIK3CG, BRAF, ARHGEF6, PIK3CD, TP53, SMAD4, NFKB1, MAPK1, ACVR1B, KRAS, RAC2, CASP9, IKBKG, PIK3CA, PIK3R5, MAPK8, AKT3, AKT2*	1.86400293	0.89942723	0.06723523	14.3005254
hsa04920: Adipocytokine signaling pathway	0.80378251	0.0134903	*CPT1C, TNF, RXRB, NFKBIE, CHKB, NFKB1, PRKCQ, TNFRSF1B, SLC2A4, IKBKG, MAPK8, PRKAA1, JAK2, AKT3, ACSL6, ACSL5, AKT2*	1.89182387	0.91784186	0.07086684	15.457126
hsa04720: Long-term potentiation	0.80378251	0.01552483	*PRKCA, ADCY1, BRAF, CREBBP, ITPR1, PRKCB, SPDYA, MAPK1, RPS6KA3, EP300, KRAS, CAMK4, GRIN2B, RPS6KA2, PPP3CB, RAP1A, PLCB2*	1.86400293	0.94380761	0.07896423	17.5875715
hsa05213: Endometrial cancer	0.66193853	0.01702413	*PIK3CG, MAPK1, TCF7, KRAS, CASP9, BRAF, PIK3CD, TP53, LEF1, PIK3CA, PIK3R5, AXIN2, AKT3, AKT2*	2.00738777	0.95754923	0.08402059	19.1258565
hsa04012: ErbB signaling pathway	0.94562648	0.01939838	*PRKCA, PIK3CG, BRAF, STAT5A, MAP2K4, STAT5B, PIK3CD, SRC, PRKCB, MAPK1, CBLB, KRAS, CDKN1B, PLCG1, PLCG2, PIK3CA, PIK3R5, MAPK8, AKT3, AKT2*	1.71402569	0.97279559	0.09282107	21.5079322
hsa04010: MAPK signaling pathway	2.26950355	0.02668452	*FGFR1, FGF5, TNF, MAP4K2, FASLG, MAP4K1, NFKB1, NFKB2, MAP3K7, ACVR1B, KRAS, MAP3K3, RAC2, RASGRP3, RASGRP1, MAP3K8, RASGRP2, PPP3CB, AKT3, RASA2, AKT2, PTPN7, PRKCA, BRAF, NF1, MAP2K4, CACNA1I, TP53, ECSIT, MECOM, CACNA2D3, STK4, PRKCB, RPS6KA5, MAPK1, PLA2G4A, RPS6KA3, DUSP2, RPS6KA2, IKBKG, CACNA1H, RAP1A, MAPK8, CACNA1F, MAP3K14, PLA2G2D, CACNA1A, MAP3K12*	1.3404066	0.99310287	0.12275106	28.4213699
hsa05222: Small cell lung cancer	0.89834515	0.02694822	*TRAF1, COL4A4, PIK3CG, FHIT, RXRB, PIK3CD, TP53, NFKB1, BIRC3, CCNE2, CDKN1B, PIAS4, CASP9, IKBKG, PIK3CA, PIK3R5, TRAF5, AKT3, AKT2*	1.68647884	0.99343832	0.12092479	28.6607497
hsa04960: Aldosterone-regulated sodium reabsorption	0.52009456	0.0400502	*PRKCA, PIK3CG, MAPK1, KRAS, PIK3CD, NR3C2, PIK3CA, PIK3R5, ATP1A2, SLC9A3R2, PRKCB*	2.00039339	0.99945834	0.17140329	39.6685018
hsa00604: Glycosphingolipid biosynthesis	0.28368794	0.04024494	*ST3GAL1, ST6GALNAC4, ST3GAL5, B3GALT4, ST8SIA5, ST8SIA1*	2.98240469	0.99947819	0.1683523	39.8196398

(*Cont'd...*)

Table 4. (*Continued*)

Term	%	*P*-value	Genes	Fold enrichment	Bonferroni	Benjamini	FDR
hsa05211: Renal cell carcinoma	0.75650118	0.04116203	*PIK3CG, EPAS1, BRAF, VHL, ARNT2, CREBBP, PIK3CD, MAPK1, EP300, KRAS, ETS1, PIK3CA, RAP1A, PIK3R5, AKT3, AKT2*	1.70423125	0.99956236	0.1681851	40.5267068
hsa04620: Toll-like receptor signaling pathway	0.9929078	0.04416942	*PIK3CG, TNF, MAP2K4, PIK3CD, NFKB1, CD40, TLR9, IRAK4, MAP3K7, MAPK1, IFNAR2, RIPK1, MAP3K8, IKBKG, IL12A, PIK3CA, PIK3R5, IRF3, MAPK8, AKT3, AKT2*	1.55025986	0.99975448	0.17576966	42.7921596
hsa04914: Progesterone-mediated oocyte maturation	0.85106383	0.06113686	*ANAPC1, PIK3CG, ADCY4, ADCY1, BRAF, ADCY7, PIK3CD, CDC26, SPDYA, MAPK1, RPS6KA3, KRAS, RPS6KA2, PIK3CA, PIK3R5, MAPK8, AKT3, AKT2*	1.56056059	0.9999909	0.23188233	54.1551262
hsa04020: Calcium signaling pathway	1.51300236	0.06304285	*ADCY4, ADCY1, ADCY7, CYSLTR1, ADORA2A, TACR1, ITPKB, ATP2B1, ADRB3, EDNRB, ATP2B3, PPP3CB, PLCB2, PRKCA, PHKG1, CACNA1I, NTSR1, PTGFR, ITPR1, PRKCB, P2RX5, P2RX4, CAMK4, PLCG1, ATP2A3, CHRM1, PLCG2, AVPR1A, CACNA1H, CACNA1F, HTR2C, CACNA1A*	1.3556385	0.99999374	0.23375948	55.2925417
hsa05120: Epithelial cell signaling in Helicobacter pylori infection	0.70921986	0.06349031	*LYN, MAP2K4, CXCR2, ATP6V1G2, NFKB1, SRC, ATP6V1A, NOD1, PLCG1, PLCG2, IKBKG, MAPK8, MAP3K14, CSK, JAM2*	1.64470847	0.99999427	0.2307826	55.5557812
hsa05322: Systemic lupus erythematosus	0.94562648	0.06406557	*HLA-DQB1, C7, TNF, HLA-DRB1, HLA-DRB3, C6, CD40, HLA-DMB, HLA-DQA2, HLA-DMA, HLA-DQA1, FCGR2B, GRIN2B, CD40LG, HIST1H4F, HLA-DPA1, HLA-DOA, HLA-DOB, CD28, HLA-DRA*	1.506265	0.99999488	0.22833484	55.8921103
hsa05214: Glioma	0.66193853	0.07095087	*PRKCA, PIK3CG, BRAF, PIK3CD, TP53, PRKCB, MAPK1, KRAS, PLCG1, PLCG2, PIK3CA, PIK3R5, AKT3, AKT2*	1.6568915	0.99999868	0.24580854	59.7401318
hsa04150: mTOR signaling pathway	0.56737589	0.07964231	*PIK3CG, MAPK1, RPS6KA3, BRAF, RPS6KA2, PIK3CD, PIK3CA, PIK3R5, PRKAA1, RPTOR, AKT3, AKT2*	1.72061809	0.99999977	0.26775988	64.1567476
hsa05216: Thyroid cancer	0.37825059	0.08317434	*MAPK1, TCF7, KRAS, BRAF, NCOA4, RXRB, TP53, LEF1*	2.05683082	0.99999988	0.27353403	65.8206999

Note: $P<0.05$ was considered statistically significant.
Abbreviations: FDR: False discovery rate; MAPK: mitogen-activated protein kinase; mTOR: mammalian target of rapamycin; VEGF: Vascular endothelial growth factor.

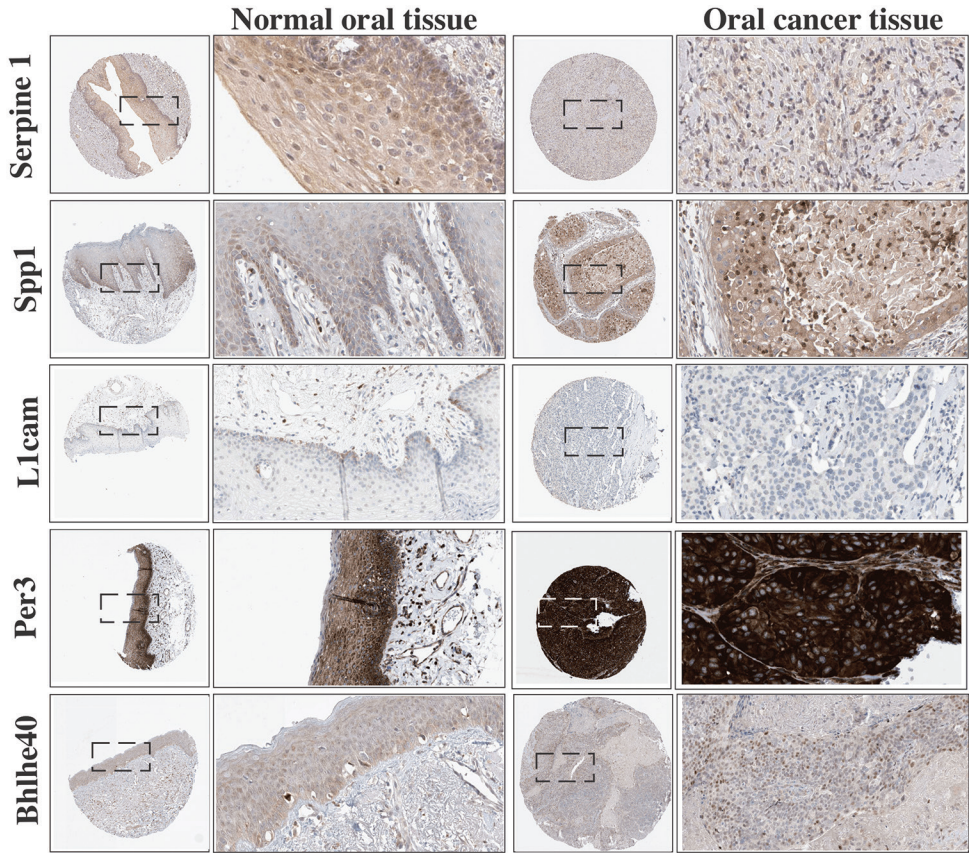

Figure 1. Representative immunohistochemical staining characteristics of *SERPINE1*, *SPP1*, *L1CAM*, *PER3,* and *BHLHE40* expressions in normal and oral cancer patients. Data were extracted from The Human Protein Atlas (https://www.proteinatlas.org/)

genome-wide biological data with molecular networks is essential for elucidating the complex mechanisms and molecular signatures linked to various disease subtypes. Several studies have identified biomarkers associated with cancer invasion, migration, and metastasis in oral cancer.[1,11,23,24] However, only a few have performed meta-analyses that encompass transcriptomic data from normal, cancerous, and lymph node samples. Our previous study demonstrated overexpression of organ-specific metastasis-associated proteins in non-metastatic lymph nodes.[8] These proteins can modify the microenvironment, attracting tumor cells and facilitating their establishment within a pre-metastatic niche.[1,4]

The purpose of our study was to identify the molecular mechanisms governing the pre-metastatic niche in OSCC. Employing a variety of analytical methods, we identified DEGs in healthy oral tissues and OSCC, non-metastatic and metastatic primary tumors, and normal and metastatic lymph nodes. Our results indicate that the upregulated genes in primary tumor samples were closely associated with cancer pathways. Validation through TCGA data confirmed these findings, demonstrating a consistent pattern in DEGs and revealing their association with 473 pre-metastatic-related genes. DAVID functional analysis of the combined pre-metastatic-related gene list and DEGs showed the activation of multiple pathways involved in cancer development. A particularly striking observation from our lymph node analysis was the inactivation of immune response pathways in metastatic lymph nodes, coupled with the upregulation of genes linked to cancer pathways and circadian rhythm. The upregulation of genes associated with Schwann cell dedifferentiation in metastatic and perineural invasion-positive tumors underscores the multifaceted nature of OSCC metastasis.

The molecular mechanisms related to the circadian rhythm in metastatic progression have been documented in tumor samples.[25-27] A previous study demonstrated that the expression patterns of circadian rhythm genes, such as *PER2* or *BMAL1*, are correlated with lymph node metastasis in breast cancer.[26] These genes are involved in melatonin production, a key regulator of circadian rhythm.[28,29]

Melatonin, an antioxidant released in response to light, plays a significant role in sleep regulation.[30,31]

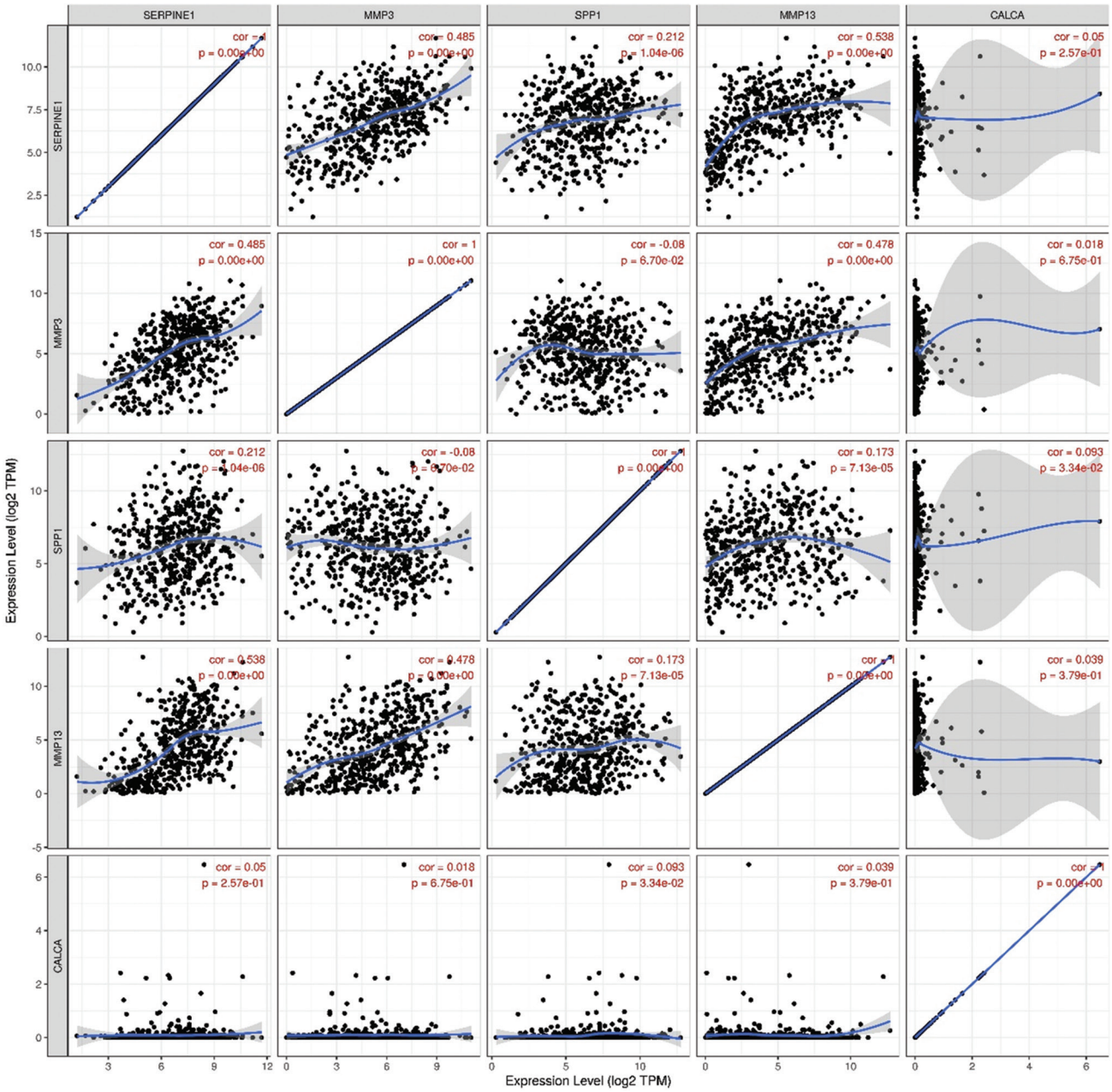

Figure 2. Correlation between *CALCA*, *SERPINE1*, *MMP13*, and *SPP1* in oral squamous cell carcinoma (The Cancer Genome Atlas). Data were extracted from the TIMER web server. $P < 0.05$ was considered statistically significant
Abbreviations: cor: Correlation; TPM: Transcripts per million.

Notably, previous studies have demonstrated that, although breast cancer patients have lower serum melatonin levels than healthy individuals, higher melatonin levels are associated with metastasis development in the distal organ.[32] Wang *et al.*[33] analyzed tissue specimens of patients with colorectal cancer and showed that overexpression of the circadian locomotor output cycles kaput (*CLOCK*) gene was associated with metastatic development in lymph nodes. Silencing the *CLOCK* gene in an animal model resulted in diminished metastatic capacity. *In vitro* analyses further demonstrated that elevated expression of the human *CLOCK* gene in colorectal cancer cell lines induced epithelial-mesenchymal transition and activated angiogenic genes.[33] On the other hand, downregulation of *PER1* has been observed in primary tumor samples from patients with OSCC.[34] In this study, we identified dysregulation of circadian rhythm genes in metastatic

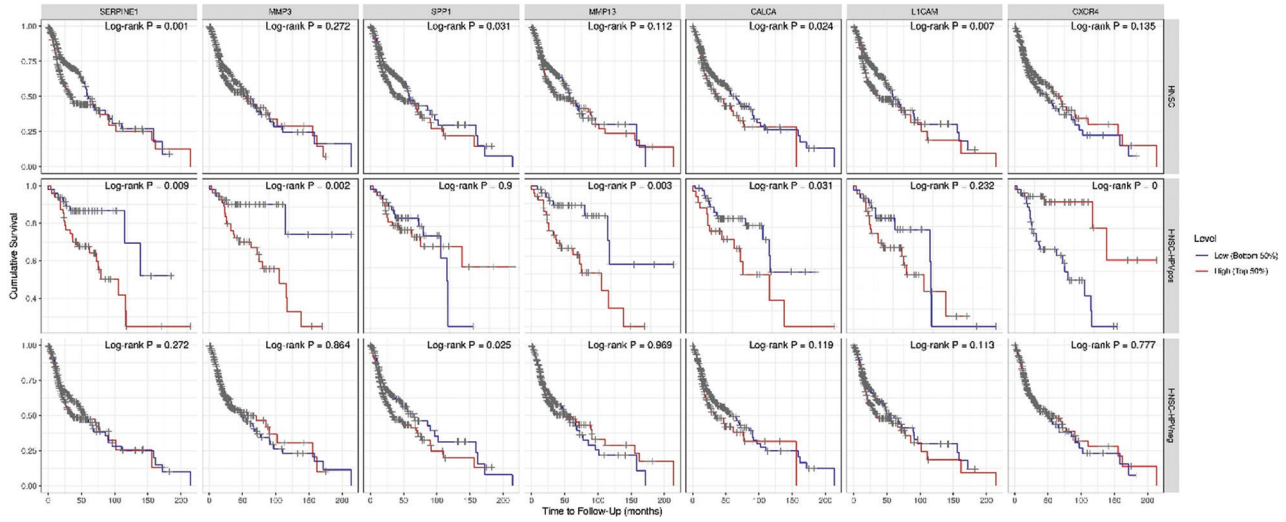

Figure 3. Kaplan–Meier analysis of *SERPINE1*, *SPP1*, *L1CAM*, *CXCR4*, and *CALCA* in oral squamous cell carcinoma (The Cancer Genome Atlas). Data were extracted from the TIMER web server. $P < 0.05$ was considered statistically significant
Abbreviations: HNSC: Head and neck cancer; HNSC-HPVneg: Head and neck cancer-human papillomavirus negative; HNSC-HPVpos: Head and neck cancer-human papillomavirus positive.

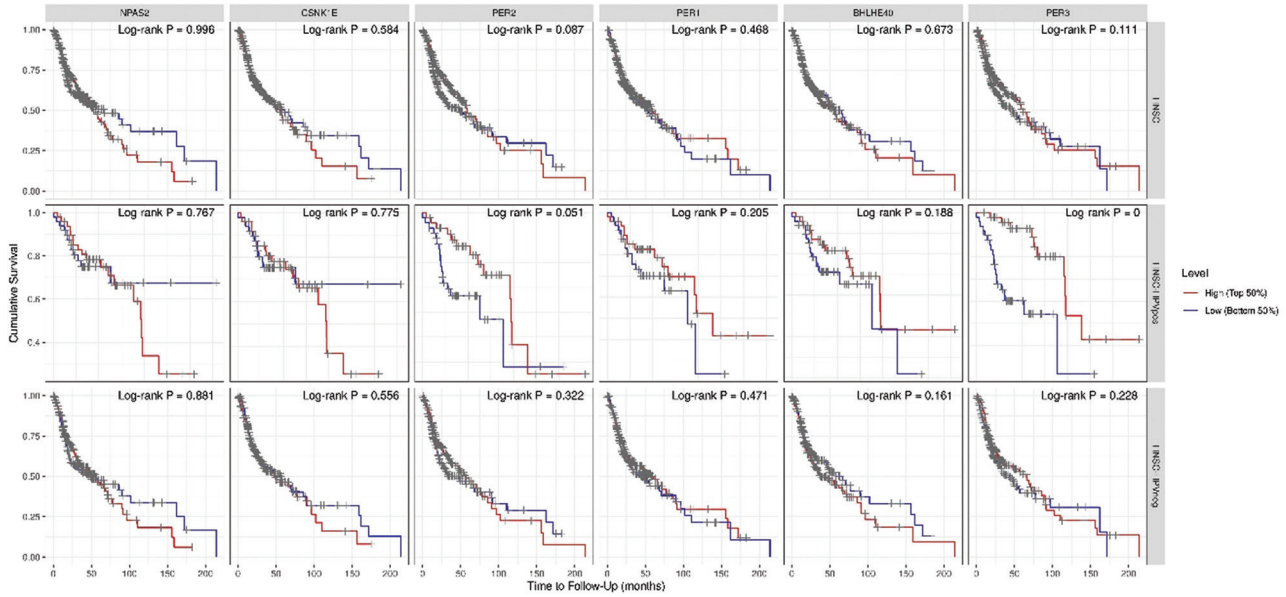

Figure 4. Kaplan–Meier analysis of *NPAS2*, *CSNK1E*, *PER2*, *PER1*, *BHLHE40*, and *PER3* in oral squamous cell carcinoma (The Cancer Genome Atlas). Data were extracted from the TIMER web server. $P < 0.05$ was considered statistically significant
Abbreviations: HNSC: Head and neck cancer; HNSC-HPVneg: Head and neck cancer-human papillomavirus positive; HNSC-HPVpos: Head and neck cancer-human papillomavirus positive.

lymph nodes. To the best of our knowledge, our study is the first to evaluate lymph node samples and the pre-metastatic niche, revealing the upregulation of circadian genes. The observed dysregulation of these genes in metastatic lymph nodes prompts further investigation of the molecular mechanisms by which altered circadian genes may contribute to metastatic spread.

We postulate that the dysregulation of circadian rhythm genes in metastasis is linked to immune response and axon guidance pathways, as these pathways were impaired in metastatic lymph nodes and negatively associated with immune-related genes in our analysis. The immune system typically functions to eliminate tumor cells; however, the tumor microenvironment can modulate immune responses

in ways that promote tumor growth. Natural killer cells, for example, can be influenced by circadian rhythm, as the downregulation of circadian genes has been shown to affect the secretion of key cytotoxic proteins such as granzymes and perforins.[35] In addition, sleep disturbances can elevate plasma levels of inflammatory cytokines, which are crucial in immune cell communication.[34,36,37] Both innate and adaptive immune cells, such as macrophages, dendritic cells, and B cells, exhibit circadian clock gene expression patterns, indicating that immune function may be closely tied to circadian rhythm.38 Leukocyte subsets also appear to adhere to a circadian pattern, demonstrating time-of-day-dependent migration to different organs.[38,39]

Axon guidance signaling is also associated with circadian rhythm, although this relationship has yet to be thoroughly explored in cancer contexts. The axon-guidance roundabout gene has been shown to alter the pace of the Drosophila circadian clock.[29,30] In primary tumor samples, genes such as *SERPENE1, L1CAM, CXCR4*, and *SPP1* facilitate cell-matrix interactions that promote tumor progression. These genes – *SERPENE1, CXCR4, L1CAM,* and *SPP1* – are multifunctional cytokines that regulate cell proliferation, survival, drug resistance, invasion, and stem-like behavior.[23,40] Our findings indicate that these genes are downregulated in metastatic lymph node samples and are associated with poor prognosis. On the other hand, *CXCR4* overexpression was associated with improved OSCC prognosis. The *CXCL12/CXCR4* pathway was implicated in the metastatic niche, as *CXCL12* can attract *CXC4+* tumor cells. This signaling axis is also involved in the mobilization of hematopoietic stem cells and the establishment of a pre-metastatic niche for cancer cells.36 Furthermore, *CXCL12/CXCR4* signaling has been shown to contribute to tumor cell proliferation and angiogenesis.

5. Conclusion

In summary, our findings suggest that during lymph node invasion, axonal guidance genes, such as *SERPENE1, L1AM, CXCR4,* and *SPP1,* are upregulated in OSCC. In addition, as neoplastic cells establish themselves, circadian rhythm genes are upregulated, contributing to immune response inhibition and promoting tumor growth. Notably, axonal guidance genes are downregulated in response to the tumor microenvironment. These insights warrant further investigation, which should include analyses of the lymph node and peripheral nerve microenvironments throughout the progression of metastasis. Such studies could provide valuable insights into the interplay between these factors, thereby enhancing our understanding of OSCC progression and informing more effective treatment strategies.

Acknowledgments

None.

Funding

This study was financed in part by the Coordenação de Aperfeiçoamento de Pessoal de Nível Superior – Brasil (CAPES) – Finance Code 001.

Conflict of interest

The authors declare they have no competing interests.

Author contributions

Conceptualization: All authors
Formal analysis: All authors
Investigation: All authors
Methodology: All authors
Writing – original draft: All authors
Writing – review & editing: All authors

Ethics approval and consent to participate

Not applicable.

Consent for publication

Not applicable.

Availability of data

The data supporting this meta-analysis were derived from GEO DataSets (https://www.ncbi.nlm.nih.gov/gds). The processed data are available upon request from the corresponding author.

Further disclosure

The version of this article is deposited in the repository of the Federal University of Alagoas (https://ud10.arapiraca.ufal.br/repositorio/publicacoes/3541).

References

1. Pastushenko I, Brisebarre A, Sifrim A, *et al*. Identification of the tumour transition states occurring during EMT. *Nature*. 2018;556(7702):463-468.

   doi: 10.1038/s41586-018-0040-3

2. Paget S. The distribution of secondary growths in cancer of the breast. 1889. *Cancer Metastasis Rev*. 1989;8:98-101.

3. Marchesi F, Piemonti L, Mantovani A, Allavena P. Molecular mechanisms of perineural invasion, a forgotten pathway of dissemination and metastasis. *Cytokine Growth Factor Rev*. 2010;21(1):77-82.

   doi: 10.1016/j.cytogfr.2009.11.001

4. Kaplan RN, Riba RD, Zacharoulis S, *et al*. VEGFR1-positive

haematopoietic bone marrow progenitors initiate the pre-metastatic niche. *Nature*. 2005;438(7069):820-827.

doi: 10.1038/nature04186

5. De Paula AM, Souza LR, Farias LC, *et al*. Analysis of 724 cases of primary head and neck squamous cell carcinoma (HNSCC) with a focus on young patients and p53 immunolocalization. *Oral Oncol*. 2009;45(9):777-782.

doi: 10.1016/j.oraloncology.2008.11.015

6. Fraga CA, Sousa A, Correa G, *et al*. High hypoxia-inducible factor-1a expression genotype associated with Eastern Cooperative Oncology Group performance in head and neck squamous cell carcinoma. *Head Neck Oncol*. 2012;4:77.

7. Silva VM, Gomes JA, Tenório LP, *et al*. Schwann cell reprogramming and lung cancer progression: A meta-analysis of transcriptome data. *Oncotarget*. 2019;10(68):7288.

doi: 10.18632/oncotarget.27204

8. Fraga CA, de Oliveira MV, de Oliveira ÉS, *et al*. A high HIF-1α expression genotype is associated with poor prognosis of upper aerodigestive tract carcinoma patients. *Oral Oncol*. 2012;48(2):130-135.

doi: 10.1016/j.oraloncology.2011.08.023

9. Deborde S, Wong RJ. How Schwann cells facilitate cancer progression in nerves. *Cell Mol Life Sci*. 2017;74(24): 4405-4420.

doi: 10.1007/s00018-017-2578-x

10. Deborde S, Omelchenko T, Lyubchik A, *et al*. Schwann cells induce cancer cell dispersion and invasion. *J Clin Invest*. 2016;126(4):1538-1554.

doi: 10.1172/JCI82658

11. Binmadi NO, Basile JR. Perineural invasion in oral squamous cell carcinoma: A discussion of significance and review of the literature. *Oral Oncol*. 2011;47(11):1005-1010.

doi: 10.1016/j.oraloncology.2011.08.002

12. Fagan JJ, Collins B, Barnes L, D'Amico F, Myers EN, Johnson JT. Perineural invasion in squamous cell carcinoma of the head and neck. *Arch Otolaryngol Head Neck Surg*. 1998;124(6):637-640.

doi: 10.1001/archotol.124.6.637

13. D'Souza G, Kreimer AR, Viscidi R, *et al*. Case-control study of human papillomavirus and oropharyngeal cancer. *N Engl J Med*. 2007;356(19):1944-1956.

doi: 10.1056/NEJMoa065497

14. Dillekås H, Rogers MS, Straume O. Are 90% of deaths from cancer caused by metastases? *Cancer Med*. 2019;8(12): 5574-5576.

doi: 10.1002/cam4.2474

15. Mascolo M, Siano M, Ilardi G, *et al*. Epigenetic disregulation in oral cancer. *Int J Mol Sci*. 2012;13(2):2331-2353.

doi: 10.3390/ijms13022331

16. Guimarães TA, Farias LC, Santos ES, *et al*. Metformin increases PDH and suppresses HIF-1α under hypoxic conditions and induces cell death in oral squamous cell carcinoma. *Oncotarget*. 2016;7:55057.

doi: 10.18632/oncotarget.10842

17. Guimaraes TA, Farias LC, Fraga CA, *et al*. Evaluation of the antineoplastic activity of gallic acid in oral squamous cell carcinoma under hypoxic conditions. *Anticancer Drugs*. 2016;27(5):407.

doi: 10.1097/CAD.0000000000000342

18. Alves L, Fraga CA, Oliveira MV, *et al*. High HIF-1α expression genotypes increase odds ratio of oral cancer. *Head Neck Oncol*. 2012;4:87.

19. Fraga CA, Oliveira MV, Domingos PL, *et al*. Infiltrating CD57+ inflammatory cells in head and neck squamous cell carcinoma: Clinicopathological analysis and prognostic significance. *Appl Immunohistochem Mol Morphol*. 2012;20(3):285.

doi: 10.1097/PAI.0b013e318228357b

20. Bray F, Laversanne M, Sung H, *et al*. Global cancer statistics 2022: GLOBOCAN estimates of incidence and mortality worldwide for 36 cancers in 185 countries. *CA Cancer J Clin* 2024;74(3):229-263.

doi: 10.3322/caac.21834

21. Pereira LX, Alves da Silva LC, de Oliveira Feitosa A, *et al*. Correlation between renin-angiotensin system (RAS) related genes, type 2 diabetes, and cancer: Insights from metanalysis of transcriptomics data. *Mol Cell Endocrinol*. 2019;493:110455.

doi: 10.1016/j.mce.2019.110455

22. Colaprico A, Silva TC, Olsen C, *et al*. TCGAbiolinks: An R/Bioconductor package for integrative analysis of TCGA data. *Nucleic Acids Res*. 2016;44(8):e71.

doi: 10.1093/nar/gkv1507

23. Zhou Y, Shurin GV, Zhong H, Bunimovich YL, HanB, Shurin MR. Schwann cells augment cell spreading and metastasis of lung cancer. *Cancer Res*. 2018;78(20): 5927-5939.

doi: 10.1158/0008-5472.CAN-18-1702

24. Lo HC, Zhang XH. EMT in metastasis: Finding the right balance. *Dev Cell*. 2018;45(6):663-665.

doi: 10.1016/j.devcel.2018.05.033

25. Rana S, Mahmood S. Circadian rhythm and its role in malignancy. *J Circad Rhythms*. 2010;8(1):3.

doi: 10.1186/1740-3391-8-3

26. Kuo SJ, Chen ST, Yeh KT, *et al*. Disturbance of circadian gene expression in breast cancer. *Virchows Arch*. 2009;454(4): 467-474.

doi: 10.1007/s00428-009-0761-7

27. Hua H, Wang Y, Wan C, *et al*. Circadian gene mPer2 overexpression induces cancer cell apoptosis. *Cancer Sci*. 2006;97(7):589-596.

doi: 10.1111/j.1349-7006.2006.00225.x

28. Humans I. Painting, firefighting, and shiftwork. In: *Iarc Monographs on the Evaluation of Carcinogenic Risks to Humans*. Vol. 98. France: IARC; 2010. p. 9-764.

29. Golombek DA, Casiraghi LP, Agostino PV, *et al*. The times they're a-changing: Effects of circadian desynchronization on physiology and disease. *J Physiol Paris.* 2013;107(4): 310-322.

doi: 10.1016/j.jphysparis.2013.03.007

30. Berger J. A two-clock model of circadian timing in the immune system of mammals. *Pathol Biol*. 2008;56(5): 286-291.

doi: 10.1016/j.patbio.2007.10.001

31. Zhu L, Zee PC. Circadian rhythm sleep disorders. *Neurol Clin*. 2012;30(4):1167-1191.

doi: 10.1016/j.ncl.2012.08.011

32. de Castro TB, Bordin-Junior NA, de Almeida EA, de Campos Zuccari DA. Evaluation of melatonin and AFMK levels in women with breast cancer. *Endocrine*. 2018;62(1):242-249.

doi: 10.1007/s12020-018-1624-2

33. Wang Y, Sun N, Lu C, Bei Y, Qian R, Hua L. Upregulation of circadian gene 'hClock' contribution to metastasis of colorectal cancer. *Int J Oncol*. 2017;50(6):2191-2199.

doi: 10.3892/ijo.2017.3987

34. Chen L, Diao L, Yang Y, *et al*. CD38-mediated immunosuppression as a mechanism of tumor cell escape from PD-1/PD-L1 blockade. *Cancer Discov*. 2018;8(9): 1156-1175.

doi: 10.1158/2159-8290.CD-17-1033

35. Cermakian N, Lange T, Golombek D, *et al*. Crosstalk between the circadian clock circuitry and the immune system. *Chronobiol Int*. 2013;30(7):870-888.

doi: 10.3109/07420528.2013.782315

36. Denkert C, Loibl S, Noske A, *et al*. Tumor-associated lymphocytes as an independent predictor of response to neoadjuvant chemotherapy in breast cancer. *J Clin Oncol*. 2010;28(1):105-113.

doi: 10.1200/JCO.2009.23.7370

37. Li Z, Dong P, Ren M, *et al*. PD-L1 Expression is associated with tumor FOXP3+ regulatory T-cell infiltration of breast cancer and poor prognosis of patient. *J Cancer*. 2016;7(7):784-793.

doi: 10.7150/jca.14549

38. Arjona A, Silver AC, Walker WE, Fikrig E. Immunity's fourth dimension: Approaching the circadian-immune connection. *Trends Immunol*. 2012;33(12):607-612.

doi: 10.1016/j.it.2012.08.007

39. Webber CA, Christie KJ, Cheng C, *et al*. Schwann cells direct peripheral nerve regeneration through the Netrin-1 receptors, DCC and Unc5H2. *Glia*. 2011;59(10):1503-1517.

doi: 10.1002/glia.21194

40. Li Z, Zhou J, Zhang J, Li S, Wang H, Du J. Cancer-associated fibroblasts promote PD-L1 expression in mice cancer cells via secreting CXCL5. *Int J Cancer.* 2019;145(7):1946-1957.

doi: 10.1002/ijc.32278

ACCSCIENCE PUBLISHING

Gene & Protein in Disease

ORIGINAL RESEARCH ARTICLE

Application of multiple inflammatory markers combined with PIVKA-II in differential diagnosis of AFP-NHCC

Wen-Tan Hu[1†], Xin-Ying Ji[2,3†], Zhi-Liang Jiang[4,5], Yi Liu[4,6], Huang-Yin Luo[5], De-Xin Zhang[1], Yi-Bin Lu[1], and Ning Luo[1*]

[1]Xinyang Central Hospital, Xinyang, Henan, China

Abstract

Alpha-fetoprotein (AFP) is a proven blood biomarker widely used in clinical detection of liver cancer, and its concentration increases immediately after liver injury, with high diagnostic specificity and low sensitivity. However, in patients with AFP-negative hepatocellular carcinoma (AFP-NHCC), also known as small liver cancer, their early stage of AFP expression is usually low or close to the normal range. Compared with AFP-positive HCC, AFP-NHCC is more likely to be subjected to missed diagnosis due to solely dependence on the measurement of blood AFP. Therefore, it is necessary to find a reliable, effective, and economical detection method for the early diagnosis of AFP-NHCC. PIVKA-II is closely related to the occurrence, development, invasion, and metastasis of liver cancer, and is also a new hematological marker widely used in the diagnosis of liver cancer in recent years. PIVKA-II effectively makes up for the limitation of negative AFP. 63.2% – 76.3% of patients with negative AFP showed positive PIVKA-II, and if only PIVKA-II detection was relied on, there would still be missed diagnosis in early patients with AFP-NHCC. In this retrospective study, we selected several commonly used inflammatory indicators to explore the diagnostic efficacy of PIVKA-II, an abnormal form of prothrombin, combined with inflammatory indicators in patients with early-stage AFP-NHCC and analyzed the relationship between some clinical features and hematological indicators in patients with AFP-NHCC. Serum levels of high-sensitivity C-reactive protein (hs-CRP), prealbumin (PA), neutrophil/lymphocyte ratio (NLR), and PIVKA-II were compared among three groups (AFP-NHCC group, benign lesion group, and healthy subjects). The diagnostic efficacy of PIVKA-II alone for AFP-NHCC and the diagnostic efficacy of three inflammatory indicators combined with PIVKA-II for AFP-NHCC were calculated, and their diagnostic specificity and sensitivity were compared. Compared with the other two groups, the AFP-NHCC group showed significant changes in three inflammatory markers and PIVKA-II, which may be related to the inflammatory progression of the tumor. Therefore, we recommend the establishment of a laboratory-based detection approach for diagnosing early-stage AFP-NHCC by combining PIVKA-II with inflammatory indicators hs-CRP, PA, and NLR, to facilitate diagnosis, treatment, and prognosis of AFP-NHCC.

Keywords: Alpha-fetoprotein-negative hepatocellular carcinoma; Prealbumin; PIVKA-II; High-sensitivity C-reactive protein

[†]These authors contributed equally to this work.

***Corresponding author:**
Ning Luo
(luoning0376@163.com)

Citation: Hu W, Ji X, Jiang Z, *et al*. Application of multiple inflammatory markers combined with PIVKA-II in differential diagnosis of AFP-NHCC. *Gene Protein Dis*. 2024;3(4):4269. doi: 10.36922/gpd.4269

Received: July 17, 2024

Accepted: November 4, 2024

Published Online: November 28, 2024

[2]Center for Molecular Medicine, Faculty of Basic Medical Subjects, Shu-Qing Medical College of Zhengzhou, Erqi District, Zhengzhou, Henan, China

[3]Department of Nuclear Medicine, Henan International Joint Laboratory for Nuclear Protein Regulation, the First Affiliated Hospital, Henan University College of Medicine, Kaifeng, Henan, China

[4]Kaifeng Municipal Key Laboratory for Infection and Biosafety, Henan International Joint Laboratory of Nuclear Protein Regulation, School of Basic Medical Sciences, Henan University College of Medicine, Kaifeng, Henan, China

[5]School of Clinical Medicine, Henan University, Kaifeng, Henan, China

[6]School of Stomatology, Henan University, Kaifeng, Henan, China

1. Introduction

Primary liver cancer is a malignant tumor with high incidence and high mortality. There were 865,269 new cases and 757,948 deaths of liver cancer in the world in 2022, making it the sixth most common cancer and the third leading cause of death from cancer in the world.[1] According to the data released by the International Agency for Research on Cancer of the World Health Organization (WHO), in 2020, there were 900,000 new cases of liver cancer worldwide, of which 46% were documented in China. The global death cases of liver cancer are 820,000, with China accounting for 47% of these cases.[2]

In China, primary liver cancer mainly includes three pathological types: hepatocellular carcinoma (HCC), intrahepatic cholangiocarcinoma, and mixed HCC-cholangiocarcinoma, among which 80% is HCC, which is the most common primary liver cancer, with most of the cases characterized by insipid onset and no specific symptoms in the early stage. Clinical detection of the disease presents substantial challenges since most of them are already in the middle and late stages when diagnosed, in addition to the rapid progression, lower-efficacy treatment, and poor prognosis. According to the WHO, nearly half of all cancers can be prevented; one-third of all cancers can be detected early and diagnosed through cancer screening, standing a higher chance for therapeutic cure.[3] Therefore, early screening of HCC plays a key role in improving the therapeutic efficacy and survival rate of patients.[4]

Alpha-fetoprotein (AFP) is a proven blood biomarker that is widely used in the clinical detection of liver cancer. AFP concentration increases after liver damage, which is characterized by high diagnostic specificity and low sensitivity.[5] However, AFP levels are low in some patients with liver cancer, a condition known as AFP-NHCC, which usually belongs to small liver cancer. Compared with HCC with positive AFP expression, AFP-NHCC presents more diagnosis challenges and is mainly confirmed by means of imaging and pathologic tests.[6] The efficacy of ultrasound screening can be easily affected by the operator's technique and inherent variations in individual subjects. Compared with ultrasound, computed tomography does not significantly improve the early detection rate. Magnetic resonance imaging (MRI) boasts high sensitivity and specificity in the detection of early-stage liver cancer, but it is expensive and time-consuming.[7] Therefore, it is necessary to find a reliable, effective, and economical detection method for the diagnosis of AFP-NHCC in the early stage.

Previous studies showed that patients with liver cancer exhibited changes in a variety of laboratory indicators, such as blood cell counts,[8] coagulation function,[9] and serum enzyme levels.[10] Recent years have seen the emergence of clinical disease diagnosis models integrated with laboratory data, which have obvious advantages including low cost and minimal invasiveness.[11,12] Therefore, the objective of this study was to examine the association between specific clinical characteristics of AFP-NHCC patients and laboratory hematological parameters, such as blood Vitamin K deficiency or antagonist-II inducer protein (PIVKA-II), a novel marker for HCC screening, which can effectively address the limitation of negative AFP. It was observed that 63.2% – 76.3% of patients with negative AFP were positive for PIVKA-II; however, relying solely on PIVKA-II detection could still result in missed diagnoses of early-stage patients with AFP-NHCC.[13]

In recent years, systemic inflammatory response (SIR) has been proven to be an important distinguishing feature of malignant tumors, and more and more studies have been conducted on inflammatory indicators in liver lesions. It is generally believed that chronic inflammation is closely related to the occurrence and development of tumors.[14] High-sensitivity C-reactive protein (hs-CRP), an acute inflammatory protein, is mainly produced by the liver. Interleukin (IL)-1) and IL-6 can stimulate the liver, increase CRP synthesis, and increase its blood level. CRP is involved in multiple aspects of the inflammatory process and is a key molecule linking innate immunity and adaptive immunity. In addition to the increase of CRP in acute infection and chronic infection, studies have reported that CRP is also increased in a variety of cancers, such as myeloma, ovarian cancer, urinary system tumors,

and primary liver cancer, and is significantly correlated with tumor stage, malignancy, and prognosis. In recent years, a growing number of studies have been conducted on inflammatory indicators in liver diseases, among which hs-CRP was commonly used.[15] Neutrophil–lymphocyte ratio (NLR), a simple prognostic indicator of inflammation derived from routine peripheral blood tests, is the focus of research on the inflammatory-related index, defined as the ratio of absolute neutrophils to lymphocytes in peripheral blood.[16] The change of NLR is an objective indicator to judge whether the body is complicated by bacterial infection. Cellular immunity involving lymphocytes is an important defense system to inhibit the occurrence and development of tumors. Immunity involving lymphocytes is an important defense system to inhibit the occurrence and development of tumors. Studies have shown that NLR can better reflect the prognosis of HCC patients, and has significant predictive value for survival and recurrence of HCC patients after liver transplantation.[17] In addition to inflammation, nutritional status is also related to the prognosis of cancer patients. Prealbumin (PA) is not only an inflammatory indicator,[18] but also an indicator of nutritional status assessment.[19] Moreover, some studies have shown that pre-operative albumin is related to the long-term prognosis of HCC patients. There are many clinical studies on the single application of PA, PIVKA-II, and NLR to assist in the diagnosis of primary liver cancer,[20-22] but relatively few studies on the combined application in the differential diagnosis of AFP-NHCC and other diseases.

In this paper, the efficacy of hs-CRP, NLR, and PA combined with PIVKA-II in the diagnosis of AFP-NHCC was analyzed and reported as follows.

2. Materials and methods

2.1. Baseline information

Ninety patients with suspected HCC and negative AFP in Xinyang Central Hospital, Xinyang, Henan, China, were recruited in this study from April 2019 to February 2023, and their diagnosis and treatment data were analyzed. Thirty-two patients diagnosed with AFP-NHCC were included in the AFP-NHCC group, and the remaining patients with non-cancerous liver diseases were included in the benign lesion group (58 cases). At the same time, 45 healthy subjects who underwent physical examination were selected and classified under the healthy control group. The baseline information is shown in Table 1. This study has been reviewed by the Ethics Review Committee (ethics number: 20240966).

2.2. Inclusion criteria

The inclusion criteria of this study are as follows:

(i) Presenting with symptoms such as liver pain, upper abdominal pain, intermittent fever, and fatigue, with weight loss and jaundice
(ii) AFP levels <20 μg/L
(iii) Having normal heart and kidney function, with an acceptable level of liver function
(iv) Obtained informed consent after explaining the research purpose, process, and significance to the patients and their families.

2.3. Exclusion criteria

The exclusion criteria of this study are as follows:

(i) Other pathological types of liver tumors
(ii) Comorbidity with other tumors, metastatic tumors, or recurrent tumors
(iii) Severe systemic infectious diseases
(iv) Incomplete clinical data
(v) Hepatic encephalopathy.

2.4. Methods

Patient data, including imaging reports and laboratory reports, were collected. Peripheral venous blood samples collected were subjected to a series of blood indicator measurements, such as PA using immunotransmission turbidimetry (PA Assay Kit, Mindray, China), hs-CRP by means of rate-scattering turbidimetry, neutrophils, and

Table 1. Comparison of baseline information

Various indicators	AFP- NHCC group (*n*=32)	Benign lesion group (*n*=58)	Healthy control group (*n*=45)	$\chi^2/F/t$	*P*
Age (year)	58.64±4.35	57.88±5.02	57.46±4.75	0.574	0.565
Gender (male/female)	20/12	28/30	25/20	1.740	0.419
History of drinking (yes/no)	23/9	40/18	30/15	0.237	0.888
History of smoking (yes/no)	19/13	30/28	25/20	0.502	0.778
Mass diameter (cm)	1.45±1.00	1.38±1.03	-	0.312	0.756
Normal liver function (yes/no)	14/18	20/38	-	0.821	0.135
Liver cirrhosis (yes/no)	20/12	35/23	-	0.175	0.359

Abbreviation: AFP-NHCC: Alpha-fetoprotein-negative hepatocellular carcinoma.

lymphocytes using blood cell analyzer, and PIVKA-II by means of chemiluminescent particle immunoassay. Afterward, the NLR was calculated.

2.5. Observation index

The laboratory test results of the three groups were compared to analyze the diagnostic efficacy of the inflammatory index combined with PIVKA-II, and PIVKA-II alone, for AFP-NHCC.

2.6. Statistical analysis

All the data were input into Statistical Package for Social Sciences (SPSS) 22.0 software (IBM SPSS Statistics, United States of America) for processing. The whole variance homogeneity test and normal distribution test were performed on continuous data. Normally distributed data that meet homogeneous variance requirements are expressed as mean ± standard deviation. One-way analysis of variance was used for comparison among multiple groups, and the LSD-t test was used for comparison between two groups. The non-normally distributed data are presented as median (M) and interquartile range (P25 and P75), and the comparison was performed using a non-parametric test. The diagnostic efficiency was analyzed using the receiver operating characteristics (ROC) curve. $P < 0.05$ was considered statistically significant.

3. Result

3.1. Comparison of baseline information

The age, gender, and living habits of the three groups of patients were found to be comparable ($P > 0.05$). In addition, there were no significant differences in the size of the tumor, normal liver function, and presence or absence of liver cirrhosis between the AFP-NHCC group and the benign lesion group ($P > 0.05$) (Table 1).

3.2. Comparison of laboratory indexes

The levels of all inflammatory indexes and PIVKA-II were the highest in the AFP-NHCC group, followed by the benign lesion group, with the healthy control group recording the lowest levels; the differences were statistically significant ($P < 0.05$) (Table 2).

3.3. Performance analysis of different diagnostic methods

The diagnostic sensitivity and specificity of PIVKA-II were 84.40% and 73.80% for AFP-NHCC, 56.70% and 68.87% for hs-CRP, and 78.10% and 56.90% for PA, respectively. The sensitivity and specificity of NLR were 75.00% and 47.80%, respectively. The sensitivity and specificity of combined diagnosis were 84.40% and 82.80%, and the area under the curve (AUC) of combined diagnosis was larger (Figures 1 and 2, Table 3).

4. Discussion

AFP is a typical and most widely used tumor marker for all kinds of liver cancers, which is of great significance for disease diagnosis and prognosis monitoring.[23] However, not all HCC patients will show increased AFP levels, and it is worth noting that other types of liver injury (hepatitis, cirrhosis, *etc.*) and even gastric cancer, teratoma, ovarian tumor, and other diseases are accompanied by increased AFP levels; this lack of disease specificity greatly limits the diagnostic value of AFP in HCC. Furthermore, the application of AFP alone cannot meet the actual clinical needs for HCC diagnosis. AFP-NHCC is a clinically special type of HCC, which loses the expression of AFP during the early stage.[24]

The prognosis of HCC depends on the stage of the tumor. In the Barcelona stage of liver cancer, liver cancer is divided into very early stage, early stage, middle stage, late stage, and terminal stage. Patients with early-stage HCC have a 5-year survival rate of more than 70%, whereas symptomatic advanced patients have a median survival of 1.0 – 1.5 years after systemic therapy. In the very early stage, patients usually have no related symptoms and signs, and only a single lesion of ≤2 cm is present at this time, with minimal liver function damage; therefore, early diagnosis

Table 2. Comparison of laboratory indexes

Group	hs-CRP (mg/L)	PA (mg/L)	NLR	PIVKA-\ (mAU/mL)
AFP-NHCC group (n=32)	74.65 (56.36, 129.43)[a,b]	45.71 (26.57, 67.46)[a,b]	3.59±1.58[a,b]	814.27 (654.64, 978.46)[a,b]
Benign lesion group (n=58)	37.26 (28.67, 63.24)[a]	92.01 (55.67, 130.35)[a]	2.82±1.04[a]	424.84 (316.65, 532.54)[a]
Healthy control group (n=45)	0.12 (0.06, 0.18)	241.15 (189.54, 290.67)	1.79±0.81	48.60 (20.04, 78.57)
χ^2	8.567	7.366	5.577	12.245
P	<0.001	0.000	0.001	0.000

Notes: Data are expressed as either M (P25, P75) or mean±SD. [a]P<0.05 compared with the healthy control group; [b]P<0.05 compared with the benign lesion group.
Abbreviations: AFP-NHCC: Alpha-fetoprotein-negative hepatocellular carcinoma; hs-CRP: High-sensitivity C-reactive protein; NLR: Neutrophil–lymphocyte ratio; PA: Prealbumin.

of HCC can provide the opportunity for timely treatment, thereby improving the survival rate of patients. Therefore, the clinical consensus is that very early intervention is the best treatment strategy.[25] However, the diagnosis rate of very early-, early-, and even middle-stage liver cancer is not high in China, and the reasons are as follows[26-28]; the pre-cancerous lesion of HCC, in which a nodule is formed from the proliferation of a single hepatocyte clone has abnormal cytology and histology, but does not meet HCC criteria; HCC is divided into low- and high DNA, there is no clear distinction between atypical hyperplastic nodules DNA and HCC. Although MRI and other high-resolution examination methods can increase the detection probability of small lesions, these techniques are not feasible during the 1st-time screening due to high cost and other inherent problems. The early-stage condition of certain patients lacks specificity and also demonstrates low awareness of the need for active examination. The diagnostic efficacy of AFP cannot meet the actual needs of clinical practice, and there is a greater possibility of false positive and false negative results which ultimately lead to the progress of liver cancer patients in the middle and late stage or terminal stage at the time of diagnosis, which is extremely unfavorable to their treatment and quality of life. With the progress of medical technology and human society, laboratory examination of tumor markers supported by bioinformatics technology has become a global research hotspot on the grounds of their minimal invasiveness and the reproducibility nature of results. The occurrence and development process of most tumors shares very similar characteristics,[29] and more and more studies have been conducted regarding the impact of chronic inflammation on the occurrence and development of tumors. Due to the low effectiveness and prolonged time required in the detection methods employing most inflammatory indexes, many researchers have become more interested in using tumor markers and inflammatory indicators with high specificity, high accuracy, and high sensitivity for tumor screening and diagnosis.

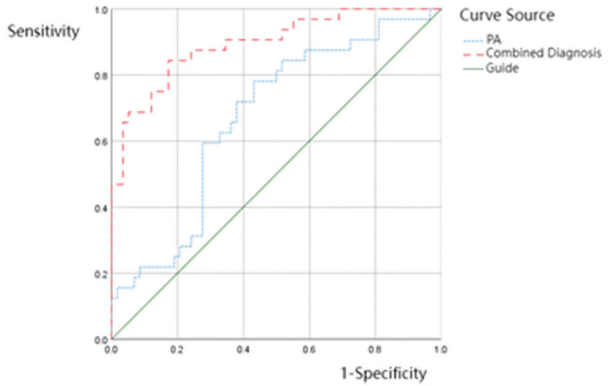

Figure 1. Diagnostic ROC curve of PA, PIVKA-II, and all inflammatory indexes for AFP-NHCC
Abbreviations: AFP-NHCC: Alpha-fetoprotein-negative hepatocellular carcinoma; PA: Prealbumin; ROC: Receiver operating characteristics.

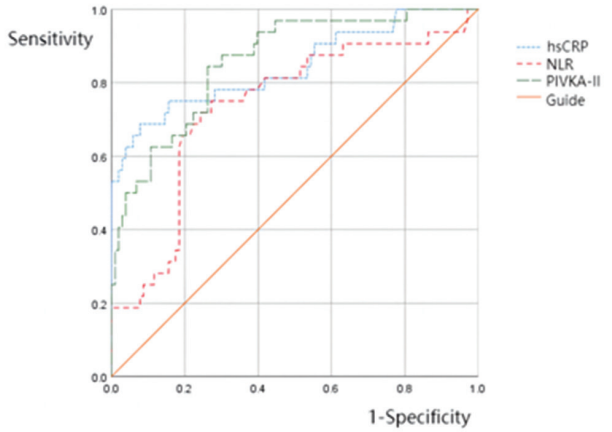

Figure 2. Diagnostic ROC curve of hs-CRP, NLR, and PIVKA-II for AFP-NHCC
Abbreviations: AFP-NHCC: Alpha-fetoprotein-negative hepatocellular carcinoma; hs-CRP: High-sensitivity C-reactive protein; NLR: Neutrophil-lymphocyte ratio; ROC: Receiver operating characteristics.

As can be seen from Table 1, the hs-CRP, PA, NLR, and PIVKA-II of patients in the benign lesion group and the AFP-NHCC group were higher than those in the healthy control group, and the levels of the above indicators in the AFP-NHCC group were also higher than those in the

Table 3: Performance analysis of different diagnostic methods

Diagnostic mode	AUC	Standard error	*P*	95% confidence interval	Sensitivity	Specificity	Youden index	Cut-off value
PIVKA-II	0.858	0.037	<0.001	0.786 – 0.930	84.40	73.80	0.582	602.16
hs-CRP	0.843	0.046	<0.001	0.754 – 0.933	56.78	68.87	0.61	59.06
PA	0.671	0.059	0.007	0.557 – 0.786	78.10	56.90	0.35	53.57
NLR	0.736	0.053	<0.001	0.632 – 0.840	75.00	72.80	0.478	1.36
PIVKA-II + inflammatory indexes	0.895	0.036	<0.001	0.825 – 0.965	84.40	82.80	0.672	-

Abbreviations: AUC: Area under the curve; hs-CRP: High-sensitivity C-reactive protein; NLR: Neutrophil-lymphocyte ratio; PA: Prealbumin.

benign lesion group. This is in line with the conclusion that it is difficult to detect the abnormal substances encoded by oncogenes, tumor suppressor genes, and other tumor-related genes in normal tissues and benign lesions.[30,31] The mechanism of tumorigenesis is complex. The discovery of a large number of white blood cells in tumor tissues in 1863 has driven more people to be acquainted with the idea that the chronic and persistent inflammatory reaction in tumor tissues or their surrounding tissues, resulting in local lymphocyte infiltration, is the root cause of tumorigenesis.[32,33] According to studies, 20% of malignant tumors are mainly caused by inflammation, and its related mechanism is not yet clear.[34] The possible reason is that the contents of active oxides and active nitrides produced by the inflammatory cells increase following the proliferation of a large number of cells. Inhibition of the antioxidant defense system results in excessive oxidative stress, and the overload of active substances can damage the stability of DNA. Eventually, gene deletion and point mutation occur.[35-37]

Although the cause of HCC is unknown, it is generally believed that the occurrence of liver cancer is basically the same as the process of hepatitis, cirrhosis, and cancerization, so HCC is perceived as a tumor originating from inflammation.[38] There have been studies reporting that SIR is closely related to the prognosis of liver cancer. Most HCCs are associated with chronic hepatitis B or C virus infection, and the host produces persistent chronic inflammation. The systemic and local inflammatory responses of the virus or tumor can provide a favorable microenvironment for tumor invasion and metastasis.[39,40] Chronic inflammation is even considered an important prognostic factor for HCC in the early stages of cancer progression. A large number of studies on advanced HCC have also shown that tumor-related inflammatory responses are associated with worse pathological staging and clinical prognosis.[41,42] Simple inflammation-related indices derived from laboratory tests have been found to have predictive value for the prognosis of liver transplantation in HCC patients.[43] Our study of inflammation markers hs-CRP, PA, and NLR, which are elevated in AFP-HCC, confirms this. Under the action of various exogenous and endogenous pathways, signal transduction and transcription activator 3, nuclear transcription factor-KB, and other signaling pathways are activated, resulting in the production of prostaglandins, leukotrienes, nitric oxide, bradykinin, and other inflammatory mediators. Recruitment of neutrophils, lymphocytes, and macrophages not only increases local inflammation but also promotes neovascularization and inhibits the immune response to tumor tissues.[44] In addition, neutrophils can release specific chemokines to accelerate the proliferation rate and colonization ability of tumor cells and assist tumor cells in immune escape.[45] In addition, tumor cells can upregulate the levels of CXCL12 and other substances in bone marrow stromal cells, and promote the increase of neutrophil levels. After the occurrence of the tumor, the expression levels of serum IL-6, IL-2, tumor necrosis factor, and other factor receptors are increased under normal circumstances, and the number of lymphocytes is correspondingly decreased, thereby inhibiting tumor proliferation and migration.[46]

The increase of neutrophil count and/or the decrease of lymphocyte number can lead to the increase of NLR, and the change of NLR can indicate the severity of inflammation and the strength of immunity and indirectly reflect the balance between the tumor-promoting environment and anti-tumor state of the body. Studies[47,48] have shown that: (i) the vast majority of tumor patients undergoing chemotherapy or surgical resection would not undergo NLR progression for a long period of time; (ii) the rapid increase of NLR indicates the potential occurrence of tumor growth or metastasis; (iii) NLR reflects an immune microenvironment that is conducive to tumor vascular invasion and inhibitory to host immune surveillance. A high NLR is associated with a poor prognosis after transplantation. hs-CRP is widely used in clinical inflammation assessment.[47] Synthesized in the liver, hs-CRP is significantly increased in level after inflammation. Another study also found that CRP levels were significantly elevated in HCC patients with negative AFP and low AFP levels (<100 μg/mL).[48] The ROC curve of this paper shows that hs-CRP alone in the diagnosis of AFP-NHCC has low sensitivity and specificity, which is unsuitable for clinical application. PA is also synthesized in the liver, and its half-life is relatively short. The application value of PA is discounted in the events of inflammation, trauma, malnutrition, or liver disease. Some literature pointed out that PA can predict the overall survival and relapse-free survival of liver cancer patients,[49] and some scholars[50,51] confirmed that PA is significantly correlated with $CD8^+$, $CD4^+$, and natural killer cells. It can predict the immune status of patients with primary liver cancer well. In this study, the diagnostic sensitivity of PA was acceptable, but the specificity was very low.

PIVKA-II, also known as abnormal prothrombin and des-γ-carboxy-prothrombin, is a liver-synthesized protein that is induced during Vitamin K deficiency, is caused by the incomplete carboxylation of the N-terminal of the chemical chain of prothrombin due to Vitamin K deficiency, resulting in the loss of the ability of prothrombin to combine with other factors. In HCC patients, Vitamin K

is deficient, and PIVKA-II is produced in large quantities due to cancer damage to hepatocytes. In recent years, the Japanese Society of Hepatology, the Asia-Pacific Society of Hepatology, the Chinese Medical Association, and other organizations have recommended PIVKA-II as an early diagnostic indicator for HCC, and the China's Chronic Hepatitis B Prevention and Treatment Guide (2019 edition) has identified PIVKA-II as an indicator for screening and diagnosis of HCC in high-risk groups. In foreign studies,[52] PIVKA-II was superior to AFP in the screening and diagnosis of early HCC, and significantly superior to AFP in terms of sensitivity and specificity in disease monitoring and prognosis assessment. Tumor staging determines the prognosis of all types of HCC. The 5-year post-operative survival rate of HCC patients diagnosed and treated early was found to exceed 70%, indicating that an earlier diagnosis could extend the median survival time of patients.[53] In Table 2 and Figure 1, although the AUC of PIVKA-II for AFP-NHCC is smaller than that of combined detection, it is still larger than 0.5 with a sensitivity as high as 84.40%, but with a lower specificity at only 73.80%. On the one hand, this index has a certain value for the diagnosis of AFP-NHCC; on the other hand, compared with combined detection, the AUC area of PIVKA-II for AFP-NHCC is higher than that of PIVKA-II for AFP-NHCC. In Table 3, we can see that the AUC of the three inflammatory indexes combined with PIVKA-II was 0.895, and the specificity and sensitivity were higher than that of the single detection, indicating that it is feasible to select PIVKA-II and inflammatory indexes (PA, hs-CRP, and NLR) as screening means for patients with negative AFP but suspected with HCC. Satisfactory results of high sensitivity and high specificity in the differential diagnosis can be obtained. At present, there are many models for the diagnosis of AFP-NHCC by combined detection of multiple biomarkers, but they are also subject to the influence of detection methods and threshold values. For example, the study of Zhang *et al.*[54] showed that the combination of AFP-L3 and Golgi Protein 73 could improve the diagnostic accuracy and sensitivity of AFP-NHCC (sensitivity 40.0%, specificity 100%, and accuracy 76.9%). In addition, a review by Zhu *et al.*[55] found that the AUC of AFP combined with platelet and alanine aminotransferase ratio in differentiating AFP-NHCC (<20 ng/mL) from non-cancer control groups and chronic hepatitis B patients was 0.839 and 0.746, respectively. The results showed that this model is an effective screening model for HCC with low or negative AFP levels. The above studies all indicate that the combination of multiple biomarkers or the combination of new biomarkers with traditional indicators or laboratory routine indicators can further improve diagnostic sensitivity. However, how the combined diagnostic model can facilitate early diagnosis needs further clinical verification and adjustment.

However, this study is not without any shortcomings. This retrospective study may be prone to research biases, warranting further verification of the results in the future through randomized controlled trials. The patients with AFP-NHCC in this study were all recruited from a single center, and the sample size was limited; therefore, more experimental subjects from different regions will be needed in the future. The etiology of AFP-NHCC samples was not classified in this study, and the diagnostic effect of AFP-NHCC induced by different causes (viral hepatitis B infection, chemical or genetic factors, *etc.*) needs to be further evaluated.

5. Conclusion

Through this study, we found that there were significant changes in PA, hs-CRP, NLR, and PIVKA-II in patients with AFP-NHCC compared with healthy individuals and patients with benign lesions. Combined detection of laboratory indicators may facilitate early diagnosis of HCC with negative or normal AFP expression by affording higher diagnostic specificity and sensitivity, thereby enabling early treatment of AFP-NHCC.

Acknowledgments

None.

Funding

This work was supported by the National Natural Science Foundation of China (Grant Nos. 31902287 and 81670988), the Kaifeng Science and Technology Development Plan (Project No. 2203008), and the Cultivation Project for Innovation Team in Teachers' Teaching Proficiency by Zhengzhou Shu-Qing Medical College (No. 2024jxcxtd01).

Conflict of interest

Xin-Ying Ji is an Editorial Board Member of this journal but was not in any way involved in the editorial and peer-review process conducted for this paper, directly or indirectly. Separately, other authors declared that they have no known competing financial interests or personal relationships that could have influenced the work reported in this paper.

Author contributions

Conceptualization: Zhi-Liang Jiang, Yi Liu
Investigation: Huang-Yin Luo, De-Xin Zhang
Methodology: Yi-Bin Lu
Writing – original draft: Wen-Tan Hu, Ning Luo, Xin-Ying Ji
Writing – review & editing: All authors

Ethics approval and consent to participate

This study has been reviewed by the Ethics Review Committee (ethics number: 20240966). The research purpose, process, and significance have been explained to the patients and their families, and all the included subjects have signed informed consent forms for participating in this clinical research.

Consent for publication

Not applicable.

Availability of data

Data are available from the corresponding author upon reasonable request.

References

1. Wen N, Cai Y, Li F, *et al*. The clinical management of hepatocellular carcinoma worldwide: A concise review and comparison of current guidelines: 2022 update. *Biosci Trends*. 2022;16(1):20-30.

   doi: 10.5582/bst.2022.01061

2. Zhang CH, Cheng Y, Zhang S, Fan J, Gao Q. Changing epidemiology of hepatocellular carcinoma in Asia. *Liver Int*. 2022;42(9):2029-2041.

   doi: 10.1111/liv.15251

3. Wang W, Wei C. Advances in the early diagnosis of hepatocellular carcinoma. *Genes Dis*. 2020;7(3):308-319.

   doi: 10.1016/j.gendis.2020.01.014

4. Villanueva A. Hepatocellular Carcinoma. *N Engl J Med*. 2019;380(15):1450-1462.

   doi: 10.1056/NEJMra1713263

5. Mao M, Wang X, Song Y, *et al*. Novel prognostic scores based on plasma prothrombin time and fibrinogen levels in patients with AFP-negative hepatocellular carcinoma. *Cancer Control*. 2020;27(1):1073274820915520.

   doi: 10.1177/1073274820915520

6. Li J, Wang Q, Yan Y, *et al*. Development and validation of a prognostic nomogram to predict the recurrence of AFP-negative and DCP-positive hepatocellular carcinoma after curative resection. *Front Oncol*. 2024;14:1414083.

   doi: 10.3389/fonc.2024.1414083

7. Tzartzeva K, Obi J, Rich NE, *et al*. Surveillance imaging and alpha fetoprotein for early detection of hepatocellular carcinoma in patients with cirrhosis: A meta-analysis. *Gastroenterology*. 2018;154(6):1706-1718.e1.

   doi: 10.1053/j.gastro.2018.01.064

8. Kurokawa T, Ohkohchi N. Platelets in liver disease, cancer and regeneration. *World Gastroenterol*. 2017;23(18):3228-3239.

   doi: 10.3748/wjg.v23.i18.3228

9. Nagel T, Klaus F, Ibanez IG, Wege H, Lohse A, Meyer B. Fast and facile analysis of glycosylation and phosphorylation of fibrinogen from human plasma-correlation with liver cancer and liver cirrhosis. *Anal Bioanal Chem*. 2018;410(30):7965-7977.

   doi: 10.1007/s00216-018-1418-7

10. Wang ZX, Jiang CP, Cao Y, Zhang G, Chen WB, Ding YT. Preoperative serum liver enzyme markers for predicting early recurrence after curative resection of hepatocellular carcinoma. *Hepatobiliary Pancreat Dis Int*. 2015;14(2):178-185.

    doi: 10.1016/s1499-3872(15)60353-8

11. Zhang LX, Lv Y, Xu AM, Wang HZ. The prognostic significance of serum gamma-glutamyltransferase levels and AST/ALT in primary hepatic carcinoma. *BMC Cancer*. 2019;19(1):841.

    doi: 10.1186/s12885-019-6011-8

12. Sylman JL, Mitrugno A, Atallah M, *et al*. The predictive value of inflammation-related peripheral blood measurements in cancer staging and prognosis. *Front Oncol*. 2018;8:78.

    doi: 10.3389/fonc.2018.00078

13. Kumar A, Jat KR, Sankar J, Lakshmy R, Lodha R, Kabra SK. Role of high-sensitivity C-reactive protein (hs-CRP) in assessment of asthma control in children. *J Asthma*. 2023;60(7):1466-1473.

    doi: 10.1080/02770903.2022.2155187

14. Yin J, Wang L, Jin T, *et al*. A cell wall-localized NLR confers resistance to Soybean mosaic virus by recognizing viral-encoded cylindrical inclusion protein. *Mol Plant*. 2021;14(11):1881-1900.

    doi: 10.1016/j.molp.2021.07.013

15. Payancé A, Dioguardi Burgio M, Peoc'h K, *et al*. Biological response under treatment and prognostic value of protein induced by vitamin K absence or antagonist-II in a French cohort of patients with hepatocellular carcinoma. *Eur J Gastroenterol Hepatol*. 2020;32(10):1364-1372.

    doi: 10.1097/meg.0000000000001652

16. Proctor MJ, Morrison DS, Talwar D, *et al*. A comparison of inflammation-based prognostic scores in patients with cancer. A glasgow inflammation outcome study. *Eur J Cancer*. 2011;47(17):2633-2641.

    doi: 10.1016/j.ejca.2011.03.028

17. Najjar M, Agrawal S, Emond JC, Halazun KJ. Pretreatment neutrophil-lymphocyte ratio: useful prognostic biomarker in hepatocellular carcinoma. *J Hepatocell Carcinoma*. 2018;5:17-28.

    doi: 10.2147/jhc.S86792

18. Zenga J, Awan MJ, Frei A, *et al*. Chronic stress promotes

an immunologic inflammatory state and head and neck cancer growth in a humanized murine model. *Head Neck*. 2022;44(6):1324-1334.

doi: 10.1002/hed.27028

19. Qiao W, Leng F, Liu T, *et al*. Prognostic value of prealbumin in liver cancer: A systematic review and meta-analysis. *Nutr Cancer*. 2020;72(6):909-916.

doi: 10.1080/01635581.2019.1661501

20. Chiang HC, Lin MY, Lin FC, *et al*. Transferrin and prealbumin identify esophageal cancer patients with malnutrition and poor prognosis in patients with normal albuminemia: A cohort study. *Nutr Cancer*. 2022;74(10):3546-3555.

doi: 10.1080/01635581.2022.2079687

21. Casadei Gardini A, Foschi FG, Conti F, *et al*. Immune inflammation indicators and ALBI score to predict liver cancer in HCV-patients treated with direct-acting antivirals. *Dig Liver Dis*. 2019;51(5):681-688.

doi: 10.1016/j.dld.2018.09.016

22. Moon G, Noh H, Cho IJ, Lee JI, Han A. Prediction of late recurrence in patients with breast cancer: Elevated Neutrophil to Lymphocyte Ratio (NLR) at 5 years after diagnosis and late recurrence. *Breast Cancer*. 2020;27(1):54-61.

doi: 10.1007/s12282-019-00994-z

23. Qian L, Li C, Luo Y, Meng S. Research progress of AFP in the diagnosis and therapy of hepatocellular carcinoma. *Sheng Wu Gong Cheng Xue Bao = Chin J Biotechnol*. 2021;37(9):3042-3060.

doi: 10.13345/j.cjb.210235

24. Wang T, Zhang KH. New blood biomarkers for the diagnosis of AFP-negative hepatocellular carcinoma. *Front Oncol*. 2020;10:1316.

doi: 10.3389/fonc.2020.01316

25. Yahoo N, Dudek M, Knolle P, Heikenwälder M. Role of immune responses in the development of NAFLD-associated liver cancer and prospects for therapeutic modulation. *J Hepatol*. 2023;79(2):538-551.

doi: 10.1016/j.jhep.2023.02.033

26. Yu C, Sun C. Diagnostic value of multislice spiral computed tomography combined with serum AFP, TSGF, and GP73 assay in the diagnosis of primary liver cancer. *Evid Based Complement Alternat Med*. 2022;2022:6581127.

doi: 10.1155/2022/6581127

27. Zhou J, Chen L, Chen L, Zhang Y, Yuan Y. Emerging role of nanoparticles in the diagnostic imaging of gastrointestinal cancer. *Semin Cancer Biol*. 2022;86(Pt 2):580-594.

doi: 10.1016/j.semcancer.2022.04.009

28. Yu H. Editorial comment: Thermal ablation plus systemic chemotherapy in colorectal cancer liver oligometastases-the optimal sequence and timing. *AJR Am J Roentgenol*. 2023;220(6):900.

doi: 10.2214/ajr.22.28846

29. Fotiadis N, De Paepe KN, Bonne L, *et al*. Comparison of a coaxial versus non-coaxial liver biopsy technique in an oncological setting: Diagnostic yield, complications and seeding risk. *Eur Radiol*. 2020;30(12):6702-6708.

doi: 10.1007/s00330-020-07038-7

30. Yin L, Chen L, Qi Z, *et al*. Gene expression-based immune infiltration analyses of liver cancer and their associations with survival outcomes. *Cancer Genet*. 2021;254-255:75-81.

doi: 10.1016/j.cancergen.2021.02.001

31. Yu H, He J, Liu W, *et al*. The transcriptional coactivator, ALL_1-fused gene from chromosome 9, simultaneously sustains hypoxia tolerance and metabolic advantages in liver cancer. *Hepatology*. 2021;74(4):1952-1970.

doi: 10.1002/hep.31870

32. Nazzal M, Sur S, Steele R, *et al*. Establishment of a patient-derived xenograft tumor from hepatitis C-Associated liver cancer and evaluation of imatinib treatment efficacy. *Hepatology*. 2020;72(2):379-388.

doi: 10.1002/hep.31298

33. Abouzed TK, Althobaiti F, Omran AF, *et al*. The chemoprevention of spirulina platensis and garlic against diethylnitrosamine induced liver cancer in rats via amelioration of inflammatory cytokines expression and oxidative stress. *Toxicol Res* (*Camb*). 2022;11(1):22-31.

doi: 10.1093/toxres/tfab118

34. Sugimoto A, Yoshizawa A, Yoshida A, *et al*. Retroperitoneal malignant extra-gastrointestinal neuroectodermal tumor with EWSR1:CREM fusion and IL-6-related systemic inflammatory symptoms: A case report. *Virchows Arch*. 2023;482(5):911-915.

doi: 10.1007/s00428-022-03442-0

35. McFarland DC, Doherty M, Atkinson TM, *et al*. Cancer-related inflammation and depressive symptoms: Systematic review and meta-analysis. *Cancer*. 2022;128(13):2504-2519.

doi: 10.1002/cncr.34193

36. Pratt HG, Steinberger KJ, Mihalik NE, *et al*. Macrophage and neutrophil interactions in the pancreatic tumor microenvironment drive the pathogenesis of pancreatic cancer. *Cancers* (*Basel*). 2021;14(1):194.

doi: 10.3390/cancers14010194

37. Schauer T, Mazzoni AS, Henriksson A, *et al*. Exercise intensity and markers of inflammation during and after (neo-) adjuvant cancer treatment. *Endocr Relat Cancer*. 2021;28(3):191-201.

doi: 10.1530/erc-20-0507

38. Patten DA, Wilkinson AL, O'Keeffe A, Shetty S. Scavenger receptors: Novel roles in the pathogenesis of liver inflammation and cancer. *Semin Liver Dis*. 2022;42(1):61-76.

doi: 10.1055/s-0041-1733876

39. Bishayee A. The role of inflammation and liver cancer. *Adv Exp Med Biol*. 2014;816:401-435.

doi: 10.1007/978-3-0348-0837-8_16

40. Lee FY, Lee SD, Tsai YT, Wu JC, Lai KH, Lo KJ. Serum C-reactive protein as a serum marker for the diagnosis of hepatocellular carcinoma. *Cancer*. 1989;63(8):1567-1571.

doi: 10.1002/1097-0142(19890415)63:8<1567:aid-cncr2820630820>3.0.co;2-j

41. Gomez D, Farid S, Malik HZ, *et al*. Preoperative neutrophil-to-lymphocyte ratio as a prognostic predictor after curative resection for hepatocellular carcinoma. *World J Surg*. 2008;32(8):1757-1762.

doi: 10.1007/s00268-008-9552-6

42. Wang Y, Attar BM, Fuentes HE, Jaiswal P, Tafur AJ. Evaluation of the prognostic value of platelet to lymphocyte ratio in patients with hepatocellular carcinoma. *J Gastrointest Oncol*. 2017;8(6):1065-1071.

doi: 10.21037/jgo.2017.09.06

43. Xu ZG, Ye CJ, Liu LX, *et al*. The pretransplant neutrophil-lymphocyte ratio as a new prognostic predictor after liver transplantation for hepatocellular cancer: A systematic review and meta-analysis. *Biomark Med*. 2018;12(2):189-199.

doi: 10.2217/bmm-2017-0307

44. Vucur M, Ghallab A, Schneider AT, *et al*. Sublethal necroptosis signaling promotes inflammation and liver cancer. *Immunity*. 2023;56(7):1578-1595.e8.

doi: 10.1016/j.immuni.2023.05.017

45. Wang H, Zhang B, Li R, *et al*. KIAA1199 drives immune suppression to promote colorectal cancer liver metastasis by modulating neutrophil infiltration. *Hepatology*. 2022;76(4):967-981.

doi: 10.1002/hep.32383

46. Guo Y, Hu HT, Xu SJ, *et al*. Correlation of serum chemokine ligand 14 with barcelona clinic liver cancer stage, lymphocyte profile, and response to transarterial chemoembolization in patients with hepatocellular carcinoma. *J Vasc Intervr Radiol*. 2023;34(6):991-998.

doi: 10.1016/j.jvir.2023.01.032

47. Kastle S, Stechele MR, Richter L, *et al*. Peripheral blood-based cell signature indicates response to interstitial brachytherapy in primary liver cancer. *J Cancer Res Clin Oncol*. 2023;149(12):9777-9786.

doi: 10.1007/s00432-023-04875-z

48. Suner A, Carr BI, Akkiz H, *et al*. C-reactive protein and platelet-lymphocyte ratio as potential tumor markers in low-alpha-fetoprotein hepatocellular carcinoma. *Oncology*. 2019;96(1):25-32.

doi: 10.1159/000492473

49. Li K, Xu Y, Hu Y, Liu Y, Chen X, Zhou Y. Effect of enteral immunonutrition on immune, inflammatory markers and nutritional status in gastric cancer patients undergoing gastrectomy: A randomized double-blinded controlled trial. *J Invest Surg*. 2020;33(10):950-959.

doi: 10.1080/08941939.2019.1569736

50. Milana F, Polidoro MA, Soldani C, *et al*. Unveiling the prognostic role of blood inflammatory indexes in a retrospective cohort of patients undergoing liver resection for intrahepatic cholangiocarcinoma. *Int J Surg*. 2024;110(11):7088-96.

doi: 10.1097/JS9.0000000000001924

51. Choi Y, Kim JW, Nam KH, *et al*. Systemic inflammation is associated with the density of immune cells in the tumor microenvironment of gastric cancer. *Gastric Cancer*. 2017;20(4):602-611.

doi: 10.1007/s10120-016-0642-0

52. Degasperi E, Perbellini R, D'Ambrosio R, *et al*. Prothrombin induced by vitamin K absence or antagonist-II and alpha foetoprotein to predict development of hepatocellular carcinoma in Caucasian patients with hepatitis C-related cirrhosis treated with direct-acting antiviral agents. *Aliment Pharmacol Ther*. 2022;55(3):350-359.

doi: 10.1111/apt.16685

53. Akuta N, Kawamura Y, Suzuki F, *et al*. Dynamics of circulating miR-122 predict liver cancer and mortality in japanese patients with histopathologically confirmed NAFLD and severe fibrosis stage. *Oncology*. 2022;100(1):31-38.

doi: 10.1159/000519995

54. Zhang Z, Zhang Y, Wang Y, Xu L, Xu W. Alpha-fetoprotein-L_3 and golgi protein 73 may serve as candidate biomarkers for diagnosing alpha-fetoprotein-negative hepatocellular carcinoma. *Onco Targets Ther*. 2016;9:123-139.

doi: 10.2147/ott.S90732

55. Zhu L, Li T, Ma X, *et al*. A simple noninvasive index can predict hepatocellular carcinoma in patients with chronic hepatitis B. *Sci Rep*. 2017;7(1):8954.

doi: 10.1038/s41598-017-09358-z

ACCSCIENCE PUBLISHING

Gene & Protein in Disease

ORIGINAL RESEARCH ARTICLE

A new gene signature associated with pyroptosis for identifying high-risk myeloma patients

Yaner Wang[1,2], Qi Wang[2], Zhenqian Huang[3], and Xinliang Mao[1,2,3]*

[1]Institute of Clinical Pharmacology, Science and Technology Innovation Center, Guangzhou University of Chinese Medicine, Guangzhou, China

[2]Guangdong and Guangzhou Key Laboratory of Protein Modification and Degradation, School of Basic Medical Sciences, Guangzhou Medical University, Guangzhou, China

[3]Department of Hematology, The First Affiliated Hospital of Guangzhou Medical University, Guangzhou, China

Abstract

Multiple myeloma (MM) is a complicated hematologic malignancy of plasma cells. However, the existing stratification systems cannot accurately predict the prognosis of MM. This study aims to evaluate the role of pyroptosis in identifying high-risk MM patients. RNA expression profiles were obtained from the Cancer Genome Atlas-MMRF CoMMpass and GTEx databases, which were treated as MM cases and controls, respectively. By applying univariate Cox regression analysis and consensus clustering, 20 pyroptosis-related genes (PRGs) were initially identified to effectively stratify MM patients into two distinct subgroups. To identify prognostic gene signature, a stepwise LASSO regression analysis was conducted following by univariate and multivariate Cox regression analyses. We identified a set of signature genes – *CASP3*, *CHMP2A*, *CHMP3*, *CHMP6*, *GZMB*, *CASP8*, *NOD2*, *PLCG1*, and *FOXO3* – that could significantly distinguish MM patients based on overall survival. We further identified that the risk score can serve as an independent prognostic indicator. The same prognostic model was also successfully constructed in the internal test cohort. Thus, a prognostic risk model for clinically predicting the survival rate of MM patients was established. Single-sample gene set enrichment analysis was employed to analyze immune infiltrating cells and immune-related pathways between two risk groups. Moreover, the mRNA expression levels of the prognostic risk signature genes were confirmed by quantitative reverse-transcription polymerase chain reaction in MM cells treated with the pyroptosis-inducing agent etoposide. In conclusion, we identified a 9-PRG signature that enables effective stratification of MM patients and serves as an independent prognostic marker. These findings underscore the need for further exploration of pyroptosis in MM therapy.

Keywords: Multiple myeloma; Pyroptosis; Signature gene; Prognosis

***Corresponding author:**
Xinliang Mao
(xinliangmao@gzhmu.edu.cn)

Citation: Wang Y, Wang Q, Huang Z, Mao X. A new gene signature associated with pyroptosis for identifying high-risk myeloma patients. *Gene Protein Dis.* 2024;3(4):4534.
doi: 10.36922/gpd.4534

Received: August 15, 2024

Accepted: December 3, 2024

Published Online: December 17, 2024

1. Introduction

Multiple Myeloma (MM) is a plasma cell malignancy more commonly affecting the elderly individuals.[1] The average age at diagnosis of MM patients is 69 years, according to the annual report of American Cancer Society website (Key Statistics About MM). The annual global incidence is approximately 2/100,000 people, making

it a relatively rare cancer.[2] Despite being rare, MM accounts for a significant proportion of deaths related to hematological malignancies.[3] The American Cancer Society website (https://www.cancer.org/cancer/types/multiple-myeloma/about/key-statistics.html) reports that there are an estimated 35,780 new myeloma cases and approximately 12,540 myeloma-associated deaths in 2024. Recently, significant strides have been made in both the understanding and management of MM.[4] Last decade has seen significant advancements in treatment against MM.[5] In addition, the advent of next-generation sequencing has provided insights into the molecular heterogeneity of MM, leading to the identification of high-risk subgroups and the development of more personalized treatment strategies.[6] According to the Revised-International Staging System (R-ISS) guideline, MM patients are mainly stratified into 4 risk categories, with a homogeneous repatrition, and those with chromosomal alterations, including del(17p), t(4;14), t(14;16), t(14;20), gain(1q), and or gene mutations such as p53 mutation, are labeled as having poor prognosis or high-risk outcomes. The disease with two or more high risk factors is regarded as a double- or multiple-hit myeloma, which may translate to poorer outcomes in the affected patients.[7] However, MM remains a largely incurable disease, with most patients experiencing relapse after initial response to therapy due to genetic heterogeneity.[8] Interestingly, in addition to traditional chromosomal translocations and gene mutations, increased lactate dehydrogenase (LDH) concentration is also taken into consideration in the R-ISS.[9] LDH is an important enzyme of the anaerobic metabolic pathway, and it is present in all tissues and increased in the blood levels when tissues and cells are injured.[10] LDH is not only a hallmark checkpoint of gluconeogenesis and DNA metabolism, but also associated with cell death, such as cell pyroptosis. In our recent study, we found that LDH is strikingly increased when MM cells undergo pyroptosis.[11]

Pyroptosis acts as a defense mechanism against microbial infections.[12] It typically manifests as cell swelling, membrane rupture, and the release of pro-inflammatory intracellular contents, leading to an inflammatory response.[13] Over the past decade, our understanding of the molecular mechanisms behind pyroptosis has significantly advanced.[14] It is now known that pyroptosis is mediated by a family of proteins called gasdermins, which are capable of forming pores in the cell membrane.[15] Pyroptosis is increasingly recognized as playing crucial roles in various diseases.[16] In infectious diseases, pyroptosis can eliminate the intracellular replication niches of pathogens and amplify the host immune response.[17] In the context of cancer, it can either inhibit or promote tumor growth, contingent on the particular circumstances.[18] The discovery of pyroptosis also opens a new avenue for the development of therapeutic strategies.[19] For example, modulating pyroptosis may enhance the efficacy of immunotherapies in cancer.[20] Despite these advances, many questions remain to be answered. For instance, the regulation of gasdermin proteins and the role of pyroptosis in non-pathogenic conditions are not fully understood.[21] Future research will likely focus on these areas and on translating the knowledge of pyroptosis into clinical applications.

Recent research has suggested a possible interplay between MM and pyroptosis, opening a promising avenue for novel therapeutic strategies.[22] Pyroptosis, through the elimination of cancerous cells and the initiation of an immune response, could be leveraged to enhance the efficacy of existing MM treatments.[23] Identifying prognostic biomarkers of pyroptosis in MM holds substantial potential to improve patient outcomes.[24] Such biomarkers could not only provide insights into a patient's likely disease course, aiding in risk stratification and personalized treatment planning, but also reveal novel targets for therapy. In particular, they could identify patients who might benefit from therapies that modulate pyroptosis, providing a new approach to combat this not-yet-curable disease.[25] Hence, while the path to fully understanding the role of pyroptosis in MM is undoubtedly challenging, it is one that holds immense promise for improving the lives of those affected by this pathological condition.[7]

Wang *et al.*[26] developed a prognostic risk scoring model based on 11 pyroptosis-related genes (PRGs) from the GSE136324 dataset. However, the small validation cohort might affect the reliability of their findings. Zhang *et al.*[27] established a prognostic model using 9 out of 33 candidate PRGs, but their model lacked experimental validation. Li *et al.*[28] proposed a 6-gene signature but it could not distinguish between disease subgroups in the validation dataset. In the present study, we conducted comparisons between MM patients and healthy controls using a larger sample dataset, and based on our results, we identified a novel and comprehensive PRG signature that can effectively classify MM patients according to disease risk.

2. Materials and methods

2.1. Data sources and processing

The clinical data and PRGs of 859 MM patients were retrieved from the Cancer Genome Atlas (TCGA)-MMRF CoMMpass project. The gene expression data were standardized using the "limma" package,[29] a scaling method to maintain data integrity and comparability. Patients lacking clinical information (n = 17) were excluded, resulting in 842 MM patients being eligible. The "caret" package was employed to divide these patients into

training group and test group, randomly. In addition, data of 70 healthy individuals, which served as controls, were retrieved from the GTEx database for analysis of bone marrow mRNA expression.

2.2. Analysis of differential PRGs

An extensive review of the literature was performed to identify 57 PRGs[30,31] as of December 2023, which are shown in Table 1. The "limma" package in R was utilized to assess the significance of differentially expressed genes (DEGs). The findings were illustrated using heatmap. The protein–protein interactions (PPIs) network of DEGs was analyzed using the GeneMANIA platform.

2.3. Establishing a prognostic risk model derived from DEGs

Univariate Cox analysis was performed with a *P*-value threshold of 0.05. This process identified preliminary prognostic genes for further study, and their prognostic significance was evaluated using consensus clustering analysis. Subsequently, the "glmnet" package in R was used to conduct a stepwise Lasso-penalized Cox regression analysis.[32] The risk scoring formula used in the Lasso regression analysis is referenced from the literature.[33] The "survival" and "timeROC" packages were used to perform receiver operating characteristic (ROC) curve analysis to evaluate the effectiveness of the prognostic model.[34] Both univariate and multivariate Cox regression analyses were employed to explore the independent prognostic value of the risk score. In addition, to visually assess the ability of PRGs to differentiate patients, we performed principal component analysis (PCA) using the "limma" and "scatterplot3d" packages in R.[35] The same algorithm was applied to construct the prognostic risk model in the internal test group.

2.4. Construction of a prognostic nomogram

The "rms" and "survival" packages in R, commonly used in medical research for prognostic modeling and survival analysis, were utilized to create prognostic nomogram.[36] For MM patients, we combined the risk score with clinical indicators such as gender, age, and disease stage to construct a prognostic model for predicting patient survival time. The prognostic model (nomogram) provides a graphical representation that incorporates multiple prognostic factors, enabling a more detailed and individualized estimation of survival time for MM patients.

2.5. Immunotherapeutic response prediction

Single-sample gene set enrichment analysis (ssGSEA) from the "GSVA" R package and the Tumor Immune Dysfunction and Exclusion (TIDE) framework were used

Table 1. Pyroptosis-related genes identified in this study

Gene symbol	Definition
AIM2	Absent in melanoma 2
APIP	Apoptosis protease-activating factor 1 Interacting Protein
BAK1	BRI1-associated receptor kinase 1
BAX	Bcl-2-associated X protein
CASP1	Cysteine-aspartic acid protease-1
CASP3	Cysteine-aspartic acid protease-3
CASP4	Cysteine-aspartic acid protease-4
CASP5	Cysteine-aspartic acid protease-5
CASP6	Cysteine-aspartic acid protease-6
CASP8	Cysteine-aspartic acid protease-8
CASP9	Cysteine-aspartic acid protease-9
CHMP2A	Charged Multivesicular Body Protein 2A
CHMP2B	Charged Multivesicular Body Protein 2B
CHMP3	Charged Multivesicular Body Protein 3
CHMP4A	Charged Multivesicular Body Protein 4A
CHMP4B	Charged Multivesicular Body Protein 4B
CHMP4C	Charged Multivesicular Body Protein 4C
CHMP6	Charged Multivesicular Body Protein 6
CHMP7	Charged Multivesicular Body Protein 7
CYCS	Recombinant Cytochrome C, Somatic
DHX9	DEAH-box helicase 9
ELANE	Elastase, neutrophil expressed
FOXO3	Forkhead box O3
GPX4	Glutathione peroxidase 4
GSDMA	Gasdermin A
GSDMB	Gasdermin B
GSDMC	Gasdermin C
GSDMD	Gasdermin D
GSDME	Gasdermin E
GZMA	Granzyme A
GZMB	Granzyme B
HMGB1	High-mobility group box-1 protein
IL18	Interleukin 18
IL1A	Interleukin 1 a
IL1B	Interleukin 1 beta
IL6	Interleukin 6
IRF1	Interferon regulatory factor 1
IRF2	Interferon regulatory factor 2
NAIP	Neuronal apoptosis inhibitory protein
NLRC4	NLR family CARD domain containing 4
NLRP1	NLR family pyrin domain containing 1
NLRP2	NLR family pyrin domain containing 2

(Cont'd...)

Table 1. ***(Continued)***

Gene symbol	Definition
NLRP3	NLR family pyrin domain containing 3
NLRP6	NLR family pyrin domain containing 6
NLRP7	NLR family pyrin domain containing 7
NLRP9	NLR family pyrin domain containing 9
NOD1	Nucleotide binding oligomerization domain containing 1
NOD2	Nucleotide binding oligomerization domain containing 2
PJVK	Pejvakin/deafness, autosomal recessive 59
PLCG1	Phospholipase C gamma 1
PRKACA	Protein kinase cAMP-activated catalytic subunit alpha
PYCARD	PYD and CARD domain containing
SCAF11	SR-related CTD associated factor 11
TIRAP	TIR domain containing adaptor protein
TNF	Tumor necrosis factor
TP53	Tumor Protein P53
TP63	Tumor Protein P63

to assess the immune environment between different risk groups.[37] TIDE aims to predict the effectiveness of initial treatments with immune checkpoint inhibitors, such as anti-*PD1* or anti-*CTLA4*, in MM patients. Compared to other markers, including *PD-L1* expression and mutation load, TIDE offers higher predictive accuracy.[38,39]

2.6. Analyzing the gene expression of the PRG signature *in vitro*

The OPM-2 MM cell line was treated with etoposide with a concentration of 0, 5, or 20 μg/mL for 48 h, and the cells were then collected to extract total RNA by using the RNAeasy™ Plus Isolation Kit (Beyotime Biotechnology Co., Ltd., Shanghai, China). The total RNAs were subjected to synthesize cDNA using TransScript Reverse Transcriptase Kit (TransGen Biotech, Beijing, China). Reverse-transcription quantitative polymerase chain reaction (qRT-PCR) was conducted in accordance to the assay manufacturer's instructions (TaKaRa Biotech, Dalian, China). The primers used for each gene are shown in Table 2. The specific steps for qRT-PCR are as follows: (1) the reaction mixture was loaded into a qPCR instrument (TaKaRa Biotech, Dalian, China), and thermal cycling conditions, typically involving denaturation, annealing, and extension phases, were set. (2) During amplification, the fluorescent dye binds to the DNA, allowing real-time quantification of DNA levels. (3) The changes in transcript levels were quantified using the comparative $2^{-\Delta\Delta CT}$ method.

Table 2. Sequence of primers used in quantitative reverse-transcription polymerase chain reaction

Caspase 3 (*CASP3*)	
Forward	5'-CATGGAAGCGAATCAATGGACT-3'
Reverse	5'-CTGTACCAGACCGAGATGTCA-3'
Caspase 8 (*CASP8*)	
Forward	5'-AAGAGCCAGGGTGGTTATTGAAAGT-3'
Reverse	5'-ATCTCCTCCTTTCTAGTGTTTAGGT-3'
Charged multivesicular body protein 2A (CHMP2A)	
Forward	5'-CTACTGCGGCAGAACCAG-3'
Reverse	5'-CATCATTCATCATCTCCTCCT-3'
Charged multivesicular body protein 3 (*CHMP3*)	
Forward	5'-ATGGGGCTGTTTGGAAAGACC-3'
Reverse	5'-TTTGCCTGTCAACAACTCTCAT-3'
Charged multivesicular body protein 6 (*CHMP6*)	
Forward	5'-AAGGCCATCCTGCAACTGAAG-3'
Reverse	5'-GCTGCTCCTGGTATCGCTT-3'
Forkhead box O3 (*FOXO3*)	
Forward	5'-CGGACAAACGGCTCACTCT-3'
Reverse	5'-GGACCCGCATGAATCGACTAT-3'
Glyceraldehyde-3-phosphate dehydrogenase (*GAPDH*)	
Forward	5'-GGAGCGAGATCCCTCCAAAAT-3'
Reverse	5'-GGCTGTTGTCATACTTCTCATGG-3'
Nucleotide-binding oligomerization domain containing 2 (*NOD2*)	
Forward	5'-TGGTTCAGCCTCTCACGATGA-3'
Reverse	5'-CAGGACACTCTCGAAGCCTT-3'
Phospholipase C gamma 1 (*PLCG1*)	
Forward	5'-GCTTCTATGTAGAGGCAAACC-3'
Reverse	5'-GCCACTTCACGGATCTTTT-3'

2.7. Statistical analysis

All statistical analyses were conducted using R software version 4.0.1, with statistical significance defined as $^{*}P < 0.05$, $^{**}P < 0.01$, and $^{***}P < 0.001$.

3. Results

3.1. The expression profile of PRGs in MM patients and healthy individuals

After a comprehensive literature review, we selected 57 PRGs for analysis. The expression landscape of these 57 PRGs was examined, and the results are illustrated in the heatmap shown in Figure 1A. Among these PRGs, 53 were identified as DEGs, of which 22 genes were markedly downregulated in MM patients, including *BAX*, *CHMP2A*, *CHMP3*, *CHMP4A*, *CYCS*, *GSDME*, *HMGB1*, *IL18*, *IL1A*, *TP63*, *CASP-6*, *-9*, *GPX4*, *GSDMA*, *GSDMC*, *NLRP2*, *NOD1*, *PLCG1*, *PRKACA*, *SCAF11*, *NAIP*, and *APIP*.

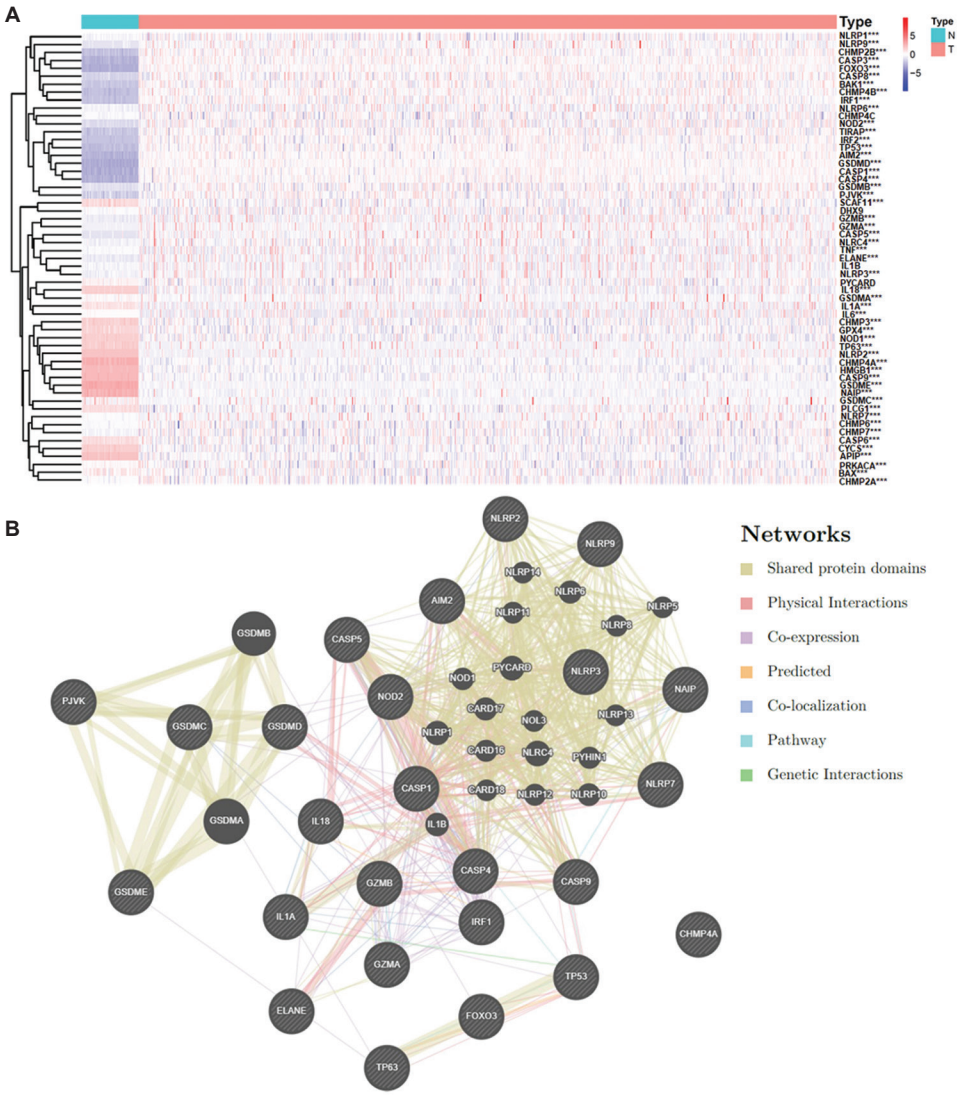

Figure 1. The expression profiles of the PRGs in MM patients. (A) The expression profile of the PRGs in normal (n = 70) and MM cells (n = 842) retrieved from GTEx database and TCGA-MMRF CoMMpass database, respectively. (B) The protein-protein interaction network diagram of DEGs.
Abbreviations: DEGs: Differentially expressed genes; MM: Multiple myeloma; PRGs: Pyroptosis-related genes.

Simultaneously, 31 genes were significantly upregulated, including *BAK1*, *CASP-1*, *-3*, *-4*, *-5*, *CHMP-2B*, *-4B*, *-6*,*- 7*, *ELANE*, *GSDMD*, *GZMB*, *IRF1*, *IRF2*, *TP53*, *AIM2*, *CASP8*, *GSDMB*, *IL6*, *NLRC4*, *NLRP-1*,*-3*, *-6*, *-7*, *-9*, *NOD2*, *PJVK*, *TIRAP*, *TNF*, *GZMA*, and *FOXO3*. DEGs are pivotal in data analysis as they reveal key genetic variations linked to specific biological processes or diseases. Identifying DEGs enables us to discover potential biomarkers and therapeutic targets, aiding in understanding MM mechanisms. Given the markedly different expression profiles of specific PRGs in MM patients and healthy individuals, it is thus possible to predict the significance of the PRGs in clinical outcomes of MM patients.

Network analysis was performed using GeneMANIA, revealing that interactions among these DEGs formed three interconnected regulatory subnetworks, specifically being associated with: (1) the caspase and granzyme family, mainly including *CASP1*, *CASP3*, *CASP4*, *CASP5*, *GZMA*, *GZMB*; (2) the gsdermin family, including *GSDMA*, *GSDMB*, *GSDMC*, *GSDMD* and *GSDME*; and (3) the NOD-like receptor family, mainly including *NLRP2*, *NLRP3*, *NLRP5*, *NLRP7*, *NLRP9*, *AIM2*, and *NOD2*. The specific interaction of these DEGs is illustrated in Figure 1B. PPIs is essential in data analysis as they help map the complex networks that regulate cellular processes. By studying PPIs, we can gain insights into MM

mechanisms, as disruptions in these interactions often lead to pathological conditions.

3.2. Neoplastic categorization according to prognostic pyroptosis modulators

Given the huge differences of critical PRGs in MM patients, we next evaluated the correlation of the PRGs in the survival of MM patients. Toward this end, a univariate Cox regression analysis was performed. The results showed that out of the 20 significant DEGs, the high expression levels of 11 genes including *BAK1*, *CASP3*, *CHMP6*, *CHMP7*, *CYCS*, *TP63*, *CASP6*, *CASP8*, *CASP9*, *IL6*, and *GZMA* were linked to reduced survival in MM patients, as indicated by hazard ratios greater than one (Figure 2A). To find whether these identified PRGs could be used to classify MM patients in terms of overall survival rate or prognosis, we performed stratification analysis. Based on the consensus clustering matrix, these patients could be classified into two groups (Figure 2B). Moreover, using the Cumulative Distribution Function (CDF) analysis to help determine the optimal number of clusters by showing the distribution of consensus values, we noted a sharp increase in the CDF plot in the form of well-defined clusters, and based upon these findings, we randomly divided the 842 patients into

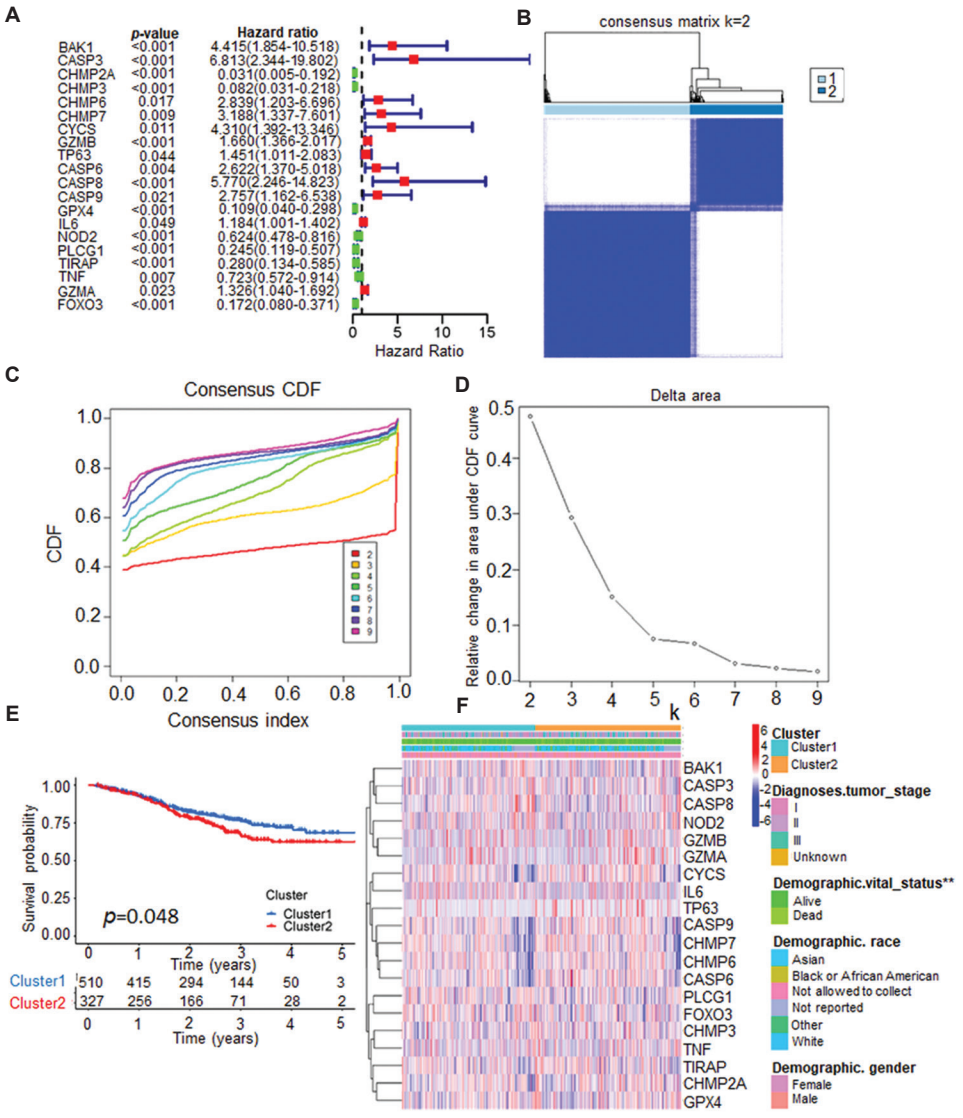

Figure 2. Classification of MM patients into two subgroups based on the initial set of 20 PRGs identified. (A) The forest plot of the preliminary 20 PRGs derived from univariate Cox regression analysis. (B) Stratification of the MM patients into 2 clusters based on the consensus clustering matrix (k = 2). (C and D) Consensus clustering model with CDF by k values. (E) The Kaplan–Meier analysis of the survival time in the two clusters. (F) The heatmap shows the preliminary 20 PRGs expression of the two clusters with different clinical pathological characteristics.
Abbreviations: CDF: Cumulative Distribution Function; MM: Multiple myeloma; PRGs: Pyroptosis-related genes.

two distinct clusters (k = 2) by CDF values (Figure 2B-D). Furthermore, the first group of patients demonstrated a survival advantage over the second group, as shown in Figure 2E, highlighting the significant prognostic impact of the preliminary PRGs. In addition, comparisons of clinical features such as tumor stage, ethnicity, and gender revealed that there were no significant differences between the two clusters (Figure 2F). These results therefore suggest that these PRGs could be used to classify MM patients.

3.3. Creation of a distinct prognostic risk model within the training set

To further examine the classification of MM patients based on the 20 PRGs as shown in Figure 2A, 842 MM patients from the TCGA-MMRF CoMMpass project were randomly divided into the training cohort (including 442 patients) and the test cohort (including 440 patients), and there were no significant differences in the general information between these cohorts (Table 3). Next, to determine whether the 20 prognostic genes could be used to create a model for predicting prognostic risk, we conducted a stepwise Lasso regression of the 20 PRGs within the training set, and the results generated a formula to calculate a risk score: risk score = (1.255 * *CASP3* exp.) + (−2.177 * *CHMP2A* exp.) + (−1.864 * *CHMP3* exp.) + (1.002 * *CHMP6* exp.) + (0.486 * *GZMB* exp.) + (1.172 * *CASP8* exp.) + (−0.554 * *NOD2* exp.) + (−1.131 * *PLCG1* exp.) + (−1.536 * *FOXO3* exp.). Using this formula, a risk model was constructed with 9 genes including *CASP3*, *CHMP2A*, *CHMP3*, *CHMP6*, *GZMB*, *CASP8*, *NOD2*, *PLCG1*, and *FOXO3*, adhering to the minimum criteria (Figure 3A and 3B). This model effectively could stratify the MM patients into two risk groups based on the median risk score (Figure 3C), with the high-risk group showing higher mortality and shorter survival time (Figure 3D). Further univariate and multivariate Cox regression analyses established the prognostic risk score as an independent predictor of patient prognosis (Figure 3E and 3F), with *P*-values below 0.001 and hazard ratios exceeding 1. The heatmap analysis further indicated significant differences in the gene expression profiles, of which *PLCG1*, *FOXO3*, *CHMP2A*, *CHMP3,* and *NOD2* were notably downregulated in the high-risk group, while other genes including *CASP3*, *CHMP6*, *GZMB,* and *CASP8* were upregulated (Figure 3G).

Table 3. Characteristics of multiple myeloma patients in two cohorts

	Training cohort	Test cohort	*P*-value
Gender			0.749
Male	230	262	
Female	172	178	
Race			0.916
White	261	301	
Asian	7	6	
Black or African American	51	61	
Unknown	83	72	
Vital status			0.919
Alive	330	321	
Dead	72	119	
Stage			0.841
Stage I	141	140	
Stage II	140	153	
Stage III	112	135	
Unknown	9	12	

MM patients in the high-risk group showed a shorter total survival rate as analyzed by the Kaplan–Meier (K–M) test, regardless of treatment (Figure 4A). The nine-gene risk model's effectiveness confirmed the predicted patient survival outcomes by the values of area under the curve (AUC, Figure 4B). AUC measures the overall performance: an AUC of 0.5 indicates no discrimination, while 1.0 signifies perfect subgroup discrimination. Finally, PCA plots demonstrated a clear distinction between the two risk groups based on 9 PRGs; however, the difference was not as evident when considering all genes or only PRGs (Figure 4C-E). Therefore, an independent prognostic model with a 9-gene set was constructed in the training cohort.

3.4. Confirmatory assessment of prognostic signature's robustness

The above study has established a 9-PRG signature gene model in the training set. To validate these 9 PRGs in the test cohort of 440 patients, both univariate and multivariate Cox regression analyses were performed, and both analyses confirmed that the risk score functions as an independent prognostic factor, with *P*-values below 0.001 and hazard ratios exceeding 1 (Figure 5A and 5B). Consistent with the finding in the training set, the high-risk group also exhibited a higher mortality rate and a similar gene expression pattern for the signature genes in the test cohort (Figure 5C-E). The K–M survival curves also showed significant differences in the survival probability (Figure 5F). Furthermore, the ROC curve analysis also found that the risk signature maintained strong prognostic accuracy (Figure 5G). The PCA analysis echoed the findings from the training cohort, effectively distinguishing patients from among the two risk groups in the test cohort (Figure 5H). Overall, these results

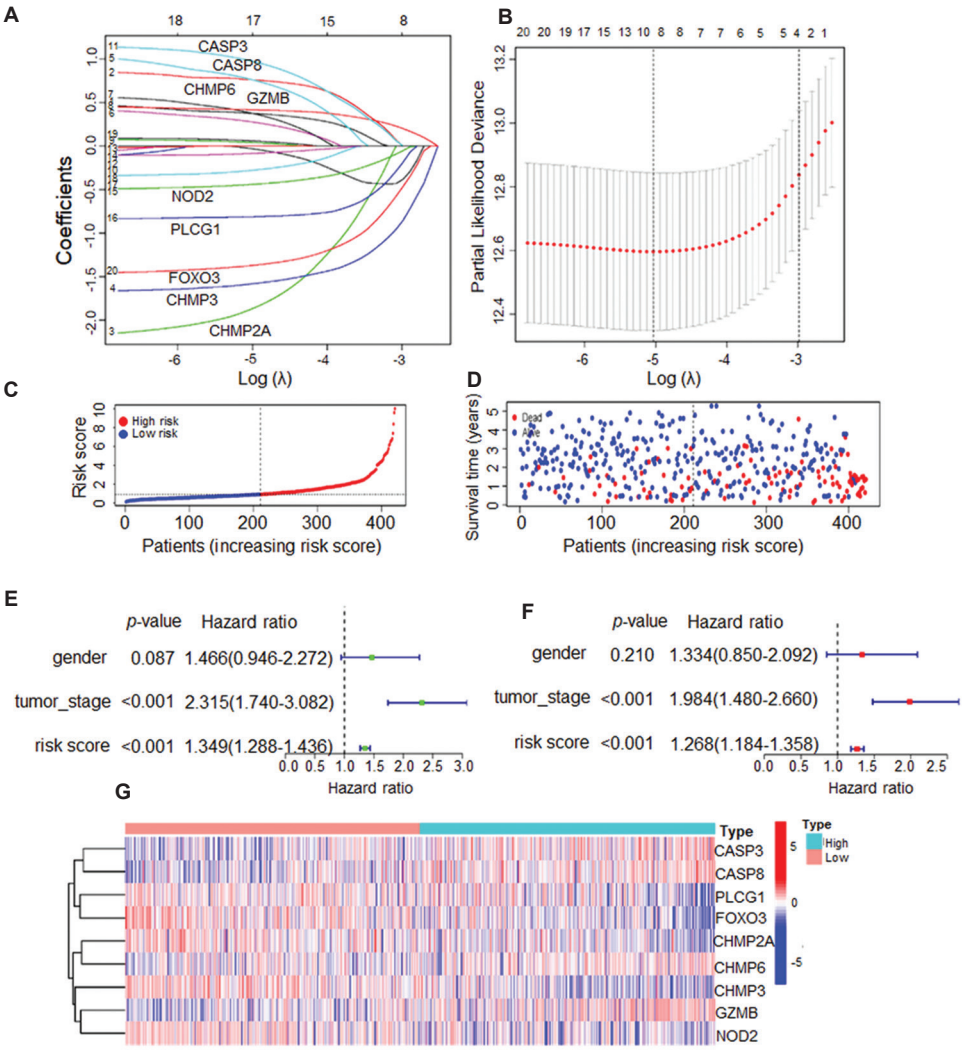

Figure 3. Construction of an independent prognostic model with a 9-gene set in the training cohort. (A and B) Construction of the LASSO regression model based on the preliminary 20 PRGs. (C and D) The risk scores and survival status of the 9 genes in the two risk groups, divided based on the median risk score derived from the LASSO regression analysis. (E and F) The univariate Cox analysis and multivariate Cox analysis to assess the independence of risk score. (G) The expression profile of the progostic risk genes in the model construction.
Abbreviation: PRGs: Pyroptosis-related genes.

confirm that the 9-PRG signature set could be used for risk stratification in MM patients.

3.5. Assessment of the prognostic signature for patient segmentation

The above studies have shown that the 9-PRG set could be used to identify the high-risk MM patients. To further estimate the capacity of this gene signature set in identification of high-risk MM patients, we examined overall survival rate in relation to clinical settings, including gender and disease stages. The correlation analysis showed that, regardless of gender or disease stages, the patients categorized as high-risk consistently had lower survival probabilities, as revealed by K–M survival analysis (Figure 6A-E). Furthermore, we developed a novel prognostic tool that combined the calculated risk scores with gender and disease stage, and the prognostic chart effectively predicted survival rate for MM patients (Figure 6F). Therefore, the above overall analyses have collectively demonstrated the 9-PRG signature set could be used to effectively distinguish between the different risk groups of MM patients.

3.6. Immune activity between the two subgroups

Given the strong association between pyroptosis and tumor immunity, as well as the impact of tumor microenvironment including immune cells on MM cells grown in bone marrow, we postulated that the gene signature set may play

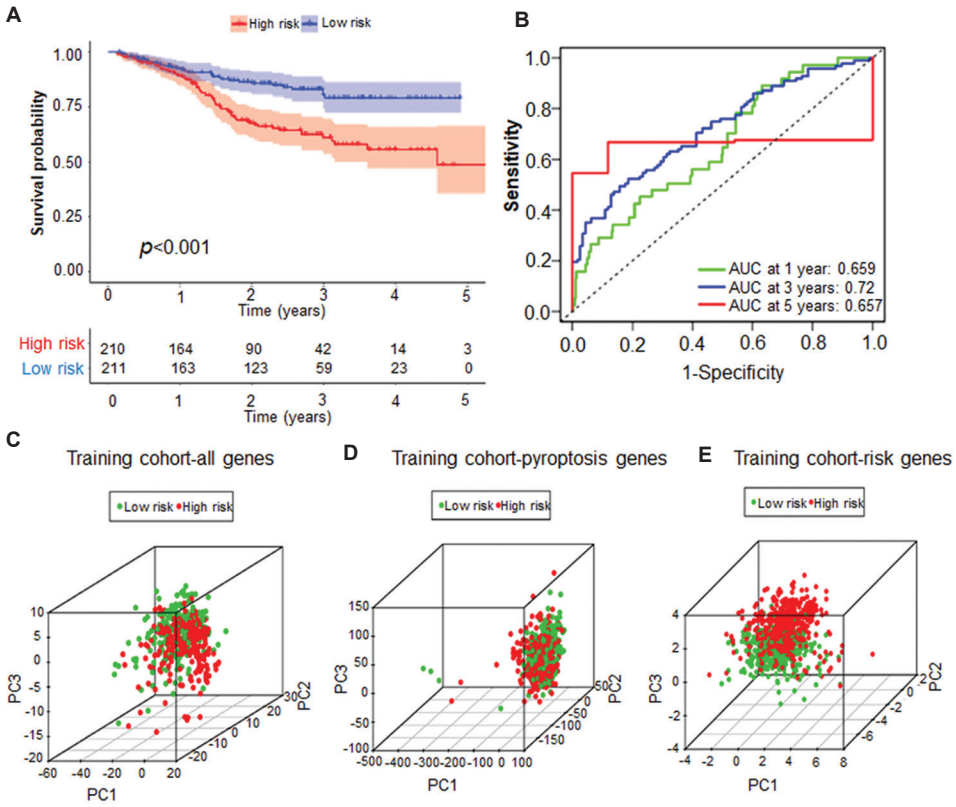

Figure 4. Validation of the prognostic risk model in the training cohort. (A) The Kaplan–Meier analysis of the survival time in two risk groups. (B) The ROC analysis of the prognostic model's efficiency to distinguish between two risk groups. (C-E) Visual results from PCA analysis for the two risk groups based on all genes (C), pyroptosis genes (D), and the 9 risk genes (E).
Abbreviations: PCA: Principal component analysis; ROC Receiver operating characteristic.

a role in MM growth confined to the bone marrow setting and modulate immune activity. To this end, we utilized the data on bone marrow cells for immune analysis because the bone marrow is the primary site of disease occurrence and can more accurately reflect the immune environment and cell–cell interactions. ssGSEA results showed a significant decrease in the presence of activated dendritic cells, dendritic cells in the high-risk group compared to the low-risk group (Figure 7A). Furthermore, the analysis revealed a significant downregulation in immune-related pathways such as antigen-presenting cell co-inhibition, C-C chemokine receptor, immune checkpoints, major histocompatibility complex (MHC) class I, and T cell co-inhibition in the high-risk group (Figure 7B). To gain a deeper understanding of tumor-immune dynamics and their impact on tumor progression and treatment outcomes, we utilized metrics such as TIDE and myeloid-derived suppressor cells (MDSC). These indicators highlighted the complex biological characteristics of MM and the interaction between the immune system and MM tumors. The high-risk group exhibited higher levels of immune dysfunction, immune exclusion, and MDSCs, as well as elevated TIDE scores (Figure 7C-F). Altogether, these findings suggest a more significant impairment of T-cell functionality in the high-risk group, potentially leading to reduced effectiveness of immunotherapeutic interventions.

3.7. Confirmation of varied expression in prognostic genes with intrinsic significance

The above-mentioned study revealed that some key genes in the signature gene set were downregulated in the high-risk patients. To find whether these genes could be upregulated by anti-MM agents, we analyzed the transcriptional levels of these genes in the MM cell treated with etoposide, which can induce cancer cell pyroptosis[40] and it also showed to induce MM cell pyroptosis.[22] The treatment with etoposide increased the mRNA levels of *CHMP2A*, *CHMP3*, *NOD2*, *PLCG1*, and *FOXO3* (Figure 8A-E), which were all found to be downregulated in high-risk MM cells (Figures 3G and 5E). Moreover, the treatment led to a decreased mRNA level of *CASP3*, *CASP8,* and *CHMP6* (Figure 8F-H) that were upregulated in the high-risk group patients. Therefore, this large-scale analysis, involving 842 MM patients and 70 healthy individuals, provides

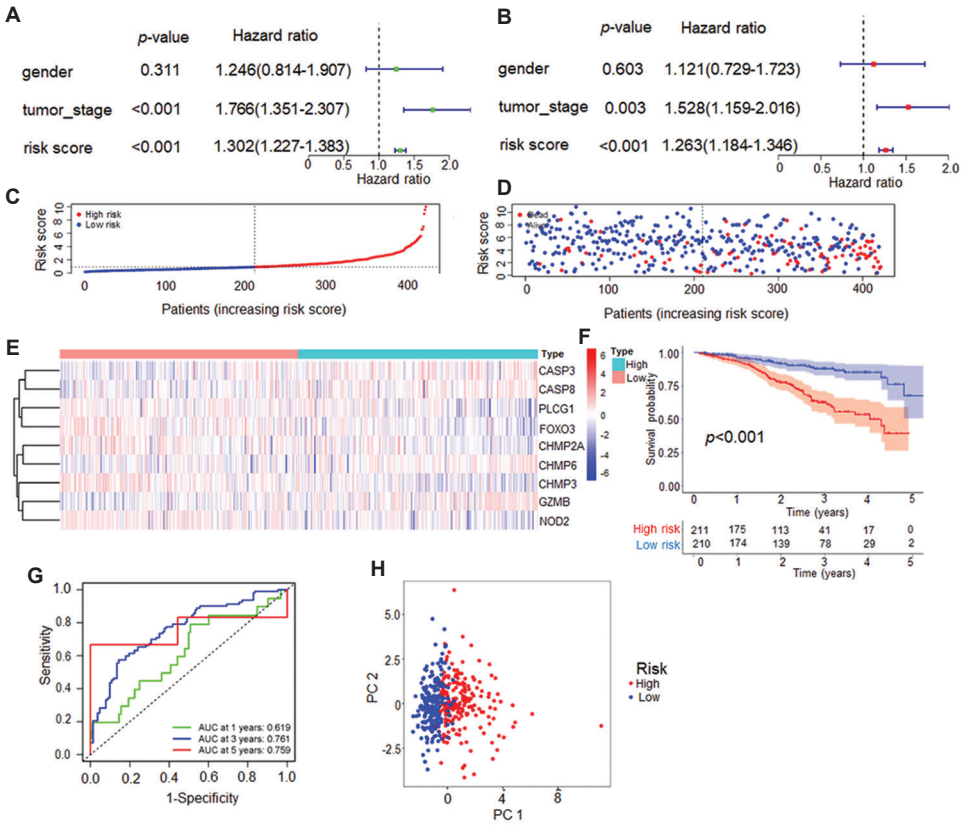

Figure 5. Internal validation of the risk model in the test cohort. (A and B) The univariate Cox analysis and multivariate Cox analysis for risk score. (C-E) The risk scores, survival status, and expression of the 9 risk genes in the two risk groups. (F) The Kaplan–Meier analysis of the survival time in the two risk groups. (G) The ROC analysis for estimating predictive efficiency. (H) The PCA analysis of two clusters based on the 9 risk genes.
Abbreviations: PCA: Principal component analysis; ROC Receiver operating characteristic.

a validated set of findings, confirming the differential expression of prognostic genes that are feasible for disease risk stratification.

4. Discussion

The main output of the present study is a novel nine PRGs signature for predicting the prognosis of MM and identifying patients with high-risk MM.

MM is a highly heterogenous plasma cell malignancy, for which a panel of treatment modalities have been proposed. The classification and stratification of the disease are key factors for guiding personalized treatment. Three principal genetic aberrations indicative of high risk are proposed in the criteria of the Updated International Staging System: translocations t(4;14) and t(14;16), as well as deletion 17p; they may occur independently or concurrently.[9] However, given the variety of genetic and epigenetic heterogeneity in MM cells, the simple classification framework of this staging system would not be fully reflective of the conditions that should be encompassed within the high-risk spectrum of MM.

One emerging field of interest is pyroptosis, a unique form of programmed cell death marked by pore formation in the plasma membrane, which subsequently triggers cell swelling and lysis.[41] A panel of genes have been reported to be involved in cell pyroptosis. There are three PRG signatures reported to predict MM prognosis and distinguish high-risk patients.[26-28] These studies reported a predictable models involved six, nine, and eleven genes, respectively. However, the limitations of these studies are conspicuous: the small sizes of MM population,[26] the relatively small panel of candidate genes,[27] and the low efficacy to distinguish high-risk patients.[28] In the present study, we analyzed a large database of cases along with controls whose data were derived from another database. The gene expression profiles of the healthy controls afford us with a comprehensive view on the expression of candidate genes, which are crucial for understanding the expression alterations of these genes in myeloma; therefore, adopting a heavy control sample in this study ensures data comprehensiveness and higher accuracy. Moreover, we reduced the candidate genes from 57 to 20 and eventually

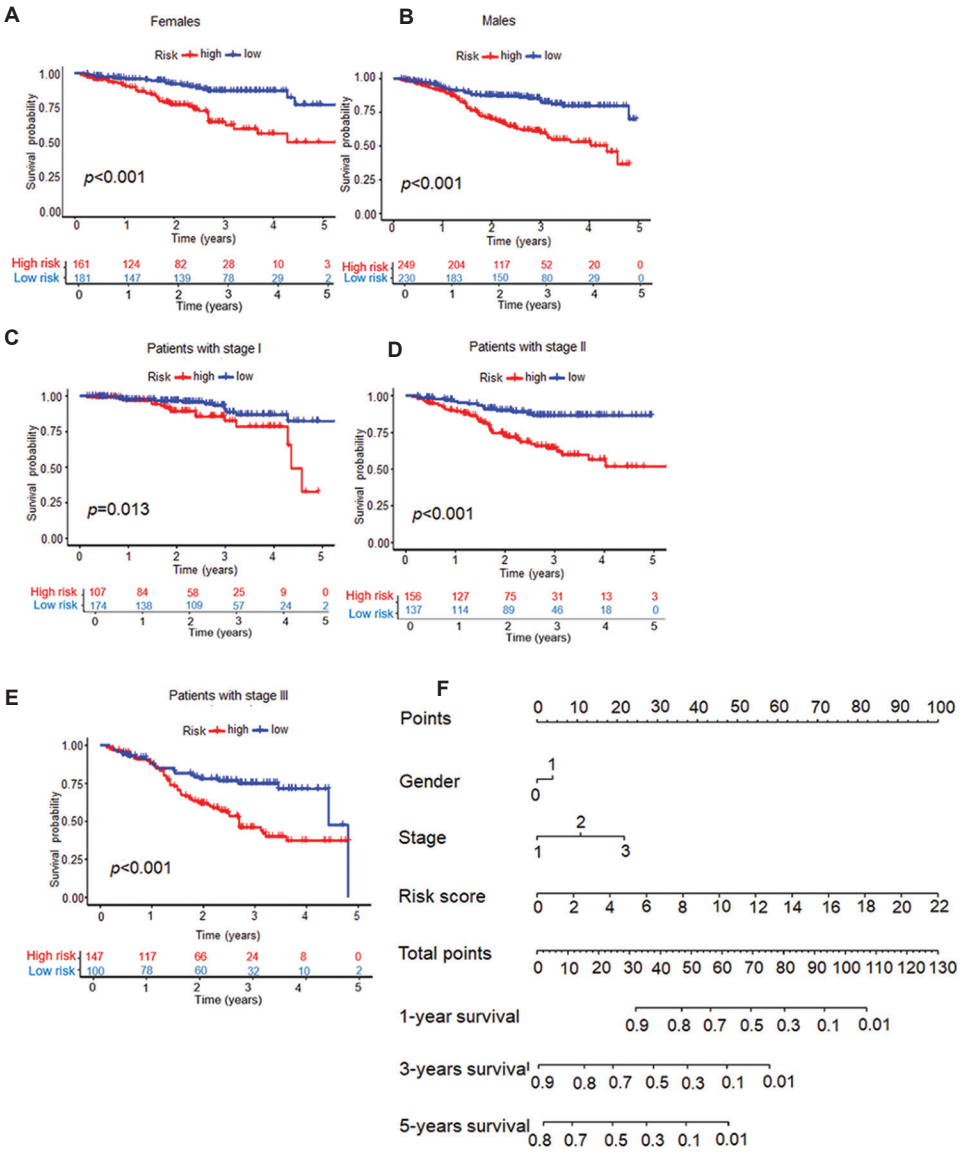

Figure 6. The MM risk differentiation using the risk model, considering gender and disease stage. (A-E) Kaplan–Meier analyses of the survival time in the two risk groups based on gender (A and B) and disease stage (C-E). (F) The nomogram established for predicting survival rate in MM patients.
Abbreviation: MM: Multiple myeloma.

to 9 in a stepwise manner. Moreover, we classified the patients into two risk groups by fully considering the clinical outcomes.

In this investigation, we conducted a comprehensive analysis of the expression patterns of PRGs in MM patients, uncovering that 22 PRGs were significantly suppressed, whereas 31 PRGs displayed high expression. Through consensus clustering analysis, we identified 20 PRGs with prognostic implications, which enable the stratification of MM patients into two distinct subgroups. Notably, these subgroups showed no distinction when evaluated by conventional clinical parameters, yet they exhibited markedly different survival outcomes, thereby offering a new dimension to clinical stratification. Further, we constructed a prognostic model employing LASSO regression analysis by focusing on these prognostic genes. The robustness of the model was confirmed in an internal validation cohort, where it was capable of effectively differentiating survival outcomes across diverse patient subsets, particularly when age and disease stage were taken into account. This novel prognostic model thus outstrips the predictive power of the existing models reported in the literature.[18,42] These 9-gene prognostic risk model could effectively classify and evaluate the survival

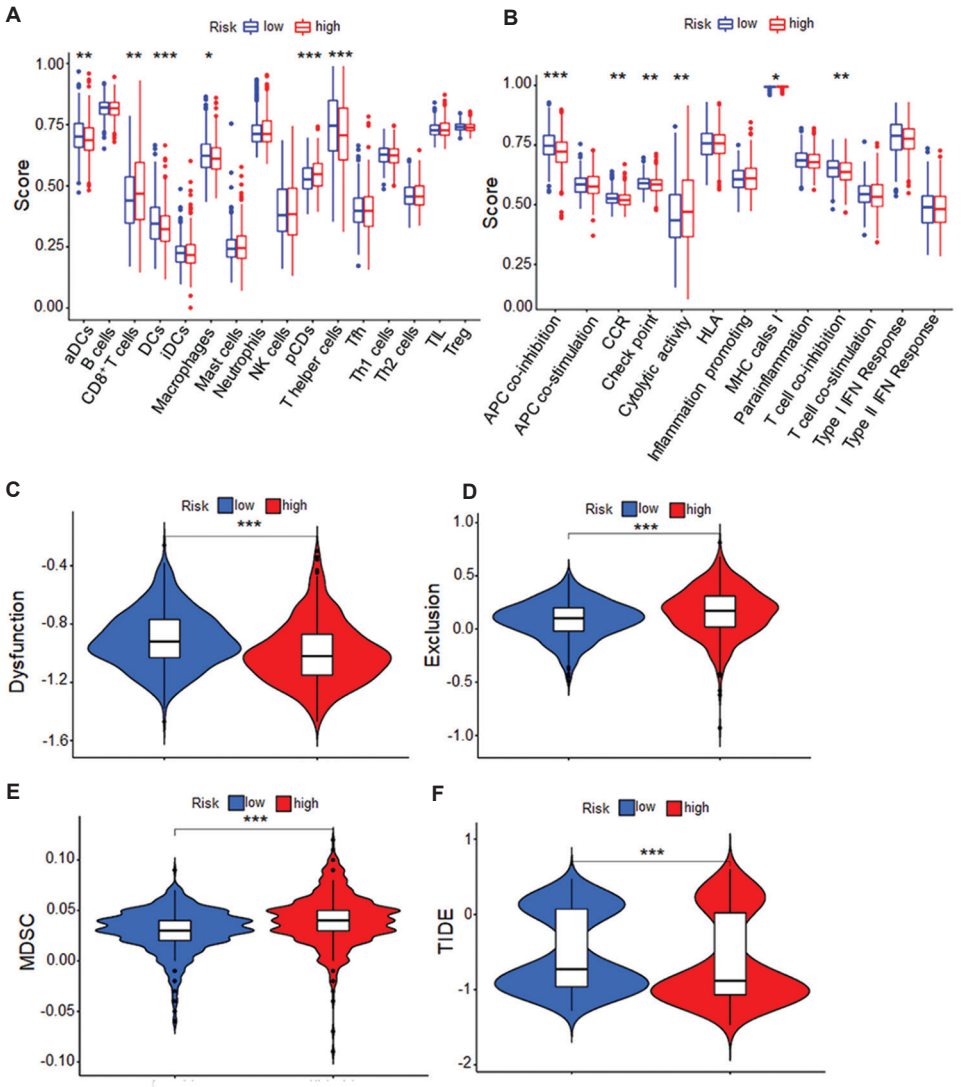

Figure 7. ssGSEA and immune correlation analysis in MM patients. (A and B) The ssGSEA scores of immune-infiltrating cells and immune pathways. (C-F) Violin plots showing dysfunction, exclusion, MDSC and TIDE scores within the two risk clusters.
Abbreviations: MDSC: Myeloid-derived suppressor cells; MM: Multiple myeloma; ssGSEA: Single-sample gene set enrichment analysis; TIDE: Tumor Immune Dysfunction and Exclusion.

of MM patients. Actually, these genes might also play key roles in MM cell survival and pyroptosis, but the roles of these genes in MM should be further studied. *FOXO3*, a known tumor suppressor gene in some cancers, was downregulated significantly in high-risk MM patients and markedly induced by etoposide, a typical anti-cancer agent to trigger cell pyroptosis. Other genes including *CHMP2A*, *CHMP3*, *NOD2*, and *PLCG1* were also downregulated but induced by etoposide; however, their specific roles in MM cell pyroptosis warrant further investigations. Interestingly, *CHMP2A* and *CHMP3* are reported to be involved in the ESCRT pathway, crucial in plasma membrane repair, a process that can avert cell death.[43] Given that plasma membrane can be penetrated by activated gasdermins, such as N-GSDMD and N-GSDME, to damage the integrity of plasma membrane, the mutations of both *CHMP2A* and *CHMP3* could potentially modulate the susceptibility of cells to this inflammatory cell death by regulating the cell's ability to mend plasma membrane disruptions.[44] Moreover, emerging research suggests that the ESCRT machinery could be involved in mediating the release of inflammatory signals during pyroptosis.[45]

In this study, we also found *NOD2* and *PLCG1* as two key determinants of high-risk MM. NOD2 is an adaptor in the formation of inflammasomes and *PLCG1*, a phospholipase C enzyme catalyzing the hydrolysis of phosphatidylinositol

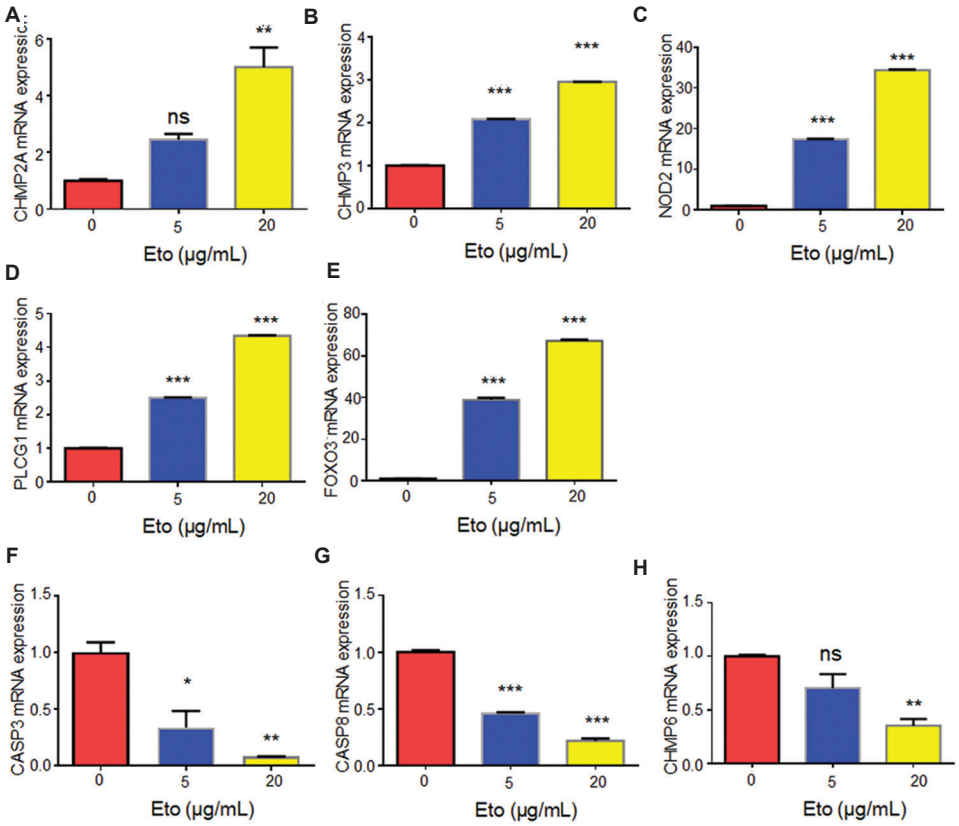

Figure 8. *In vitro* validation of the expression of 9 PRGs in MM cells treated with the pyroptosis-inducing agent etoposide. (A-H) The mRNA expressions of CHMP2A (A), CHMP3 (B), NOD2 (C), PLCG1 (D), FOXO3 (E), CASP3 (F), CASP8 (G), and CHMP6 (H) in the MM cells treated with varying concentrations of etoposide.
Abbreviations: MM: Multiple myeloma; PRGs: Pyroptosis-related genes.

4,5-bisphosphate (*PIP2*) into diacylglycerol (*DAG*) and inositol trisphosphate (*IP3*), both of which are critical in controlling inflammasome activation and pyroptosis.[46] However, given that MM cells undergo pyroptosis mainly through *GSDME*- but not *GSDMD*-mediated pathway, the specific roles of these genes in MM cell pyroptosis should be further investigated.

5. Conclusion

The present study establishes a novel PRG-based independent prognostic model that is powerful to predict the overall survival of MM patients and effective for distinguishing among MM patients with different disease risk profile. However, our PRG signature set does not encompass genes related to karyotype or mutations in the IPSS system, making it a novel and effective model for stratifying MM patients and predicting prognosis, that is not governed by the current IPSS system's classification and not restricted by karyotype profiles. Moreover, we also found several key genes that might play key roles in MM cell pyroptosis. Our future work will continue to deepen our understanding of the roles of pyroptosis in MM prognosis, thereby facilitating the development of precision medicine.

Acknowledgments

None.

Funding

This project was partly supported by the National Key Research and Development Program of China (#2022YFC2705003), National Natural Science Foundation of China (#82170176), and Guangzhou Medical University Discipline Construction Funds (Basic Medicine) (#JCXKJS2022A05).

Conflict of interest

Xinliang Mao is the Editorial Board Member of this journal but was not in any way involved in the editorial and peer-review process conducted for this paper, directly or indirectly. Separately, other authors declared that they have no known competing financial interests or personal relationships that could have influenced the work reported in this paper.

Author contributions

Conceptualization: Xinliang Mao, Yaner Wang
Formal analysis: Yaner Wang, Qi Wang, Zhenqian Huang
Investigation: Yaner Wang
Writing–original draft: Yaner Wang, Xinliang Mao
Writing–review & editing: Yaner Wang, Xinliang Mao

Ethics approval and consent to participate

Not applicable.

Consent for publication

Not applicable.

Availability of data

The clinical data and PRGs for 859 MM patients were retrieved from The Cancer Genome Atlas (TCGA)- MMRF CoMMpass project (https://portal.gdc.cancer.gov/ repository). In addition, the GTEx database was utilized to analyze mRNA expression in the bone marrow of 70 healthy individuals, who served as the controls.

References

1. Rajkumar SV. Multiple myeloma: 2016 update on diagnosis, risk-stratification, and management. *Am J Hematol*. 2016;91(7):719-734.

   doi: 10.1002/ajh.24402

2. Kazandjian D. Multiple myeloma epidemiology and survival: A unique malignancy. *Semin Oncol*. 2016;43(6):676-681.

   doi: 10.1053/j.seminoncol.2016.11.004

3. Palumbo A, Anderson K. Multiple myeloma. *New Engl J Med*. 2011;364(11):1046-1060.

   doi: 10.1056/NEJMra1011442

4. Puig N, Paiva B, Lasa M, *et al*. Flow cytometry for fast screening and automated risk assessment in systemic light-chain amyloidosis. *Leukemia*. 2019;33(5):1256-1267.

   doi: 10.1038/s41375-018-0308-5

5. Moreau P, Attal M, Hulin C, *et al*. Bortezomib, thalidomide, and dexamethasone with or without daratumumab before and after autologous stem-cell transplantation for newly diagnosed multiple myeloma (CASSIOPEIA): A randomised, open-label, phase 3 study. *Lancet*. 2019;394(10192):29-38.

   doi: 10.1016/s0140-6736(19)31240-1

6. Walker BA, Morgan GJ. The genomic features associated with high-risk multiple myeloma. *Oncotarget*. 2018;9(84): 35478-35479.

   doi: 10.18632/oncotarget.26269

7. Rajkumar SV. Multiple myeloma: 2022 update on diagnosis, risk stratification, and management. *Am J Hematol*. 2022;97(8):1086-1107.

   doi: 10.1002/ajh.26590

8. Kumar SK, Dispenzieri A, Lacy MQ, *et al*. Continued improvement in survival in multiple myeloma: Changes in early mortality and outcomes in older patients. *Leukemia*. 2014;28(5):1122-1128.

   doi: 10.1038/leu.2013.313

9. van de Donk N, Pawlyn C, Yong KL. Multiple myeloma. *Lancet*. 2021;397(10272):410-427.

   doi: 10.1016/S0140-6736(21)00135-5

10. Farhana A, Lappin SL. Biochemistry, lactate dehydrogenase. In: *StatPearls*. Treasure Island, FL: StatPearls Publishing; 2023.

11. Liang JP, He YM, Cui YL, *et al*. Proteasomal inhibitors induce myeloma cell pyroptosis via the BAX/GSDME pathway. *Acta Pharmacol Sin*. 2023;44(7):1464-1474.

    doi: 10.1038/s41401-023-01060-3

12. Jorgensen I, Miao EA. Pyroptotic cell death defends against intracellular pathogens. *Immunol Rev*. 2015;265(1):130-142.

    doi: 10.1111/imr.12287

13. Shi J, Zhao Y, Wang K, *et al*. Cleavage of GSDMD by inflammatory caspases determines pyroptotic cell death. *Nature*. 2015;526(7575):660-665.

    doi: 10.1038/nature15514

14. Chen X, He WT, Hu L, *et al*. Pyroptosis is driven by non-selective gasdermin-D pore and its morphology is different from MLKL channel-mediated necroptosis. *Cell Res*. 2016;26(9):1007-1020.

    doi: 10.1038/cr.2016.100

15. Ding J, Wang K, Liu W, *et al*. Pore-forming activity and structural autoinhibition of the gasdermin family. *Nature*. 2016;535(7610):111-116.

    doi: 10.1038/nature18590

16. Li T, Zheng G, Li B, Tang L. Pyroptosis: A promising therapeutic target for noninfectious diseases. *Cell Prolif*. 2021;54(11):e13137.

    doi: 10.1111/cpr.13137

17. Man SM. Inflammasomes in the gastrointestinal tract: Infection, cancer and gut microbiota homeostasis. *Nature Rev Gastroenterol Hepatol*. 2018;15(12):721-737.

    doi: 10.1038/s41575-018-0054-1

18. Fang Y, Tian S, Pan Y, *et al*. Pyroptosis: A new frontier in cancer. *Biomed Pharmacother*. 2020;121:109595.

    doi: 10.1016/j.biopha.2019.109595

19. Xia X, Wang X, Cheng Z, *et al*. The role of pyroptosis in cancer: Pro-cancer or pro-"host"? *Cell Death Dis*. 2019;10(9):650.

doi: 10.1038/s41419-019-1883-8

20. Shi M, Tang C, Wu JX, *et al*. Mass spectrometry detects sphingolipid metabolites for discovery of new strategy for cancer therapy from the aspect of programmed cell death. *Metabolites*. 2023;13(7):867.

doi: 10.3390/metabo13070867

21. Rao Z, Zhu Y, Yang P, *et al*. Pyroptosis in inflammatory diseases and cancer. *Theranostics*. 2022;12(9):4310-4329.

doi: 10.7150/thno.71086

22. He Y, Jiang S, Cui Y, *et al*. Induction of IFIT1/IFIT3 and inhibition of Bcl-2 orchestrate the treatment of myeloma and leukemia via pyroptosis. *Cancer Lett*. 2024;588:216797.

doi: 10.1016/j.canlet.2024.216797

23. Chen LL, Chen X, Choi H, *et al*. Exploiting antitumor immunity to overcome relapse and improve remission duration. *Cancer Immunol Immunother*. 2012;61(7):1113-1124.

doi: 10.1007/s00262-011-1185-1

24. Guner A, Kim HI. Biomarkers for evaluating the inflammation status in patients with cancer. *J Gastric Cancer*. 2019;19(3):254-277.

doi: 10.5230/jgc.2019.19.e29

25. Yu P, Zhang X, Liu N, Tang L, Peng C, Chen X. Pyroptosis: Mechanisms and diseases. *Signal Transduct Target Ther*. 2021;6(1):128.

doi: 10.1038/s41392-021-00507-5

26. Wang H, Shao R, Lu S, *et al*. Integrative analysis of a pyroptosis-related signature of clinical and biological value in multiple myeloma. *Front Oncol*. 2022;12:845074.

doi: 10.3389/fonc.2022.845074

27. Zhang C, Wu S, Chen B. A novel prognostic model based on pyroptosis-related genes for multiple myeloma. *BMC Med Genomics*. 2023;16(1):32.

doi: 10.1186/s12920-023-01455-5

28. Li C, Liang H, Bian S, Hou X, Ma Y. Construction of a prognosis model of the pyroptosis-related gene in multiple myeloma and screening of core genes. *ACS Omega*. 2022;7(38):34608-34620.

doi: 10.1021/acsomega.2c04212

29. Yuan C, Yuan M, Chen M, *et al*. Prognostic implication of a novel metabolism-related gene signature in hepatocellular carcinoma. *Front Oncol*. 2021;11:666199.

doi: 10.3389/fonc.2021.666199

30. Ye J, She X, Liu Z, *et al*. Eukaryotic initiation factor 4A-3: A review of its physiological role and involvement in oncogenesis. *Front Oncol*. 2021;11:712045.

doi: 10.3389/fonc.2021.712045

31. Chen W, Zhang W, Zhou T, Cai J, Yu Z, Wu Z. A newly defined pyroptosis-related gene signature for the prognosis of bladder cancer. *Int J Gen Med*. 2021;14:8109-8120.

doi: 10.2147/ijgm.S337735

32. Du H, Xie S, Guo W, *et al*. Development and validation of an autophagy-related prognostic signature in esophageal cancer. *Ann Transl Med*. 2021;9(4):317.

doi: 10.21037/atm-20-4541

33. Yang Y, Wu G, Li Q, *et al*. Angiogenesis-related immune signatures correlate with prognosis, tumor microenvironment, and therapeutic sensitivity in hepatocellular carcinoma. *Front Mol Biosci*. 2021;8:690206.

doi: 10.3389/fmolb.2021.690206

34. Fang Y, Huang S, Han L, Wang S, Xiong B. Comprehensive analysis of peritoneal metastasis sequencing data to identify LINC00924 as a Prognostic biomarker in gastric cancer. *Cancer Manag Res*. 2021;13:5599-5611.

doi: 10.2147/cmar.S318704

35. Yuan M, Wang Y, Sun Q, *et al*. Identification of a nine immune-related lncRNA signature as a novel diagnostic biomarker for hepatocellular carcinoma. *Biomed Res Int*. 2021;2021:9798231.

doi: 10.1155/2021/9798231

36. Dai Y, Qiang W, Lin K, Gui Y, Lan X, Wang D. An immune-related gene signature for predicting survival and immunotherapy efficacy in hepatocellular carcinoma. *Cancer Immunol Immunother*. 2021;70(4):967-979.

doi: 10.1007/s00262-020-02743-0

37. Zhao WJ, Ou GY, Lin WW. Integrative analysis of neuregulin family members-related tumor microenvironment for predicting the prognosis in gliomas. *Front Immunol*. 2021;12:682415.

doi: 10.3389/fimmu.2021.682415

38. Fu J, Li K, Zhang W, *et al*. Large-scale public data reuse to model immunotherapy response and resistance. *Genome Med*. 2020;12(1):21.

doi: 10.1186/s13073-020-0721-z

39. Jiang P, Gu S, Pan D, *et al*. Signatures of T cell dysfunction and exclusion predict cancer immunotherapy response. *Nature Med*. 2018;24(10):1550-1558.

doi: 10.1038/s41591-018-0136-1

40. Wang Y, Gao W, Shi X, *et al*. Chemotherapy drugs induce pyroptosis through caspase-3 cleavage of a gasdermin. *Nature*. 2017;547(7661):99-103.

doi: 10.1038/nature22393

41. Shi J, Gao W, Shao F. Pyroptosis: Gasdermin-mediated programmed necrotic cell death. *Trends Biochem Sci*. 2017;42(4):245-254.

doi: 10.1016/j.tibs.2016.10.004

42. Ju X, Yang Z, Zhang H, Wang Q. Role of pyroptosis in cancer cells and clinical applications. *Biochimie*. 2021;185:78-86.

doi: 10.1016/j.biochi.2021.03.007

43. Verma R, Marchese A. The endosomal sorting complex required for transport pathway mediates chemokine receptor CXCR4-promoted lysosomal degradation of the mammalian target of rapamycin antagonist DEPTOR. *J Biol Chem*. 2015;290(11):6810-6824.

doi: 10.1074/jbc.M114.606699

44. Raab M, Gentili M, de Belly H, *et al*. ESCRT III repairs nuclear envelope ruptures during cell migration to limit DNA damage and cell death. *Science*. 2016;352(6283):359-362.

doi: 10.1126/science.aad7611

45. Tian Z, Tong X, Sheng G, *et al*. Printable magnesium ion quasi-solid-state asymmetric supercapacitors for flexible solar-charging integrated units. *Nat Commun*. 2019;10(1):4913.

doi: 10.1038/s41467-019-12900-4

46. Zhang S, Li X, Zhang X, Zhang S, Tang C, Kuang W. The pyroptosis-related gene signature predicts the prognosis of hepatocellular carcinoma. *Front Mol Biosci*. 2021;8:781427.

doi: 10.3389/fmolb.2021.781427

Our Journals

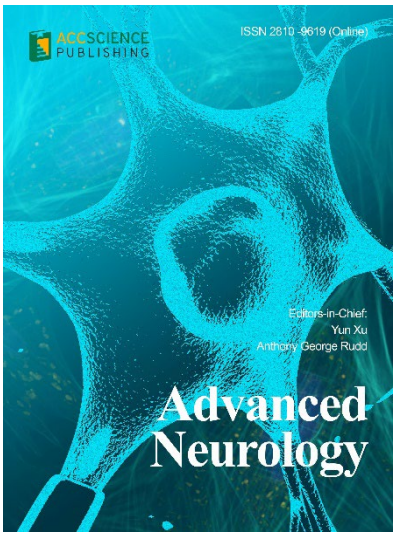

Advanced Neurology is a peer-reviewed and open-access journal that aims to publish and disseminate novel research in the breadth of neurology and neuroscience. The journal aims to advance our understanding in the nervous system and provide a platform to neuroscientists and physicians to showcase their findings in original fundamental and clinical research as well as to present new ideas that highlight the changes in the neurological clinical practice.

Advanced Neurology covers subject areas, including but not limited to the following:

- Neurological disorders
- Neurodegenerative disease
- Cerebrovascular disease
- Epilepsy and movement disorders
- Neuroimmune disease
- Neurological infections
- Muscle disease
- Molecular and cellular neuroscience
- Systems neuroscience
- Cognitive neuroscience
- Computational modeling of nervous system

Global Translational Medicine is a quarterly journal that focuses on medicine, biological sciences, and biomaterials engineering. The goal of *Global Translational Medicine* is to provide a platform to researchers for showcasing their latest research works in translational medicine so as to advance the field towards the betterment of human health. Despite the advancement of omics and new technologies, the process of transforming these technologies and scientific research results into effective therapies and putting them into clinical use still has a long way to go. *Global Translational Medicine* provides a platform to fill the gaps in preclinical and inter-disciplinary research, to promote clinical translation of scientific research results, and to contribute to the conception of new and improved preventive measures as well as diagnostic and therapeutic techniques of diseases.

Global Translational Medicine covers the following themes: cardiovascular disease, metabolism/diabetes/obesity, neuroscience/neurology, cancer, biomaterials and their applications in medicine, proteomics/metabolomics, pharmacogenomics, biomarkers, bioinformatics and data mining, animal and clinical research, and medical methods arising from interdisciplinary crossover.

Start a new journal

Write to us via email if you are interested to start a new journal with AccScience Publishing. Please attach your CV, professional profile page and a brief pitch proposal in your email. We shall inform you of our decision whether we are interested to collaborate in starting a new journal.

Contact: info@accscience.com

https://accscience.com/journal/GPD

Contact
www.accscience.com
8 Burn Road, #15-03 Trivex, Singapore 369977
Email: editorial@accscience.com
Phone: +65 8182 1586